TAMPEREEN TEKNILLINEN YLIOPISTO
TAMPERE UNIVERSITY OF TECHNOLOGY

Ville Jouppila

Modeling and Control of a Pneumatic Muscle Actuator

Julkaisu 1199 • Publication 1199

Tampere 2014

Tampereen teknillinen yliopisto. Julkaisu 1199
Tampere University of Technology. Publication 1199

Ville Jouppila

Modeling and Control of a Pneumatic Muscle Actuator

Thesis for the degree of Doctor of Science in Technology to be presented with due permission for public examination and criticism in Frami B Building, Auditorium 2, at University Consortium of Seinäjoki, on the 4th of April 2014, at 12 noon.

Tampereen teknillinen yliopisto - Tampere University of Technology
Tampere 2014

ISBN 978-952-15-3258-0 (printed)
ISBN 978-952-15-3428-7 (PDF)
ISSN 1459-2045

ABSTRACT

This thesis presents the theoretical and experimental study of pneumatic servo position control systems based on pneumatic muscle actuators (PMAs). Pneumatic muscle is a novel type of actuator which has been developed to address the control and compliance issues of conventional cylindrical actuators. Compared to industrial pneumatic cylinders, muscle actuators have many ideal properties for robotic applications providing an interesting alternative for many advanced applications. However, the disadvantage is that muscle actuators are highly nonlinear making accurate control a real challenge.

Traditionally, servo-pneumatic systems use relatively expensive servo or proportional valve for controlling the mass flow rate of the actuator. This has inspired the research of using on/off valves instead of servo valves providing a low-cost option for servo-pneumatic systems. A pulse width modulation (PWM) technique, where the mass flow is provided in discrete packets of air, enables the use of similar control approaches as with servo valves. Although, the on/off valve based servo-pneumatics has shown its potential, it still lacks of analytical methods for control design and system analysis. In addition, the literature still lacks of studies where the performance characteristics of on/off valve controlled pneumatic systems are clearly compared with servo valve approaches.

The focus of this thesis has been on modeling and control of the pneumatic muscle actuator with PWM on/off valves. First, the modeling of pneumatic muscle actuator system controlled by a single on/off valve is presented. The majority of the effort focused on the modeling of muscle actuator nonlinear force characteristics and valve mass flow rate modeling. A novel force model was developed and valve flow model for both simulation and control design were identified and presented.

The derived system models (linear and nonlinear), were used for both control design and utilized also in simulation based system analysis. Due to highly nonlinear characteristics and uncertainties of the system, a sliding mode control (SMC) was chosen for a control law. SMC strategy has been proven to be an efficient and robust control strategy for highly nonlinear pneumatic actuator applications. Different variations of sliding mode control, SMC with linear model (SMCL) and nonlinear model (SMCNL) as well as SMC with integral sliding surface (SMCI) were compared with a traditional proportional plus velocity plus acceleration control with feed-forward (PVA+FF) compensation. Also, the effects of PWM frequency on the system performance were studied.

Different valve configurations, single 3/2, dual 2/2, and servo valve, for controlling a single muscle actuator system were studied. System models for each case were formulated in a manner to have a direct comparison of the configuration and enabling the use of same sliding mode control design. The analysis of performance included the sinusoidal tracking precision and robustness to parameter variations and external disturbances. In a similar manner, a comparison of muscle actuators in an opposing pair configuration controlled by four 2/2 valves and servo valve was executed.

Finally, a comparison of a position servo realized with pneumatic muscle actuators to the one realized with traditional cylinder was presented. In these cases, servo valve with SMC and SMCI were used to control the systems. The analysis of performance included steady-state error in point-to-point positioning, the RMSE of sinusoidal tracking precision, and robustness to parameter variations.

PREFACE

The work in this thesis has been carried out in the Department of Mechanics and Design at Tampere University of Technology during the years 2008-2012. The research was mainly supported by the Graduate School of Concurrent Engineering funded by the Ministry of Education. The work was supported financially (received grants) also by Finnish Foundation for Technology Promotion (TES), Alfred Kordelin Foundation, and Science Fund of City of Tampere.

I would like to express my gratitude to my supervisor professor Asko Ellman for the guidance and support during the research work. I am also grateful to Dr. Andrew Gadsden, professor Gary M. Bone and professor Saied R. Habibi for their strong professional support, valuable ideas, and constructive feedback during the research work. In addition, I thank my thesis reviewers, professor Petter Krus and professor Matti Pietola, for providing their insightful and valuable comments on the work.

I would also like to express my gratitude to the professor Erno Keskinen and professor Michel Cotsaftis for their critical and constructive feedback in the Graduate School seminars.

I want to thank all my colleagues and staff of the Department of Mechanics and Design for providing a pleasant and supportive working atmosphere.

I wish to express my loving gratitude to my family, especially my wife Hanna, my father Tuomo and my mother Arja as well as to my friends for their support and encouragement throughout my life.

TABLE OF CONTENTS

LIST OF PUBLICATIONS AND AUTHOR CONTRIBUTIONS

This thesis consists of an introductory part, literature review of the topic and the summary of the publications.

Publication 1: Ville Jouppila, Andrew Gadsden, Asko Ellman, "Modeling and Identification of a Pneumatic Muscle Actuator System Controlled by an On/Off Solenoid Valve", in *Proceedings of 7th International Fluid Power Conference,* Aachen Germany, March 2010, 15 pages

Publication 2: Ville Jouppila, Asko Ellman, "Position Control of PWM-actuated Pneumatic Muscle Actuator System", in *Proceeding of the ASME 2011 International Mechanical Engineering Congress and Exposition (ASME IMECE 2011),* Denver, USA, November 2011, 13 pages

Publication 3: Ville Jouppila, Andrew Gadsden, Gary Bone, Asko Ellman, Saeid Habibi, "Sliding Mode Control of a Pneumatic Muscle Actuator System with a PWM Strategy", accepted for publication in *International Journal of Fluid Power.*

Publication 4: Ville Jouppila, Asko Ellman, "A Pneumatic Position Servo Based on On/Off Valve Actuated Muscle Actuators in Opposing Pair Configuration" in *Proceedings of Bath/ASME Symposium on Fluid Power & Motion Control (FPMC 2012), Bath, UK, September 2012, pp. 243-258*

Publication 5: Ville Jouppila, Andrew Gadsden, Asko Ellman, "Experimental Comparisons of Sliding Mode Controlled Pneumatic Muscle and Cylinder Actuator" accepted for publication in *ASME Journal of Dynamic Systems, Measurement and Control.*

The thesis candidate is the first author of all publications contributing the main research work of the publications including the modeling, simulations, experiments and writing. Prof. Asko Ellman has been the supervisor of this thesis providing support and facilities for this research. Dr. Andrew Gadsden has provided his experience on control and estimation, as well as scientific writing. Prof. Saeid Habibi provided his broad experience on control systems and estimation and facilities to do this research work at McMaster University during the years 2009 and 2010. Prof. Gary Bone provided his experience on pneumatic servo systems for this research.

LIST OF FIGURES

LIST OF TABLES

LIST OF ABBREVIATIONS

ANFMRC	Adaptive Neuro-Fuzzy Model-Reference Control
ADVSC	Adaptive Discrete Variable Structure Control
AGPC	Adaptive Generalized Predictive Control
ARMA	Auto Regressive Moving Average
CARIMA	Controlled Auto-Regressive Integrated Moving Average
CSLM	Continuous Sliding Mode
DSLM	Discrete Sliding Mode
FF	Feed-Forward
ITAE	Integral of Time-weighted Absolute Error
LTI	Linear Time Invariant
LTV	Linear Time Variant
LVQNN	Learning Vector Quantization Neural Network
MIMO	Multi-input-multi-output
MRAC	Model-Reference Adaptive Control
NN	Neural Networks
NMPC	Nonlinear model predictive control
PID	Proportional-Integral-Derivative
PMA	Pneumatic Muscle Actuator
PVA	Proportional-Velocity-Acceleration
PWM	Pulse Width Modulation
PΔP	Proportional plus differential pressure
RLS	Recursive Least Squares
RMSE	Root mean squared error
SISO	Single-input-single-output
SMC	Sliding Mode Control
STC	Self-Tuning Control
VSC	Variable Structure Control

NOMENCLATURE

Symbols of Latin alphabet

C_v	valve conductance
D	diameter of the actuator
F	force
K	stiffness
K_D	derivative gain
K_I	integral gain
K_P	proportional gain
K_{p_eq}	equivalent proportional gain
K_{v_eq}	equivalent velocity feedback gain
K_{a_eq}	equivalent acceleration feedback gain
K_{SMC}	switching gain
L, L_0	length of the actuator, initial length
M	payload, total moving mass
M_p	overshoot
S, $S(x,t)$	sliding surface, state and time dependent sliding surface
S_i	total inner surface
T_settle	settling time
V	volume of the actuator chamber
W_{in}	input work
W_{out}	output work
b	length of one braid strand
b_v	valve critical pressure ratio
$f(.)$	system dynamics function
$b(.)$	control gain function
i	index numbering
k	corrective coefficient

k_g	gas stiffness
k_p	elastic constant
n	number of times the strand encircles the actuator, system order
p ,p’	absolute pressure, relative pressure
p_0	environment pressure
t_{reach}	reaching time
u	control signal
u_{eq}	equivalent control
u_{sw}	switching control
x	output of interest (e.g. position of the load)
x_d	desired output of interest (e.g. position of the load)

Symbols of Greek alphabet

β	gain margin
ε	contraction ratio, boundary layer width
ζ	damping coefficient
η	convergence rate, positive constant
θ, θ_0	braid angle, initial braid angle
λ	control bandwidth
Φ	boundary layer thickness
ω_n	natural frequency

1. INTRODUCTION

1.1 Problem overview

Servo control in industrial applications has traditionally been limited to two main technologies: electromagnetic motors and hydraulic actuators. Electric servo motors provide clean and reliable operation but they are usually high-speed, low torque actuators, and need transmission elements to convert power to a more useful form. Also, mechanical elements are required to convert the rotary motion to linear motion if needed.

Hydraulic actuators have favorable force/speed characteristics, and can be directly coupled with payload. On the other hand, hydraulic systems are noisy and they are well known for their leakage. One positive aspect shared by electromagnetic and hydraulic actuators is ease of control. Linear models provide a good approximation for both systems, and conventional linear controllers can often provide adequate performance.

Pneumatic actuators have many desirable properties for servo applications. The actuators themselves are often of simple construction, widely available, easily maintained and low in cost. They have a high power-to-weight ratio, are fast acting, and unlike electric motors, can apply a force at a fixed position over a prolonged period of time with no ill effects. Also, compressed air is readily available in most industrial environments. Like electromagnetic actuators, pneumatics offer clean and reliable operation. Like hydraulic actuators, pneumatics can be coupled directly to a payload, without the need of transmission elements for power or motion conversion. Unlike electro-magnetic and hydraulic actuators, a pneumatic actuator exhibits significant nonlinear behavior due to compressibility of air, valve fluid flow characteristics, friction etc. The compressibility of air gives a very low stiffness compared to hydraulic and electric systems. In addition, the stiffness of a cylinder actuator depends also on its position. Friction in mechanical systems is dependent on a number of variables such a temperature, pressure and surface roughness and may change from day to day. Pneumatic valves, as with most flow control devices, are nonlinear in that the flow is not directly proportional to the control variable. In addition, valves may exhibit high hysteresis. These nonlinear characteristics result in a complex and difficult system to model and control accurately preventing linear control systems from providing acceptable servo control of the pneumatic actuator. Although pneumatic actuators are widely used in robotics and automation, these effects are the main reason that they are still commonly avoided for advanced applications and mainly been limited to the simple positioning tasks realized with simple on-off control valves and mechanical stops. However, relatively recent developments in control valves and actuators with low friction properties and high reliability allow for improved control of servo-

pneumatics, making their performance competitive with traditional servo technologies. On the other hand, these improvements increase the capital cost of a pneumatic positioning systems, thus negating economy as their most attractive feature.

Each of the main actuator technologies has application fields for which it is particularly suited and in which it performs effectively. On the other hand, there has also been a lot of research work for new actuators technologies among which the most promising is the family of pneumatic muscle actuators (PMA) which have been developed to address the control and compliance issues of conventional cylindrical actuators. Compared to industrial pneumatic cylinders, muscle actuators have many ideal properties for robotic applications: high force-to-weight ratio, flexibility, light structure and good efficiency. In a McKibben actuator, which is the most popular version of PMAs, the cylinder/piston structure is replaced by a compliant braided shell that still retains the positive attributes of good power/weight performance, simplicity, etc. This technology provides an interesting alternative actuation source for many advanced applications. However, the disadvantage is that muscle actuators are highly nonlinear making accurate control a real challenge.

Traditionally, servo-pneumatic systems use expensive servo or proportional control valves, and the cost of valves dominates the cost of actuator in almost all cases. This has inspired the research of Pulse Width Modulated (PWM) control that offers the ability to provide servo control of pneumatic actuators at a significantly lower cost by utilizing low-cost on/off solenoid valves instead of proportional servo valves. Instead of continuously varying the resistance of the control valve as in the case of proportional-valve-based systems, PWM controlled systems meter the power delivered to the actuator discretely by delivering packets of fluid mass via valve that is either completely open or closed. If delivery of these packets of mass occur on a time scale that is significantly faster than the system dynamics (i.e. dynamics of the actuator and load), then the system will respond in essence to the average mass flow rate into and out of actuator, in a similar to the continuous case. Although the PWM-pneumatics has shown its potential, it still lacks of analytical methods for control design and system analysis. Also, there have not been studies where the performance of PWM-actuated systems is compared with the ones with servo or proportional valves and where the advantages and disadvantages of PWM servo-pneumatics are fully addressed. The fact is that, in order to make PWM-actuated servo systems attractive and compatible for industrial applications, it should provide a performance close enough to a system with traditional servo valves and provide significant savings in system costs.

1.2 Problem statement and thesis contributions

This thesis focuses on the modeling and control of pneumatic servo systems, actuated by pneumatic muscle actuator(s) and PWM-controlled on/off valve(s). The problem statement and thesis contributions are formulated as follows:

1) As the overall pneumatic system is highly nonlinear, a detailed mathematical model for both simulation and control design purposes is required. The simulation model should be as realistic as possible in order to provide means for system analysis and for design and testing control laws.

   A dynamic model of the muscle actuator system was built, based on physical principles and dedicated experimental identification, where special attention was given to the modeling of the muscle actuator and on/off solenoid valve. These models were validated by experiments.

   a) Pneumatic muscle actuator introduces a highly nonlinear force-pressure-displacement relation and a significant hysteresis making the accurate modeling of the pneumatic system even more challenging.

      Special attention was given to the modeling of the muscle actuator force characteristics. As a result a novel and accurate force model was developed.

   b) When PWM-actuated on/off valve(s) is used instead of a servo valve, the valve switching introduces a discontinuous system dynamics which is difficult to handle from the point of view of control design.

      In order to enable conventional analytical model-based control approaches, a valve model transforming the discontinuities into a continuous form was developed. Also, a detailed model of the valve operation for simulation purposes was developed.

2) Highly nonlinear nature of pneumatic systems makes the accurate control extremely difficult. As such, classical linear control approaches provide only poor performance and more complex control strategies are needed.

   Due to highly nonlinear characteristics of the muscle actuator system and uncertainties present in the system, a sliding mode control (SMC) was chosen for a control law. SMC strategy has been proven to provide an efficient, robust and simple approach for controlling nonlinear and uncertain systems. The effectiveness of the chosen strategy was compared with traditional linear PVA+FF control approach.

3) Although PWM-pneumatics has been studied during the past two decades, their performance compared to traditional servo valve controlled system has not been completely addressed. Also, the literature lacks robustness study of the PWM –pneumatic systems to parameter variations.

   A comparison of PWM- on/off valve and servo valve controlled pneumatic system with the same control law (SMC) was performed. The robustness of the approaches against parameter variations was verified by changing the loading conditions of the system. With the comparison the advantages and disadvantages of PWM-approach were addressed.

4) Although pneumatic muscle actuators are widely studied they are still rare in industrial servo applications. The main reasons for this are: their highly nonlinear behavior, lack of simple and effective control strategies for providing sufficient performance, their totally different working principle from the traditional cylinder preventing direct replacement of the cylinder.

   A comparison of pneumatic position servo system realized with traditional cylinder and pneumatic muscle actuators was executed. With the comparison the advantages and disadvantages of pneumatic muscle actuators were addressed.

1.3 Thesis outline

The thesis is written in a set book format unlike the traditional PhD thesis manuscript. The content is based on five publications which are appended at the end of the thesis. In the first Chapter, introduction to the research problem, as well as the thesis objectives and main contributions were stated. In Chapter 2, a summary of literature review including most significant works related to modeling and control of traditional servo valve controlled and PWM-controlled pneumatic servo systems are represented. In Chapter 3, the basic concepts and properties of pneumatic muscle actuators including literature of modeling and control issues are discussed.

Chapter 4 summarizes the five publications containing the publication objectives, approaches, important results, conclusions and significant contributions.

Chapter 5 presents overall conclusions and restates the major research contributions of this study.

The Appendices present main fundamental principles and concepts of control approaches used in this work providing support for the reader.

2. LITERATURE REVIEW

2.1 Introduction

In this chapter the literature related to pneumatic servo control system is reviewed. The review will be divided in three sub areas: pneumatic system modeling, control of a pneumatic servo system based on a servo or proportional valve, and control of pneumatic servo systems with on/off valves and pulse width modulation (PWM).

A typical arrangement of components used in pneumatic servo systems is shown in Figure 2-1. Traditionally, pneumatic cylinder with its variations is used as an actuator in pneumatic systems. However, pneumatic muscle actuator (PMA) with its high force-to-weight characteristics has found some applications especially in robotics. In servo-pneumatics, the actuator is typically controlled with servo valve that has an integrated closed-loop controller for the spool position. An alternative to servo valve is a proportional valve that is operated in an open-loop manner having a proportional magnet for providing a proportional relation between control signal and spool position. On-off solenoid valves are usually used in simple point-to-point positioning systems with e.g. mechanical stops. However, the use of pulse width modulation (PWM) technique with on/off valves results in an averaged flow for which the actuator responses in a similar way as in case of servo valve system.

A wide variety of controllers can be used with pneumatic servo system ranging from simple linear controllers to advanced nonlinear model-based controllers. In a selection of a controller, the design objectives are very important factors. Positioning control, or point-to-point control, deals with applications in which the exact trajectory is not as important as the static positioning error of the system. Servo control, instead, is defined as an actuator's ability to follow an arbitrary trajectory, and is considered more demanding of the controller.

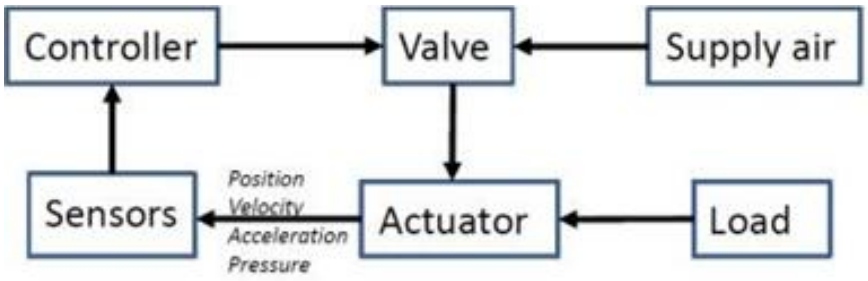

Figure 2-1: A typical configuration of pneumatic servo systems

There are two basic methods of dealing with control problems: the linear and the nonlinear approach (see Figure 2-2). Generally speaking, most physical systems are nonlinear in nature.

However, if the operating range of a control system is small, and if the involved nonlinearities are smooth, then the control system may be approximated by a set of linear differential equations with a sufficient accuracy. For linear systems, there exist many well-established analysis and design techniques such as root-locus, Bode plot, Nyquist criterion, state-feedback, pole placement etc. Examples of popular linear fixed gain controllers in industrial applications are Proportional-Derivative (PD), Proportional-Integral-Derivative (PID), and Proportional-Velocity-Acceleration (PVA) that are typically designed using the above design techniques.

Traditional servo actuators – electric motors and hydraulic cylinders – may be modeled as linear mechanisms without significant error and linear control methods may therefore be applied with an adequate control performance. However, the linear approach obviously has its drawbacks for those systems that are strongly nonlinear in nature. When the state of the system is far from the equilibrium point used for linearization, nonlinearities can degrade system performance and possibly impair the stability of the system. In addition, so called "hard nonlinearities" such as Coulomb friction, actuator saturation, valve dead-zones, and gear backlash possess a discontinuous feature that can't be described by a linear approximation (Slotine & Li, 1991).

Pneumatic systems are highly nonlinear for which conventional linear control approaches can't provide good performance (Brun et al., 1998). If linear controllers are employed, for instance, trajectory tracking performance is highly influenced by the position at which its approximate models are defined. (Virvalo, 1995; Nouri et al., 2000). Also, these systems suffer from the highly nonlinear behavior associated to compressibility effects (Bobrow & McDonell, 2002) and dry-friction at near zero velocities (Guenther et al., 2006; Khayati et al., 2009). For these reasons, nonlinear control techniques are usually applied for controlling pneumatic servo systems. Nonlinear control theory studies how to apply existing linear methods to more general control systems. Additionally, it provides methods that cannot be analyzed using the linear time-invariant (LTI) system theory. Control design techniques for nonlinear systems can be subdivided into different categories (Fig 2-2). The adaptive control attempts to treat the system as a linear system in a limited range of operation and use linear design techniques for each region. The basic idea in adaptive control is to estimate the uncertain plant parameters on-line. There three main approaches for constructing adaptive controllers are the model-reference adaptive control method (MRAC), the self-tuning control (STC) method, and the gain scheduling method (Slotine & Li, 1991). Techniques that attempt to introduce auxiliary nonlinear feedback in such a way that the system can be treated as linear for purposes of control design is called a feedback linearization technique. The Lyapunov based methods can be divided in Lyapunov redesign, nonlinear damping, back-stepping and sliding mode control. Sliding mode controller which has its' roots in variable structure systems is the most

commonly used nonlinear controller and it can be used to control both linear and nonlinear systems. The most important advantage of a sliding mode controller is its low sensitivity/robustness to disturbances and system parameter variations. Therefore even an approximate process model can provide good performance, at least theoretically (Slotine & Li, 1991). The intelligent control is a class of control techniques that use various artificial intelligent computing approaches like neural networks, fuzzy logic, machine learning and genetic algorithms.

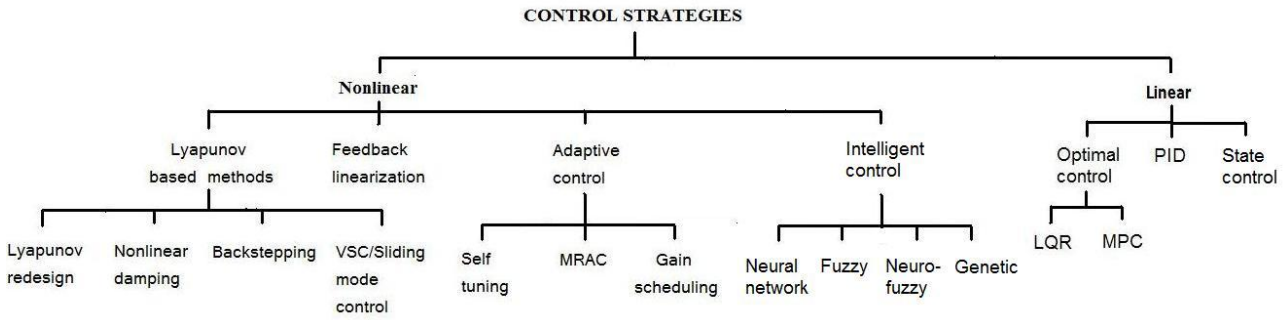

Figure 2-2: Summary of main control techniques

2.2 Modeling of pneumatic systems

A review of modeling issues of pneumatic systems is briefly introduced. The mathematical analysis of pneumatic systems requires a consideration of thermodynamics, fluid dynamics and the dynamics of the load and the actuator. It is clear, that accurate model of the pneumatic actuator is an important tool for both control design and optimizing its operation.

The pioneering work on the servo-pneumatics is the studies by J.L. Shearer in the 1950's (Shearer, 1956 & 1957). He studied the pneumatic processes in the motion control, and set up a complete mathematical model for a double-rod cylinder involving the compressibility of air in the actuator chambers and the characteristics of the airflow through the control valve. As a result of this study, a third-order linear mathematical model was obtained. Shearer's work has provided a solid theoretical basis for further research and his model has been widely used for pneumatic control system dynamic analysis and controller design.

In 1966, a further study on Shearer's model using the root locus technique was made in (Burrows, 1966), where the effects of the combinations of valve center types and frictions levels on the linear system model were investigated. It was concluded, that the effect of an open center valve was similar to that of viscous friction in that it improved system stability. In 1969, Burrows extended Shearer's work by providing the model for the whole stroke and made a conclusion that

the system was less stable when operating about the mid-stroke position compared with any other position (Burrows, 1969).

A paper by (Liu & Bobrow, 1988) expanded on Shearer's work by examining the potential use of direct-drive pneumatic servo-actuators in robotic applications. They derived a complete linear state-space model of the actuator based on an arbitrary operating point and developed a straightforward experimental procedure to determine the unknown flow constant of this linear model. Their analysis showed that the linear model represented the dominant dynamics of the pneumatic system with an adequate precision and claimed that pneumatic systems were practical for use in servo-control applications.

In (Bobrow & Jabbari, 1991), a system identification method was used to determine a linear ARMA (Auto Regressive Moving Average) model for a pneumatic force control system. They found that the order of the dominant dynamics was shown to vary with the position of the mechanism. The problem of sensor resolution and noise was the most difficult to handle. They also found that if the order of the system was underestimated, the control performance was more satisfactory. However, after they used the on-line identified linear model for position adaptive control, they concluded that the model obtained from the identification algorithm was not adequate for control purpose.

Pu and his group have studied the models and control strategies of pneumatic servo systems over a wide range of operating conditions, both theoretically and experimentally. In (Pu et al., 1992), they pointed out that the stability and damping characteristics of pneumatic servo systems are inherently complex and difficult to model. This complexity was primarily caused by the compressibility of working fluid which resulted in nonlinearities relating to choked flow, pressure drop along transmission pipes, leakage and possibly time varying lubrication conditions leading to variable friction characteristics. They concluded that it is extremely difficult to predict actual motion characteristics when different types of motion are required since the stability and transient response of pneumatic servo are highly nonlinear: being position dependent, velocity/acceleration dependent and direction dependent. In their research, a simplified linear model was used for guidance in interpreting the behavior of pneumatic servo rather than as an exact design tool.

In (Uebing et al., 1997), a new linear model for a pneumatic servo system took into account unequal piston area, charging and discharging conditions resulting from the unequal chamber pressures, and predicted the position and direction of motion dependency of the dynamic behavior. They found that the system dynamics are not only actuator displacement dependent but also motion direction dependent. Their simulation results showed that the direction dependency is even more dominant than the displacement dependency.

In his thesis (McDonell, 1996), McDonell developed a nonlinear model for a three degree of freedom pneumatic robot control system and designed a controller directly based on this nonlinear model. He developed this model by following Shearer's, Liu's and Bobrow's methodologies but made further identification of the pressure-flow characteristics of the servo valve. Experimental measurements proved that the actual pressure flow characteristics of the valve was quite different than the theoretical one described by Shearer. Therefore the curve fitting method was used to find mass flow model from the measured data in his work. Then this identified mass flow model was combined with the dynamic model of the cylinder chamber so that the nonlinear model of the whole system was completed for use in nonlinear controller design.

Nonlinear models have been presented in a number of other papers, notably in (Richer & Hurmuzlu, 2000). Their model included the effects of propagation delay and friction losses in air hoses, which can be significant between valve and actuator.

In (Wang et al., 2001), a nonlinear model for their pneumatic servo took into account the effect of residual volume associated with connecting pipes and mechanical structure and the uneven distribution of friction force.

Some efforts for analytical modeling of pneumatic actuator with on/off valves can be found. In (Kunt & Singh, 1990) Floquet Theory was applied to analyze the dynamic response of the on-off valve controlled pneumatic systems based on the linear time varying (LTV) model. In (Ye et al., 1992) two models for the pneumatic PWM solenoid valves, in which the valves were considered as on-off devices with opening and closing delays were proposed.

In (Messina et al., 2005) an extensive set of experiments and a related mathematical model investigating the dynamics of pneumatic actuators controlled by on/off solenoid valves, whose opening and closing time response based on a PWM technique was presented. The analytical-experimental comparisons showed the ability of the theoretical model to provide an accurate mean expectation of the position of the actuator less than about 2 mm for several operating and initial conditions. The presented theoretical model dealing with a non-linear and highly transient dynamics should be considered as an attempt aimed at providing a valuable tool for designing control strategies without the need for expensive physical models.

In (Taghizadeh et al., 2009a) a nonlinear dynamic model of a PWM-driven pneumatic fast switching valve was presented. The electro-magnetic, mechanical and fluid sub-systems of the valve were investigated including their interactions. Unknown parameters were identified using direct search optimization and model validation by comparing the simulated and measured current curves. In order to use the model in PWM control applications, a simplification strategy was also

proposed and a static model was obtained between the PWM duty cycle and the moving average of the spool position.

2.3 Control of pneumatic systems

A review of the main studies on the control methods in the field of pneumatic position servo systems is given in this chapter. The review will begin on the studies, where proportional or servo-valves have been used to control a pneumatic actuator, and then continues to studies where on/off valves have been applied to servo-pneumatic systems.

2.3.1 Servo/proportional valve controlled pneumatic systems

Conventional linear control approaches, e.g. PID-control – and, by extension, P, PI and PD control, are very popular in industrial applications due to their simple architecture, easy tuning, cheap and excellent performance. However, it is very difficult to determine the appropriate PID gains in case of nonlinear and unknown controlled systems. Typically, their use has been limited to simple pneumatic positioning and point-to-point systems and even then a reasonable performance requires modifications to the control law. In tracking-type servo systems linear control approaches are not typically used as they perform poorly and more advanced control approaches are required to obtain adequate performance. However, note that the linear controllers are often used as a reference for new control strategies.

Many linear control strategies have been proposed for servo-pneumatic systems such as PVA state feedback (Weston et al., 1984), (Moore et al., 1985 & 1986), (Brun et al.,1999), PD and PD + pressure feedback (Liu & Bobrow, 1988), PVA with genetic algorithms (Jeon et al., 1998), PD with gain tuning (Fok & Ong, 1999), PID with acceleration feedback (Wang et al., 1999). In these works it was stated that velocity and acceleration/pressure feedback control can improve both dynamic and static performance dramatically and that pneumatic systems are practical for use in servo-control applications. Traditional linear control approaches have been studied also in (Pu & Weston, 1988), (Pu et al., 1992).

Feedback linearization with PID controller has been studied in the works (Kimura et al., 1995 & 1997) and (Lee et al., 2002). In (Richard & Scavarda, 1996), (Brun et al.,1999), (Brun et al., 2002) and (Wang et al., 2007), (Perondi et al., 2010), a control law consisting of an input-output linearization via a static nonlinear state feedback was proposed. More recently, in (Sobczyk et al., 2012) a feedback linearization with friction compensation applied to a pneumatic positioning system was proposed.

In order to reduce the effects of nonlinearities (friction, compressibility, etc.) some adaptive control strategies with traditional linear control approaches have been proposed; adaptive pole

placement compensator (Bobrow & Jabbari, 1991), (McDonell & Bobrow, 1993), PID with self-tuning control (STC) (Shih & Tseng, 1994), adaptive PI control (Hamiti et al., 1996), self-tuning P-controller (Richardson et al., 2001), fuzzy PID gain scheduling (Situm et al., 2004).

Variable structure control (VSC) and its' derivative sliding mode control (SMC) has gained a lot of attention also in pneumatic servo systems. In (Surgenor et al., 1995), a proposed continuous sliding mode control (CSLM) did not improve the accuracy obviously but was indeed more robust than PVA and PΔP (proportional plus differential pressure) when the loading conditions change.

In (Song, 1997), a robust SMC scheme for pneumatic servo systems with two proportional pressure servo valves was presented. The experimental results demonstrated good tracking performance (< 2mm) and reasonable steady state error (0.2 mm). This controller was robust to mass load change from 30 kg to 100 kg.

In (Smaoui et al., 2004) a 2^{nd} order SMC approach with the main objective to demonstrate that the undesired chattering phenomenon can be avoided while retaining the same robustness of first order sliding mode control. In (Smaoui et al., 2006), the same authors presented a design of multi-input/multi-output (MIMO) back-stepping and sliding mode control laws for a pneumatic servo system. Experimental results showed that satisfactory control performance was obtained by both control laws resulting in an average steady state position error about 0.1 mm. They claimed that the back-stepping controller suits better for controlling a pneumatic system due to undesirable chattering effect in SMC approach.

In (Ning & Bone, 2005) and (Ning & Bone, 2007), three control algorithms; PVA+FF+DZC, linear SMC, and nonlinear SMC were compared. The results indicated that SMC approaches could provide significantly better performance than PVA+FF+DZC and the tracking control performance was stated to be better than those previously reported for similar systems. The SMC based on nonlinear plant model improved the tracking performance by 18 % compared to linear approach.

In (Tsai & Huang, 2008), the proposed multiple-surface sliding controller (MSSC) was able to give good performance regardless of the uncertainties and time-varying payload.

In (Meng et al., 2013), the proposed adaptive robust trajectory tracking control based on sliding mode approach was able to effectively compensate the nonlinearities and parametric uncertainties present in the pneumatic servo system.

VSC or SMC for pneumatic servo systems have been studied also in (Tang & Walker, 1995), (Pandian et al., 1997 & 2000), (Richer & Hurmuzlu, 2000a & 2000b), (Chiang et al., 2005), (Chen et al. 2009).

In (Rao & Bone, 2008), a new modeling approach and a novel multiple-input-single-output (MISO) nonlinear position control law was designed using the back-stepping methodology.

Maximum tracking errors of ± 0.5 mm for a 1-Hz sine wave trajectory, and steady state errors within ± 0.05 mm for an S-curve trajectory were achieved.

Since 1990's fuzzy control and neural network control with pneumatic servo systems have been studied by many researchers such as (Matsukuma, et al., 1997), (Song, et al., 1997), (Tanaka et al., 1998), (Schulte & Hahn, 2004), (Kaitwanidvilai & Parnichkun, 2005). The most important advantage of these strategies is that they do not need any mathematical model of the system being suitable for controlling highly nonlinear and time-variant systems. Quite often fuzzy and neural network approaches have been used to adapt and tune the controller gains of traditional linear controllers such as PID or to identify model parameters online.

2.3.2 On/Off -valve controlled pneumatic systems

Servo-pneumatic systems are usually realized by the continuously acting servo or proportional valves. In order to decrease the cost of the system, a considerable amount of research has been performed to develop inexpensive servo-pneumatic systems using on/off solenoid valves with pulse-width modulation (PWM) technique. Pulse width modulation offers considerable advantages in the control of DC motors and hydraulic servos as it can reduce the effects of nonlinearities such as hysteresis, threshold, stick friction, dead-zone and null-shift, and improve the system reliability and performance. Previous efforts have shown the potential of PWM-controlled pneumatics of which the main works are presented next.

The early works by (Morita et al., 1985), (Noritsugu, 1985) and (Noritsugu, 1987a & 1987b) showed the potential of the use of on/off valves with the PWM –strategy in pneumatic systems. Linear control approaches, such as state feedback control (Marchant et al., 1988), a dual-mode PVΔP (Linnett & Smith, 1989), a dual-loop (PI, PD) (Lai et al., 1990 & 1992) provided reasonable steady state accuracies (< 1 mm) for pneumatic positioning.

The most significant linear control approach was presented in (Van Varseveld & Bone, 1997) where a discrete PID controller with added friction compensation and position feed-forward term was proposed. The results indicated a worst case steady-state accuracy of 0.21 mm and S-curve tracking error less than 2.0 mm.

In (Gentile & Giannoccaro, 2002) a novel pulse-width modulation algorithm with a PI controller and position feed-forward component for an on/off solenoid valve controlled positioning system was applied. They stated that the performance of the system was comparable to those achieved by other researchers using servo valves.

Fuzzy state (position, velocity, acceleration) feedback controller was studied in (Choi et al., 1995) and fuzzy PD controller in (Wang et al., 1996) and in (Shih & Hwang, 1997). In (Shih & Ma,

1998b), a controller which combined the fuzzy logic with neural network (NN) for a PWM pneumatic positioning system was studied. Experimental results showed that the system performance was good with steady state error within ±0.1 mm. In (Shih & Lee, 1998), the same idea was used with a pneumatic positioning system controlled by servo valve and by on/off valves separately. Experimental results showed good system performance with the steady state error ±0.08 mm for on/off control and ±0.05 mm for servo valve control.

In (Paul et al., 1994) a reduced sliding mode switching controller based on a "reduced-order" nonlinear model neglecting the major nonlinearities was presented. When the position error was close to zero, the system switched the sliding mode control to proportional control.

In (Shih & Ma, 1998a), a sliding mode control with the modified differential PWM method to eliminate the dead-zone was proposed. The experimental results showed that the steady state error was distributed from -0.07 mm to +0.03 mm.

In (Barth et al., 2002 & 2003), a control design methodology for systems characterized by discontinuous (i.e. PWM switching) dynamics was presented. The proposed control methodology transforms a discontinuous switching model into a linear continuous equivalent model enabling the use of conventional control designs.

In (Shen et al., 2006a) a method for nonlinear model based PWM control of a pneumatic servo actuator based on the full nonlinear model of such systems was presented. Specifically, their paper extended the authors' previously published averaging techniques to nonlinear systems. The nonlinear averaging technique was then utilized as the basis for the development of a PWM-based sliding mode approach (Shen et al., 2006b) to the control of pneumatic servo systems.

In (Ahn & Yokota, 2005), a novel valve pulsing algorithm was developed that allowed the use of multiple on/off solenoid valves in place of costly servo valves. A comparison between the system response of the standard PWM technique and that of the modified PWM technique with a PVA state feedback controller showed that control performance was significantly increased.

In (Song & Liu, 2006) two effective algorithms for improving the performance of a pneumatic actuator were studied. PVA control with friction compensation and a CARIMA model referenced adaptive generalized predictive control (AGPC) to overcome time delay problem were presented. The experimental results of the proposed approaches were impressive for both the steady state and dynamic tracking.

In (Nguyen et al., 2007) a sliding mode controller using four low-cost solenoid valves without PWM strategy was proposed. The control law has an energy-saving mode that saves electrical power, reduces chattering, and prolongs the valve's life. Their results showed that the tracking performance was not significantly degraded without PWM approach.

In (Taghizadeh et al., 2009a), simple P- and PD-controller for a pneumatic cylinder with only one fast switching valve were compared. Despite the internal nonlinearities, the proposed pneumatic circuit lead to a quasi-linear input-output relation between duty cycle and cylinder piston velocity. Experimental results indicated that sufficient tracking performances were achieved with the PD-controller. In (Taghizadeh et al., 2009b), the pneumatic circuit with two fast switching valves was modified such that an identical PWM signal was demanded by both valves. A simple PWM algorithm was applied to compensate the dead zones in the relation between the duty cycle input and the valve flow output. Closed-loop tests were implemented and high tracking performance for frequencies up to 5 Hz were obtained. In (Taghizadeh et al., 2009c), a multi-model PD-controller was realized by identifying linear model for several constant loads and PD-controller tuned for each case. Then, a switching algorithm was applied which determined the best model and selected the corresponding controller in any load condition. Experimental results indicated the high performances of the multi-model controller under variable load conditions.

PWM-pneumatics has also been applied to control a clutch actuator for heavy duty trucks. The most interesting works in that field are back-stepping control (Sande et al., 2007), (Langjord et al., 2008), dual-mode switching controller (Langjord et al., 2009) and NMPC (nonlinear model predictive) controller (Grancharova & Johansen, 2011).

2.3.3 Summary of control approaches in pneumatic servo systems

Many control strategies have been applied to pneumatic servo systems. A direct comparison of control approaches is difficult as the system configurations and experimental conditions can be very different. In order to make the comparison easier, Tables 2.1-2.4 summarize the main information of the previous studies of pneumatic control systems. The tables include only the works where experimental results have been reliably given. The works with only simulation results given are not included. The tables include information of the used actuator and valve, the control strategy, the payload, reference position (control objective) and the control performance in terms of steady-state and tracking error. Other performance indicators such as response and settling time, stability, robustness, are not included, but they can be found in the corresponding works.

Most of the previous studies have concentrated only on the performance of the system for point-to-point control. In Table 2.1, the works where servo or proportional valve has been used to control the actuator for positioning tasks are presented. In Table 2.2, the works with on/off valves for positioning tasks are presented, respectively. For most of the studies with servo valves, the steady state position accuracy that the system could achieve was ±0.2 to ±0.1 mm. The lowest steady state error reported in the literature was ±0.02 mm. The lowest steady state error reported

with on/off valves was even better ±0.01 mm. It is interesting to note, that in positioning tasks the performance of the systems with on/off valves are comparable to those with servo/proportional valves. Also, it should be noted, that linear control strategies and their modifications can be used in positioning tasks to provide reasonable steady state accuracy. However, the lowest steady state errors can be obtained using nonlinear control strategies.

Many of the previous studies have concentrated also on the performance of the system for trajectory tracking control. The tracking of arbitrary movement profiles is important especially for applications in robotics. In Table 2.3, the works where servo or proportional valve has been used to control the actuator for tracking tasks are presented. Table 2.4 gathers the works with on/off valves for tracking tasks, respectively. It can be clearly seen that the conventional linear control approaches perform poorly in tracking control. Note also, that sliding mode control (SMC) approaches have been very popular resulting in good tracking performance. With servo/proportional valves the best tracking accuracy reported has been 0.36 % of the total motion range. In overall, significantly better tracking accuracies have been obtained with servo/proportional valves than with on/off valves. With on/off valves the best tracking accuracy reported has been 2 % of the total motion range.

Positioning task with proportional or servo valves						
Author	**Actuator type & size**	**Valve**	**Control strategy**	**Payload [kg]**	**Reference position**	**Steady state error**
Tsai & Huang, 2008	Symmetric (40 / - /1000)	5/3 - servo	Multiple-surface SMC	12-18 kg	Step 500 mm	sse < 0.02 mm
Rao & Bone, 2008	Asymmetric (9.5/3.2 /25.4)	4 x 2/2-proportional valve	MISO backstepping	1.5 kg	S-curve: 20 mm	sse < 0.05 mm
Shih & Lee, 1998	Rodless cylinder	Servo valve	Fuzzy control	Unknown	Step 150 mm	sse < 0.05 mm
Tanaka, et al., 1998	Symmetric, (55/22 /170)	2 x prop. pressure control valve	MRAC + NN	Unknown	Step 50 mm	sse < 0.08 mm
Chiang, et al. , 2005	Symmetric (50/20/ 200)	5/3 servo valve	Self-tuning adaptive + discete VSC	2 kg	Step 180 mm	sse < 0.1 mm
Jeon et al., 1998	Rodless (21.6/ - / 600)	2 x 3/2-servo valve	PVA with genetic algorithm	3 kg	Step 300 mm	sse < 0.1 mm
Song, et al., 1997	Asym.,low frict, (63/ ?/ 300)	2 x prop. pressure control valve	NN I-PD	30 kg	Step 10 mm	sse < 0.1 mm
Weston, et al., 1984	Asymmetric, (25/10/400)	5/3-servo valve	PVA	No payload	Step 50 mm	sse < 0.1 mm
Surgenor et al., 1995	Asymmetric, (25/10/120)	5/3-servo valve	SMC	2.2 kg	Step 50 mm	sse < 0.2 mm
Brun et al., 1998	Asymm. (32 / 20 / 500)	2 x 3/2-servo valve	State feedback (fixed gain)	17 kg	Step 50 mm	sse < 0.2 mm
Brun et al., 1998	Asymm. (32 / 20 / 500)	2 x 3/2-servo valve	State Feedback linearization	17 kg	Step 50 mm	sse < 0.2 mm
Song, 1997	Asym.,low-frict, (63 / ? /300)	2 x prop. pressure control valve	SMC	30-100 kg	50 mm, cont. Profile	sse < 0.2 mm
Fok & Ong, 1999	Rodless, (40 / - / 1800)	5/3 - servo valve	PD + gain tuning methodology	40-80kg	Step 1500 mm	sse < 0.3 mm
Marchant_1988	Cylinder	5-port proportional valve with 50 Hz PWM	State feedback with pole placement	No payload	Step -80..125 mm	sse < 0.5 mm
Hamiti, et al., 1996	Asymmetric, (40/16/250)	5/3 -servo	Autotuning PI	0.4 - 12 kg	Step 150 mm	sse < 0.5 mm
Chen et al. 2009	Asym. (? / ? / ?)	5/3 -servo	Integral SMC	Unknown	Step: 150 mm	sse < 0.5 mm
Chen et al. 2009	Asym. (? / ? / ?)	5/3 -servo	Fuzzy control	Unknown	Step: 150 mm	sse < 0.5 mm
Shih & Tseng, 1995	Asymmetric (45/12/200)	5/3 - servo	PID optimal control	Unknown	Step 150 mm	sse < 1.9 mm

Table 2-1: Summary of pneumatic servo positioning with servo/proportional valves

Positioning task with on/off valves						
Author	Actuator type & size	Valve	Control strategy	Payload [kg]	Reference position	Steady state error
Shih & Ma, 1998	Rodless cylinder	2 x 3/2 -on/off	SMC with modified differential PWM	Unknown	Step 150 mm	sse < 0.01 mm
Shih & Ma, 1998	Rodless cylinder	2 x 3/2 -on/off	Fuzzy control + modified diff. PWM	Unknown	Step 150 mm	sse < 0.075 mm
Shih & Lee, 1998	Rodless cylinder	On/off valve	Fuzzy PD control	Unknown	Step 150 mm	sse < 0.08 mm
Wang, et al., 1996	Asymmetric, (25/10 /300)	6 x 3/2- on/off	Hybrid (fuzzy PD, PCM and PWM)	No payload	Steps 50-300 mm	Ave. RMSE = 0.08 mm
Nguyen et al., 2007	Rodless, (25.4 / - /610)	4 x 2/2 on/off valve	SMC without PWM	2 kg	Step : -20..20 mm	sse < 0.1 mm
Choi, et al., 1995	Asymmetric	On/off valves	State feedback PVA + fuzzy logic	Unknown	Step ?	sse < 0.1 mm
Ahn & Yokota, 2005	Rodless, (32 / - / 1000)	8 x 2/2 -on/off	PVA + mod.PWM algorithm+LVQNN	No payload, 10/20/30 kg	Step 600 mm	sse < 0.2 mm 30 kg: sse < 0.4 mm
Van Varseveld & Bone, 1998	Asymm., low-frict., (27/ ? /152)	2 x 3/2 on/off valve	PID+friction comp + pos. FF	0.94 kg	S-curve :64 mm	sse < 0.21 mm
Song &Liu, 2006	Asymmetric, (27 / ? / 100)	2 x 3/2 -on/off with PWM	AGPC (model ref. adaptive predictive	Unknown	Step: 50 mm	sse < 0.25 mm
Song &Liu, 2006	Asymmetric, (27 / ? / 100)	2 x on/off valves with PWM	PVA + friction compensation	Unknown	Step: 50 mm	sse < 0.28 mm
Gentile et al, 2002	Asymmetric, (25/? /100)	2 x 3/2 -on/off	PI+FF (with PWM)	0.25 - 1.5 kg	Ramp 60 mm	sse < 0.33 mm
Linett & Smith, 1989	Symm.,low-frict., (64 / ? / 295)	2 x 2-way on/off valves	Dual mode PV + differential pressure	37 kg	Step 300 mm	sse < 1 mm
Paul, et al., 1994	Symm,low fric., (25.4/ ?/ 305)	2 x 2/2 -on/off	Reduced order SMC	No payload	Step 126 mm	sse < 1 mm
Tang & Walker, 1995	Symmetric, 32 mm	On/off valves	VSC	Unknown	Step 100 mm	sse < 5 mm

Table 2-2: Summary of pneumatic servo positioning with on/off valves

Tracking task with proportional or servo valves						
Author	Actuator type & size	Valve	Control strategy	Payload [kg]	Reference position	Performance (te = tracking error [mm], RMSE [mm]
Bone & Ning, 2007	Rodless, (25 / - / 600)	5-3-servo valve	SMC based on nonlinear model	5.8kg	Sine: 70 mm, 0.25 Hz Sine: 70 mm, 1.0 Hz	te < 0.5 **(0.36 %)**,RMSE: 0.194 (0.15%) - , RMSE: 0.62 (0.44%),
Smaoui, et al., 2006	Asymmetric, (32 / 20 / 500)	2 x 3/2-proportional	MIMO SMC	17 kg	250 mm, cont. profile	te < 1.27 **(0.51 %)**
Ning & Bone, 2005	Rodless, (25 / - / 600)	5/3-servo valve	SMC based on linear model	5.8kg	Sine: 70 mm, 0.25 Hz Sine: 70 mm, 1.0 Hz	te < 0.75 **(0.55%)**, RMSE: 0.34 (0.25%), te < 2.4 (1.7 %), RMSE:0.75 (0.54%),
Smaoui, et al., 2006	Asymmetric, (32 / 20 / 500)	2 x 3/2-proportional	MIMO backstepping	17 kg	250 mm, cont. profile	te < 1,5 mm **(0.6 %)**
Meng et al. 2013	Rodless, (25/ - / 500)	5/3-proportional	Adaptive SMC	1.88 kg	Sine:125 mm, 0.25 Hz Sine:125 mm, 0.5 Hz Sine:125 mm, 0.75Hz	te < 1.5 **(0.6 %)**, RMSE: 0.78 (0.32 %) te < 2.9 (1.2 %), RMSE: 1.4 (0.56 %) te < 4.6 (1.9 %), RMSE: 3.2 (1.3 %)
Brun et al., 1998	Asymm. (32 / 20 / 500)	2 x 3/2-servo valve	State Feedback linearization	17 kg	Ramp 400 mm (in 2s)	te < 3 **(0.75 %)**
Brun et al., 1998	Asymm. (32 / 20 / 500)	2 x 3/2-servo valve	State feedback (fixed gain)	17 kg	Ramp 400 mm (in 2s)	te < 4 **(1 %)**
Chen et al. 2009	Asym. (? / ? / ?)	5/3 -servo	Integral SMC	Unknown	Sine: 200 mm, 0.1 Hz	te < 5 **(1.25 %)**
Ning & Bone, 2005	Rodless, (25/ - /600)	5/3-servo valve	PVA+FF+DZC	5.8kg	Sine: 70 mm, 0.25 Hz Sine: 70 mm, 1.0 Hz	te < 1.7 **(1.3 %)** , RMSE: 0.74 (0.53 %), te < 5.0 (3.6 %), RMSE: 1.74 (1.25 %),
Rao & Bone, 2008	Asymmetric (9.5/3.2 /25.4)	4 x 2/2-proportional	MISO backstepping	1.5 kg	S-curve: 20mm Sine: 7.5 mm, 1.0 Hz	te < 0.3 **(1.5 %)**, RMSE: 0.074 (0.37 %) te < 0.5 (3.3 %) , RMSE=0.136 (1%),
Carneiro et al. 2011	Asym. (32/ 16 / 400)	2x 5/3 -servo valves	VSC	2.69-kg	Sine: 160 mm, 1.0 Hz	te < 8 **(2.5 %)**
Tsai & Huang, 2008	Symmetric (40 / - /1000)	5/3 - servo	Multiple-surface SMC	12-18 kg	Sine: 200 mm, 0.1 Hz Sine: 200 mm, 0.5Hz	te < 12.5 **(3.1 %)** te < 50 (12.5 %)
Song, 1997	Asym.,low-frict, (63 / ? /300)	2 x prop. pressure control	SMC	30-100 kg	50 mm, cont. profile	te < 2.0 **(4 %)**
Richardson et al, 2001	Asym., low frict. (18/ ? /38)	2 x prop. pressure control	P-control + self-tuning	4.5 kg	Sine: 80 mm, 0.04 Hz	te < 8.0 **(5 %)**
Lee et al. 2002	Rodless, (25/ - / 200)	5/3-servo	Cascaded PID with friction comp.	2.7 kg	Sine: 70 mm, 0.5 Hz	te < 15.6 **(11%)** , RMSE = 7.3 (5.2%)
Carneiro et al. 2011	Asym. (32/ 16 / 400)	2x 5/3 -servo valves	PID	2.69 kg	Sine: 160 mm, 1.0 Hz	te < 65 **(20 %)**
Carneiro et al. 2011	Asym. (32/ 16 / 400)	2x 5/3 -servo valves	State feedback	2.69 kg	Sine: 160 mm, 1.0 Hz	te < 70 **(22 %)**

Table 2-3: Summary of pneumatic servo tracking with servo/proportional valves

Tracking task with on/off valves						
Author	**Actuator type & size**	**Valve**	**Control strategy**	**Payload [kg]**	**Reference position**	**Performance (te = tracking error [mm], RMSE [mm]**
Taghizadeh et al., 2009	Asymmetric, (25/ ? /125)	3/2 -on/off valve	PV + feedback linearization	No payload	Sine: 20 mm, 1.0 Hz Sine: 20 mm, 2.0 Hz	te < 0.7 **(2 %)** te < 1.5 (4 %)
Van Varseveld & Bone, 1998	Asymm., low-frict., (27/ ? /152)	2 x 3/2 on/off valve	PID+friction comp + pos. FF	0.94 kg	S-curve :64 mm	te < 2.0 **(3.1 %)**
Song &Liu, 2006	Asymmetric, (27 / ? / 100)	2 x 3/2 -on/off with PWM	AGPC (model ref. adaptive predictive	Unknown	Sine : 38 mm, 0.25 Hz	te < 3.27 **(4.4 %)**, av.error: 0.76
Shen et al., 2006	Asymmetric, 27/6.4/100)	2 x 3/2 on/off valve	SMC+PWM + nonlinear averaging	10 kg	Sine: 20 mm, 0.25 Hz Sine : 20 mm, 0.5 Hz Sine :20 mm, 1.0 Hz	te < 2 **(5 %),** te < 3.5 (9 %) te < 4 (10 %)
Nguyen et al., 2007	Rodless, (25.4 / - /610)	4 x 2/2 on/off valve	SMC without PWM	2 kg	Sine: 20 mm, 0.5 Hz	te < 2.5 **(6.3 %)**
Gentile et al, 2002	Asymmetric, (25/? /100)	2 x 3/2 -on/off	PI+FF (with PWM)	0.25 - 1.5 kg	Ramp 60 mm	te < 4 **(6.7 %)**
Song &Liu, 2006	Asymmetric, (27 / ? / 100)	2 x on/off valves with PWM	PVA + friction compensation	Unknown	Sine : 38 mm, 0.25 Hz	te < 6.29 **(8.4 %)** , av.error: 2.78

Table 2-4: Summary of pneumatic servo tracking with on/off valves

3. PNEUMATIC MUSCLE ACTUATORS (PMAs)

3.1 Concept and operation

Pneumatic muscle actuators (PMAs) are contractile or extensional devices operated by pressurized air filling a pneumatic bladder (Schulte, 1961). The most traditional version of PMAs is the McKibben actuator which consists of an expandable internal bladder (an elastic tube) surrounded by a braided sleeving (Fig. 3-1) (Chou & Hannaford, 1996). The braided shell (Nylon, Kevlar) is placed on the inner tube in a manner that an angle is formed between the braids and the longitudinal axis of the actuator. The angle and initial dimensions of the inner tube and braided net as well as the used materials affect critically the actuator's characteristics. When the internal bladder is pressurized, it expands in a balloon-like manner against the braided shell that acts to constrain the expansion in order to maintain a cylindrical shape. As the volume of the internal bladder increases due to the increase in pressure, the actuator shortens/contracts and produces force on a coupled mechanical load. The generated force depends on the applied pressure and the muscle's rate of contraction resulting in highly nonlinear characteristics. Due to the unidirectional operation a paired or antagonistic setup (Fig. 3-2) or other return force is needed to generate bidirectional force or movement.

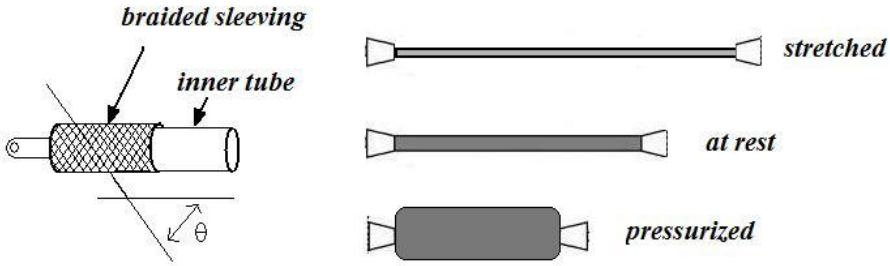

Figure 3-1: Structure and operating principle of a typical pneumatic muscle actuator

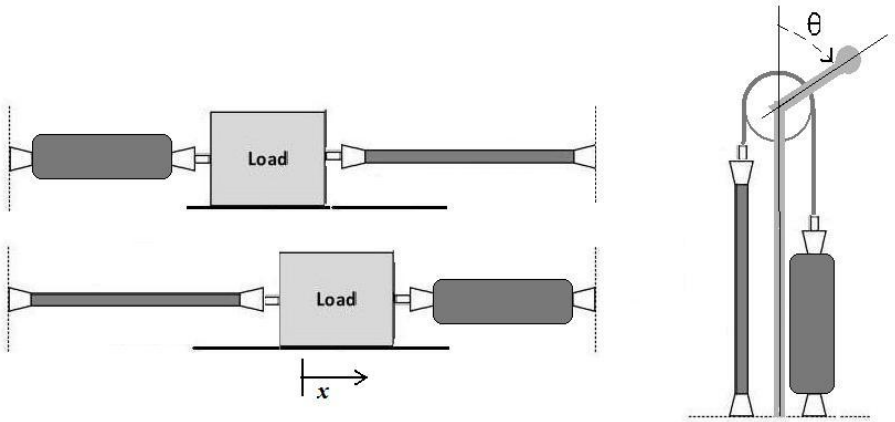

Figure 3-2: Antagonistic set-up with pneumatic muscle actuators

3.2 History

The history of the muscle actuator began in 1940, when Pierce (Pierce, 1940) patented an application referred to as the "Expansible Cover" that is the earliest example of braided pneumatic actuators. The application was proposed to be used in the coal mining industry instead of dynamite. Due to the weave used in the construction, the pressurized air inside the device caused an expansion of the cover applying a braking force to the coal. Although Pierce observed the longitudinal contraction of the device it was until 1949 when De Haven (De Haven, 1949) obtained a patent for a "Tensioning Device For Providing a Linear Pull". In De Haven's device an expandable inner tube was surrounded by a double helically woven tube. The device reached a maximum force of approximately 7000 N and was capable of contracting by 30 % when pressurized to 3 MPa. The actuator was proposed for tension pilot safety belts upon crashing. The operation of the device was based on the sudden ignition of gunpowder inside the device. It released the compressed gas providing an activation time of only 2-3 ms.

By 1958, Gaylord (Gaylord, 1958) patented a "Fluid Actuated Motor System and Stroking Device" that based essentially on the same principle, but having an external power source. Gaylord was first to analyze the system mathematically providing the equation for the force generated by the muscle actuator motor system.

According to (Baldwin, 1969), the term "McKibben Muscle" was given for the device by the American atomic physicist Joseph L. McKibben who proposed using the actuator in the area of Prosthetics and Orthotics in the late 1950's. The invention was marketed as an orthopaedic device fastening on the arm or the forearm and serving as a substitute for the weak musculature as shown in Figure 3-3.

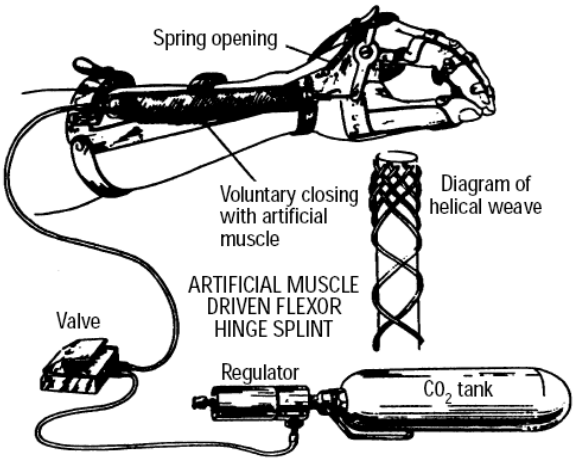

Figure 3-3: Original use of McKibben muscle as forearm musculature orthotics to open/close the handicapped hand fingers (Tondu & Lopez, 2000)

In 1961, Schulte (Schulte, 1961) published a paper containing details of the use of the McKibben muscle and much of the mathematical analysis previously included in Gaylord's patent. At the time, the power/weight performance of the actuator and the inherent compliance were seen as positive features but the complexity of control remained a problem and development of the actuator was discontinued.

Interest in alternative pneumatic systems increased in the 1980's due to improvements in control techniques. Bridgestone started to develop a commercial version of pneumatic muscle which was called "Rubbertuator" (Takagi, 1986). The company developed and marketed two industrial robots RASC and Soft Arm (Inoue, 1987) based on the Rubbertuator actuators. Despite some use of these robots in practical applications the work on the Rubbertuator stopped by the 1990's. However, the potential of pneumatic muscle for mechatronic applications was already recognized by several research groups that continued the development and progressing of the technology.

Nowadays, the only commercially available muscle actuators are the Air Muscle provided by Shadow Robot Company (Shadow Robot Company, 2012) and Fluidic Muscle by Festo (Festo, 2002). The Air Muscle has been very popular among research institutes, but for industrial usage the Fluidic Muscle (MAS) (Fig. 3-4) suites better. The Fluidic Muscle has all of the same operational principles as the traditional McKibben muscle, but possesses an important characteristic of having the fibre mesh embedded inside the expandable bladder, much like fibre or metal reinforcements are embedded in a tire or high-pressure hose. Due to its construction, the Festo actuator possesses a very long life period of at least 10 million switching cycles. In addition, the actuator has a significant restoring force which will thus decrease the exhaust time of the actuator, resulting in an increase in bandwidth and decreased hysteresis (Festo, 2002).

Figure 3-4: Festo Fluidic Muscle (Festo, 2002)

3.3 Properties

The specific structure of the pneumatic muscle gives the actuator a number of desirable characteristics. In the following are described the advantages of muscle actuators:

- ***Low cost***: They are quite easy to produce in a range of lengths and diameters. Pneumatic muscle actuators are significantly cheaper than pneumatic cylinders or electric drives with the same maximum force.
- ***Powerful***: Due to light structure the actuator has an exceptionally high power and force to weight/volume ratios. Especially, when fully stretched, the muscle actuator is capable of producing an incredibly high force. Compared to conventional actuators (pneumatic, as well as hydraulic and electric), PMAs excel in this respect (Plettenburg, 2005). In application where total amount of mass is highly critical, PMAs might be an alternative.
- ***Wide range of working environments****:* Pneumatic muscle actuators can be applied in a very dusty, humid or wet environment. This is contradictory to conventional (electrical, mechanical or pneumatic) actuators, which must be kept clean and dry.
- ***Flexibility***: Muscle actuator can be operated when twisted axially, bent around a corner, and need no precise aligning.
- ***Compliance:*** Muscle actuator systems are inherently compliant as they "give in" without increasing the force in the actuation when a force is exerted on the actuator. This is an important feature when the muscle actuator is used in robotic applications interacting with humans, or when delicate operations have to be carried out.
- ***Smooth operation:*** Muscle actuator provides a smooth and natural movement as it has an immediate response and does not have stick friction, which is a significant problem with pneumatic cylinders.
- ***Damping:*** Muscles are also self-dampening when contracting (speed of motion tends to zero), and their flexible material makes them inherently cushioned when extending.
- ***Similarity to biological muscles:*** PMAs show great similarity with biological muscles. In (Klute et al., 1999) a comparison, based on experiments, between pneumatic and biological muscles was made. In (Klute et al., 2002), the PMAs were compared to the Hill model, a model describing the behaviour of biological muscles. The similarity was based upon the length – stiffness relation of the muscles. The length – damping relation was different for McKibben muscles and biological muscles; the damping in McKibben muscles was much lower. Also compared with natural muscle PMA can provide up to 10 times more force for a similar cross-sectional area (Caldwell et al., 2000).

Obviously these attributes make pneumatic muscle actuators an interesting option for use in many applications but as with conventional systems there are also some disadvantages:

- ***Highly nonlinear:*** The major disadvantage of PMAs, is that the relations defining its behaviour are nonlinear. Both the stiffness and damping depend in a nonlinear manner on the actual muscle length and the pressure.
- ***Compliance:*** The compliance is a disadvantage from control theory point of view. A model describing the actuator behaviour is required in order to have the actuator generating a required output force.
- ***Hysteresis:*** PMAs suffer from hysteresis due to friction between the tube and the braid and between nylon fibres of the braid.
- ***Short stroke:*** PMAs can provide a maximum contraction/stroke of approximately 30 % of its nominal length. Thus, longer strokes will need longer muscles.
- ***Low bandwidth:*** The bandwidth (less than 5 Hz) is often considered to be too low for practical success in many robotic applications.
- ***Short fatigue life:*** In some cases, the fatigue life of the PMA has been considered to be too short for practical applications (Klute & Hannaford, 1998) (Kingsley & Quinn, 2002). However, the Festo Fluidic Muscle makes an exception (Festo, 2002).

Due to disadvantages, especially the highly nonlinear characteristics, accurate control of the PMAs has been very difficult to obtain. In addition, a different working principle compared to traditional pneumatic cylinder actuator has prevented the breakthrough of muscle actuator in the area of industrial applications. The main applications have been restricted in academic use for robotic applications.

3.4 Modeling

As with all actuation systems, effective design with pneumatic muscle actuators relies on being able to accurately model and predict the forces that will be generated under any operating conditions. In developing a static force model of the muscle, the main approach has been based on energy modelling (Chou & Hannaford, 1996), (Tondu & Lopez, 2000). The approach considers virtual work and conservation of energy without losses providing a relationship between the actuator force, pressure and length. The key to the actuator performance is the braided structure shown in Figure 3-1, which determines the length or degree of the contraction and the diameter of the muscle through which the forces are generated. The geometric model (Fig 3-5) with the length L and the diameter D of the actuator are given by

$$L = b\cos\theta$$
$$D = \frac{b\sin\theta}{n\pi} \tag{3.1}$$

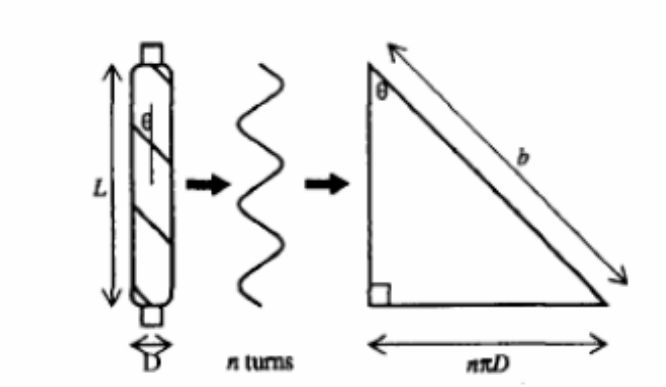

Figure 3-5: Geometric model of McKibben actuator (Chou & Hannaford, 1996)

where b is the length of one braid strand, and n is the number of times a strand encircles the muscle's circumference from end-cap to end-cap, and θ is the braid angle. Assuming ideal cylindrical shape the volume enclosed can be expressed with equation (Chou & Hannaford, 1996):

$$V = \frac{b^3}{4\pi n^2}\cos\theta\sin^2\theta \tag{3.2}$$

It should be noted that in reality the muscle shape is not ideally cylindrical resulting in an error for the volume prediction. Also, bladder thickness and muscle elasticity affect the accuracy of the model. Thickness of the bladder was considered in (Chou & Hannaford, 1996) and the shape of the muscle end-caps in (Tsagarakis & Caldwell, 2000). A comparison between theoretical muscle volume models and different measurement techniques were studied in (Varga et al, 2011). Instead of using the analytical volume model, a common approach has been to experimentally define the volume and then use a fitting function to model the volume.

Based on energy conservation and ideal cylindrical volume model, the input work W_{in} is done in the muscle actuator when pressurized air pushes the inner bladder surface. This can be described by

$$dW_{in} = \int_{S_i}(p - p_0)d\mathbf{l_i}\cdot d\mathbf{s_i} = (p - p_0)\int_{S_i} d\mathbf{l_i}\cdot d\mathbf{s_i} = p'dV \tag{3.3}$$

where p is the absolute internal pressure, p_0 is the environment pressure, p' is the relative pressure, S_{i} is the total inner surface, $d\mathbf{s_i}$ is the area vector, $d\mathbf{l_i}$ is the inner surface displacement

vector, and dV is the volume change. The output work W_{out} is done when the actuator shortens associated with the volume change, which is

$$dW_{out} = -FdL \tag{3.4}$$

where F is the axial force, and dL is the axial displacement. From the view of energy conservation with an assumption of lossless operation and without energy storage, the input work should equal the output work

$$\begin{aligned} &dW_{out} = dW_{in} \\ &\Rightarrow -FdL = p'dV \end{aligned} \tag{3.5}$$

Based on the geometric model, the generated force model for muscle type actuators given in (Chou & Hannaford, 1996) is

$$F = p'\frac{b^2}{4\pi n^2}(3\cos^2\theta - 1) \tag{3.6}$$

which is equivalent to

$$F = p'\frac{\pi D_{\max}^2}{4}(3\cos^2\theta - 1) \tag{3.7}$$

where $D_{\max}=b/n\pi$ designates the theoretical but non-physically reachable maximum muscle diameter for braid angle θ=90°, which is the same form used in (Schulte, 1961). As the braid angle is difficult to measure in practice, a more useful model was proposed by (Tondu & Lopez, 1997)

$$\begin{aligned} &F = \frac{\pi D_{\max}^2}{4} p'\left[a(1-\varepsilon)^2 - b\right] \\ &a = \frac{3}{\tan^2\theta_0} \quad b = \frac{1}{\sin^2\theta_0} \quad \varepsilon = \frac{L_0 - L}{L_0} \end{aligned} \tag{3.8}$$

with the muscle force F, the relative muscle pressure p', the initial/rest measurable braid angle θ_0 and the contraction ratio ε. However, they recognized (Tondu & Lopez, 2000) that the model given by (Eq. (3.8)) predicted forces higher than were actually being generated. They pointed out that the more a muscle contracts, the less cylindrical it becomes. The ends of the muscle take on a conic shape and to account for this systematic error, a corrective factor k was introduced. The factor amplifies the contraction ratio ε, thereby reducing the predicted force at high contraction ratios. The modified model was given by

$$F = \frac{\pi D_{\max}^2}{4} p\left[a(1-k\varepsilon)^2 - b\right], \quad 0 \le \varepsilon \le \varepsilon_{\max} \tag{3.9}$$

In (Chou & Hannaford, 1996) also a simplified and linearized force length relation was given by

$$F = k_g (p' - p_{th})(L - L_{\min}) + k_p (L - L_0) \tag{3.10}$$

with k_g a supposed constant gas stiffness, k_p an elastic constant for the shearing force, the actual length L, the minimal length L_{min} (at maximum contraction), the initial length L_0, and a threshold pressure p_{th} at which the tube and braid touch. According to the definition of minimal length, the force due to the air in the muscle is zero if the actual and the minimal length are equal. Despite adjusting the parameters, the models developed are not able to match well with the measured data of the force generated by Fluidic muscle actuator (θ_0=23.5°, L_0=0.3 m, D_0=0.01 m) used in this work as can be seen in Figure 3-6.

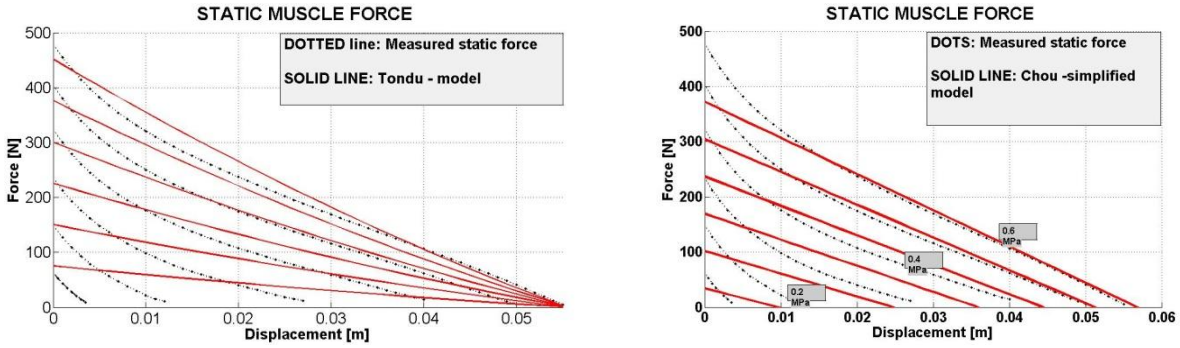

Figure 3-6: Comparison of traditional force models with measured force of Festo Fluidic Muscle

The reason for the difference between the models and actual force is most likely due to the different structure of the Festo actuator compared to traditional McKibben structure. While the pneumatic muscle of the published literature use an inner tube covered by a rhomboidal mesh, the mesh of the Festo pneumatic muscles is embedded in the tubing. As a result, hysteresis due to the friction between the mesh and the inner tube is drastically reduced in the Festo pneumatic muscles. As the traditional models are not able to predict the force produced by the Festo Fluidic muscle, a new force model was developed and discussed in Publication 1.

Due to compressibility of gas all pneumatic actuators show a compliant behaviour. In addition to this, a pneumatic muscle actuator has its dropping force to contraction curve as a second source of compliance: even if the pressure is maintained at a fixed level, the muscle acts spring-like due to the change of force with regard to length. Using equation (Eq.(3.5)), the stiffness of the muscle actuator can be expressed as (Daerden & Lefeber, 2002)

$$K = \frac{dF}{dL} = -\frac{d(p'\frac{dV}{dL})}{dL} = -\frac{dp'}{dV}\left(\frac{dV}{dL}\right)^2 - p'\frac{d^2V}{dL^2} \tag{3.11}$$

It can be clearly seen in Figure 3-7, that the stiffness of the muscle actuator is highly dependent on the displacement/contraction of the muscle. When the actuator length is close to its nominal, the actuator is in the high-stiffness region. When it contracts, the stiffness decreases being smallest at higher displacements (low-stiffness region). It is clear that the actuator system is thus more sensitive to external disturbances in the low-stiffness region than in the high-stiffness region. The pressure affects also the stiffness, as the stiffness increases as a function of pressure, being proportional with fixed displacements.

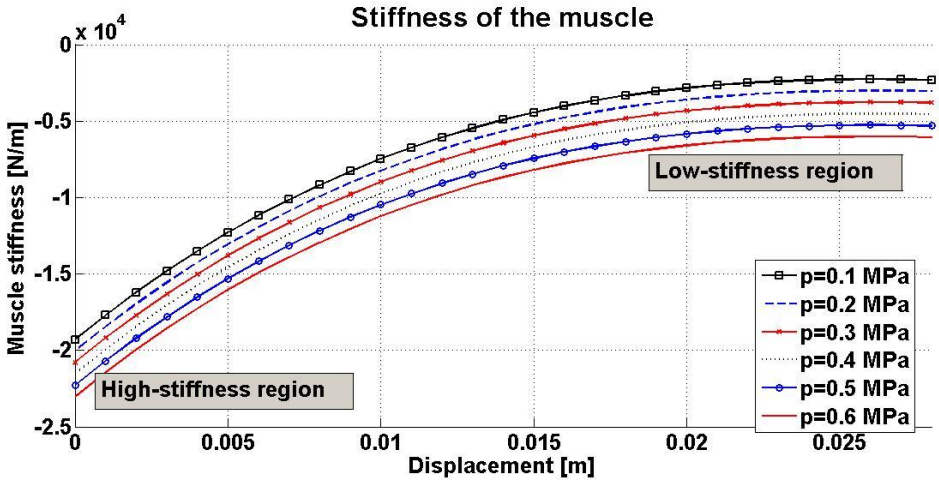

Figure 3-7: Stiffness of the Fluidic muscle actuator (θ_0=23.5°, °, L_0=0.3 m, D_0=0.01 m)

Friction has been identified as the most significant nonlinearity in servo-pneumatic actuators (Pfreundschuh et al., 1991). In the literature, a number of methods have been developed to model, analyze, and counteract the effects of friction. Despite the effort to develop an accurate model for friction in mechanism, in many applications friction may be an unknown, yet bounded, disturbance to the system. In (Wang et al., 2001) it was demonstrated, that the static friction of a pneumatic cylinder varies as a function of both the cylinder position as well as pressure in the chambers and direction of movement. This variation in friction appears to be a random variable, without an identifiable trend along the stroke. Also, the stick-slip effect (stick friction, stiction) is a serious problem and can prevent certain motions from being realized. Figure 3-8 illustrates some commonly used friction models with pneumatic actuation.

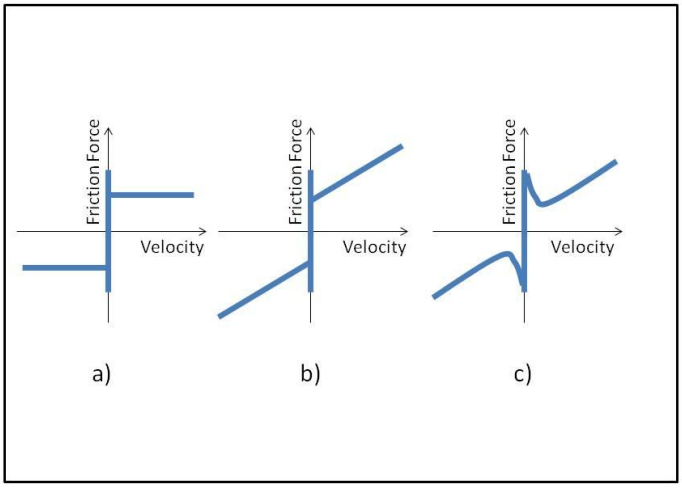

Figure 3-8: Common Friction Models: a) static + Coulomb friction, b) static + Coulomb + viscous friction, c) Stribeck friction

As pneumatic muscle actuators are single-piece devices without any sliding contacts within the actuator they are capable of providing stick-slip free operation. On the other hand, friction between braid strands and tube and between the strands themselves as well as non-elastic deformation of the diaphragm will show up as dry friction and hysteresis. Due to the friction, a threshold pressure needs to be exceeded in order to start radial diaphragm deformation and movement. Hysteresis is a complex nonlinearity with memory that complicates tracking control. In pneumatic muscle actuators, the hysteretic phenomenon was first reported in (Inoue, 1987) where it was indicated that this kind of hysteresis was caused by the inherent hysteresis of the elastic bladder, the friction between braided cords and rubber bladder, and the friction between cords themselves. These causes were also listed in (Tondu & Lopez, 2000), (Chou & Hannaford, 1996) amongst them the friction between cords being the most significant. In (Tondu & Lopez, 2000) a dry-friction model was added to the static force model in order to increase the accuracy of the static and dynamic response, but this study was limited to the assumption that hysteresis is due to only the thread-to-thread dry friction between the cords. In (Davis & Caldwell, 2006) the hysteresis was tried to capture statistically when braids friction was carefully considered. However, these studies give rise to complex problems in terms of control, since there are many parameters that are difficult to quantify. The work in (Chou & Hannaford, 1996) gave an insight into hysteretic characteristics in McKibben muscle actuator, such as quasi-rate independency, history dependency, but they did not really go further into modelling that hysteresis. They modelled it simply by adding a Coulomb friction offset that was added to and subtracted from the static force equation depending on the direction of movement. More recently hysteresis has been considered in (Van Damme et al. 2008) and (Vo-Minh

et al., 2011). In the latter work, a Maxwell-slip model used as a lumped-parametric quasi-static model to capture the force/length hysteresis of muscle actuator was proposed. The obtained model was claimed to be simple and easy to handle in terms of control.

Dynamic modeling of the pneumatic muscle actuator has been studied in (Reynolds et al., 2003) where a three-element actuator model was developed consisting of a contractile element, a spring, and a dashpot damper. In (Colbrunn et al., 2001b) the muscle actuator model consisted of parallel nonlinear spring, constant viscous damper and Coulomb friction. In (Balasubramanian et al., 2003) and (Kercher et al., 2006), the muscle dynamics has been modeled as a mass-spring-damper system with a nonlinear pressure dependent damper and nonlinear spring. As the accurate identification of the damping and viscous friction of the muscle actuator is a difficult task, the viscous friction and damping are often modelled with a constant coefficient.

3.5 Control

Due to many advantages of pneumatic muscle actuators, great research effort in the modeling and control field has been carried out in order to address the control problem of PMAs. They have been largely envisioned as an interesting alternative to hydraulic and electric actuators in many applications. In order to realize satisfactory control performance, many control strategies have been proposed to handle the effect of nonlinear factors of the pneumatic muscle actuator. This section gives an overview of previous works on the muscle actuator control.

A pioneering work by the group of Caldwell includes control schemes such as the traditional PID-controller with feed-forward term (Caldwell et al, 1993) and an adaptive controller (Caldwell, et al., 1995). The adaptive controller was applied to an antagonistic pair of McKibben muscles. In their system the flexor muscle was used for controlling the motion and the extensor used as a passive return spring limiting the actuator capabilities. Therefore, the authors considered a true antagonistic pair for which the adaptive pole placement scheme in (Medrano-Cerda et al., 1995). The authors have announced that the position regulation of the joints of their arm prototype was better than ±2°.

One major category to solve the nonlinear control problem is the combination of linear control methods with higher-level computation (adaptive, fuzzy control, etc.), which addresses the nonlinearity through modulation of control parameters. Approaches in this category include the generalized variable structure MRAC by (Nouri et al., 1994), NN PID by (Hesselroth et al., 1994) the gain scheduling approach for force regulation by (Repperger et al., 1999a & 1999b), fuzzy PD+I controller by (Chan et al., 2003), nonlinear PID controller with neural network by (Thanh & Ahn,

2006) and fuzzy PID gain scheduling control by (Situm & Herceg, 2008). Though such approaches afford a certain level of compensation for nonlinearities, a low sampling frequency of control parameters possess a potential conflict with the fast dynamics.

Variable structure control was studied by (Hamerlain, 1995) and (Repperger et al., 1998). Model-based cascaded PI controller to improve the control of humanoid arm driven by pneumatic muscle actuators was proposed in (Schröder et al., 2003). In the approaches proposed by (Carbonell et al., 2001), (Lilly, 2003) and (Lilly & Yang, 2005), a three-element actuator model developed by (Reynolds et al., 2003) was used, which consists of a contractile element, a spring, and a dashpot damper. Based on this model, in (Carbonell et al., 2001) a robust back-stepping controller, an adaptive back-stepping controller, and a sliding mode controller were developed and compared in the presence of model uncertainties and external perturbations through simulations. Ultimate boundedness was proved for the back-stepping tracking controllers and exponential stability for the sliding mode controller. The tracking was well achieved by the sliding-mode and the adaptive back-stepping controller. In (Lilly, 2003), it was stated that adaptive control technique was superior to fixed PID controller. In (Lilly & Yang, 2005), it was stated that the SMC approach was a very promising control approach for pneumatic muscle actuator, resulting in proven closed loop stability as well as bounded steady-state tracking error. The disadvantage of these papers is that the control performance was studied only by simulation without any experimental implementation.

In (Ahn & Thanh, 2004), a fast, accurate and inertial load independent pneumatic muscle manipulator was studied. The proposed learning vector quantization neural network (LVQNN) was used to recognize the weighting conditions of external inertial load and to select suitable gains of PID controller for each case. In (Ahn & Thanh, 2005a), a nonlinear PID controller with neural network was presented. The proposed controller was very effective in the accurate position control of the PAM manipulator, but also made the system more robust with respect to the change inertial load. The controller had an adaptive control capability where the control parameters were optimized via the back propagation algorithm. In order to improve the damping of the system, in (Ahn & Thanh, 2005b) a magneto-rheological brake (MRB) was equipped to the joint of the manipulator. The muscle actuators were controlled by a conventional PID controller while the MRB was controlled by a phase plane switching control method. The steady state error with respect to various loads (up to 1000 %) was reduced within ±0.05°. In (Thanh & Ahn, 2007), a new concept of phase plane switching control using a magneto-rheological brake (MRB) was proposed and applied to a 2-axis artificial muscle manipulator to improve the control performance under various external loads. They used conventional PID control for muscle actuators and novel phase plane switching control for MRB. The results showed that the proposed control algorithm was highly effective in the

tracking control of a sinusoidal trajectory, had high gain control, good control performance, fast response and strong, robust stability with respect to variation of both external loads and reference input frequency. The results also suggested that the proposed phase plane switching control algorithm using MRB was one of the most effective methods for developing a practically available, human-friendly robot by using a PAM manipulator.

In (Van Damme et al., 2007), a proxy-based sliding-mode control for a 2-DOF planar manipulator has been proposed. A proxy-based method can be seen as an extension to both conventional PID and sliding mode control. The principal advantage of the proposed control method was the increased safety for people interacting with the 2-DOF planar manipulator actuated by pleated pneumatic muscles.

An adaptive robust posture control structure for a parallel manipulator driven connected by a spherical joint to the base with three pneumatic muscles (PMDPM) each controlled by on/off valves has been presented in (Zhu, Tao, Yao, & Cao, 2008). To deal with the uncertainties effectively, an adaptive robust control strategy based on back-stepping approach was applied.

The motion control of pneumatic actuators using a flatness-based approach has been studied in several papers. The first investigations addressed hoisting applications and involved a vertical operation of the carriage using a single pneumatic muscle in (Hildebrandt et al., 2002). Then a horizontal operation of the carriage with a pair of pneumatic muscles arranged at opposite sides of this carriage was thoroughly investigated in (Aschemann & Hofer, 2004), (Aschemann & Hofer, 2005) and (Aschemann et al., 2006). Based on their previous works (Aschemann & Schindele, 2008) presented a cascaded sliding-mode control scheme for a pneumatic linear axis, where a guided carriage was driven by a nonlinear mechanism consisting of a rocker with an antagonistic pair of pneumatic muscle actuators arranged at both sides. The differential flatness of the system was exploited in combination with sliding mode techniques to stabilize the error dynamics in view of un-modelled dynamics. Experimental results showed a maximum tracking error of 3.5 mm and negligible position steady-state error. The robustness of the proposed control was shown by measurements with an almost doubled carriage mass.

In (Shen, 2010) a nonlinear model-based control of pneumatic artificial muscle servo systems, where a full nonlinear model including the flow dynamics, pressure dynamics, force dynamics and load dynamics of the system was developed. Based on the SISO model, nonlinear control approach in terms of sliding mode control was developed and implemented on an experimental system. Experimental results with sinusoidal tracking (with amplitude of 7.5 mm for a frequency range of 0.5-1.5 Hz) showed accuracies of +/- 0.5 mm to +/-1.2 mm.

There are only a few studies discussing the control of pneumatic muscle actuators with on/off valves and PWM strategy. In (Van Ham et al., 2003), a rotative joint actuated by two pneumatic muscles and controlled by an adaptive PID angle controller combined with two bang-bang pressure controllers was designed. The low-level bang-bang controller with dead-zone was claimed to be excellent pressure controller. Unfortunately, they did not provide any details of positioning accuracy of the proposed controller.

In (Sarosi et al., 2009, 2010 & 2011), a position control method based on relay type sliding mode for a robot arm driven by pneumatic muscle actuator was studied. They compared the system controlled by six 2/2 on/off valves (3 per each actuator) to the one controlled by a proportional valve. The steady state positioning error with on/off valves for a 15 mm step change was within ±0.02 mm and ±0.01 mm with proportional valve. However, the effectiveness of the system for tracking tasks neither the robustness of the system was not studied.

POSITIONING TASK WITH PNEUMATIC MUSCLE ACTUATOR SYSTEM

Author	**Muscle Actuator** (Diameter [mm]/Length [mm]), **Configuration**	Valve	Control strategy	Payload [kg]	Reference position	Performance (sse = steady state error)
Sarosi et al., 2009	2 x Festo DMSP (D=10 / L=250) , Linear	5/3 -Servo valve	SMC	Unknown	Step: 15 mm	sse < 0.01 mm (0.1 %)
Hildebrandt et al., 2002	1 x Festo DMSP (D=40 / L=?), Vertical	Proportional valve (Festo MPYE)	Flatness based feed-forward + position feedback	90 kg	Smooth step (50 mm)	sse < 0.1mm (0.2 %)
Sarosi et al., 2009	2 x Festo DMSP (D=10 / L=250) , Linear	On/off valves	SMC	Unknown	Step: 10 mm	sse < 0.02 mm (0.2 %)
Sarosi & Gyeviki, 2011	2 x Festo DMSP (D=10 / L=250) , Rotation	MPYE Servo valve	SMC	Unknown	Step: 15°	sse < 0.04° (0.3 %)
Ahn & Thanh, 2005b	2 x Festo DMSP (D=10 / L=220), Rotation	Proportional valve (Festo MPYE)	PID + Magneto-rheological brake	20 kgcm2	Step: 15 °	sse < 0.05 ° (0.35 %)
Ahn & Thanh, 2004	2 x Festo DMSP (D=10 / L=220), Rotation	Proportional valve (Festo MPYE)	PID + LVQNN	20-620 $kgcm^2$	Step: 15 °	sse < 0.1 ° (0.7 %)
Medrano-Cerda et al., 1995	(D=12.7 /L= 79), Rotation	Piezo-electric valves (50 Hz) ,PWM	Adaptive pole-placement PID with on-line estimation	No load	Step: 80°	sse < 2 ° (2.5 %)
Nouri et al., 1994	(D=? /L= ?), Rotation	Pressure regulator	Generalized variable structure Model Reference Adaptive Control	0.6 kg	S-curve: 1.4 rad	sse < 0.07 rad (5 %)
Caldwell et al., 1995	(D=12.7 /L= 79), Rotation	Piezo-electric valves (50 Hz) ,PWM	Adaptive PID	No load	Step: 9 °	sse < 1 ° (11 %)

Table 3-1: Summary of control approaches for positioning tasks with pneumatic muscle actuators

TRACKING TASK WITH PNEUMATIC MUSCLE ACTUATOR SYSTEM

Author	Muscle Actuator (Diameter [mm]/Length [mm]), Configuration	Valve	Control strategy	Payload [kg]	Reference position	Performance (te =tracking error)
Aschemann,2008	2 x Festo DMSP (D=40 /L=?), Linear	Proportional valve (Festo MPYE)	Cascaded SMC	Unknown	Continuous profile - 300...+300 mm	te < 3,5 mm (0.6 %)
Balasubramanian, 2003a	Single muscle, (D=40 /L=?), Vertical	Pressure regulator	Fuzzy PV	Unknown	Continuous profile 0-125 mm	te < 1 mm (0.8 %)
Aschemann,2008	2 x Festo DMSP (D=40 /L=?), Linear	5/3 -Proportional valve	Proxy based SMC	Unknown	Continuous profile - 300...+300 mm	te <5 mm (0.84 %)
Aschemann,2008	2 x Festo DMSP (D=40 /L=?), Linear	5/3 -Proportional valve	Flatness based control	Unknown	Continuous profile - 300...+300 mm	te < 6 mm (1 %)
Chan et al, 1999	Single muscle, vertical	Pressure control valve	Fuzzy PD+I learning control	29 kg	Sine: 17.8 mm, 0.1 Hz	te < 1.1 mm (3 %)
Shen, 2010	2 x Festo DMSP (D= 20 /L=200), Linear	5/3 -servo valve	SMC	10 kg	Sine:7.5 mm, 0.5 Hz	te < 0.5 mm (3.3 %)
Hildebrandt, 2002	Single Festo DMSP (D=40 /L=?), Vertical	5/3 -Proportional valve	Flatness based feed-forward + position feedback	90 kg	Smooth step (50 mm)	te < 2 mm (4 %)
Thanh et al, 2006	2 x Festo DMSP (10 /L=220), Rotation	5/3 -proportional valve	Nonlinear PID with NN		Sine: 20 °, 0.2 Hz	te < 2 ° (5 %)
Zhu et al., 2008	Parallel platform manipulator (3 x Festo DMSP)	On/off valves	Adaptive back-stepping control	Unknown	Sine: 5°, 0.05 Hz	te < 0.6° (6 %)
Van Damme et al. 2007	2-DOF Manipulator with pleated PAMs (Rot.)	Proportional pressure regulator	Proxy-based sliding mode control	2.6 kg	Sine: 35 mm, 0.1 Hz	te < 10 mm (15 %)
Thanh et al, 2006	2 x Festo DMSP (D= 10 /L=220), Rotation	5/3 -proportional valve	PID	Unknown	Sine: 20 °, 0.2 Hz	te < 8.5 ° (24 %)

Table 3-2: Summary of control approaches for tracking tasks with pneumatic muscle actuators

Tables 3.1 and 3.2 summarize the control strategies applied to pneumatic muscle actuators. A direct comparison of the control approaches is once again quite difficult as the actuator sizes and configuration can be quite different. In order to enable some kind of comparison, the control approaches are ordered based on the relative steady-state and tracking error. The lowest steady state error reported in the literature was ±0.01 mm which is compatible with the ones obtained with pneumatic cylinders. The lowest relative tracking error reported in the literature was 0.6 % which is slightly poorer compared to the one (0.36 %) obtained with pneumatic cylinders. This indicates that it is possible to develop compatible servo systems with pneumatic muscle actuators if the control strategy is carefully chosen.

4. SUMMARY OF PUBLICATIONS

4.1 "Modeling and Identification of a Pneumatic Muscle Actuator System Controlled by an On/Off Solenoid Valve" (Published in *Proceedings of 7th International Fluid Power Conference,* Aachen Germany, March 2010)

4.1.1 Objectives

As the pneumatic muscle actuator system driven by a single PWM-controlled on/off solenoid valve is highly nonlinear, an accurate nonlinear model was required, for both simulation and control design purposes. Special attention was given for both modeling the muscle actuator and the on/off solenoid valve. The resulting simulation models should be as realistic as possible in order to provide means for system analysis and for testing control laws.

Pneumatic muscle actuator introduces a highly nonlinear force-pressure-displacement relation and a significant hysteresis making the accurate modeling of the pneumatic system even more challenging. The objective was to provide an accurate model for the actuator force as well as provide study of existing hysteresis.

When PWM-actuated on/off valve is used for controlling the motion of the actuator, the valve switching introduces a discontinuous system dynamics which is difficult to handle in control design. Thus, the objective was to provide a continuous nonlinear model of the system enabling the implementation of conventional analytical model based control approaches.

4.1.2 Approaches

The modeling was applied to a one degree of freedom pneumatic muscle actuator system for which the nonlinear system model was developed as a combination of analytical and empirical methods. The four major processes of the system, including the flow dynamics, pressure dynamics, force dynamics, and load dynamics were studied to develop a full nonlinear model that captures major nonlinearities of the system.

- It was noted, that the previously introduced models for predicting the force generated by the muscle actuator did not provide sufficient results with Festo Fluidic Muscle used in this work. For that reason, a novel model for capturing the nonlinear relation between the force, pressure and displacement of the actuator was developed.
- In this work, the hysteresis of the actuator was measured with isobaric test which refers to force/length hysteresis, when the pressure inside the actuator was maintained constant. It was observed that for different levels of pressure the width of the hysteresis curve was almost the same and remained almost the same also for the entire stroke. As a result, the

hysteresis was modelled as a Coulomb friction with a constant offset depending on the direction of movement.

- The velocity dependent viscous friction/damping was assumed to be pressure independent. The damping factor was determined experimentally with a setup where the muscle actuator was attached to a load cell and low friction cylinder actuator with known estimated friction characteristics. A set of experiments was executed to determine the total friction as a function of velocity. The viscous friction of the muscle actuator was then determined by subtracting the cylinder friction from the measured total friction.
- For simulation purposes a common mass flow rate model was used for which the parameters (C_v, b_v) were experimentally determined. The experimental setup was based on ISO 6358 standard. This mass flow rate model was combined with valve switching delay and opening and closing time of the valve spool in order to provide realistic flow behaviour of the PWM valve. This semi-empirical and discontinuous mass flow rate model was denoted as a non-analytical modeling approach in the publication.
- The use of PWM results in a discontinuous mass flow rate that is difficult to handle from the viewpoint of control design. A continuous mass flow rate model for control design includes the determination of an equivalent mass flow rate as a function of PWM duty ratio and actuator pressure. For experimentally determined data, a ^{2nd} order bi-polynomial fitting function was applied. As the function is continuous and invertible, it can be used to map the controller output (mass flow rate) with measured actuator pressure to a corresponding PWM duty ratio. The model is not only able to capture the nonlinear mass flow characteristics very accurately but also makes the control design easier. Note, that this empirical mass flow rate model was denoted as an analytic modeling approach in the publication. The notations “analytic” and “non-analytic” used in the original publication mean that the analytic and continuous model enables the use of traditional control design techniques and non-analytic (discontinuous) model does not.

4.1.3 Results

The novel force model developed in this paper gives a very accurate prediction compared to traditional force models as shown in Figure 4-1. An accurate prediction of force gives a good basis for achieving a sufficient control performance with pneumatic muscle actuators.

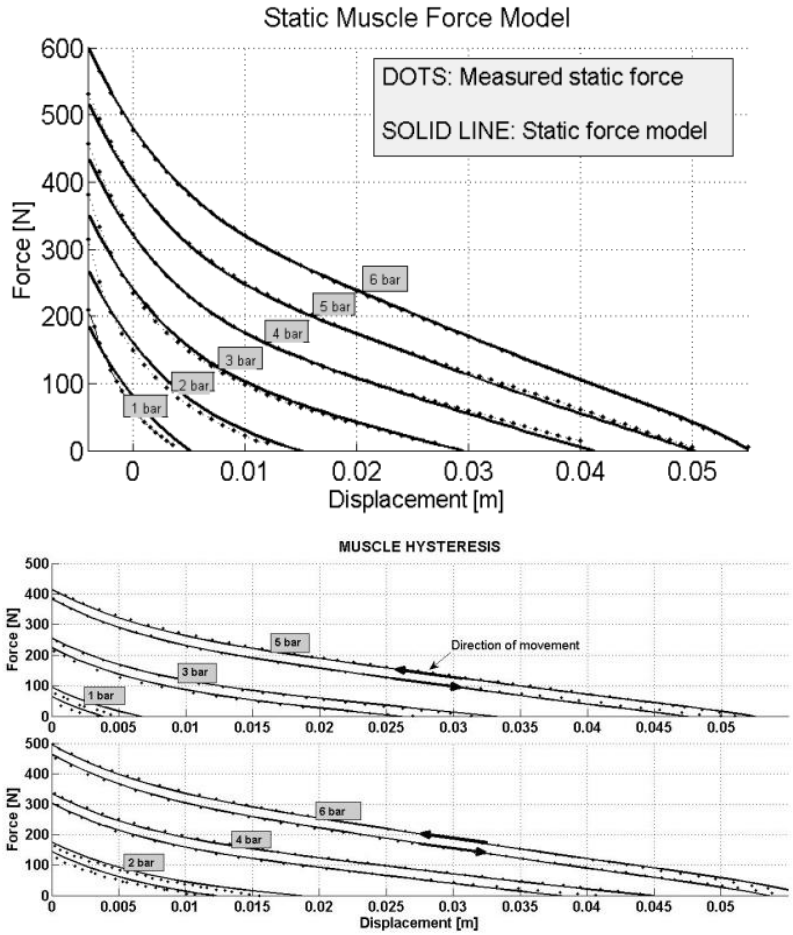

Figure 4-1: Novel force model with hysteresis for predicting the force generated by the muscle actuator

In the paper, the mass flow rate of the PWM-operated on/off valve was experimentally estimated as an equivalent mass flow rate as a function of PWM duty ratio and actuator pressure as shown in Figure 4-2. Then a 2nd order bi-polynomial function was fitted for the estimated data with a reasonably good accuracy.

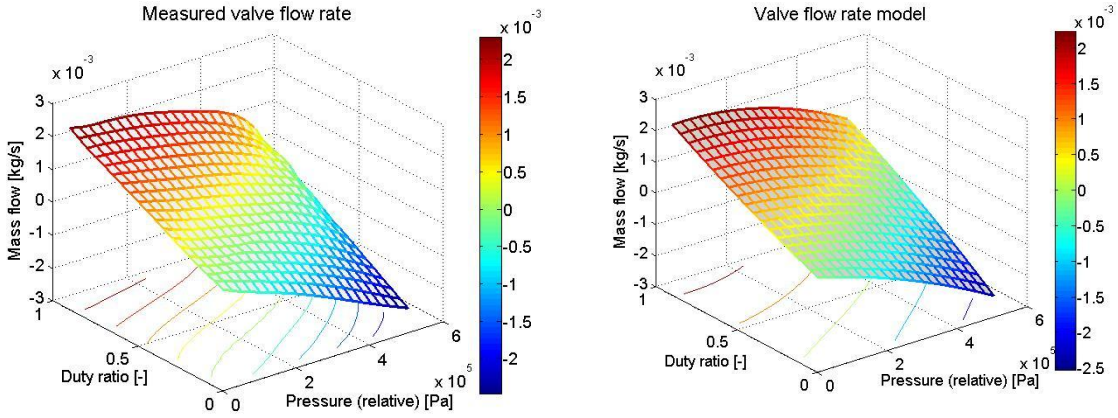

Figure 4-2: Estimated equivalent mass flow rate as a function of PWM duty ratio and actuator pressure (left) and its 2nd order bi-polynomial fitting (right)

The identified valve mass flow models (continuous and discontinuous) were both validated by pressurizing and depressurizing a constant volume with different PWM duty ratios with PWM frequency 50 Hz. The results showed that both models can accurately describe the mass flow rate characteristics of the valve as they were capable of accurately predict the pressure in the closed chamber.

The overall system model was verified with a set of triangle waveform input signals (PWM duty ratio) and measuring the position of the actuator with a constant payload (see Publication 1 for more details). The results showed reasonably good modeling accuracy in comparison to experimental data. The modeling errors were mainly caused by the inaccurate friction modeling and dynamic hysteresis.

The simulation models were used for initial tuning of a traditional PI-controller. When implementing the controller into a real system only a slight fine tuning was needed to improve the control performance.

4.1.4 Conclusions and Contributions

An accurate prediction of nonlinear force characteristics of the muscle actuator is important to the analysis and investigation of muscle actuator based systems. A novel force model developed in this work provided accurate force prediction of the muscle actuator used in this work. Also, frictional characteristics including hysteresis were studied.

The modeling of mass flow characteristics of the control valve is very important to the analysis of the system as well as from the viewpoint of control design. For simulation purposes, a detailed model of the on/off valve was developed based on analytical and empirical methods. From the point of view of control design, discontinuous switching is difficult to handle. In order to provide a continuous valve flow model, a recently introduced method of 2^{nd} order bi-polynomial function was utilized and applied for determining an accurate prediction of flow as a function of pressure and PWM duty ratio. As the resulting model is invertible, the flow model can be utilized in the control design loop to remove the nonlinear flow characteristics from the model used in the controller design. As a result, the flow model enables the use of effective linear tools for analysis and stability as well as the use of analytical model-based control approaches.

4.2 "Position Control of PWM-Actuated Pneumatic Muscle Actuator System" (*In Proceedings of the ASME 2011 International Mechanical Engineering Congress and Exposition (ASME IMECE 2011)*

4.2.1 Objectives

Highly nonlinear nature makes an accurate control of pneumatic systems extremely difficult. As such, classical linear control approaches usually can't provide good performance and more complex control strategies are needed. Due to highly nonlinear characteristics of the muscle actuator system and uncertainties present in the system, a sliding mode control (SMC) was chosen for a control law. SMC strategy has been proven to provide an efficient, robust and simple approach for controlling nonlinear and uncertain systems. In order to verify the performance of SMC approach, a comparison to a conventional linear proportional-velocity-acceleration plus feed-forward (PVA+FF) control approach was performed. Another objective was to study the effect of PWM frequency on the control performance. In the original publication only simulation results were introduced. For that reason experimental results are introduced in the section of Results. In addition to the original publication, a study of sliding mode control with integral sliding surface (SMCI) is also performed.

4.2.2 Approaches

- The system under study was a one degree of freedom pneumatic muscle actuator system attached to a pneumatic cylinder with a nominal payload mass M=2 kg. The muscle actuator was controlled by a single on/off valve in PWM mode while the cylinder provided a constant returning force.
- A nonlinear model of the muscle actuator and valve including discontinuities developed in (4.1) was used as a "real" plant model in simulations. This model was used for analyzing and tuning the controller performances by simulations before implementing in the real application.
- The mass flow rate model for the PWM-valve introduced in (4.1) was utilized to provide a continuous and invertible description of mass flow rate for controller designs.
- Two different control algorithms (PVA+FF and SMCL) based on the linearized system model were developed. A sliding mode control based on the nonlinear system model (SMCNL) was also developed and compared to linear control approaches. As an extension to the paper, also a sliding mode control with integral sliding surface (SMCI) was developed and compared to SMCNL approach.
- The initial tuning of the controllers was performed and their performances for sinusoidal tracking tasks with an amplitude 14 mm and various frequencies were first studied by

simulations. Finally, the control approaches were applied and studied with the experimental setup.

- The stability and performance analysis included the effects of friction modeling error and valve modeling error. The robustness of the controllers was tested by varying the payload mass from 50 % to 150 percent of nominal system.
- The effect of the PWM frequency was studied by comparing the performance with PWM frequencies 50 and 100 Hz.

4.2.3 Results

In the publication, only simulation results were introduced for the controllers PVA+FF, SMCL and SMCNL. As the experimental results were not included in the original paper, they are given and discussed here. Please, see the detailed simulation results in the Publication 2.

Experimental tests were performed with payload mass 1, 2 and 3 kg. Sinusoidal input trajectories with frequencies 0.25, 0.5, 0.75 and 1.0 Hz were used. The experimental tuning enabled a slight higher gains compared to simulations resulting in boundary layer thickness Φ=50 for PWM 50 Hz and Φ=40 for PWM 100 Hz. The other parameters were the same as in the simulations: $\lambda=\omega_n=85$ rad/s, $\zeta=0.1$, K_{sw}=2e-3 resulting in equivalent PVA gains K_{p_eq}=0.289, K_{v_eq}=0.00068 and K_a=4e-5 for PWM 50 Hz and K_{p_eq}=0.36, K_{v_eq}=0.00085 and K_a=5e-5 for PWM 100 Hz. Similar filtering for obtaining the velocity and acceleration was used as in the simulations.

Table 4-1 gathers the RMSE tracking error of the controllers with the nominal payload mass. The results indicate that PVA+FF and SMCL provide similar performance as expected. The SMCNL improves the performance up to 20 % with both PWM 50 Hz and PWM 100 Hz. The use of PWM 100 Hz will result in an approximately 20 % better tracking performance, mainly due to smaller PWM introduced dither in the position signal as well as faster control loop. This corresponds to the results obtained in simulations. Figure 4-3 shows the tracking performance of PVA+FF and SMCNL for PWM 50 Hz and PWM 100 Hz. Note, that PWM 100 Hz results in a significant improvement also in terms of maximum tracking error compared to PWM 50 Hz.

Frequency	**PVA+FF** (PWM 50)	**SMCL** (PWM 50)	**SMCNL** (PWM 50)	**PVA+FF** (PWM 100)	**SMCL** (PWM 100)	**SMCNL** (PWM 100)
0.25 Hz	0.428	0.431	0.390	0.327	0.327	0.298
0.5 Hz	0.563	0.578	0.495	0.449	0.442	0.383
0.75 Hz	0.811	0.835	0.673	0.596	0.602	0.503
1 Hz	1.078	1.120	0.887	0.758	0.764	0.628
Total RMSE	2.880	2.964	2.445	2.130	2.135	1.812

Table 4-1: Comparison of RMSE (mm) values for nominal payload (2 kg) with PWM 50 Hz and 100 Hz

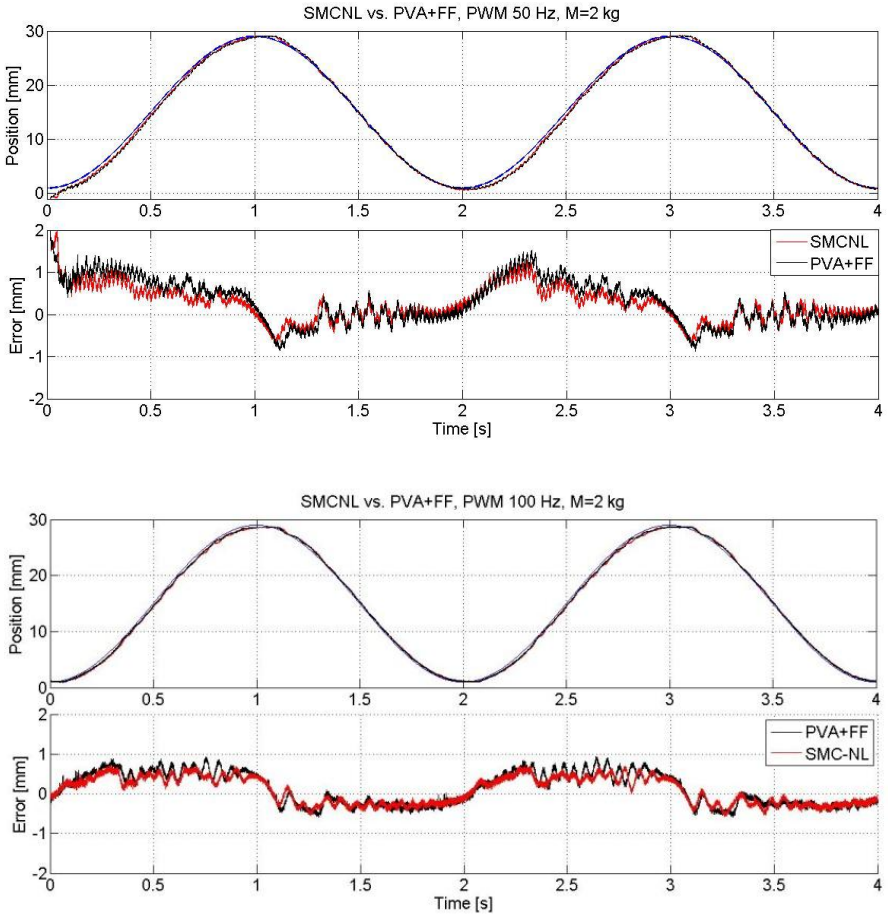

Figure 4-3: Comparison of SMCNL and PVA+FF with nominal payload (*M*=2 kg), 0.50 Hz sinusoidal. In the upper figure PWM 50 Hz is used in the lower figure PWM 100 Hz is used.

Frequency	PVA+FF (PWM 50)	SMCL (PWM 50)	SMCNL (PWM 50)	PVA+FF (PWM 100)	SMCL (PWM 100)	SMCNL (PWM 100)
0.25 Hz	0.397	0.405	0.362	0.327	0.330	0.282
0.5 Hz	0.568	0.580	0.489	0.441	0.439	0.371
0.75 Hz	0.821	0.862	0.698	0.593	0.596	0.487
1 Hz	1.074	1.159	0.944	0.749	0.753	0.612
Total RMSE	2.860	3.006	2.493	2.115	2.118	1.752

Table 4-2: Comparison of RMSE (mm) values for increased payload (3 kg) with PWM 50 Hz and 100 Hz

Table 4-2 shows the comparison of the controller performances in terms of RMSE values for increased payload *M*=3 kg. In overall, the tracking accuracy was actually improved due to the decreased motion dither caused by the increased inertia. Figure 4-4 illustrates the control performance SMCNL for PWM 50 Hz and PWM 100 Hz with sinusoidal input 0.5 Hz. It should be noted, that low damping coefficient ζ=0.1 tends to increase oscillations when the inertia of the system increases. However, it can be seen that PWM 100 Hz not only provides better accuracy but also provides better damping. This can be clearly seen at negative velocity region. In that case, the

cylinder provides the driving force and the muscle actuator works as a brake making the control of the system more difficult. Also, note the performance at motion reversals where PWM 100 Hz can provide better performance against muscle actuator hysteresis.

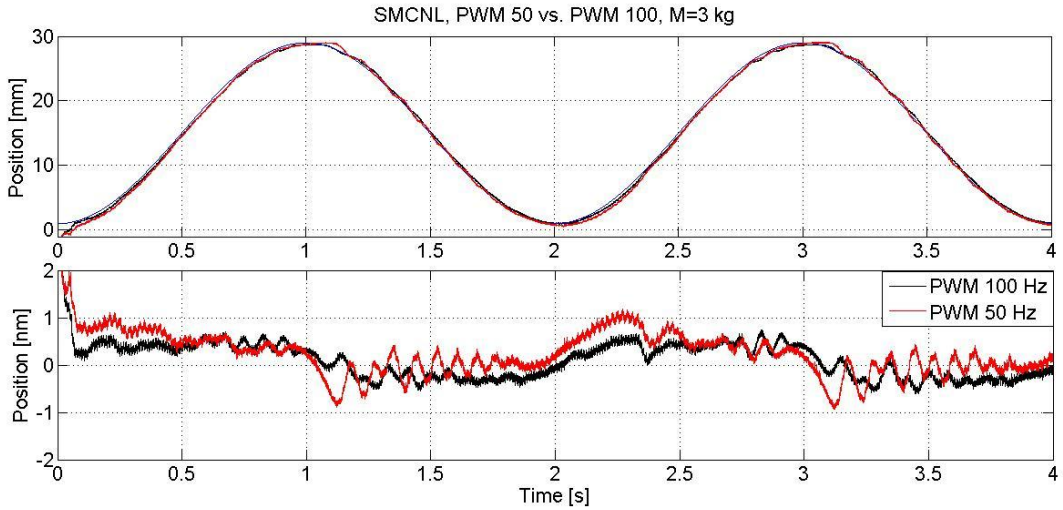

Figure 4-4: Comparison of PWM 50 (red) and 100 Hz (black) with SMCNL and payload *M*=3 kg

Table 4-3 shows the comparison of the controller performances in terms of RMSE values with decreased payload mass *M*=1 kg. It was noted, that the tracking accuracy decreased 15 % in average for all controllers from the nominal case. This was due to smaller inertia which increased the magnitude of position dither. The SMCNL was capable of providing an improved tracking performance up to 20 % compared to PVA+FF and SMCL. It should be noted, that the SMCNL became more efficient at higher input frequencies. Figure 4-5 illustrates the control performance of PVA+FF and SMCNL for PWM 50 Hz and PWM 100 Hz. Note, the increased dither due to decreased inertia and increased oscillation of PVA+FF controller. Again, the PWM 100 Hz can provide significantly better performance compared to PWM 50 Hz.

Frequency	**PVA+FF** (PWM 50)	**SMCL** (PWM 50)	**SMCNL** (PWM 50)	**PVA+FF** (PWM 100)	**SMCL** (PWM 100)	**SMCNL** (PWM 100)
0.25 Hz	0.517	0.517	0.480	0.395	0.390	0.376
0.5 Hz	0.653	0.662	0.569	0.540	0.531	0.460
0.75 Hz	0.894	0.914	0.771	0.724	0.726	0.618
1 Hz	1.140	1.175	0.959	0.926	0.915	0.756
Total RMSE	3.204	3.268	2.779	2.585	2.562	2.210

Table 4-3: Comparison of RMSE (mm) values for decreased payload (*M*=1 kg) with PWM 50 Hz and 100 Hz

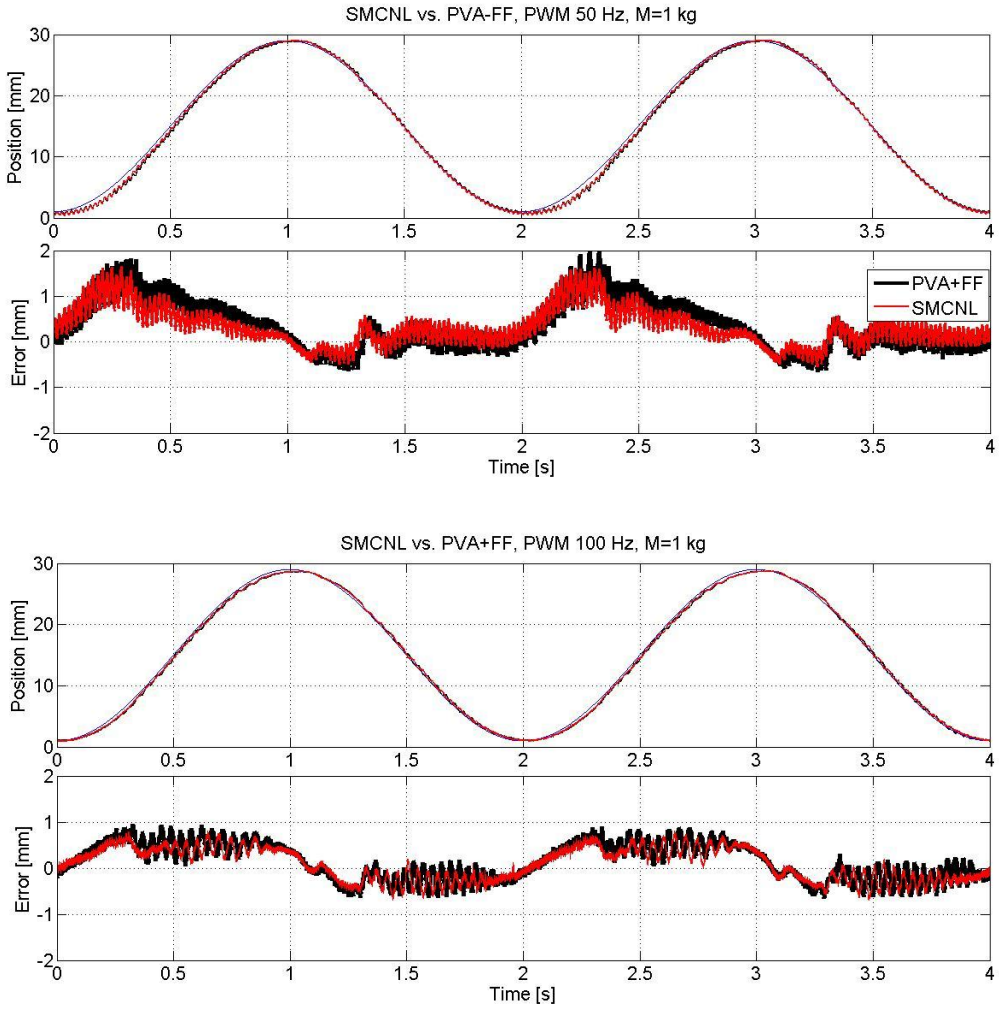

Figure 4-5 Comparison of PVA+FF and SMCNL with decreased payload (*M*=1 kg) and PWM 50 and 100 Hz

Frequency	**SMCNL** (PWM 50)	**SMCI** (PWM 50)	**SMCNL** (PWM 100)	**SMCI** (PWM 100)
0.25 Hz	0.390	0.212	0.298	0.174
0.5 Hz	0.495	0.306	0.383	0.262
0.75 Hz	0.673	0.523	0.503	0.411
1 Hz	0.887	0.836	0.628	0.607
Total RMSE	2.445	1.877	1.812	1.454

Table 4-4: Comparison of RMSE (mm) values of SMCNL and SMCI for nominal payload (*M*=2 kg) with PWM 50 Hz and 100 Hz

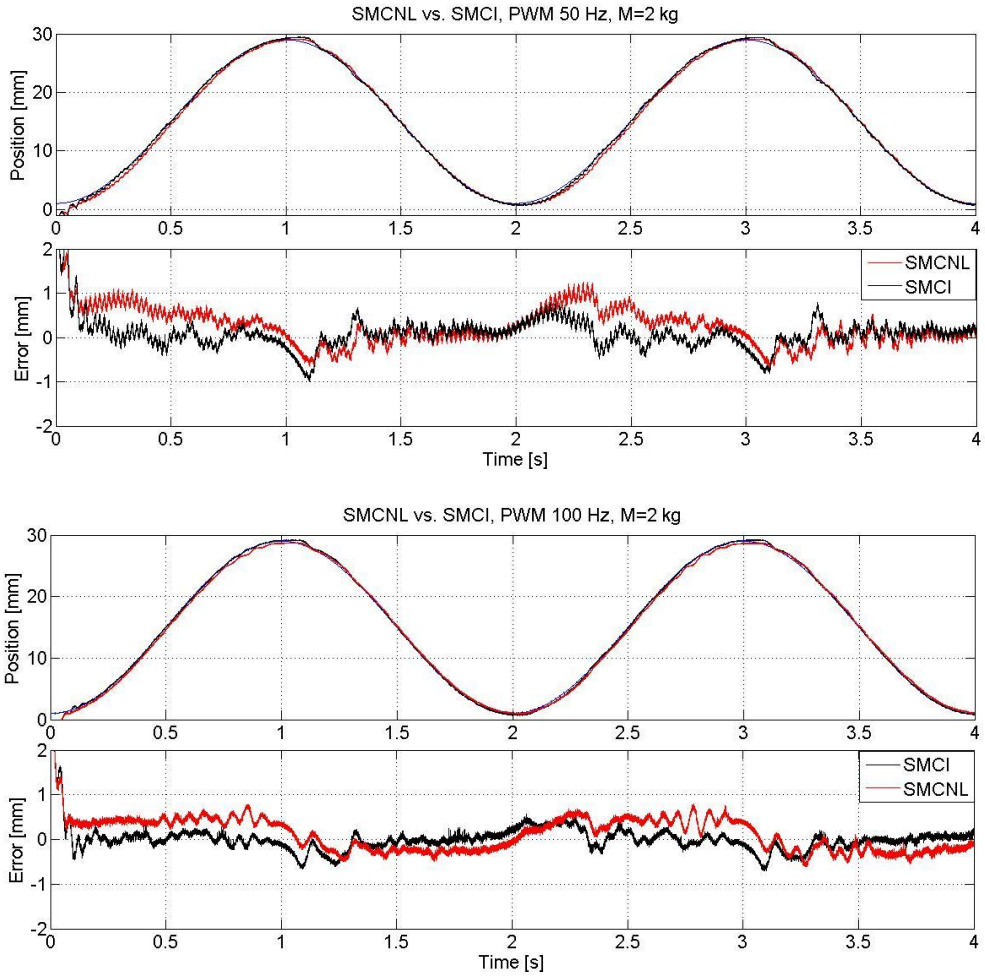

Figure 4-6: Comparison of SMCNL and SMCI with nominal payload and PWM 50 Hz and PWM 100 Hz

For the sliding mode control with the integral sliding surface (SMCI) the tuned controller gains were $\lambda=\omega_n=70$ *rad/s*, $\zeta=0.1$, K_{sw}=2e-3 and $\phi=35$) for PWM 50 Hz and ($\lambda=\omega_n=70$ *rad/s*, $\zeta=0.1$, K_{sw}=2e-3 and $\phi=30$) for PWM 100 Hz. It can be noted, that integral action will significantly improve the tracking performance especially at low input frequencies. Table 4-4 shows the comparison between the SMCNL and SMCI designs. The integral term improves the tracking between the end points as can be seen in Figure 4-6. However, at higher input frequencies the overshooting caused by the integral term at turning points will deteriorate the performance. Also, it should be noted that adding integral term in the system will decrease the damping properties of the system. The results correspond well with the simulation results.

With increased payload M=3 kg the use of integral sliding surface shows quite similar performance as with nominal payload. It significantly (up to 40 %) improves the performance at low input frequencies, but the performance degrades at higher frequencies. Also, there were slight

increased oscillations compared to nominal case due to low damping properties. Table 4-5 compares SMCNL to SMCI.

Frequency	**SMCNL** (PWM 50)	**SMCI** (PWM 50)	**SMCNL** (PWM 100)	**SMCI** (PWM 100)
0.25 Hz	0.362	0.201	0.282	0.181
0.5 Hz	0.489	0.331	0.371	0.268
0.75 Hz	0.698	0.591	0.487	0.404
1 Hz	0.944	0.865	0.612	0.594
Total RMSE	2.493	1.877	1.752	1.447

Table 4-5: Comparison of RMSE (mm) values of SMCNL and SMCI for nominal payload (*M*=3kg) with PWM 50 Hz and 100 Hz

With decreased payload mass *M*=1 kg the SMCI approach with PWM 50 Hz showed a poor performance especially at input frequencies 0.25 Hz and 1 Hz as there were significant oscillations in the motion. The controller gains were too high in comparison to increased noise (low inertia) leading to poor performance as shown in Figure 4-7. The oscillation can be removed by increasing the boundary layer thickness at the cost of decreased tracking accuracy. The performance with PWM 100 Hz showed also increased oscillations but still provided better tracking accuracy. Table 4-6 shows the RMSE values for SMCNL and SMCI with PWM 50 and 100 Hz.

Frequency	**SMCNL** (PWM 50)	**SMCI** (PWM 50)	**SMCNL** (PWM 100)	**SMCI** (PWM 100)
0.25 Hz	0.480	0.829	0.376	0.174
0.5 Hz	0.569	0.440	0.460	0.314
0.75 Hz	0.771	0.557	0.618	0.451
1 Hz	0.959	1.241	0.756	0.648
Total RMSE	2.779	3.067	2.210	1.587

Table 4-6: Comparison of RMSE (mm) values of SMCNL and SMCI for nominal payload (*M*=1 kg) with PWM 50 Hz and 100 Hz

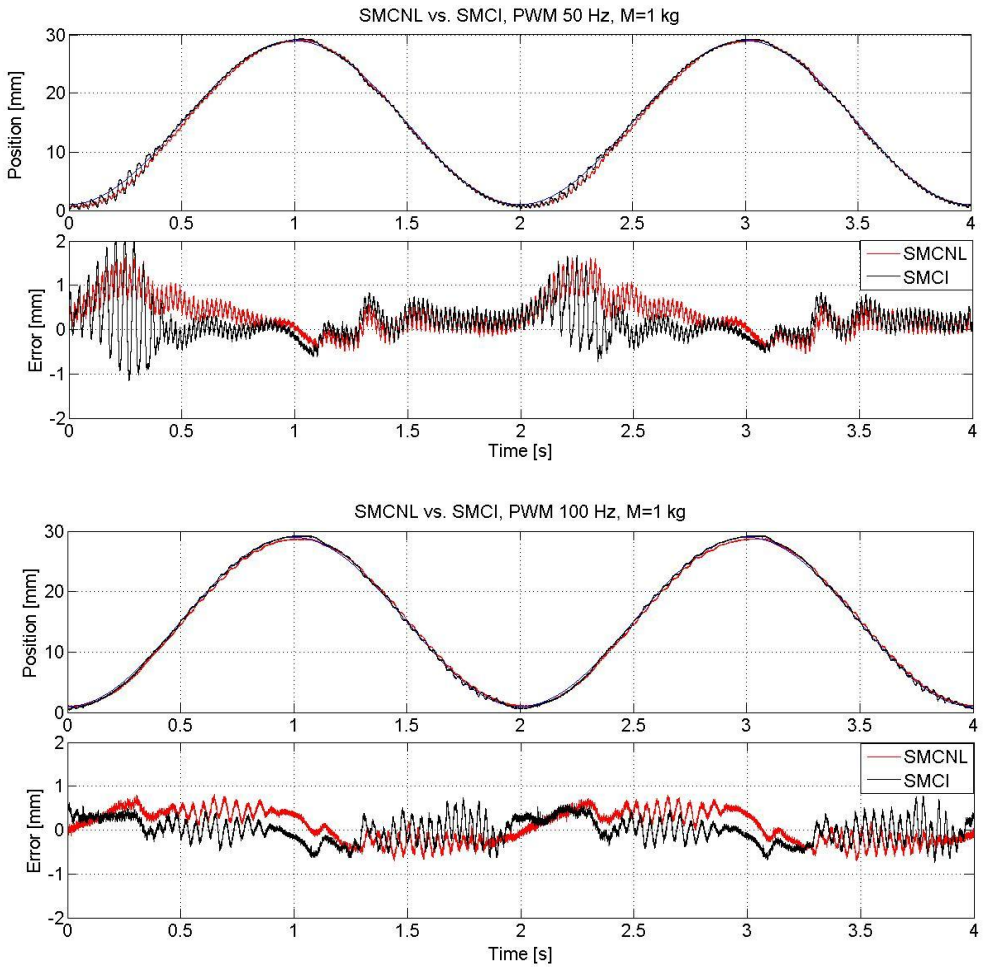

Figure 4-7: Comparison of SMCNL and SMCI with decreased payload (*M*=1 kg) and PWM 50 Hz and PWM 100 Hz

4.2.4 Conclusions and Contributions

This paper provides a low-cost approach to control pneumatic muscle actuator systems by using high-speed on/off valve(s) with PWM technique instead of costly proportional and servo valves. A full nonlinear modelling including pressure, flow and load dynamics of the system was derived and used for initial tuning and analysis of the controllers. The continuous valve model was exploited in the control design by converting the controller output (mass flow rate) into PWM duty ratio signal simplifying the control design. Due to highly nonlinear nature of the system under study, a sliding mode control (SMC) approach was chosen for control law. The SMC approach should provide means for accurate control of nonlinear systems as well as guarantee robustness to modeling errors and uncertain parameters. The effectiveness of the SMC approach with its variants SMCL, SMCNL and SMCI were compared to a conventional PVA+FF control law.

As expected, the results indicated that PVA+FF and SMCL resulted in almost identical performance with a similar set of feedback gains. By using the boundary layer approach with SMC,

the control law transforms into a state feedback controller (comparable to PVA) as the system enters the boundary region. The main difference between the approaches is thus in the computation of model-based component; equivalent control term with SMC and feed-forward (FF) term with PVA+FF. As the FF control component uses desired state vectors as inputs and the inverse of the linear system model, the resulting control signal is noiseless. In contrast, with SMC the equivalent term is computed based on the error of desired and measured states. Thus, the noise associated with estimated velocity and acceleration signals affects the control performance negatively.

With a similar set of feedback gains, SMCNL can improve the tracking performance approximately by 15 % compared to above mentioned linear approaches. This difference becomes from the better prediction of desired control action through computed equivalent control term.

Sliding mode control with an integral sliding surface (SMCI) can provide a significant tracking improvement (up to 40 %) compared to nonlinear SMC. The advantage of integral action becomes significant especially with low frequency tracking tasks as the tracking error is decreased during the movement. It was notable, that the effectiveness of the integral action decreased with higher frequencies, especially due to overshooting when the direction of the movement was changed. Combined with the hysteresis of the muscle actuator and integral wind-up the maximum tracking error increased in those cases. Commonly, SMC approach is considered as a “high gain” state feedback controller. However, in case of PWM-pneumatics this is not true. It was notable, that SMC approaches (SMCL and SMCNL) did not enable use of higher control gains than PVA+FF approach. This was caused by the PWM control delay where the control signal is sampled once per PWM cycle. Thus, the PWM delay is very harmful reducing the performance and robustness of the SMC approach.

The used PWM frequency has a significant effect on the system performance. The PWM frequency should be significantly higher than the system dynamics in order to provide smooth mass flow rate. However, the maximum PWM frequency is limited by the speed of the valve as the switching time determines the maximum reasonable frequency. In this work, the effect of PWM frequency was studied by operating the system with PWM frequencies 50 Hz and 100 Hz. It was notable, that the higher PWM frequency resulted in clearly better performance in terms of tracking accuracy and robustness. The faster control loop results in smaller dither in the position signal as well as enables the use of higher low-pass cut-off frequencies for estimating the velocity and acceleration from the measured position. Thus, the choice of filter cut-off frequency is a trade-off between the phase delay and noise. In addition, higher PWM frequency enables higher control gains improving the tracking performance. Also, due to faster control loop a better robustness to

parameter variations and disturbances is obtained. Ideally, in order to better exploit the advantages of SMC strategy the PWM frequency should be higher requiring faster control valves.

4.3 "Sliding Mode Control of a Pneumatic Muscle Actuator System with a PWM Strategy" (Accepted for publication in *International Journal of Fluid Power*)

4.3.1 Objectives

Although PWM-pneumatics has been studied during the past two decades, their performance compared to traditional servo valve controlled system has not been clearly addressed. Also, the literature lacks robustness study of the PWM –pneumatic systems to parameter variations and disturbances. The objective of this paper is to provide a comparison of PWM- on/off valve and servo valve controlled pneumatic system with the same sliding mode control law. Also the robustness of the approaches against parameter variations should be verified by e.g. changing the loading conditions of the system as well as against external disturbances.

4.3.2 Approaches

- The system under study was a one degree of freedom pneumatic muscle actuator system attached to a pneumatic cylinder with a nominal payload mass M=2 kg. Three different valve configurations; single on/off valve (Case 1), two on/off valves (Case 2), and servo valve (Case 3), were used.
- The mass flow rate model for the PWM-valve introduced in (4.1) was utilized to provide a continuous and invertible description of flow for SMC control design. The same modeling approach was used in all valve cases in order to provide similar controller structure.
- A detailed description of controller tuning was introduced, that made the choice of switching gain K_{SMC} and boundary layer thickness Φ easier.
- The effect of damping ratio ζ on the system performance was studied for all valve cases.
- The performance of the different valve configurations was studied with sinusoidal position tracking tasks. PWM frequency 100 Hz was used with on/off valve approaches. The robustness of the system was analyzed by changing the payload from 0.5 to 4 kg (25 % - 200 % from the nominal M=2 kg). The robustness to external disturbances was studied by varying the cylinder return force.

4.3.3 Results

The mean RMSE values for the control performance of the valve configurations for sinusoidal tracking with nominal payload are gathered in Table 4-7. For the normal conditions, as

demonstrated by the results, the two valves system provided the best tracking with sinusoidal frequencies 0.25 Hz and 0.5 Hz. The two valves and servo valve configurations improved the tracking performance up to 30 % compared with the single on/off valve case. It is also notable that the tracking performance with the two valve configuration was slightly better than compared to the servo valve system (overall).

Frequency	Single On/Off	Dual On/Off	Servo Valve
0.25 Hz	0.196	**0.087**	0.091
0.5 Hz	0.268	**0.170**	0.205
1 Hz	0.448	0.378	**0.367**
Total RMSE	0.912	**0.635**	0.663

Table 4-7: Comparison of RMSE (mm) values averaged over five measurements for the three valve configurations

The RMSE results for payload variation are summarized in Tables 4-8 and 4-9. It is interesting to observe that the on/off valve configurations were extremely robust to decreased payload mass as the total tracking accuracy was actually improved when compared with the normal case. Conversely, the performance of the servo valve configuration decreased with payload mass M=0.5 kg by approximately 37% when compared with the normal case.

For the increased payload M=4 kg, the performance of the case with two on/off valves degraded 79% on average, and 46% with the single valve compared with the normal case. In terms of robustness, the best performance to increased payload mass was obtained with the servo valve configuration, as the performance decreased only by 16%.

Frequency	Single On/Off	Two On/Off	Servo Valve
0.25 Hz	0.163	**0.079**	0.135
0.5 Hz	0.230	**0.142**	0.232
1 Hz	0.470	**0.354**	0.543
Total RMSE	0.863	**0.575**	0.910

Table 4-8: Comparison of average RMSE (mm) with payload M=0.5 kg

Frequency	Single On/Off	Two On/Off	Servo Valve
0.25 Hz	0.231	0.193	**0.131**
0.5 Hz	0.356	0.313	**0.209**
1 Hz	0.748	0.633	**0.434**
Total RMSE	1.335	1.139	**0.774**

Table 4-9: Comparison of average RMSE (mm) with M=4 kg

With all of the valve configurations, oscillations occurred in the motion signal with increased inertia. This was due to a relatively low damping ratio $\xi = 0.1$ which is a design parameter in the definition of the closed loop control dynamics, and began to affect the performance with increased inertia. With the nominal payload M=2 kg, the tracking performance degraded significantly with higher damping ratio. A higher damping ratio magnified the noise in the system, which resulted in poor performance, especially with on/off valve configurations. The servo valve configuration had a faster control loop, which provided better robustness to increased noise. Under the M=4 kg condition, the systems started to oscillate when low damping ratios were implemented, thus a higher damping ratio was needed. The best performance was obtained by using a damping ratio of 0.4 with the servo valve and two valves systems, and 0.7 with the single valve system. Note also that a high damping ratio decreased the tracking accuracy which could be seen amongst all of the configurations (see the publication for details).

Robustness to external disturbances was tested by applying sinusoidal and stepwise force inputs with a load cylinder. The amplitude of the force disturbance was 25 N and the mean value was 50 N. Frequencies of 1 Hz and 2 Hz were used for the sinusoidal disturbance, and 0.75 Hz for the stepwise disturbance. Table 4-10 summarizes the RMSE values of the control performance when the input tracking trajectory was a sinusoidal signal with amplitude 10 mm at 0.25 Hz. Although each of the valve configurations was capable of providing a reasonable response for the applied disturbance signals, the best performance was clearly obtained with the servo valve configuration.

Disturbance	Single On/Off	Two On/Off	Servo Valve
1 Hz (Sine)	0.173	0.149	**0.120**
2 Hz (Sine)	0.288	0.238	**0.178**
0.75 Hz (Step)	0.280	0.237	**0.177**
None	0.123	**0.083**	0.097

Table 4-10: Comparison of averaged RMSE (mm) with external disturbance

4.3.4 Conclusions and Contributions

This paper continued the study of PWM-driven pneumatic muscle actuator applications. As the literature lacks studies of the comparison between PWM-operated on/off valve and traditional servo valve controlled pneumatic systems, this paper provides a performance and robustness study of those two approaches. Three different valve configurations were studied: single on/off valve, two on/off valves and servo valve. As the mechanical structure of the system remained same in each case and the flow characteristics of the valve configurations were modeled using inverse mapping,

the resulting system model used for control design was identical in each case. As a consequence, the equivalent control term in the sliding mode control law was identical for each case enabling the use of similar sliding surface design. Then, a switching gain was defined based on the velocity requirements of the system leaving the boundary layer thickness as the only control parameter to adjust for each case individually. This kind of procedure made it possible to compare performance characteristics of different valve configurations for tracking tasks and robustness to parameter variations and external disturbances.

The results indicated that PWM-operated on/off valve approach can provide a compatible performance for servo valve approach. Especially, the system with two on/off valves can provide similar tracking accuracy in nominal conditions as the servo valve approach. The performance of single on/off valve approach was not as good as with the other. However, this was expected as the valve is switching continuously (there is flow in or out all the time) increasing the amplitude of dither and noise in the system. However, it should be noted that the single valve approach is certainly cheapest of the configurations and is still capable of providing reasonable performance.

The disadvantages of on/off valve approaches arise when the system parameters change. The robustness in this sense was verified by changing the payload mass. The results showed that the servo valve approach performed much better with increased payload mass than the on/off valve approaches. With decreased payload mass, the performance of the servo valve approach decreased due to increased control chattering. The on/off valve approaches showed good robustness to decreased inertia. The servo valve approach was the most robust against bounded external disturbances due to its faster control loop. Thus, the problem of on/off valve approaches to increased inertia can be summarized as a combination of signal noise (due to PWM switching) and the PWM introduced control delay.

In overall, under nominal conditions, the PWM actuated on/off valve controlled muscle actuator system can provide a considerable low-cost option for servo valve controlled system.

4.4 "A Position Servo Based on On/Off Valve Actuated Muscle Actuators in Opposing Pair Configuration" (in *Proceedings of Bath/ASME Symposium on Fluid Power & Motion Control (FPMC 2012), 2012)*

4.4.1 Objectives

As the muscle actuator is unidirectional, a typical way to provide return force is to use another muscle actuator. They can be attached horizontally or vertically as an opposing pair configuration to provide linear motion or in parallel connected via a pulley to provide a rotational movement. These kinds of setups are also known as agonist/antagonistic configurations. A typical way to control the

position of the system is to use a servo or proportional valve. In this paper, the objective is to show that the muscle actuator system can be controlled accurately also with on/off valves with PWM strategy. Although, the use of on/off valves leads to a MISO system, the control problem can still be converted to a SISO form for which the same control law as with servo valve can be utilized. Thus, in this paper a performance comparison of on/off valve and servo valve controlled system with identical sliding mode control law in terms of tracking accuracy and robustness to payload variations is conducted.

4.4.2 Approaches

- The system under study was a one degree of pneumatic system, where two actuators were mounted horizontally and coupled to a linear slide carrying a payload mass M=2 kg.
- In the on/off valve approach, each actuator was controlled by two 2/2 valves, one for controlling the inflow and the other for controlling the outflow. This kind of configuration can be seen similar as the system controlled with 5/3 way servo valve.
- In order to enable a direct comparison, the chosen servo valve and on/off valves used have the same nominal flow capacity.
- The system model was defined in a SISO canonical control form typical to servo valve controlled systems. In case of servo valve, it was assumed that the valve control signal U results in a symmetric valve opening area for mass flow A and mass flow B. Similarly, in case of on/off valves, it was assumed that the PWM control signal (duty ratio) results in a similar effective valve opening area with respective valves for mass flow rate A and B.
- Traditional mass flow rate model was used, where a mass flow of an ideal gas through a converging nozzle was assumed. The model parameters were obtained by least squares fitting of experimental data to the respective mass flow rate equation.
- A normalized control variable [-1..1] was used in both valve approaches, which was then converted to a real valve control signal. In both cases, also dead zone compensation was used. The dead zone range was experimentally defined.
- A sliding mode controller based on a 2^{nd} order sliding surface definition was designed. Initial tuning of the control parameters was done with the help of simulations and then refined with experimental setup. A similar set of controller parameters was used in order to provide a direct comparison of the systems.
- The performance of the on/off valve and servo valve approach was studied with sinusoidal position tracking tasks up to 2 Hz with amplitude 15 mm. The robustness of the system was analyzed by changing the payload from 2 up to 6 kg.

4.4.3 Results

The mean RMSE values for the control performance of the servo valve and on/off valves configuration with SMC approach for sinusoidal tracking with nominal payload (M=2 kg) are gathered in Table 4-11. It can be seen that on/off valve approach results in only 22 % poorer performance in total than the servo valve approach for the whole input frequency range. Especially, at low input frequencies (< 1 Hz) on/off valve approach is capable of providing surprisingly good performance as the performance is almost identical to servo valve approach. The maximum negative and positive tracking error for each frequency is also shown in Table 4-11. It is notable that servo valve approach provides better accuracy in terms of maximum tracking error in overall. The maximum error occurs mostly at times when the direction of movement is changed when the effect of muscle actuator hysteresis is most significant. With servo valve approach the control loop is much faster (1 ms) than with on/off valve approach (10 ms) resulting in better response to control commands at motion reversals.

Frequency	**On/Off Valve** (RMSE)	**On/off valve** (Max. error)	**Servo valve** (RMSE)	**Servo valve** (Max. error)
0.25 Hz	0.143	$-0.4 \dots + 0.4$	0.144	$-0.35 \dots + 0.35$
0.5 Hz	0.195	$-0.5 \dots + 0.6$	0.195	$-0.5 \dots + 0.3$
0.75 Hz	0.220	$-0.5 \dots + 0.6$	0.240	$-0.6 \dots + 0.3$
1 Hz	0.348	$-0.6 \dots + 0.7$	0.324	$-0.6 \dots + 0.45$
1.5 Hz	0.725	$-1.1 \dots + 1.5$	0.500	$-0.8 \dots + 0.7$
2.0 Hz	1.126	$-1.5 \dots + 2.0$	0.750	$-1.15 \dots + 1.0$
Total RMSE	2.757	–	2.153	–

Table 4-11: Comparison of RMSE (mm) and maximum tracking error (mm) values of the valve configurations with nominal payload mass M=2 kg and SMC approach.

The sum of the mean RMSE values of control performances for sinusoidal tracking at 0.25, 0.5, 0.75 and 1.0 Hz under payload variation is used as a robustness indicator. It is interesting to see, that servo valve approach is extremely robust to increased payload mass as the tracking performance is maintained up to M=6 kg (see the publication for details). In contrast, the on/off valve approach is capable of maintaining reasonable robustness up to M=4 kg after which the performance starts to degrade more clearly. A significantly better robustness of servo valve approach is due its faster

control loop combined with smaller position dither in the system. As the SMC strategy is quite sensitive to delay and noise, it starts to affect the performance with PWM strategy that results in a 10 ms control delay and more noise due to PWM switching. In order to demonstrate the effect of control delay, the servo valve approach was used with a sampling time T_s=10 ms that corresponds with the PWM 100 Hz. It was noted, that the control delay degrades the control performance especially at higher payload masses decreasing the robustness of the controller. With on/off valve approach the effect of control delay and system noise has a more significant effect on the performance. Another critical factor affecting the controller performances is the value of damping ratio used in the sliding surface design. A smaller damping ratio significantly decreases the magnitude of sensor noise (velocity, acceleration) and in the nominal case a higher value of damping ratio than 0.3 resulted in a poor performance due to magnified noise. It should be noted, that the damping ratio determines the damping properties of the control dynamics. Thus, a small value will provide fast response with low damping resulting in a poor performance with increased system inertia. A higher damping ratio will provide better damping properties with slower response resulting in better performance especially with increased inertia. For that reason, the controllers were not able to provide good results with payload masses much higher than M=6 kg with a damping ratio 0.3.

4.4.4 Conclusions and Contributions

This paper provides a low-cost approach to control pneumatic muscle actuator systems by using high-speed on/off valves instead of costly proportional and servo valves. The system under study consisted of pneumatic muscle actuators in the opposing pair configuration driven by four PWM operated 2/2 on/off valves. In order to provide a comparison between on/off valve and servo valve approaches, a full nonlinear modelling of the system in SISO canonical control form was derived for which SMC strategy was applied. As the resulting controller structure was same for both valve configurations, a direct comparison between the approaches was possible. In nominal conditions, the on/off valve approach resulted in good results as the tracking accuracy was almost identical with the servo valve approach. In terms of maximum tracking error, the servo valve approach provided slightly better performance due to its faster control response at motion reversals when the muscle actuator hysteresis is most significant. At higher tracking frequencies servo valve approach performed better mostly due to its higher flow capacity compared to on/off valve approach. The robustness of the approaches was tested by increasing the payload mass up to 6 kg. It was noted, that servo valve approach was extremely robust against it, but the performance of on/off valve approach started do degrade clearly at higher payloads. This difference between the approaches is

caused by the PWM switching introduced control delay and higher system noise that significantly affects the performance of SMC controlled PWM approaches. However, the results indicate that on/off valve approach can provide a reasonable performance and an interesting option for servo-pneumatic systems with limited uncertainties and parameter variations.

4.5 Experimental Comparisons of Sliding Mode Controlled Pneumatic Muscle and Cylinder Actuators (Accepted for publication in *ASME Journal of Dynamic Systems, Measurement and Control*)

4.5.1 Objectives

Although pneumatic muscle actuators are widely studied they are still rare in industrial applications. The main reasons for this are: their highly nonlinear behavior, lack of simple and effective control strategies for providing sufficient performance, their totally different working principle from the traditional cylinder preventing direct replacement of the cylinder. On the other hand, pneumatic muscle actuators have some advantages over cylinders such as higher force-to-weight ratio and stick-slip free operation that are desirable features in many applications. In order to better address the advantages and disadvantages of pneumatic muscle actuators a comparison of pneumatic position servo system realized with traditional cylinder and pneumatic muscle actuators is performed in this paper.

4.5.2 Approaches

- Two linear pneumatic position servo systems controlled by a servo valve were studied. The first application was composed of pneumatic muscle actuators (Festo MAS10-300) in an opposing pair configuration. In the second application traditional pneumatic asymmetric cylinder (Festo DSNU-25-100-PPV-A) was used. The actuators were mounted horizontally and coupled to a linear slide carrying a payload mass M=5 kg.
- The size of the cylinder was chosen to provide corresponding force range as the pneumatic muscle actuator system. Within the determined working range [-15 mm, 15 mm] the maximum force of the muscle actuator system at the pressure 0.6 MPa is 300 N. The theoretical maximum force of the cylinder is 295 N for a positive stroke. The similar force range of the systems enables the comparison of the applications.
- Both systems were modelled in a SISO canonical control form where control signal U resulted in a symmetric valve opening area for mass flow rate A and B. Traditional mass flow rate model was used, where a flow of an ideal gas through a converging nozzle was assumed. The flow model parameters were obtained by least squares fitting of experimental

data to the respective flow equation. Experimentally determined valve dead zone compensation was used.

- A sliding mode controller based on a 2nd order sliding surface definition and SMC based on integral sliding surface (SMCI) were used as control laws. Initial tuning of the control parameters was done with the help of simulations and then refined with experimental setup. A cost function based on tracking error and control effort was used for determining the boundary layer thickness.
- The performance of the applications was studied with simple point-to-point positioning task as well as with sinusoidal tracking tasks with amplitude 15 mm. The robustness of the system was analyzed by changing the inertia of the system.

4.5.3 Results

Figures 4-11 and 4-12 illustrate the control performance of cylinder and muscle actuator configurations with SMC and SMCI law. It is interesting to see, that the muscle actuator configuration is capable of providing significantly better steady-state accuracy than the cylinder configuration. The cylinder friction introduces a maximum steady-state error of approximately 0.2 mm with SMC. With SMCI the integral action tries to decrease the steady state error, but due to friction introduces overshooting around the target position. In contrast, the muscle actuator configuration with SMC can provide better overall steady state accuracy compared to cylinder approach with a maximum steady-state error of 0.2 mm. With SMCI, the steady state error decreases to approximately ± 0.1 mm with a small dither around the target position. With SMCI approaches, note the overshooting for step-wise commands. This is due to integral action that decreases overall system damping combined with a relative small closed loop damping factor ζ=0.3.

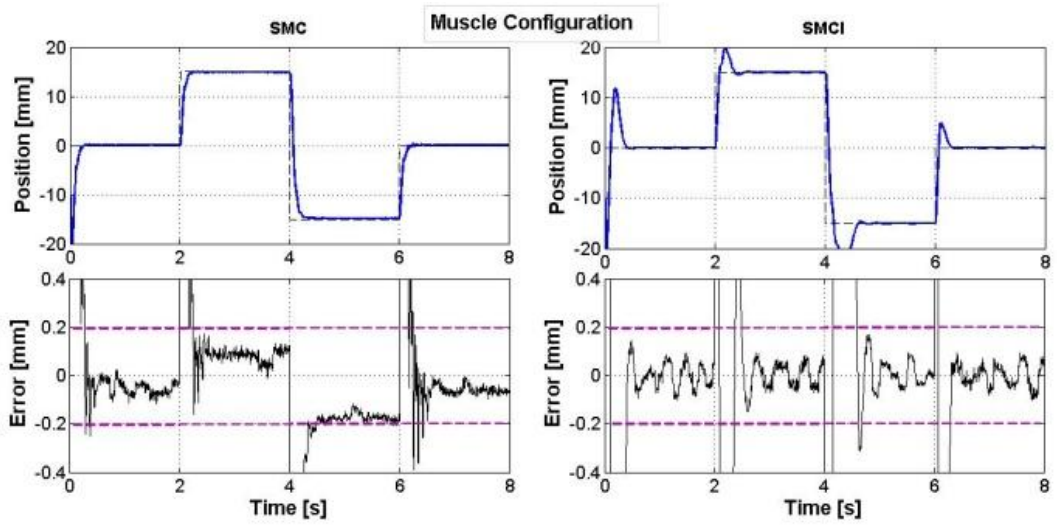

Figure 4-8: Point-to-point positioning with muscle configuration

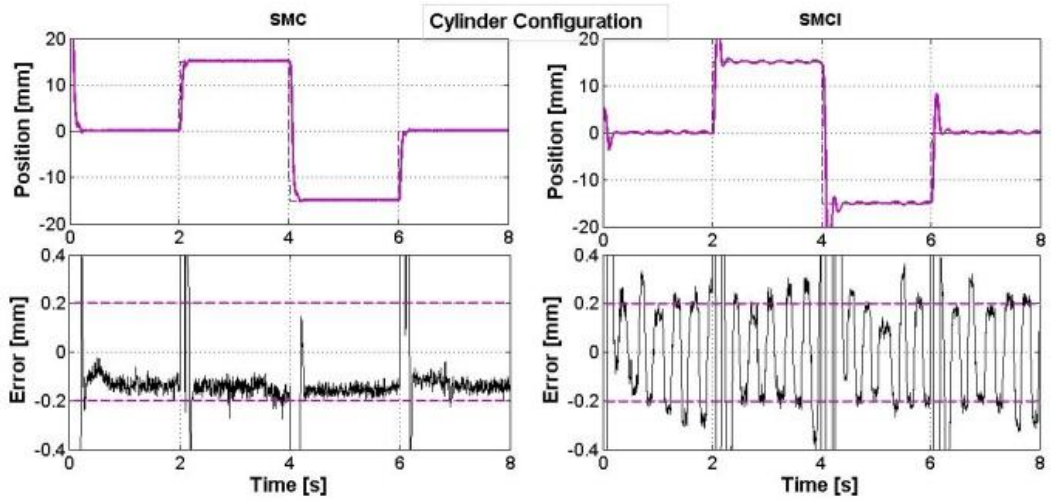

Figure 4-9: Point-to-point positioning with cylinder configuration

The mean RMSE values for the sinusoidal tracking with a nominal payload M=5 kg are gathered in Table 4-12. In Table 4-13 are gathered the maximum errors during the task. It is clearly seen that the integral action can provide better tracking performance compared to traditional SMC especially at lower input frequencies. At higher input frequencies, the integral action causes overshooting at reversals of motion resulting in a decreased performance (see maximum error values). It is very interesting to note, that the best performance at low input frequencies (< 0.5 Hz) is obtained with muscle actuator configuration and SMCI control law. As the muscle actuator can provide a stick-slip free motion, the maximum error at motion reversals is much smaller than with the cylinder reflecting also to the RMSE value. At higher tracking frequencies the cylinder actuator performs clearly better than the muscle actuator. This is caused partially by the higher bandwidth of the cylinder actuator and larger modeling uncertainties in the system with muscle actuators. Figures from 4-13 to 4-15 illustrate the performance of muscle actuator and cylinder system with SMCI control law for sinusoidal tracking 0.25, 1.0 and 1.5 Hz.

Frequency	Muscle SMC	Muscle SMCI	Cylinder SMC	Cylinder SMCI
0.25 Hz	0.164	**0.062**	0.189	0.106
0.5 Hz	0.325	**0.131**	0.209	0.138
0.75 Hz	0.437	0.268	0.231	**0.159**
1.0 Hz	0.560	0.439	0.242	**0.191**
1.5 Hz	0.784	0.865	0.291	**0.268**
2.0 Hz	1.020	1.510	**0.299**	0.332
Total RMSE	3.290	3.276	1.461	1.194

Table 4-12: Comparison with nominal payload *M*=5 kg (RMSE [mm])

Frequency	Muscle SMC	Muscle SMCI	Cylinder SMC	Cylinder SMCI
0.25 Hz	-0.35..0.33	**-0.16..0.20**	-0.45..0.22	-0.41..0.33
0.5 Hz	-0.57..0.40	**-0.33..0.38**	-0.56..0.34	-0.53..0.63
0.75 Hz	-0.73..0.62	-0.56..0.58	-0.70..0.38	**-0.51..0.47**
1.0 Hz	-0.95..0.82	-0.86..0.86	-0.70..0.36	**-0.53..0.60**
1.5 Hz	-1.30..1.10	-1.60..1.60	-0.74..0.50	**-0.67..0.70**
2.0 Hz	-1.60..1.60	-2.50..2.60	**-0.73..0.46**	-0.71..0.75

Table 4-13: Comparison with nominal payload *M*=5 kg (Max. error [mm])

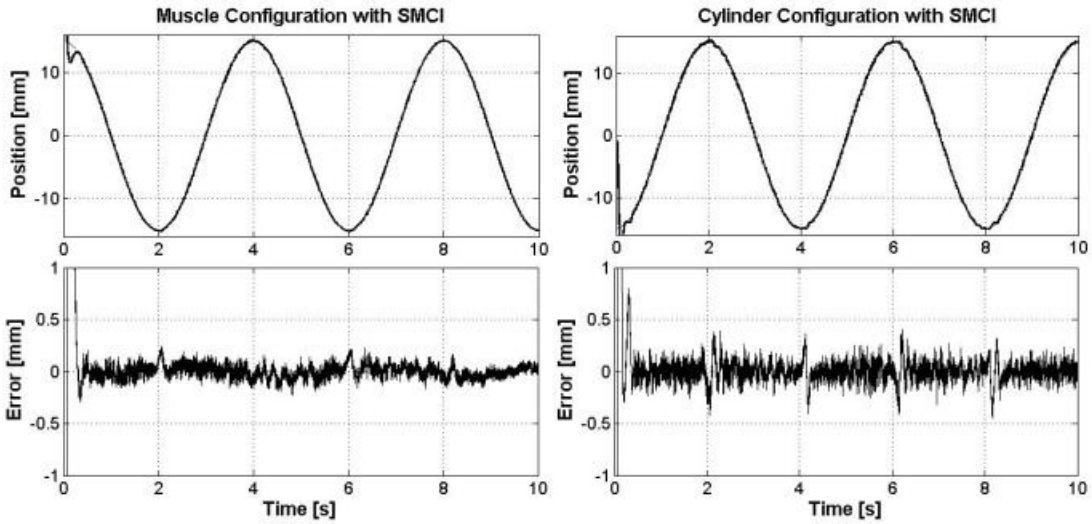

Figure 4-10: Sinusoidal 0.5 Hz tracking

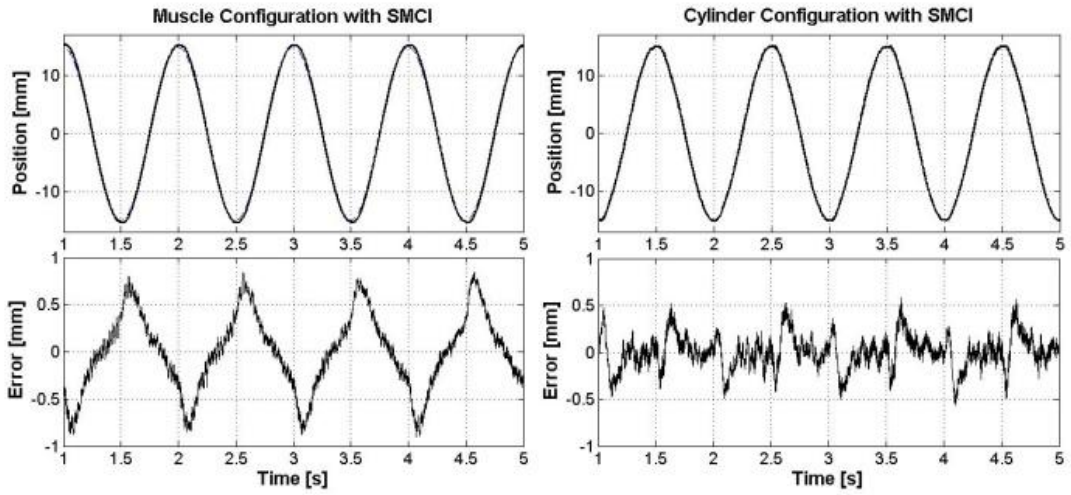

Figure 4-11: Sinusoidal 1.0 Hz tracking

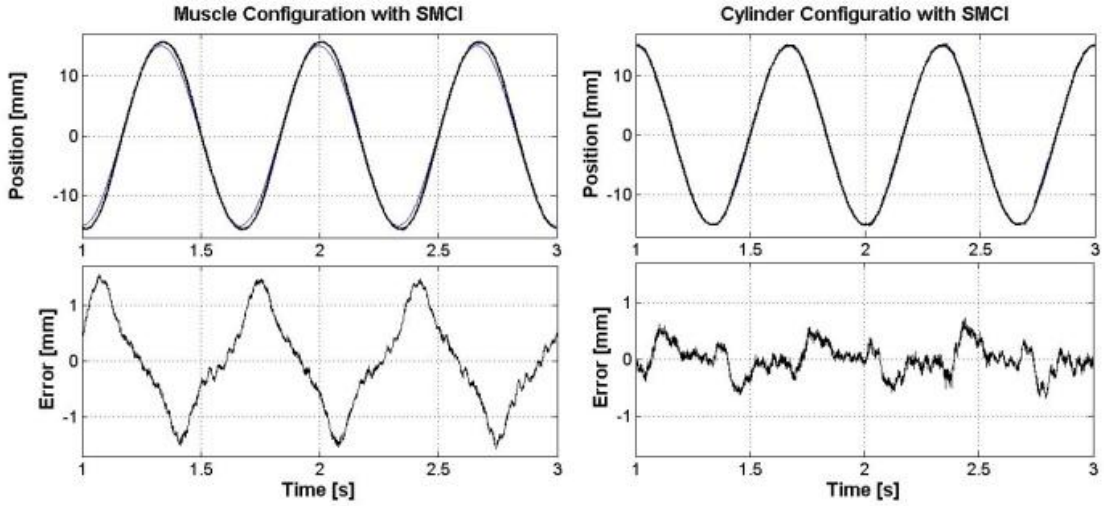

Figure 4-12: Sinusoidal 1.5 Hz tracking

The robustness of the control approaches were tested by changing the payload mass from the nominal M=5 kg. The robustness is validated by calculating the sum of the averaged RMSE values (5 measurements for each) for input frequencies 0.25, 0.5, 0.75 and 1.0 Hz and normalized with respect to the nominal case. Figure 4-13 illustrates that the sliding mode control strategy is not very robust against decreased payload mass. With decreased inertia the control effort is too strong resulting in increased chattering. This could be avoided by selecting a smaller control gains at the cost of losing tracking accuracy in the nominal case. Against increased payload mass the control laws are quite insensitive providing a reasonably good performance in overall. This corresponds well with the fact that the SMC strategy is commonly stated as a robust control law. However, it can be noted that the system with muscle actuators can provide very good robustness as the

performance hardly changes from the nominal case. In case of cylinder actuator, the performance starts to degrade slightly especially at higher inertias mostly due to friction at low velocities.

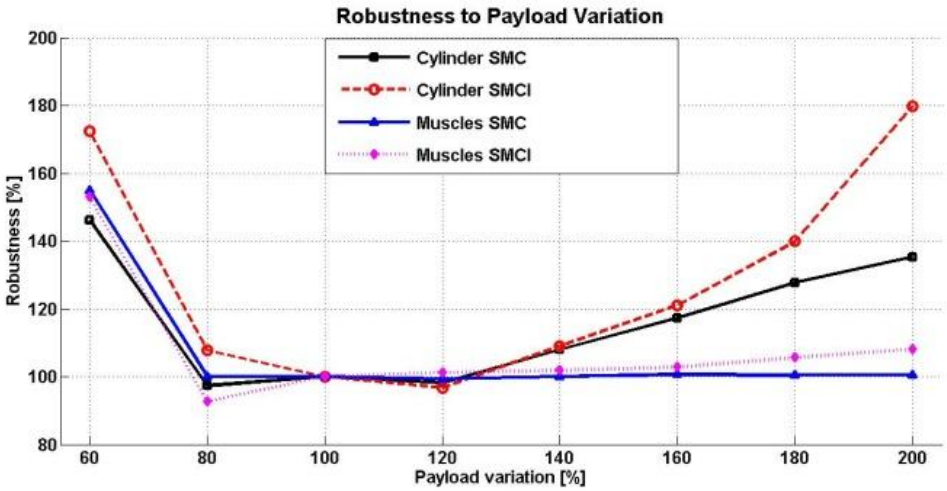

Figure 4-13: Robustness to payload variation

4.5.4 Conclusions and Contributions

A pneumatic muscle actuator is an interesting option to cylinder as it has a very high force-to-weight relation and very low friction. Although widely studied and many control strategies proposed to handle the nonlinearities, the muscle actuators are still not widely used in industrial applications. This is mainly caused by the totally different operating principle compared to traditional cylinder actuator as well as lack of information how and in what conditions the muscle actuator can outperform the cylinder actuator. In this paper, the focus was to experimentally verify and compare the performance of the position servo system composed of muscle actuators to the one composed of a traditional cylinder actuator.

Based on the derived system models given in a SISO affine form, a sliding mode control (SMC) law and SMC law with an integral action (SMCI) were applied. As the resulting controller structures were same for both configurations, a direct comparison between the approaches was enabled. The tuning of the controllers was based on the same criteria with minimizing a cost function where the tracking error and control effort were considered.

The system performances were verified with a simple positioning task and with sinusoidal position tracking tasks. Maximum tracking error and RMSE value were used as performance criteria. It was interesting to note that the system with the muscle actuators resulted in a smaller steady state error and RMSE than the system with the cylinder for positioning task as well as for low frequency (<0.5 Hz) sinusoidal tracking task. This was caused by the stick-slip free smooth

operation of muscle actuators at low velocities, whereas the static friction degrades the performance with the cylinder actuator. At higher tracking frequencies the cylinder actuator outperformed the muscle actuators. Reasons for this are the higher bandwidth of the cylinder actuator and probably smaller modeling errors. With SMCI approach the system performance could be significantly improved at low tracking frequencies. At higher frequencies, the overshooting at motion reversals started to increase the tracking error. It was also notable, that the steady state error increased with cylinder and SMCI compared to SMC as the friction caused small oscillations around the target position. In case of muscle actuators this phenomena was significantly smaller. The robustness of the approaches was tested by changing the payload mass from 60 to 200 %. It was noted, that the system with muscle actuators was very robust to increased payload mass resulting in almost no change in the performance compared to nominal case. With the cylinder the performance started to degrade at higher payload masses (more with SMCI) mostly due to friction at smaller tracking frequencies. It was also noted, the performance of all approaches started to decrease at smaller inertias, which is quite typical effect for SMC strategy due to increased chattering.

5. CONCLUSIONS, KEY RESULTS AND CONTRIBUTIONS

In this thesis, the focus of the research work was on the modeling and control of the pneumatic muscle actuator based system for position servo applications. Introduction to the research problem and literature review of the topic were discussed in the beginning of the thesis. The five publications that have been published or submitted for review were summarized with respect to the objectives, approaches, results, conclusions and research contributions.

The overall objective of the research work was to provide information and new findings for pneumatic servo applications based on pneumatic muscle actuator. A particular pneumatic positioning system based on single or double muscle actuators controlled by on/off or servo valve was used. The key conclusions and results of this research are summarized as following.

1. An accurate model of the nonlinear pneumatic system is a key feature for analysis and control design. The simulation of the system is very efficient way to analyze, verify and test new control strategies. Especially, in case of nonlinear system its' importance is even higher. The pneumatic muscle actuator system controlled by on/off valves results in a very nonlinear system.
    a. An accurate prediction of nonlinear force characteristics of the muscle actuator is important to the analysis and investigation of muscle actuator based systems. A novel force model developed in this work provided accurate force prediction of muscle actuator used in this work. Also, frictional characteristics including hysteresis were studied.
    b. The modeling of mass flow characteristics of the control valve is very important to the analysis of the system as well as from the viewpoint of control design. For simulation purposes, a detailed model of the on/off valve was developed based on analytical and empirical methods. From the point of view of control design, the discontinuous switching is difficult to handle. In order to provide a continuous valve flow model, a recently introduced method of 2^{nd} order bi-polynomial function was utilized and applied for determining an accurate prediction of flow as a function of pressure and PWM duty ratio. As the resulting model is invertible, the flow model can be utilized in the control design loop to remove the nonlinear flow characteristics from the model used in the controller design. As a result, the flow model enables the use of effective linear tools for analysis and stability as well as the use of analytical model-based control approaches.

2. Due to highly nonlinear nature of the system under study, a sliding mode control (SMC) approach was chosen for control law. The SMC approach should provide means for accurate control of nonlinear systems as well as guarantee robustness to modeling errors and uncertain parameters. The effectiveness of the SMC approach with its variants SMCL, SMCNL and SMCI were compared to a conventional PVA+FF control law.
    a. As expected, the results indicated that PVA+FF and SMCL resulted in almost identical performance with a similar set of feedback gains. By using the boundary layer approach with SMC, the control law transforms into a state feedback controller (comparable to PVA) as the system enters the boundary region. The main difference between the approaches is thus in the computation of model-based component; equivalent control term with SMC and feed-forward (FF) term with PVA+FF. As the FF control component uses desired state vectors as inputs and the inverse of the linear system model, the resulting control signal is noiseless. In contrast, with SMC the equivalent term is computed based on the error of desired and measured states. Thus, the noise associated with estimated velocity and acceleration signals affects the control performance negatively.
    b. With a similar set of feedback gains, SMC approach based on the nonlinear system model can improve the tracking performance approximately by 15 % compared to above mentioned linear approaches. This difference becomes from the better prediction of desired control action through computed equivalent control term.
    c. Sliding mode control with an integral sliding surface (SMCI) can provide a significant tracking improvement (up to 40 %) compared to nonlinear SMC. The advantage of integral action becomes significant especially with low frequency tracking tasks as the tracking error is decreased during the movement. It was notable, that the effectiveness of the integral action decreased with higher frequencies, especially due to overshooting when the direction of the movement was changed. Combined with the hysteresis of the muscle actuator and integral wind-up the maximum tracking error increased in those cases.
3. Commonly, SMC approach is considered as a “high gain” state feedback controller. However, in case of PWM-pneumatics this is not true. It was notable, that SMC approaches (SMCL and SMCNL) did not enable use of higher control gains than PVA+FF approach. This was caused by the PWM control delay where the control signal is sampled once per PWM cycle. Thus, the PWM delay is very harmful reducing the performance and robustness of the SMC approach.

4. The used PWM frequency has a significant effect on the system performance. The PWM frequency should be significantly higher than the system dynamics in order to provide smooth flow. However, the maximum PWM frequency is limited by the speed of the valve as the switching time determines the maximum reasonable frequency. In this work, the effect of PWM frequency was studied by operating the system with PWM frequencies 50 Hz and 100 Hz. It was notable, that the higher PWM frequency resulted in clearly better performance in terms of tracking accuracy and robustness. The faster control loop results in smaller dither in the position signal as well as enables the use of higher low-pass cut-off frequencies for estimating the velocity and acceleration from the measured position. Thus, the choice of filter cut-off frequency is a trade-off between the phase delay and noise. Simulation and experimental studies indicated that higher PWM frequency enabled the use of higher cut-off frequencies. In addition, higher PWM frequency enables higher control gains improving the tracking performance. Also, due to faster control loop a better robustness to parameter variations and disturbances is obtained. Ideally, in order to better exploit the advantages of SMC strategy the PWM frequency should be as high as possible requiring faster control valves.
5. The main advantage of on/off valves for controlling the actuator is their low economical cost compared to traditional servo valve system. However, it should be clear that it is difficult to obtain better or even similar performance as with servo valves. As the literature lacks studies of the comparison between PWM-operated on/off valve and traditional servo valve controlled pneumatic systems, they are discussed in Publication 3 and 4. In Publication 3, three different valve configurations (single 3/2 on/off, dual 2/2 on/off and servo) were experimentally compared with a setup where single muscle actuator was driving a cylinder load. In Publication 4, the two muscle actuators in an opposing pair configuration controlled by four 2/2 on/off valves and single servo valve was studied.
    a. Due to similar mechanical system structure and similar valve flow modeling using inverse mapping, the resulting system model used for control design enables the use of similar SMC structure. Then, a switching gain was defined based on the velocity requirements of the system leaving the boundary layer thickness as the only control parameter to adjust for each case individually. This kind of procedure made it possible to compare performance characteristics of different valve configurations for tracking tasks and robustness to parameter variations and external disturbances. The results indicated that PWM-operated on/off valve approach can provide a compatible performance for servo valve approach. Especially, the system with two on/off valves

can provide similar tracking accuracy in nominal conditions as the servo valve approach. The performance of single on/off valve approach was not as good as with the others. However, it should be noted that the single valve approach is certainly cheapest of the configurations and is still capable of providing reasonable performance. The disadvantages of on/off valve approaches arise when the system parameters change. The robustness tests showed that the servo valve approach performed much better with increased payload mass than the on/off valve approaches. With decreased payload mass, the performance of the servo valve approach decreased due to increased control chattering. In contrast, the on/off valve approaches showed good robustness to decreased inertia. The servo valve approach was the most robust against bounded external disturbances due to its faster control loop. Thus, the problem of on/off valve approaches to increased inertia can be summarized as a combination of signal noise (due to PWM switching) and the PWM introduced control delay. In overall, under nominal conditions, the PWM actuated on/off valve controlled muscle actuator system can provide a considerable low-cost option for servo valve controlled system at present valve technology.

b. In Publication 4, the system under study consisted of pneumatic muscle actuators in the opposing pair configuration driven by four PWM operated 2/2 on/off valves or servo valve. In this case, a traditional mass flow rate model commonly used with servo valves was used also with on/off valve case. Thus, the system models were again comparable enabling similar control approach and comparison. In nominal conditions, the on/off valve approach resulted in good results as the tracking accuracy was almost identical with the servo valve approach. In terms of maximum tracking error, the servo valve approach provided slightly better performance due to its faster control response at motion reversals when the muscle actuator hysteresis is most significant. At higher tracking frequencies servo valve approach performed better mostly due to its higher flow capacity (although the nominal flow capacities were the same) compared to on/off valve approach. The robustness of the approaches was tested by increasing the payload mass up to 300 %. Similar result were obtained as in Publication 3 as the servo valve approach was extremely robust against it, but the performance of on/off valve approach started do degrade clearly at higher payloads. In overall, the results indicate that on/off valve approach can provide a reasonable performance and an interesting option for servo-pneumatic systems with bounded uncertainties and parameter variations at present technology.

6. A pneumatic muscle actuator is an interesting option to cylinder as it has a very high force-to-weight relation and stiction-free operation. Although widely studied and many control strategies proposed to handle the nonlinearities, the muscle actuators are still not widely used in industrial applications. This is mainly caused by the totally different operating principle compared to traditional cylinder actuator as well as lack of information how and in what conditions the muscle actuator can outperform the cylinder actuator. In (4.5), a position servo system realized with muscle actuators was compared to one realized with traditional cylinder actuator. Both systems were controlled by servo valve and SMC or SMCI law. Following are the main findings.
    a. Simple step-wise positioning tasks showed that the system with the muscle actuators controlled by SMC law resulted in a lower steady-state error than the system with the cylinder actuator. This was caused by the stick-slip free smooth operation of muscle actuators, whereas the static friction degrades the performance with the cylinder actuator. Both systems were tested also with SMCI control law in order to provide better steady state accuracy. It was observed, that the steady state error increased with cylinder and SMCI compared to SMC as the friction caused small oscillations around the target position. In case of muscle actuators, the SMCI improved the steady state accuracy (less that 0.1 mm) although slight oscillatory behavior was observed around the desired position. However, compared to cylinder the performance was significantly better.
    b. In sinusoidal tracking tasks the muscle actuator system outperformed the cylinder at low frequencies (<0.5 Hz) with both SMC and SMCI strategies. At higher tracking frequencies the cylinder actuator outperformed the muscle actuators. Reasons for this are the higher nominal bandwidth of the cylinder actuator and probably smaller modeling errors. With SMCI approach the system performance could be significantly improved at low tracking frequencies. At higher frequencies, the overshooting at motion reversals started to increase the tracking error.
    c. The robustness of the approaches was tested by changing the payload mass from 60 to 200 %. It was noted, that the system with muscle actuators was very robust to increased payload mass resulting in almost no change in the performance compared to nominal case. With the cylinder the performance started to degrade at higher payload masses (more with SMCI) mostly due to friction at smaller tracking frequencies. It was also noted, the performance of all approaches started to decrease

at smaller inertias, which is quite typical effect for SMC strategy due to increased chattering.

BIBLIOGRAPHY

Ahn, K. K., Thanh, T. D. C. (2004). Improvement of the Control Performance of Pneumatic Artificial Muscle Manipulators Using an Intelligent Switching Control Method. *KSME International Journal ,* Vol.18, No. 8, pp.1388-1400.

Ahn, K. K., Thanh, T. D. C. (2005a). Nonlinear PID Control to Improve the Control Performance of the Pneumatic Artificial Muscle Manipulator Using Neural Network. *Journal of Mechanical Science and Technology,* Vol.19, No. 1, pp.106-115.

Ahn, K. K., Thanh, T. D. C., Ahn, Y. K. (2005b). Performance Improvement of Pneumatic Artificial Muscle Manipulators Using Magneto-Rheological Brake. *Journal of Mechanical Science and Technology (KSME International Journal),* Vol.19, No. 3, pp.778-791.

Ahn, K. K., Yokota, S. (2005). Intelligent Switching Control of Pneumatic Actuator Using On/off Solenoid Valves. *Mechatronics ,* Vol.15, pp.683-702.

Aschemann, H., Hofer, E. P. (2004). Flatness-based Trajectory Control of Pneumatically Driven Carriage with Uncertainties. *Proceedings of NOLCOS*, Stuttgart, Germany, pp. 239-244.

Aschemann, H., Hofer, E. P. (2005). Flatness-based Trajectory Planning and Control of a Parallel Robot Actuated by Pneumatic Muscles. *Proceedings of ECCOMAS Thematic Conference on Multibody Dynamics*, Madrid, Spain, (pp. CD-ROM).

Aschemann, H., Schindele, D. (2007). Sliding Mode Control of a Linear Axis Driven by Pneumatic Muscle Actuators. *Proceedings of MMAR*, Miedzyzdroje, Poland, (pp. CD-ROM).

Aschemann, H., Schindele, D. (2008). Sliding-Mode Control of a High-Speed Linear Axis Driven By Pneumatic Muscle Actuators. *IEEE Transactions on Industrial Electronics ,* Vol. 55, No. 11, pp. 3855-3864.

Aschemann, H., Schindele, D., Hofer, E. P. (2006). Nonlinear Trajectory Control of a High-speed Linear Axis Driven by Pneumatic Muscle Actuators. *Proceedings of IECON*, Paris, France, pp. 3857-3862.

Balasubramanian, K., Rattan, K., (2003a). Fuzzy Logic Control of a Pneumatic Muscle System Using a Linearizing Control Scheme. *Int. Conf. North American Fuzzy Information Processing Society*, pp. 432-436.

Balasubramanian, K., Rattan, K., (2003b). Feed-forward Control of a Nonlinear Pneumatic Muscle System Using Fuzzy Logig. *IEEE Int. Conf. on Fuzzy Systems*, Vol. 1, pp. 272-277.

Baldwin, H. A. (1969). Realizable Models of Muscle Function. *Proceedings of the First Rock Biomechanics Symposium*, New York, USA, pp. 139-148.

Barth, E. J., Zhang, J., Goldfarb, M. (2003). Control Design for Relative Stability in a PWM-Controlled Pneumatic Systems. *ASME Journal of Dynamic Systems, Measurement and Control* , Vol. 125, No. 3, pp. 504-508.

Barth, E. J., Zhang, J., Goldfarb, M. (2002). Sliding Mode Approach to PWM-controlled Pneumatic Systems. *The American Control Conference*, Anchorage, AK., pp. 2362-2367.

Bobrow, J. E., Jabbari, F. (1991). Adaptive Pneumatic Force Actuation and Position Control. *ASME Journal of Dynamic Systems, Measurement and Control* , Vol. 113, pp. 267-272.

Bobrow, J. E., McDonell, B. (2002). Modeling, Identification, and Control of a Pneumatically Actuated, Force Controllable Robot. *IEEE Transactions on Robotics and Automation*, Vol. 14, No.5, pp. 732-742.

Brun, X., Belgharbi, M., Sesmat, S., Scavarda, S. (1999). Control of an electropneumatic actuator: Comparison Between Some Linear and Non-linear Control Laws. *Proceedings of the Institution of Mechanical Engineers, Part 1: Journal of Systems and Control Engineering*, pp. 387-405.

Brun, X., Thomasset, D., Bideaux, E. (2002). An Accurate Tracking Control of an Electropneumatic Actuator. *1st Fluid Power Net International Ph.D Symposium*, pp. 215-226.

Burrows, C. R. (1966). Use of Root Loci in Design of Pneumatic Servo-Motors. In *Control*, pp. 469-477.

Burrows, C. R. (1969). Effect of Position of the Stability of Pneumatic Servomechanisms. *Journal Mechanical Engineering Science* , Vol.11, No. 6, pp.615-616.

Caldwell, D. G., Medrano-Cerda, G. A., Goodwin, M. J. (1993). Braided Pneumatic Actuator Control of a Multi-Joined Manipulator. *Proceedings of the IEEE International Conference on Systems, Man and Cybernetics*, Le Touquet, France, pp. 423-428.

Caldwell, D. G., Razak, A., Goodwin, M. J. (1993). Braided Pneumatic Muscle Actuators. *IFAC Conference on Intelligent Autonomous Vehicles.* Southampton, UK.

Caldwell, D. G., Medrano-Cerda, G. A., & Goodwin, M. J. (1995). Control of Pneumatic Muscle Actuators. *IEEE Control Systems Magazine* , Vol. 15 , No. 1, pp.40-48.

Caldwell, D. G., Tsagarakis, N., Medrano-Cerda, G. A. (2000). Biomimetic Actuators: Polymeric Pseudo Muscular Actuators and Pneumatic Muscle Actuators. *Mechatronics*, Vol.10, pp.499-530.

Carbonell, P., Jiang, Z. P., Repperger, D. W. (2001a). Nonlinear Control of a Pneumatic Muscle Actuator: Backstepping vs. Sliding-Mode. *Proceedings of IEEE International Conference on Control Applications*, pp. 167-172.

Carbonell, P., Jiang, Z.-P., Repperger, D. W. (2001b). A Fuzzy Backstepping Controller for a Pneumatic Muscle Actuator System. *Proceeding of the 2001 IEEE Int. Symp. on Intelligent Control*, pp.353-358.

Carbonell, P., Jiang, Z.-P., Repperger, D. W. (2001c). A Comparative Study of Nonlinear Control of a Pneumatic Muscle Actuator System. *Proceeding of the 5th IFAC Symp. on Nonlinear Control Systems*.

Chan, S. W., Lilly, J. H., Repperger, D. W., Berlin, J. E. (2003). Fuzzy PD+I Learning Control for a Pneumatic Muscle. *Proceedings of IEEE International Conference on Fuzzy Systems*, Vol. 1, pp. 278-283.

Chen, C.-L., Chen, P.-C., Chen, C.-K. (1993). A Pneumatic Model-Following Control System Using a Fuzzy Adaptive Controller. *Automatica* , Vol.29, No. 4, pp.1101-1105.

Chen, H.-M., Chen, Z.-Y., Chung, M.-C. (2009). Implementation of an Integral Sliding Mode Controller for a Pneumatic Cylinder Position Servo Control System. *2009 Fourth International Conference on Innovative Computing, Information and Control*, pp. 552-555.

Chiang, M.-H., Chen, C.-C., Tsou, T.-N. (2005). Large Stroke and High Precision Pneumatic-Piezoelectric Hybrid Positioning Control Using Adaptive Discrete Variable Structure Control. *Mechatronics* , Vol. 15, No. 5, pp. 523-545.

Choi, S. H., Ahn, C., Lee, C. O. (1995). Application of Fuzzy Logic Adaptor to the Position COntrol of a Pneumatic System Using On-Off Valves. *FRST-Vol. 2 Fluid Power Systems and Technology ASME*, pp. 21-28.

Chou, C.-P., Hannaford, B. (1996). Measurement and Modeling of a McKibben Pneumatic Artificial Muscles. *IEEE Transactions on Robotics and Automation* , Vol. 12, No. 1, pp.90-102.

Colbrunn, R. W., Nelson, G. M., Quinn, R. D., (2001a). Design and Control of a Robotic Leg with Braided Pneumatic Actuators. *Proceedings of the 2001 IEEE/RSJ Int. Conf. on Intelligent Robots and Systems* , Hawaii, USA, pp. 992-998.

Colbrunn, R. W., Nelson, G. M., Quinn, R. D., (2001b). Modeling of Braided Pneumatic Actuators for Robotic Control. *Proceedings of the 2001 IEEE/RSJ Int. Conf. on Intelligent Robots and Systems* , Hawaii, USA, pp. 1964-1970.

Daerden, F., Lefeber, D. (2002). Pneumatic artificial muscles: actuators for robotics and automation. *European Journal of Mechanical and Environmental Engineering* , Vol.47, No.1, pp. 10-21.

Davis, S., Caldwell, D. G. (2006). Braid Effects on Contractile Range and Friction Modeling in Pneumatic Muscle Actuators. *International Journal of Robotics Res.* , Vol.25, No. 4, pp.359-369.

De Haven, H. (1949). *Patent No. 2,483,088.* USA.

Drakunov, S., Hanchin, G. D., Su, J., Özguner, U. (1997). Nonlinear Control of a Rodless Pneumatic Servoactuator, or Sliding Modes Versus Coulomb Friction. *Automatica* , Vol. 33, No.7, pp. 1401-1408.

Festo. (2002). *Fluidic Muscle MAS, Festo Brochure.*

Fok, S. C., Ong, E. K. (1999). Position Control and Repeatibility of a Pneumatic Rodless Cylinder System for Continuous Positioning. *Robotics and Computer Integrated Manufacturing* , Vol. 15, pp. 365-371.

Gao, X., Feng, Z.-I. (2005). Design Study of an Adaptive Fuzzy-PD Controller for Pneumatic Servo System. *Control Engineering Practice* , Vol. 13, pp. 55-65.

Gaylord, R. H. (1958). *Patent number 2,844,126.* USA.

Gentile, N., Giannoccaro, N. I. (2002). Experimental Tests on Position Control of a Pneumatic Actuator Using On/Off Solenoid Valves. *IEEE/ICIT Conference on Industrial Technology,* Bangkok, Thailand, pp. 555-559.

Grancharova, A., Johansen, T. A. (2011). Design and Comparison of Explicit Model Predictive Controllers for an Electropneumatic Clutch Actuator Using On/Off Valves. *IEEE/ASME Transactions on Mechatronics* , Vol. 16, No.4, pp. 665-673.

Gross, D. C., Rattan, K. S. (1998). An Adaptive Multilayer Neural Network for Trajectory Tracking Control of a Pneumatic Cylinder. *System, Man and Cybernetics 1998 IEEE International Conference*, Vol.2, pp. 1662-1667.

Guenther, R., Perondi, E.A., de Pieri, E.R., Valdiero, A.C., (2006). Cascade Controlled Pneumatic Positioning System with LuGre Model Based Friction Compensation. *Journal of Brasilian Society of Mechanical Sciences & Engineering,* Vol. 28, No. 1, pp. 48-57.

Hamerlain, M., (1995). An Anthropomorphic Robot Arm Driven by Artificial Muscles Using a Variable Structure Control. *IEEE/RSJ Int. Conf. Intelligent Robots and Systems* , Vol. 1, pp. 550-555.

Hamiti, K., Voda-Besanqon, A., Roux-Boisson, H. (1996). Position Control of a Pneumatic Cylinder Under the Influence of Stiction. *Control Engineering Practice* , Vol. 4, No. 8, pp. 1079-1088.

Hesselroth, T., Sarkar, K., van der Smagt, P., Schulten, K. (1994). Neural Network Control of a Pneumatic Robot Arm. *IEEE Trans. Syst. Man. Cybernetics,* Vol. 24, No. 1, pp. 28-38.

Hildebrandt, A., Sawodny, O., Neumann, R., Hartmann, A. (2002). A Flatness Based Design For Tracking Control of Pneumatic Muscle Actuators. *Proceedings of 7th International Conference on Automation, Robotics and Vision*, Singapore, pp. 1151-1161.

Inoue, K. (1987). Rubbertuators and Applications for Robotics. *4th International Symposium on Robotics,* pp. 57-63

Iordanou, H. N., Surgenor, B. W. (1997). Sliding Surface Design for Discrete Sliding Mode Control and Application to a Pneumatic Positioning System. *10th International Bath Fluid Power Workshop.* Bath, UK.

ISO6358. (1989). *Pneumatic Fluid Power - Components using Compressible Fluids - Determination of Flow-rate Characteristics.*

Jeon, Y.-S., Lee, C.-O., Hong, Y.-S. (1998). Optimization of the Control Parameters of a Pneumatic Servo Cylinder Drive Using Genetic Algorithms. *Control Engineering Practice* , Vol.6, No. 7, pp.847-853.

Kaitwanidvilai, S., Parnichkun, M. (2005). Force Control in a Pneumatic System Using Hybrid Adaptive Neuro-Fuzzy Model Reference Control. *Mechatronics* , Vol. 15, pp.23-41.

Kawamura, S., Miyata, K., Hanafusa, H., Isida, K. (1989). PI-type Hierarchical Feedback Control Scheme for Pneumatic Robots. *IEEE International Conference on Robotics and Automation*, Vol. 3, pp. 1853-1858.

Kerscher, T., Albiez, J., Zöllner, J. M., Dillman, R. (2005). Evaluation of the Dynamic Model of Fluidic Muscles Using Quick-Releases, *The First IEEE/RAS-EMBS International Conference on Biomedical Robotics and Biomechatronics*, Pisa, Italy, pp.637-642.

Khayati, K., Bigras, P., Dessaint, L.-A. (2008). Force Control Loop Affected by Bounded Uncertainties and Unbounded Inputs for Pneumatic Actuator Systems. *JASME Journal of Dynamic Systems, Measurement, and Control* , Vol.130, No.1, 9 pages

Khayati, K., Bigras, P., Dessaint, L.-A. (2009). LuGre Model-Based Friction Compensation and Positioning Control for a Pneumatic Actuator Using Multi-Objective Output-Feedback Control via LMI Optimization. *Mechatronics* , Vol.19, No.9, pp. 535-547.

Kimura, T., Hara, S., Fujita, T., Kagawa, T. (1995). Control for Pneumatic Actuator Systems Using Feedback Linearization with Disturbance Rejection. *Proceedings of the 1995 American Control Conference*, Seattle, WA, USA, pp. 825-829.

Kimura, T., Hara, S., Fujita, T., Kagawa, T. (1997). Feedback Linearization for Pneumatic Actuator Systems with Static Friction. *Control Engineering Practice* , Vol.5, No.10, pp. 1385-1394.

Kingsley, D. A., Quinn, R. D. (2002). Fatigue life and frequency response of braided pneumatic actuators. *IEEE International Conference on Robotics and Automation Conference.* Washington, USA, pp. 2830-2835.

Klute, G. K., Hannaford, B. (1998). Fatigue Characteristics of McKibben Artificial Muscle Actuators. *Proceedings of the IEEE/RSJ International Conference on Intelligent Robots and Systems.* Victoria, Canada.

Klute, G. K., Czerniecki, J. M., Hannaford, B. (2002). Artificial Muscles: Actuators for Biorobotic Systems. *International Journal of Robotics Research* , Vol. 21, pp.295-309.

Klute, G. K., Czerniecki, J. M., Hannaford, B. (1999). McKibben Artificial Muscles: Pneumatic Actuators with Biomechanical Intelligence. *International Conference on Advanced Intelligent Mechatronics,* Atlanta, USA, pp. 221-226.

Kunt, C., Singh, R. (1990). A Linear Time Varying Model For On-Off Valve Controlled Pneumatic Actuators. *ASME Journal of Dynamic Systems, Measurement and Control* , Vol. 112, pp. 740-747.

Lai, J.-Y., Menq, C.-H., Singh, R. (1990). Accurate Position Control of a Pneumatic Actuator. *ASME Journal of Dynamic Systems, Measurement and Control* , Vol. 112, pp. 734-739.

Lai, J.-Y., Singh, R., Menq, C.-H. (1992). Development of PWM Mode Position Control for a Pneumatic Servo System. *Journal of the Chinese Society of Mechanical Engineers* , Vol. 13, No.1, pp. 86-95.

Langjord, H., Johansen, T. A., Bratli, C. (2009). Dual-mode Switched Control of an Electropneumatic Clutch Actuator with Input Restrictions. *Proceedings of European Control Conference*, Budapest, Hungary, pp. 2085-2090.

Langjord, H., Johansen, T. A., Hespanha, J. P. (2008). Switched Control of an Electropneumatic Clutch Actuator Using On/Off Valves . *Proceedings of American Control Conference*, Seattle, WA, USA, pp. 1513-1518.

Lee, H. K., Choi, G. S., Choi, G. H. (2002). A study on Tracking Position Control of Pneumatic Actuators. *Mechatronics* , Vol.12, pp.813-831.

Lilly, J. H. (2003). Adaptive tracking for Pneumatic Muscle Actuator in Bicep and Tricep Configurations. *IEEE Transactions on Neural Systems and Rehabilitation Engineering* , Vol. 11, No.3, pp.333-339.

Lilly, J. H., Yang, L. (2005). Sliding Mode Tracking for Pneumatic Actuators in Opposing Pair Configuration. *IEEE Transactions on Control Systems Technology* , Vol. 13, No.4, pp. 550-558.

Linnett, J. A., Smith, M. C. (1989). An Accurate Low-Friction Pneumatic Position Control System. *Proceedings of Institution of Mechanical Engineering, Part B, Journal of Engineering Manufacture,* pp.159-165.

Liu, S., Bobrow, J. E. (1988). An Analysis of a Pneumatic Servo System and Its Application to a Computer-Controlled Robot. *ASME Journal of Dynamic Systems, Measurement, and Control* , Vol.110, pp. 228-235.

Marchant, J. A., Street, M. J., Gurney, P., Bensin, J. A. (1988). Design and Testing of a Servo Controller for Pneumatic Cylinders. *Proceedings of Institution of Mechanical Engineering, Part E, Journal of Process Mechanical Engineering* , pp. 21-27.

Matsukuma T., Fujiwara, A., Namba, M., Ishida, Y. (1997). Non-linear PID Controller Using Neural Networks. *The 1997 IEEE International Conference on Neural Networks*, Houston, USA, pp. 811-814.

McDonell, B. W. (1996). *Modeling, Identification, and Control of a Pneumatically Actuated Robotic Manipulator.* Ph.D Thesis, Department of Mechanical Engineering, University of California, Irvine, USA.

McDonell, B. W., Bobrow, J. E. (1993). Adaptive Tracking Control of an Air Powered Robot Actuator. *ASME Journal of Dynamic Systems, Measurement and Control* , Vol. 115, pp. 427-433.

Medrano-Cerda, G. A., Bowler, C. J., Caldwell, D. G. (1995). Adaptive Position Control of Antagonistic Pneumatic Muscle Actuators. *IEEE/RSJ International Conference on Intelligent Robots and Systems*, Vol.1, Pittsburgh, pp. 378-383.

Meng, D., Tao, G., Zhu, X. (2013). Adaptive Robust Motion Trajectory Tracking Control of Pneumatic Cylinders. *Journal of Central South University*, Vol.20, No.12, pp. 3445-3460.

Messina, A., Giannoccaro, N. I., Gentile, A. (2005). Experimenting and Modeling the Dynamics of Pneumatic Actuators Controlled by Pulse Width Modulated (PWM) Technique. *Mechatronics* , Vol.15, pp. 859-889.

Moore, P. R., Weston, R., Thatcher, T. W. (1985). Compensation in Pneumatically Actuated Servomechanisms. *Trans Inst M C* , Vol.7, No.5, pp. 238-244.

Moore, P., Ssenkungo, F. W., Weston, R. H., Thatcher, T. W., Harrison, R. (1986). Control Strategies for Pneumatic Servo Drives. *International Journal of Production Research* , Vol. 24, No.6, pp. 1363-1382.

Morita, Y. S., Shimizu, M., Kagawa, T. (1985). An Analysis on Pneumatic PWM and Its Application to a Manipulator. *Proceedings of International Symposium on Fluid Control and Measurement*, Tokyo, Japan, pp. 3-8.

Nguyen, T., Leavitt, J., Jabbari, F., Bobrow, J. E. (2007). Accurate Sliding-Mode Control of Pneumatic Systems Using Low-Cost Solenoid Valves. *IEEE/ASME Transactions on Mechatronics* , Vol. 12, No.2, pp. 216-219.

Ning, S., Bone, G. M. (2005). Experimental Comparison of Two Pneumatic Servo Position Control Algorithms. *Proceedings of the IEEE International Conference on Mechatronics & Automation*, Niagara Falls, Canada, pp. 37-42.

Ning, S., Bone, G. M. (2007). Experimental Comparison of Position Tracking Control Algorithms for Pneumatic Cylinder Actuators. *IEEE/ASME Transactions on Mechatronics* , Vol. 12, No.5, pp. 557-561.

Noritsugu, T. (1985). Pulse-Width Modulated Feedback Force Control of a Pneumatically Powered Robot Hand. *Proceedings of International Symposium on Fluid Control and Measurement*, Tokyo, Japan, pp. 47-52.

Noritsugu, T. (1987a). Development of PWM Mode Electro-Pneumatic Servomechanism, Part I: Speed Control of a Pneumatic System. *Journal of Fluid Control* , Vol. 7, No.1, pp. 65-79.

Noritsugu, T. (1987b). Development of PWM Mode Electro-Pneumatic Servomechanism, Part II: Position Control of a Pneumatic System. *Journal of Fluid Control* , Vol. 17, No.2, pp. 7-28.

Noritsugu, T.;& Takaiwa, M. (1995). Robust Positioning Control of Pneumatic Servo System with Pressure Control Loop. *IEEE International Conference on Robotics and Automation*, Vol. 3, Nagoya, Japan, pp. 2613-2618.

Nouri, A. S., Gauvert, C., Tondu, B., Lopez, P. (1994). Generalized Variable Structure Model Reference Adaptive Control of One-Link artificial Muscle Manipulator in Two Operating Modes. *Proceedings of IEEE International Conference on Systems, Man and Cybernetics, Human, Information and Technology*, Vol. 2, pp. 1944-1950.

Nouri, B., Al-Bender, F., Swewers, J., Vanherck, P., Van Brussel, H. (2000). Modelling a Pneumatic Servo Positioning System with Friction. *Proceedings of IEEE International Conference on Systems, Man and Cybernetics, Human, Information and Technology*, Vol. 2, pp. 1944-1950.

Pandian, S. R., Hayakawa, Y., Kamoyama, Y., Kawamura, S. (2000). Practical Design of Adaptive Model-Based Sliding Mode Control of Pneumatic Actuators. *Fluid Power System: Journal of the Japanese Hydraulics and Pneuamtics Society* , Vol.31, 107-114.

Pandian, S. R., Takemura, F., Hayakawa, Y., Hayakawa, S. (2002). Pressure Observer-Controller Design for Pneumatic Cylinder Actuators. *IEEE/ASME Transactions of Mechatronics* , Vol.7, No.4, pp. 490-499.

Pandian, S. R., Hayakawa, Y., Kanazawa, Y., Kamoyama, Y., Kawamura, S. (1997). Practical Design of a Sliding Mode Controller for Pneumatic Actuators. *ASME Journal of Dynamic Systems, Measurement and Control* , Vol. 119, pp.666-674.

Paul, A. K., Mishra, J. K., Radke, M. G. (1994). Reduced Order Sliding Mode Control for Pneumatic Actuator. *IEEE Transactions on Control System Technology* , Vol. 2, No.3, pp. 271-276.

Perondi, E., Suzuki, R., Sobczyk, M. (2010). Feedback Linearization Control Applied to a Pneumatic Actuator System. In *XVIII Congresso Brasileiro de Automatica (CBA2010)*, pp. 2473-2478.

Pfreundschuh, G. H., Kumar, V., Sugar, T. G. (1991). Designing and Control of a 3 DOF In-parallel Actuated Manipulator. *IEEE International Conference on Robotics and Automation*, Sacramento, CA, USA, pp. 1659-1664.

Pierce, R. C. (1940). *Patent No. 2,211,478.* USA.

Plettenburg, D. H. (2005). Pneumatic Actuators: a Comparison of Energy-to-Mass Ratio's. *Proceedings of the 2005 IEEE 9th International Conference on Rehabilitation Robotics*, Chicago, IL, USA, pp. 545-549.

Pu, J. S., Weston, R. H., Moore, P. (1992). Digital Motion Control and Profile Planning for Pneumatic Servos. *ASME Journal of Dynamic Systems, Measurement and Control* , Vol. 114, pp. 634-640.

Pu, J., Weston, R. H. (1988). Motion Control of Pneumatic Drives. *Microprocessors and Microsystems* , Vol.12, No.7, pp.373-382.

Rao, Z., Bone, G. M. (2008). Nonlinear Modeling and Control of Servo Pneumatic Actuators. *IEEE Transactions on Control Systems Technology* , Vol. 16, No.3, pp. 562-569.

Repperger, D. W., Johnson, K. R., Phillips, C. A., (1998). A VSC Position Tracking System Involving a Large Scale Pneumatic Muscle Actuator. *Proceedings of 37th IEEE International Conference on Decision & Control*, Florida, USA, pp. 4302-4307.

Repperger, D. W., Phillips, C. A., Krier, M. (1999a). Controller Design Involving Gain Scheduling for a Large Scale Pneumatic Muscle Actuator. *Proceedings of IEEE International Conference on Control Applications,* pp. 285-290.

Repperger, D. W., Johnson, K. R., Phillips, C. A., (1999b). Nonlinear Feedback Controller Design of a Pneumatic Muscle Actuator System. *Proceedings of the American Control Conference,* California, USA, pp. 1525-1529.

Reynolds, D. B., Repperger, D. W., Phillips, C. A., Bandry, G. (2003). Modeling the Dynamic Characteristics of Pneumatic Muscle. *Annals of Biomedical Engineering,* Vol. 31, pp. 310-317.

Richard, E., Scavarda, S. (1996). Comparison between Linear and Nonlinear Control of a Pneumatic Servodrive. *ASME Journal of Dynamic Systems, Measurement and Control* , Vol. 118, No.2, pp. 245-252.

Richardson, R., Plummer, A. R., Brown, M. D. (2001). Self-tuning Control of a Low-Friction Pneumatic Actuator Under the Influence of Gravity. *IEEE Transactions on Control System Technology* , Vol. 9, No.2, pp. 330-334.

Richer, E., Hurmuzlu, Y. (2000a). A High Performance Pneumatic Force Actuator System: Part I - Nonlinear Mathematical Model. *ASME Journal of Dynamic Systems, Measurement and Control* , Vol. 122, No.3, pp. 416-425.

Richer, E., Hurmuzlu, Y. (2000b). A High Performance Pneumatic Force Actuator System: Part II - Nonlinear Control Design. *ASME Journal of Dynamic Systems, Measurement and Control* , Vol.122, No.3, pp. 426-434.

Sande, H., Johansen, T. A., Kaasa, G. O., Snare, S. R., & Bratli, C. (2007). Switched Backstepping Control of an Electropneumatic Clutch Actuator Using On/Off Valves. *Proceedings Oof American Control Conference*, New York, pp. 76-81.

Sarosi, J., Gyeviki, A., Veha, A., Toman, P. (2009). Accurate Position Control of PAM Actuator in Labview Environment. *IEEE 7th International Symposium on Intelligent Systems and Informatics,* pp. 301-305.

Sarosi, J., Gyeviki, A., (2010). Experimental Setup for the Positioning of Humanoid Upper Arm. *Analecta Technica Szegedinensia, Review of Faculty of Engineering 2010/2-3,* pp. 222-226.

Sarosi, J.,Gyeviki, A., (2011). Accurate Positioning of Humanoid Upper Arm. *International Journal of Engineering, Annals of Faculty of Engineering Hunedoara,* pp. 33-36.

Schröder, J., Kawamura, K., Gockel, T., Dillmann, R., (2003). Improved Control of a Humanoid Arm Driven by Pneumatic Actuators. *Proc. of the 3rd IEEE Int. Conf. on Humanoid Robots,* Munich, Germany, 20 pages.

Schulte, H. F. (1961). The Characteristics of the McKibben Artificial Muscle. *The Application of External Power in Prosthetics and Orthotics. Publication 874,* Lake Arrowhead: National Academy of Sciences - National Research Council, pp. 94-115

Schulte, H., Hahn, H. (2004). Fuzzy State Feedback Gain Scheduling Control of Servo-Pneumatic Actuators. *Control Engineering Practice ,* Vol.12, pp. 639-650.

Shadow Robot Company. (2012). *http://www.shadowrobot.com/airmuscles/.*

Shearer, J. L. (1957). Nonlinear Analog Study of a High-Pressure Servomechanism. *ASME Transactions ,* Vol. 79, pp. 465-472.

Shearer, J. L. (1956). Study of Pneumatic Processes in the Continuous Control of Motion with Compressed Air (I,II). *ASME Transactions ,* Vol. 78, pp. 233-249.

Shen, X. (2010). Nonlinear Model-Based Control of Pneumatic Artificial Muscle Actuator System. *Control Engineering Practice ,* Vol. 18, pp.311-317.

Shen, X., Zhang, J., Barth, E. J., Goldfarb, M. (2006a). Nonlinear Averaging Applied to the Control of Pulse Width Modulated (PWM) Pneumatic Systems. *The American Control Conference*, Boston, USA, pp. 4444-4448.

Shen, X., Zhang, J., Barth, E. J., Goldfarb, M. (2006b). Nonlinear Model-Based Control of Pulse Width Modulated Pneumatic Servo Systems. *ASME Journal of Dynamic Systems, Measurement and Control ,* Vol. 128, 663-669.

Shih, M. C., Tseng, S. I. (1994). Pneumatic Servo-Cylinder Position Control by PID Self-tuning Controller. *JSME International Journal, Series C ,* Vol. 37, No.3, pp. 565-572.

Shih, M. C., Tseng, S.-I. (1995). Identification and Control of a Servo Pneumatic Cylinder. *Control Engineering Practice ,* Vol.3, No.3, pp.1285-1290.

Shih, M., Hwang, C. (1997). Fuzzy PWM Control of the Positions of a Pneumatic Robot Cylinder Using High Speed Solenoid Valve. *JSME International Journal ,* Vol. 40, No.3, pp. 469-476.

Shih, M., Ma, M.-A. (1998a). Position Control of a Pneumatic Rodless Cylinder Using Sliding Mode M-D-PWM Control the High Speed Solenoid. *JSME International Journal ,* Vol. 41, No.2C, pp. 236-241.

Shih, M., Ma, M.-A. (1998b). Position Control of a Pneumatic Cylinder Using Fuzzy PWM Control Method. *Mechatronics ,* Vol. 8, pp. 241-253.

Shih, M.-C., Lee, T.-W. (1998). On-line Learning Neural Fuzzy Control the Position of a Pneumatic Cylinder. *Proceeding of the 3rd International Conference on Advanced Mechatronics.* Japan.

Situm, Z., Pavkovic, D., Novakovic, B. (2004). Servo-Pneumatic Position Control Using Fuzzy PID Gain Scheduling . *ASME Journal of Dynamic Systems, Measurement and Control,* Vol.12, No.2, pp. 376-387.

Situm, Z., Herceg, S., (2008). Design and Control of a Manipulator Arm Driven by Pneumatic Muscle Actuators . *16th Mediterranean Conf. on Control and Automation*, Ajaccio, France, pp. 926-931.

Slotine, J., & Li, W. (1991). *Applied Nonlinear Control.* Englewood Cliffs, New Jersey: Prentice Hall.

Smaoui, M., Brun, X., Thomasset, D. (2004). Robust Position Control of an Electropneumatic System Using Second Order Sliding Mode. *IEEE Intenational Symposium on Industrial Electronics*, Vol. 1, pp. 429-434.

Smaoui, M., Brun, X., Thomasset, D. (2006). Systematic Control of an Electropneumatic System: Integrator Backstepping and Sliding Mode Control. *IEEE Transactions on Control Systems Technology* , Vol. 14, No.5, pp. 905-913.

Sobczyk, M., Perondi, E., Suzuki, R. (2012). Feedback Linearization Control with Friction Compensation Applied to a Pneumatic Positioning System. *ABCM Symposium Series in Mechatronics*, Vol. 5 , pp. 252-261.

Song, J. (1997). A Robust Sliding Mode Control for Pneumatic Servo Systems. *International Journal of Engineering Science* , Vol. 35, No.8, pp. 711-723.

Song, J., Bao, X., Ishida, Y. (1997). An Application of MNN Tained by MEKA for the Position Control of Pneumatic Cylinder. *The 1997 IEEE International Conference on Neural Networks*, pp. 829-833.

Song, Q., Liu, F. (2006). Improved Control of a Pneumatic Actuator Pulsed with PWM. *Proceedings of the 2nd IEEE/ASME International Conference on Mechatronic and Emdedded Systems and Applications*, pp. 1-4.

Surgenor, B. W., Vaughan, N. D. (1995). Continuous Sliding Mode Control of a Pneumatic Actuator. *Journal of Dynamic Systems, Measurement and Control,*Vol.119, No.3, pp. 578-581.

Taghizadeh, M., Ghaffari, A., Najafi, F. (2008). A Linearization Approach in Control of PWM-driven Servo-Pneumatic Systems. *Proceedings of the 40th Southeastern Symposium on System Theory*, New Orleans, LA, USA., pp. 395-399.

Taghizadeh, M., Ghaffari, A., Najafi, F. (2009a). Modeling and Identification of a Solenoid Valve for PWM Control Applications. *C R Mechanique* , Vol. 337, pp. 131-140.

Taghizadeh, M., Ghaffari, A., Najafi, F. (2009b). Improving Dynamic Performances of PWM-driven Servo-Pneumatic Systems Via a Novel Pneumatic Circuit. *ISA Transactions* , Vol. 91, pp. 512-518.

Taghizadeh, M., Ghaffari, A., Najafi, F. (2009c). Increased Tracking Ability Pulse Width Modulation-driven Pneumatic Servo Systems Via a Modified Pneumatic Circuit. *Electrical Engineering* , Vol. 91, pp.79-87.

Taghizadeh, M., Najafi, F., Ghaffari, A. (2009). Multimodel PD-control of a Pneumatic Actuator UNder Variable Loads. *The International Journal of Advanced Manufacturing Technology* , Vol.48, No.5-8, pp.655-662.

Takagi, T. (1986). *Patent No. 4,615,260.* USA.

Tanaka, K., Yamada, Y., Sakamoto, M., Ushikado, S. (1998). Model Reference Adaptive Control with Neural Network for Electro-Pneumatic Servo System. *Proceedings of the 1998 IEEE International Conferences on Control Application*, Italy, pp. 1130-1134.

Tang, J., Walker, G. (1995). Variable Structure Control of a Pneumatic Actuator. *ASME Journal of Dynamic Systems, Measurement and Control* , Vol. 117, pp.88-92.

Thanh, T. D. C., Ahn, K. K. (2006). Nonlinear PID Control to Improve the Control Performance of 2 Axes Pneumatic Artificial Muslce Manipulator Using Neural Network. *International Journal of Mechatronics* , Vol. 16, pp.15-38.

Thanh, T. D. C., Ahn, K. K. (2006). Intelligent Phase Plane Switching Control of Pneumatic Artificial Manipulators with Magneto-Rheological Brake. *International Journal of Mechatronics,* Vol. 16, pp. 85-95.

Thanh, T. D. C. Ahn, K. K. (2007). Control of Two-Axis Pneumatic Artificial Muscle Manipulator with a New Phase Plane Switching Control Method. *Journal of Mechanical Science and Technology,* Vol. 21, pp.1018-1027.

Tondu, B., Lopez, P. (1997). The McKibben Muscle and Its Use in Actuating Robot-Arms Showing Similarities with Human Arm Behaviour. *Industrial Robot* , Vol.24, No.6, pp.432-439.

Tondu, B., Lopez, P. (2000). Modeling and Control of McKibben Artificial Muscle Robot Actuators. *IEEE Control Systems Magazine* , Vol. 20, No.2, pp.15-38.

Tsai, Y.-C., Huang, A.-C., (2008). Multiple-Surface Sliding Controller Design for Pneumatic Servo Systems. *Mechatronics* , Vol.18 , pp. 506-512.

Tsagarakis, N., Caldwell, D. G., (2000). Improved Modelling and Assessment of Pneumatic Muscle Actuators, *International Conference on Robotics and Automation* , San Francisco, pp.3641-3646.

Uebing, M., Vaughan, N. D., Surgenor, B. W. (1997). On Linear Dynamic Modeling of a Pneumatic Servo System. *The Fifth Scandinavian Conference on Fluid Power, SICFP'97*, pp. 364-378.

Utkin, V. I. (1977). Variable Structure Systems with Sliding Modes. *IEEE Transactions on Automatic Control* , Vol. 22, No.2, pp. 212-222.

Utkin, V. (1993). Variable Structure Systems and Sliding Mode: State of the Art Assessment. In K.-K. D. Young (Ed.), *Studies in Automation and Control 10: Variable Structure Control for Robotics and Aerospace Applications,* Amsterdam: Elsevier Science Publishers, pp. 9-32.

Van Damme, M., Vanderborght, R., Van Ham, R., Verrelst, B., Daerden, F., Lefeber, D. (2007). Proxy-based Sliding Mode Control of a Manipulator Actuated by Pleated Pneumatic Artificial Muscle. *Proceedings of IEEE International Conference on Robotics and Automation,* Rome, Italy, pp. 4355-4360.

Van Damme, M., Beyl, P., Vanderborght, B., Van Ham, R., Vanderniepen, I., Versluys, R. (2008). Modeling Hysteresis in Pleated Pneumatic Artificial Muscles. *Proceedings of IEEE International Conference on Robotics, Automation and Mechatronics* , pp. 471-476.

Van Ham, R., Daerden, F., Verrelst, B., Lefeber, D. (2003). Control of a joint actuated by two Pneumatic Artificial Muscles with fast ON-OFF Valves. *6th National Congress on Theoretical and Applied Mechanics,* (CD-ROM).

Van Varseveld, R. B., Bone, G. M. (1997). Accurate Position Control of a Pneumatic Actuator Using On/Off Solenoid Valves. *IEEE/ASME Transactions on Mechatronics* , Vol. 2, No.30, pp. 195-204.

Varga, Z., Keski-Honkola, P., Moucka, M. (2011). Comparison Between Muscle Volume Models and Measurements. *The Twelfth Scandinavian International Conference on Fluid Power, SICFP'11,* A4: pp. 149-158.

Virvalo, T., (1995). Modeling and Design of a Pneumatic Position Servo System Realized with Commercial Components. Ph.D Thesis, Tampere University of Technology, Tampere, Finland.

Wang, H., Mo, J. T., Chen, N. (1996). Hybrid Fuzzy Logic Algorithm For Position Control of Pneumatic Actuator with 3/2-way Solenoid Valves. *Proc Instn Mech Engrs Vol 210, Part C: Journal of Mechanical Engineering Science*, pp.167-176.

Wang, J., Wang, D. J., Moore, P. R., & Pu, J. S. (2001). Modelling Study, Analysis, and Robust Servocontrol of Pneumatic Cylinder Actuator Systems. *IEEE Process Control Theory and Applications* , Vol.148, No.1, pp.35-42.

Wang, J., Kotta, U., Ke, J. (2007). Tracking Control of Nonlinear Pneumatic Actuator Using Static State Feedback Linearization of Input/Output Map. *Proceedings of Estonian Academy on Science, Physics and Mathematics* , Vol. 56, p. 47-66.

Wang, J. Pu, J., Moore, P. (1999). A Practical Control Strategy for Servo-Pneumatic Actuator Systems. *Control Engineering Practice* , Vol. 7, No.12, pp. 1483-1488.

Weston, R. H., Moore, P., Thatcher, T. W. (1984). Computer Controlled Pneumatic Servo Drives. *Proceedings of the Institution of Mechanical Engineers, Part B: Journal of Engineering Manufacture* , Vol.198, pp. 275-281.

Vo-Minh, T., Tjahjowidodo, T., Ramon, H., Van Brussel, H. (2011). A New Approach to Modeling Hysteresis in a Pneumatic Artificial Muscle Using the Maxwell-Slip Model. *IEEE/ASME Transactions on Mechatronics* , Vol. 16, No.1, pp.177-186.

Xiang, F., Wikander, J., Eriksson, B., (1998). Nonlinear Control of Pneumatic Servo – a Feedback Linearization Approach. *Proceedings of the 1st International Fluid Power Conference*, Aachen, Germany.

Xiang, F., Wikander, J., (2004). Block-Oriented Aproximated Feedback Linearization for Control of Pneumatic Actuator System. *Control Engineering Practice*, Vol. 12, No.4, pp. 387-399.

Ye, N., Scavarda, S., Betemps, M., Jutard, A. (1992). Models of a Pneumatic PWM Solenoid Valve for Engineering Applications. *ASME Journal of Dynamic Systems, Measurement and Control,* Vol. 114, No.4, pp. 680-688.

Zhu, X., Tao, G., Yao, B., Cao, J. (2008). Adaptive Robust Posture Control of a Parallel Manipulator Driven by Pneumatic Muscles. *Automatica* , Vol. 44, No.9, pp. 2248-2257.

APPENDIX A: Control Approaches

In this chapter the control strategies used in this study are introduced. First, basic principles of classical proportional plus integral plus derivative (PID) feedback controller are presented. Then, the structure of the proportional plus velocity plus acceleration plus feed-forward (PVA+FF) controller and a pole-placement method for determining the controller gains are discussed. Finally, the concept of Sliding Mode Control (SMC) is discussed.

A.1 Classical PID control

Depending on the complexity and the linearity of the plant, the first approach of control design is usually based on "classical control" strategies. The purpose of the control law in a closed loop system is to generate appropriate control signals to the plant in order to force the output states to follow the desired inputs in a stable and accurate fashion, i.e. force the error signals to reach zero. A block diagram of a typical feedback control system is shown in Figure A-1. As stated, this classical control form is designed to force the system output states to follow the desired inputs based on error signals only. Thus, this controller does not contain any information about the plant and responds only to the error signal, its derivative and/or its integral (e.g. PID); and it is called a "non-model-based" controller. There are a few approaches available to tune the controller gains including a trial and error approach and structured tuning procedure such as the Ziegler-Nichols method. However, the classical controller is not robust in terms of performance and stability since its design does not usually directly take into account the existence of external perturbations such as noise.

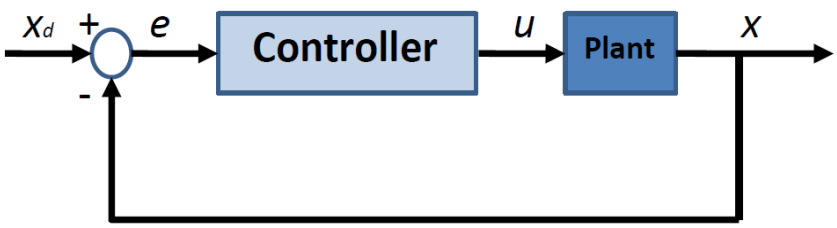

Figure A-1: A classical feedback control loop

Error signal between the desired input x_d and output x is

$$e = x_d - x \tag{A.1}$$

where control signal u can be formulated in the form of a classical PID controller as:

$$u = K_p e + K_I \int e dt + K_D \frac{de}{dt} \tag{A.2}$$

where K_P, K_I and K_D are constant gains. This controller structure was applied in Publication 1.

A.2 PVA+FF Control

The PVA control algorithm has been used in pneumatic positioning control by many researchers. The closed loop control system with PVA controller is shown schematically in Figure A-2. The transfer function of PVA controller is given by

$$u = K_p e - K_v s - K_a s^2 \tag{A.3}$$

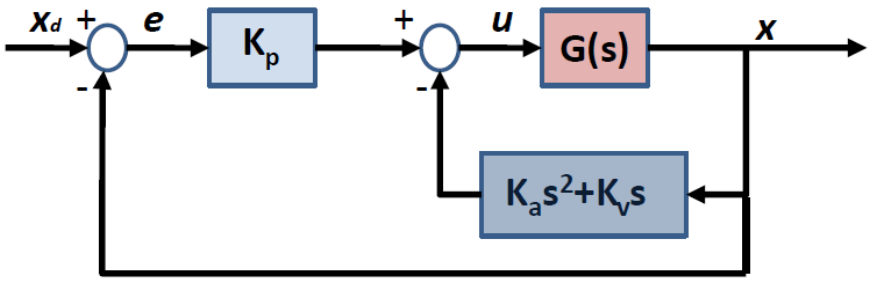

Figure A-2: Block diagram of PVA control system

K_p, K_v and K_a as the proportional, velocity and acceleration gains, respectively. It is generally stated, that both velocity and acceleration feedback are essential to ensure adequate performance in pneumatic servo applications. When velocity feedback control is used, the control signal is proportional to the actuators velocity (rate of change of the actual position). Since the velocity feedback acts based upon the velocity, it tends to increase damping and improve the stability of the system but degrades tracking error. Thus, a high velocity feedback gain tends to slow down (over-damp) the response to a commanded position change. Acceleration feedback tends to further increase the damping of the system and improve the stability properties. Velocity and acceleration feedback with improved damping properties enable the use of higher proportional gain in the system. In practice, acceleration is often avoided as the double differentiation of the position signal

generally produces a noisy signal even with filtering. On the other hand, current sensor technology provides relatively inexpensive methods for direct measurement of acceleration.

The PVA-controller gains can be obtained by using a pole-placement method introduced in (Ning & Bone, 2005). Consider a typical 3rd transfer function model of

$$G(s) = \frac{n_0}{s\left(s^2 + d_2 s + d_1\right)} \tag{A.4}$$

For a pneumatic positioning control system with PVA controller and given plant model the closed-loop transfer function is

$$G_{cl}(s) = \frac{X(s)}{X_d(s)} = \frac{n_0 K_p}{s^3 + (d_2 + n_0 K_a)s^2 + (d_1 + n_0 K_v)s + n_0 K_p} \tag{A.5}$$

Usually, the performance of the closed loop will be judged by its time-domain response. Specifically, standard step response criteria are used. Among these criteria, peak-overshoot may be used to estimate the relative stability of the system and the settling time T_{settle}, may be used to estimate the speed of the response if the peak-overshoot is fixed. It is well known from the linear control theory that these time-domain criteria are determined by the positions of the poles and zeros of the closed-loop transfer function. For the closed-loop transfer function described by equation (A.4) the time domain response will be determined by the position of its three poles in the s-plane. To theoretically guarantee the stability, all of the poles need to be located in the left hand side of the s-plane (negative real part).

Suppose the poles of the closed-loop transfer function are

$$\begin{aligned} s_{1,2} &= -\xi\omega_n \pm i\omega_n\sqrt{1-\xi} \\ s_3 &= -r\xi\omega_n \end{aligned} \tag{A.6}$$

Equation (A.4) becomes

$$\begin{aligned} G_{cl}(s) = \frac{X(s)}{X_d(s)} &= \frac{n_0 K_p}{\left(s + r\xi\omega_n\right)\left(s^2 + 2\xi\omega_n s + \omega_n^2\right)} \\ &= \frac{n_0 K_p}{s^3 + \left(r\xi\omega_n + 2\xi\omega_n\right)s^2 + \left(2r\xi^2\omega_n^2 + \omega_n^2\right)s + r\xi\omega_n^3} \end{aligned} \tag{A.7}$$

In order to make the two complex conjugate poles the dominant poles, the real pole s_3 needs to be located far to the left of these two conjugate complex poles.

Equating equation (A.6) with (A.5), the control gains can be calculated as follows:

$$\begin{aligned} K_p &= r\xi\omega_n^3 / n_0 \\ K_v &= \left(2r\xi^2\omega_n^2 + \omega_n^2 - d_1\right)/ n_0 \\ K_a &= \left(r\xi\omega_n + 2\xi\omega_n - d_2\right)/ n_0 \end{aligned} \tag{A.8}$$

From the linear control theory we know that the peak-overshoot depend only on the damping ratio ζ. The smaller the value of ζ, the bigger is the overshoot. If ζ>1.0, the system becomes an over-damped system and the overshoot disappears. For practical industrial applications the overshoot should be small, and usually a criteria ζ>0.8 is used. Term ω_n can be determined according to the desired settling time T_{settle} (Surgenor et al., 1995)

$$\begin{aligned} T_{settle} &= \frac{4}{\xi\omega_n} \Leftrightarrow \omega_n = \frac{4}{T_{settle}\xi} \\ M_p &= 100e^{-\xi\pi/\sqrt{1-\xi^2}} \end{aligned} \tag{A.9}$$

In order to get a fast response, the value of ω_n should be as large as possible i.e. T_{settle} should be as small as possible as long as no saturation in control occurs. If saturation happens then the actual settling time may be much larger than the desired one.

Tracking error is another important performance criterion for a positioning system. For the pneumatic servo positioning system to be useful in applications such as robotics it is necessary that the payload can dynamically follow a desired trajectory as precisely as possible. This is known as the tracking control problem. A common PVA control algorithm performs poorly in tracking control as the velocity and acceleration feedback tend to decrease tracking accuracy at a cost of providing a better damping properties for the system. In order to improve tracking performance a feed-forward (FF) control is commonly used. The block diagram of the system with PVA plus FF is shown in Figure A-3, where

$$\begin{aligned} G(s) &= \frac{X(s)}{U(s)} = \frac{n_0}{s\left(s^2 + d_2 s + d_1\right)} \\ H(s) &= K_a s^2 + K_v s \end{aligned} \tag{A.10}$$

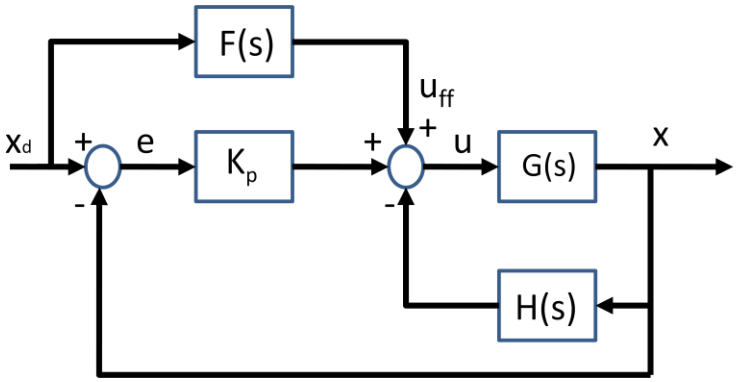

Figure A-3: Block diagram of PVA+FF control system

The goal of the feed-forward design is to make the output track the input perfectly, i.e.

$$\frac{X(s)}{X_d(s)} = 1 \Rightarrow$$
$$\frac{X(s)}{X_d(s)} = \frac{K_p G(s) + F(s)G(s)}{1 + K_p G(s) + H(s)G(s)} = 1 \tag{A.11}$$

This objective is obtained by setting:

$$F(s) = \frac{1 + G(s)H(s)}{G(s)} \tag{A.12}$$

Substituting Equation (A.10) into (A.12) we have

$$F(s) = \frac{1}{n_0} s^3 + (\frac{d_2}{n_0} + K_a) s^2 + (\frac{d_1}{n_0} + K_v) s \tag{A.13}$$

In the time domain the feed-forward control output is given by

$$u_{ff}(t) = \frac{1}{n_0} \dddot{x}_d(t) + (\frac{d_2}{n_0} + K_a) \ddot{x}_d(t) + (\frac{d_1}{n_0} + K_v) \dot{x}_d(t) \tag{A.14}$$

A.3 Sliding Mode Control

Background of sliding mode control

Vadim Utkin (Utkin V. I., 1977) introduced the concept of sliding mode control (SMC). Sliding mode control is a simple approach to robust control having its' roots in Variable Structure Control (VSC). The characteristic feature of VSC is that a sliding mode occurs on a prescribed manifold, or switching surface, where switching control is employed to maintain the state on that surface.

Generally a sliding mode may appear in any dynamic system governed by ordinary differential equations with discontinuous right-hand sides. The sliding mode occurs in the system if the control action switches at a sufficiently high frequency. Sliding mode control enhances the advantages of variable structure control, mainly an insensitivity to plant variance and the ability to achieve state trajectories not available through conventional control methods. The disadvantages of both variable structure and sliding mode control is that they both require a controller capable of high frequency switching, which is characterized by chattering of the output device. This, in turn may excite un-modeled high-frequency behavior in the system. In (Utkin V. , 1993) Utkin reviewed more recent development in VSC and discussed mathematical analysis methods, controller designs and practical applications researchers have developed. Already in the 90's the application of VSC had produced quantifiable economic benefits in several industries.

Relay control

When a system state switches at high (theoretically infinite) frequency, sliding mode motion can occur. In order to illustrate this, consider the simplest form of sliding mode control, a relay control, with a simple first order system, as shown in Figure A.4 and with equation

$$\dot{x} = f(x) + u \tag{A.15}$$

where *f(x)* is the system dynamics, *x* is the output of interest and *u* is the control input. For a bounded function *f(x)*, $|f(x)|<f_0$ (a constant), and tracking error

$$e = x_d - x \tag{A.16}$$

where x_d as the desired state, the control signal *u* in Eq. (A.15) is given as

$$u = \begin{cases} K_{SMC}, & e > 0 \\ -K_{SMC}, & e < 0 \end{cases} \tag{A.17}$$

with K_{SMC} as a switching gain. Given a certain value of $K_{SMC} > f_0 + |\dot{x}_d|$, the value of error *e* and $\dot{e} = \dot{x}_d - f(x) - K_{SMC} sign(e)$ have opposite signs, where *sign* is the sign-function. The magnitude of the tracking error *e* thus decays at a certain rate and reaches zero after a finite time interval t_{reach}, as illustrated in Figure A.5. The motion after t_{reach} is called the sliding mode.

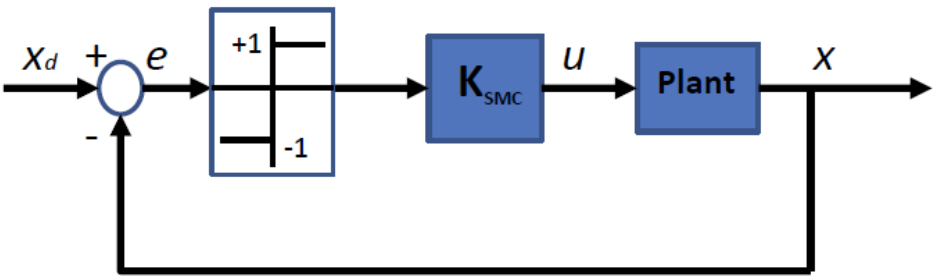

Figure A-4: Pure relay control

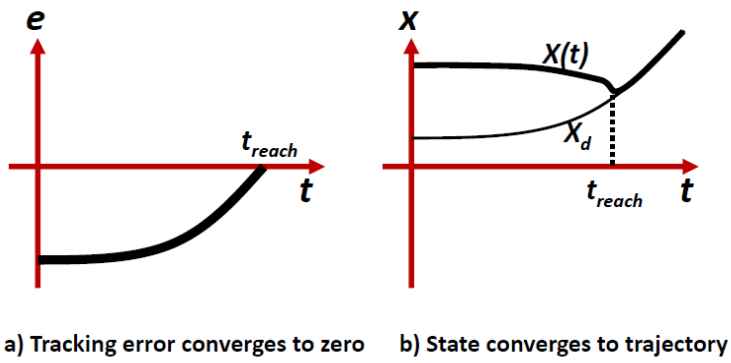

Figure A-5: Tracking control using pure relay function

It is obvious, that the relay control action requires an infinitely fast switching on the sliding surface. The switching around the sliding surface generates a point of discontinuity. This can't be implemented in any realistic application, because of imperfections in switching devices due to mechanical delays, dead zones and hysteresis. These imperfections may lead to high-frequency oscillations that are undesirable in practice.

Sliding surfaces

Sliding mode control is one implementation of variable structure control and it introduces the concept of *S* as the sliding surface or manifold (Utkin V. I., 1977). Consider the n^{th} order single-input dynamic system

$$x^{(n)} = f(\mathbf{x}) + b(\mathbf{x})u \tag{A.18}$$

where the scalar x is the output of interest (e.g. the position of the actuator), the scalar u is the control input, and $\mathbf{x}=[x,x^{(1)}\ldots x^{(n-1)})]^T$ is the state vector, and n is the number of the system order. The function $f(\mathbf{x})$ (generally nonlinear) is not exactly known but it is bounded by a known continuous function of $\mathbf{x}$. Similarly, the control gain $b(\mathbf{x})$ is not exactly known but is of known sign and is

bounded by a known continuous function **x**. The objective is to design a controller to get the state **x** to track a desired time varying state $\mathbf{x}_d=[x_d, x_d^{(1)} \ldots x_d^{(n-1)}]^T$ in the presence of model imprecision on $f(\mathbf{x})$ and $b(\mathbf{x})$. In order to achieve the tracking task using a finite control u, the initial desired state $\mathbf{x}_d(0)=\mathbf{x}(0)$.

Let

$$\mathbf{e} = \mathbf{x} - \mathbf{x}_\mathbf{d} = \left[e \quad \dot{e} \quad \cdots e^{(n-1)}\right]^T \tag{A.19}$$

be the tracking error vector. Define a time-varying surface $S(t)$ in the state space by the scalar equation

$$S(\mathbf{x},t) = (\frac{d}{dt} + \lambda)^{(n-1)} e = 0 \tag{A.20}$$

where λ is a strictly positive constant denoted as control bandwidth, whose value must be properly chosen in surface design. For example, if n=2,

$$S(\mathbf{x},t) = \dot{e} + \lambda e \tag{A.21}$$

If n=3

$$S(\mathbf{x},t) = \ddot{e} + 2\lambda\dot{e} + \lambda^2 e \tag{A.22}$$

Given the initial condition $\mathbf{x}_d(0)=\mathbf{x}(0)$, i.e. $e(0)=0$, the perfect tracking $\mathbf{x}\equiv\mathbf{x}_\mathbf{d}$ ($\mathbf{e}\equiv 0$) is obtained as long as the system state remains on the surface S after $t > 0$, which means the tracking problem is translated into that of keeping the scalar quantity S at zero.

For all single input systems a suitable candidate of Lyapunov functions is $V(\mathbf{x}) = ½S^2$ which is globally positive definite. The states outside of the sliding surface S are guaranteed to converge after a finite time by choosing the proper control law u satisfying a "sliding condition" (Slotine & Li, 1991)

$$\frac{1}{2}\frac{d}{dt}S^2 = S\frac{dS}{dt} \le -\eta\,|S| \tag{A.23}$$

where η is a strictly positive constant. Equation (A.23) can always be established, which indicates that the state trajectory converges to the surface and is restricted to the surface for all subsequent time (Slotine & Li, 1991) as shown in Figure A-6. In other words the control algorithm

should drive the states towards the sliding surface if it is not already on the surface. To achieve this, the control input u can be defined as

$$u = -K_{SMC} sign(S) \tag{A.24}$$

where the switching gain K_{SMC} should be large enough to compensate for the system uncertainties and disturbances.

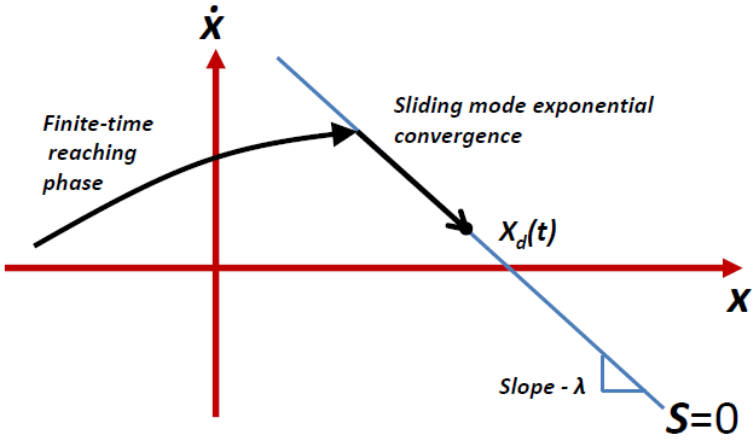

Figure A-6: A graphical interpretion of the sliding condition (n=2), (based on (Slotine & Li, 1991)).

Equivalent control approach

In order to utilize the system model in sliding mode control law, the equivalent control approach was introduced by (Slotine & Li, 1991). Once on the sliding surface and staying on the surface the dynamics of the system is given by

$$\dot{S} = 0 \tag{A.25}$$

If the system model is absolutely accurate and there is no disturbance, we can formally solve the above equation for the control input u and obtain an expression called the equivalent control u_{eq}, which can be interpreted as a control law that would satisfy the Equation (A.25). The equivalent control term corresponds with the feed-forward (FF) compensation used e.g. with PVA+FF control approach. For a third order system (n=3), the equivalent control term u_{eq} is defined as

$$u_{eq} = b(\mathbf{x})^{-1}\left(\dddot{x}_d - f(\mathbf{x}) - 2\lambda\ddot{e} - \lambda^2\dot{e}\right) \tag{A.26}$$

However, for practical tracking control problems, model imprecision and disturbances are evitable and the system may run outside the sliding surface. Therefore, the total control input u is composed of equivalent control component and the switching component

$$u = u_{eq} + u_{sw} \tag{A.27}$$

As stated before, the purpose of switching control u_{sw} is to force the plant state outside the sliding surface to go back to the surface.

$$u_{sw} = -K_{SMC} sign(S) \tag{A.28}$$

The switching gain K_{sw} can be related to uncertainties of the system, if they are upper-bounded. If

$$| \hat{f}(\mathbf{x}) - f(\mathbf{x}) | \leq F(\mathbf{x}) = a\hat{f}(\mathbf{x}) \tag{A.29}$$

where $\hat{f}(\mathbf{x})$ is an estimate of $f(\mathbf{x})$, the estimation error on f is assumed to be bounded by some known function $F(\mathbf{x})$, with a as an uncertainty factor.

Also, let control gain $b(\mathbf{x})$ to be unknown but of known bounds (possibly time-varying or state-dependent) by

$$0 < b_{\min}(\mathbf{x}) \leq b(\mathbf{x}) \leq b_{\max}(\mathbf{x}) \tag{A.30}$$

where the minimum $b_{min}(\mathbf{x})$ and maximum $b_{max}(\mathbf{x})$ can be defined based on some assumptions of system parameter bounds, e.g. payload variation. Since the control input enters multiplicatively in the dynamics, it is natural to choose the estimate of $b(\mathbf{x})$ as the geometric mean of the above bounds:

$$\hat{b}(\mathbf{x}) = \sqrt{b_{\min}(\mathbf{x}) b_{\max}(\mathbf{x})} \tag{A.31}$$

Bounds (A.30) can then be written in the form

$$\begin{aligned} &\beta^{-1} \leq \frac{\hat{b}(\mathbf{x})}{b(\mathbf{x})} \leq \beta, \quad where \\ &\beta = \sqrt{\frac{b_{\max}(\mathbf{x})}{b_{\min}(\mathbf{x})}} \end{aligned} \tag{A.32}$$

with β as a gain margin, by analogy to the terminology used in linear control. The switching gain can then be defined to guarantee robustness in the presence of uncertainties by (Slotine & Li, 1991)

$$K_{SMC} \geq \beta(F+\eta)/\hat{b}(\mathbf{x}) + (\beta - 1)\,|u_{eq}\,| \qquad \text{(A.33)}$$

It can be seen from the above description that an advantage of the sliding mode control is that the nth order tracking control problem for state x is reduced to a 1st order stabilization problem in S. This advantage makes the control simple and practical.

Boundary layer control

Due to the discontinuous nature of a control action, ideal sliding mode control demands infinitely fast switching. The high-frequency switching can excite un-modeled dynamics such as parasitic dynamics, which are often ignored in the open-loop model design if the associated poles are well damped and outside the desired bandwidth of the control system. At the same time, imperfect switching can be the result of a relay with hysteresis or a mechanical delay. These two mechanisms can lead to the chattering phenomenon in real SMC applications and the system will oscillate in the vicinity of the switching plane as shown in Figure A-7.

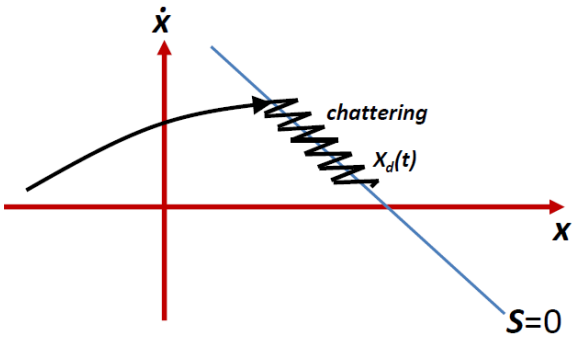

Figure A-7: Chattering phenomenon in an imperfect switching (n=2), (based on (Slotine & Li, 1991)).

The most common solution to smoothen out the chattering is a boundary layer control. The basic idea is to apply a thin boundary layer neighboring the switching surface. To do this, Equation (A.28) should be replaced by

$$u_{sw} = -K_{SMC} sat(S, \phi) \tag{A.34}$$

where

$$sat(S, \phi) = \begin{cases} \text{sgn}(S/\phi), & for\ |S/\phi| > 1 \\ S/\phi, & for\ |S/\phi| \le 1 \end{cases} \tag{A.35}$$

As shown in Figure A-8 (for case n=2), the vertical dimension Φ is the boundary layer thickness, and the horizontal dimension ε is the boundary layer width that is related to Φ by

$$\varepsilon = \frac{\phi}{\lambda^{n-1}} \tag{A.36}$$

Thus, the control bandwidth λ and boundary layer thickness Φ determine the tracking precision. Within the shaded area, the control function is continuous. Outside the shaded area, the control function is discontinuous.

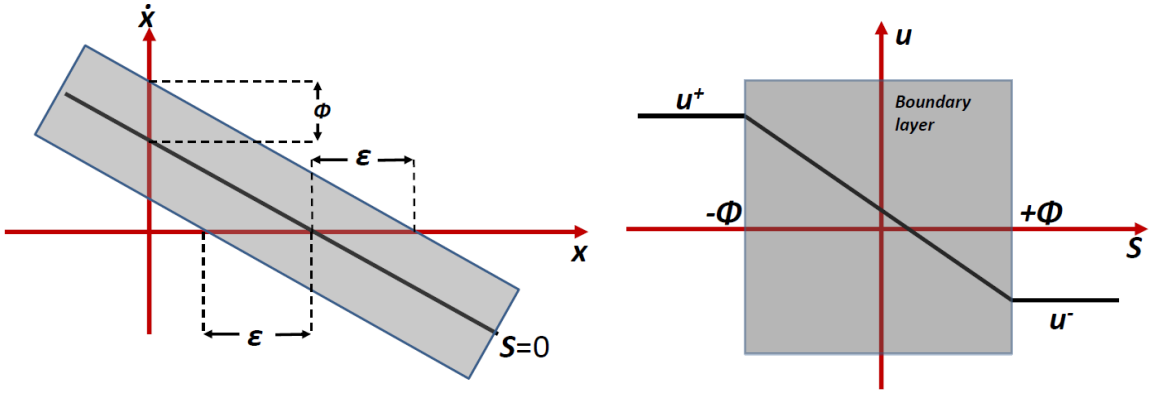

Figure A-8: Boundary layer control (based on (Slotine & Li, 1991)).

Figure A-8 gives an interpretation of the control law u in the boundary layer, where a slope is used to negate for the abrupt jump between u+ and u-.

It should be noted that the continuation of control inside the boundary layer, in fact acts like a low-pass filter on the switching action. Thus, the high-frequency chattering is effectively eliminated at the cost of losing tracking precision and robustness to un-modeled dynamics. As a result, a trade of between these factors must be taken into account when designing the control law.

Example of a sliding mode control

To illustrate the sliding motion, consider a 3rd order linear model given by Equation (A.4)

$$\dddot{x} = -d_2\ddot{x} - d_1\dot{x} + n_0 u \tag{A.37}$$

where u is the control input signal (e.g. mass flow rate) to the system, and x is the position of the actuator. Assume ideal conditions without external disturbances and sensor noise. Defining a sliding surface based on the equation (A.22), SMC control signal can be defined as:

$$\begin{aligned} u &= u_{eq} - K_{SMC}\,\mathrm{sgn}(S) \quad with \\ S &= \ddot{e} + 2\lambda\dot{e} + \lambda^2 e \\ u_{eq} &= (\ddot{x}_d + d_2\ddot{x} + d_1\dot{x} - 2\lambda\ddot{e} - \lambda^2\dot{e})/n_0 \end{aligned} \tag{A.38}$$

and K_{sw} is the switching gain for compensating modeling uncertainties. Figure A-9 illustrates the control performance for a sinusoidal tracking, when only equivalent control and switching control is used. It is shown, that the pure equivalent control, although assumed a perfect system model, can't follow the trajectory exactly. This is due to velocity and acceleration feedback resulting in phase delay in the response. The switching control, instead, is capable of providing a good tracking performance (>10 times better than the equivalent control) with a cost of highly switching control signal. The tracking accuracy can be further increased by combining the equivalent and switching component as illustrated in Figure A-9. However, the high frequency switching (chattering) of the control signal is often undesirable and can be reduced by applying a boundary layer around the sliding surface. As shown in Figure A-9, the chattering has disappeared and the control performance maintained.

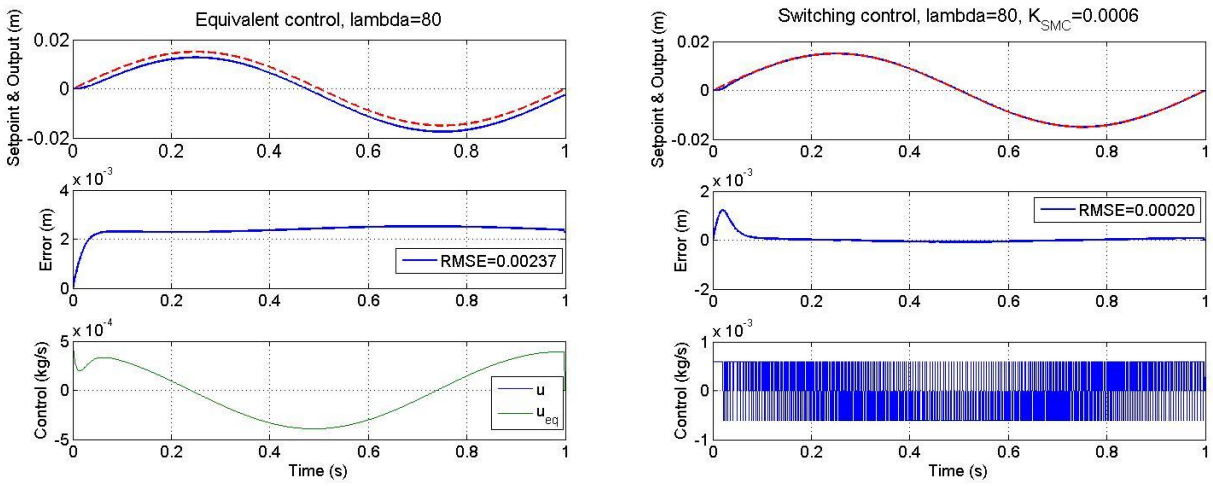

Figure A-9: Equivalent and switching control with perfect system model

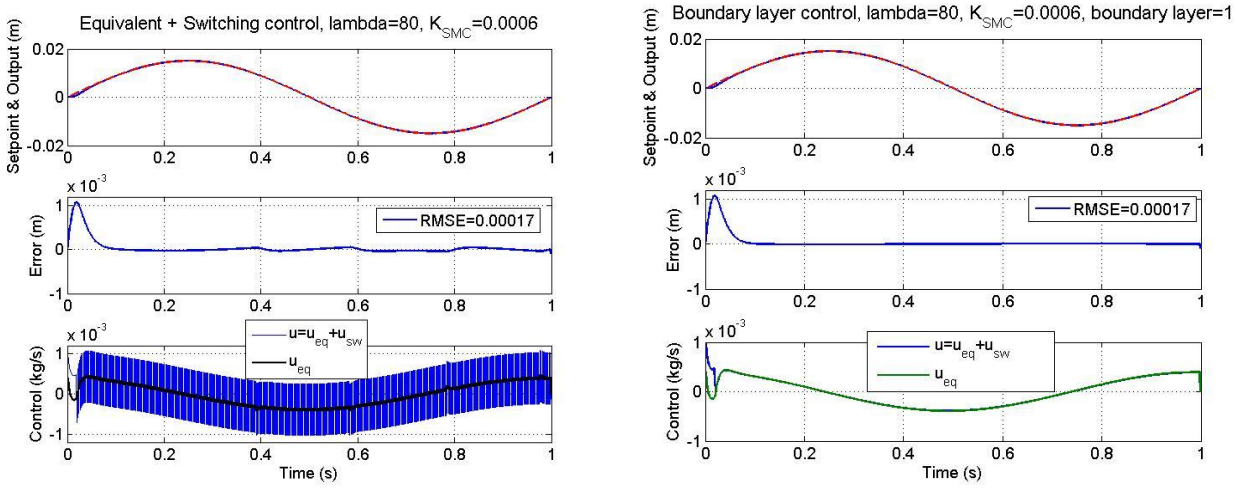

Figure A-10: Sliding mode control with sign-function and boundary layer with a perfect system model

Often, the model of the plant used for controller design is inaccurate. Figure A-11 illustrates the performance of the combined equivalent and switching control and boundary layer control with imperfect plant model (moving mass increased by 500 %). It can be seen, that SMC is extremely robust to parameter variation. However, it should be noted, that boundary layer control decreases the robustness of the system although not clearly seen in this case.

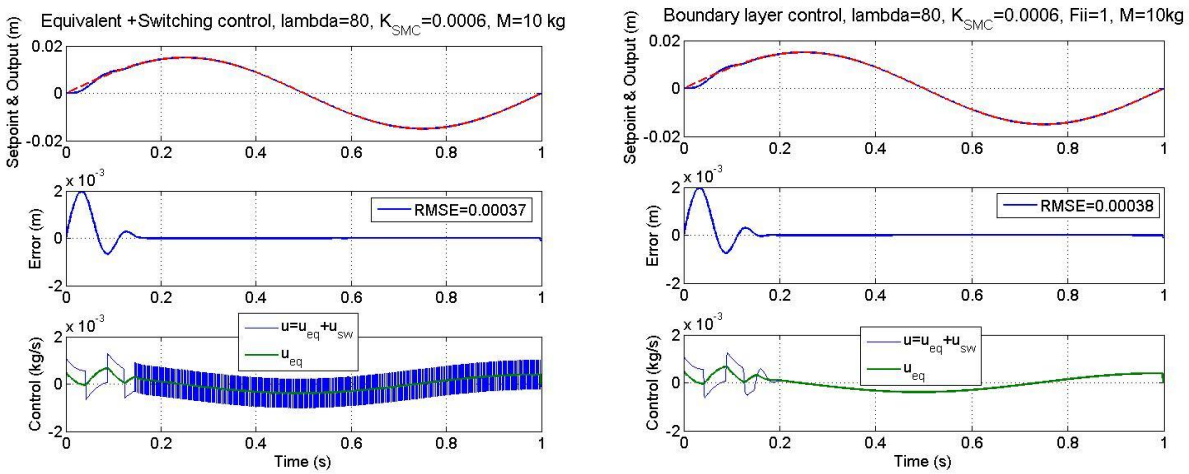

Figure A-11: Sliding mode control with sign-function and boundary layer with an imperfect plant model (moving mass increased by 500 %)

In practical applications, there are always delays in the system that will affect the system performance. In PWM pneumatic systems, the PWM sampling will introduce a sample-and-hold – type delay as the control signal is sampled only once in every PWM period. From the viewpoint of sliding mode control, the delay is extremely difficult to handle as SMC relies on the fast switching. Figure A-12 illustrates the effect of delay on the SMC performance. It can be seen, that due to delay

the boundary layer thickness needs to be increased significantly in order to avoid chattering and limit cycles.

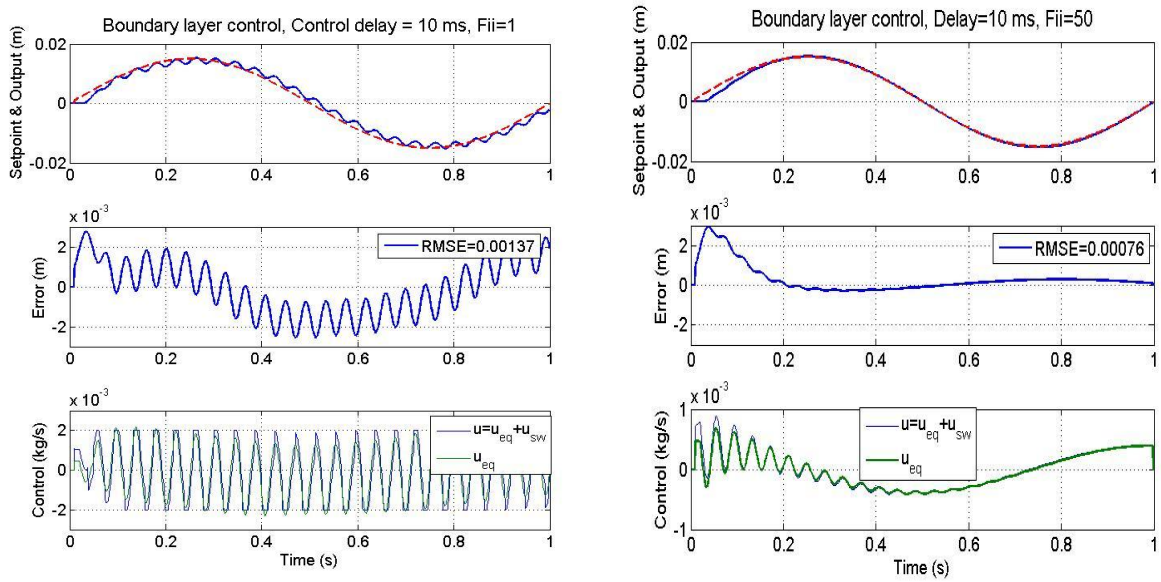

Figure A-12: Boundary layer control with control delay

Figure A-13 illustrates how the control performance (in terms of RMSE) is degraded as a function of control delay with a constant boundary layer thickness (Φ=1, 10, 50).

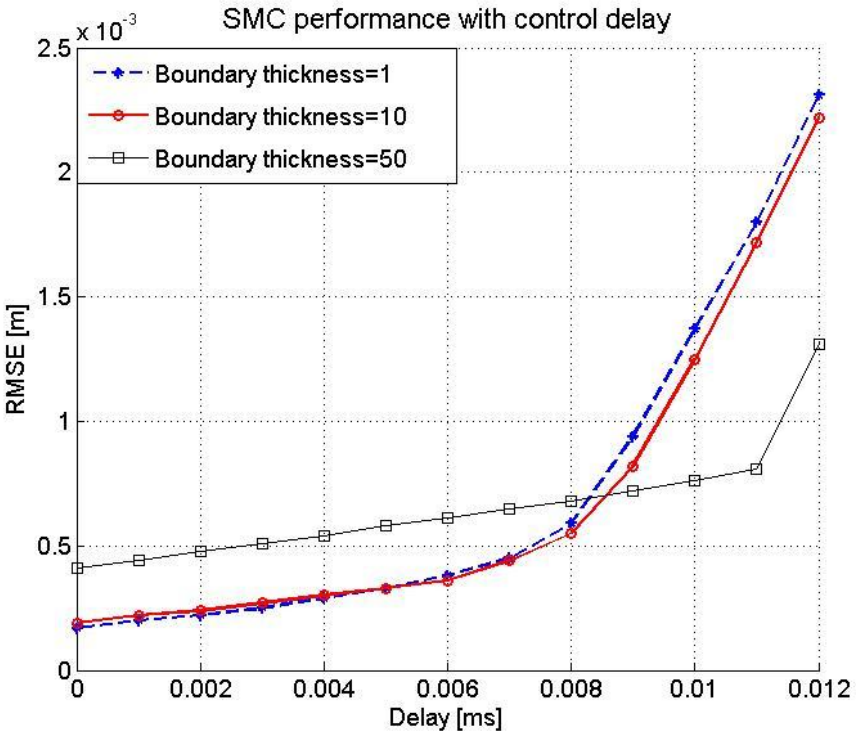

Figure A-13: Boundary layer control with control delay

PUBLICATIONS

PUBLICATION 1

Modeling and Identification of a Pneumatic Muscle Actuator System Controlled by an On/Off Solenoid Valve

Ville Jouppila, Andrew Gadsden andAsko Ellman

Reprinted, with permission, from the *Proceedings of 7th International Fluid Power Conference,* Aachen Germany, 2010

Modeling and Identification of a Pneumatic Muscle Actuator System Controlled by an On/Off Solenoid Valve

Ville Jouppila

Department of Mechanics and Design, Tampere University of Technology, Tampere, Finland

Andrew Gadsden

Department of Mechanical Engineering, McMaster University, Hamilton, Canada

Asko Ellman

Department of Mechanics and Design, Tampere University of Technology, Tampere, Finland

ABSTRACT

Pneumatic actuators offer desirable properties for many applications, such as compactness, low costs, high power-to-weight ratios, reliability, and simplicity. However, due to many nonlinearities (air compressibility, friction, air flow through valve), accurate position and force control of pneumatic actuators is extremely difficult and expensive to achieve. There is a growing interest in PWM-controlled pneumatic systems using low cost on/off solenoid valves instead of servo valves in order to develop less expensive pneumatic servo systems. In addition, a new type of pneumatic McKibben muscle actuator possesses significant advantages like a very high force/weight and force/volume performance, quick response, and wide operational ranges in a variety of environments.

In this paper, a high speed on/off valve is applied to control a pneumatic McKibben muscle actuator system. However, the complex nonlinear dynamics of the actuator in addition to those already mentioned make the modeling and accurate control of the pneumatic system a difficult challenge. As a result, the designed model is nonlinear and may still contain unknown parameters that require identification in order to obtain reasonable dynamical matching with the real system. Furthermore, the discontinuous switching nature of the on/off valve causes transients in the system, making the analytic modeling of the system even more complex.

The objective of this research is to develop an analytical model of the system which includes the nonlinearities of the system, and the transformation of the discontinuities into a continuous form. The use of analytical models enables the implementation of conventional analytical control approaches, such as sliding mode control, and provides a tool for the analysis of stability and robustness. In this paper, the modeling process is applied to a one degree of freedom pneumatic system for which the analytical nonlinear system model is developed by a combination of physical and empirical methods. An extensive set of experimental tests are performed to characterize the dynamics of the overall system. A non-analytic and analytic model of the system are developed and validated by a comparison of the simulated results with the experimental implementation of the system.

1 INTRODUCTION

Pneumatic actuators are commonly avoided for advanced applications due to problems with control caused by the compressibility of air and other nonlinear effects. Pneumatic control systems are mainly used in simple industrial applications with limited requirements for accurate control of motion and force. However, high power-to-weight ratios, compactness, ease of maintenance, and the safety of pneumatic actuators, offer desirable features for many industrial designs. The pneumatic McKibben muscle actuator is a new type of actuator that offers a high force-to-weight ratio and is able to operate in a wide range of environments. The compressibility of air, the nonlinear air flow characteristics through the valves, friction and the nonlinear characteristics of the McKibben muscle actuator result in a complex and difficult system to model and control.

In the theoretical analysis of pneumatic systems a combination of thermodynamics, fluid dynamics and the dynamics of the motion is required. The mathematical analysis requires the consideration of the mass flow rates through the valve, the determination of the pressure, volume and temperature of the air in the actuator, and the determination of the dynamics of the load. Furthermore, identification techniques, although usually based on linear methods, can be used for finding the mathematical model of the pneumatic system. An accurate model of the actuator is an important condition for both control design and for optimizing its operation.

2 SYSTEM MODELING

2.1 System setup and structure

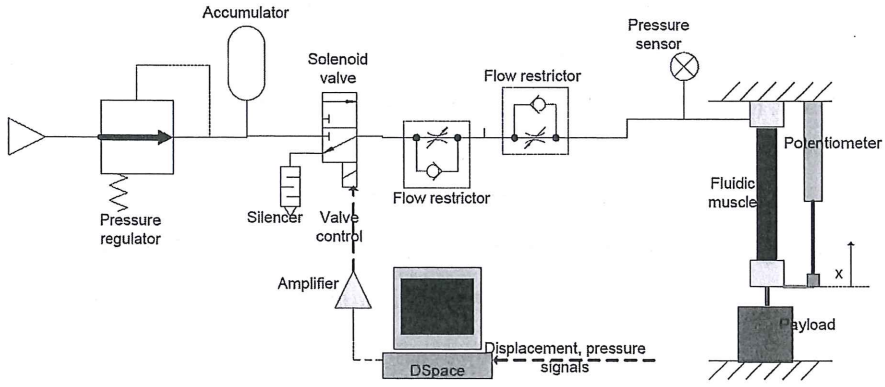

Figure 1: System setup

The system hardware is illustrated schematically in Fig. 1. The Festo fluidic muscle (MAS10-300 mm) is hanging vertically, actuating (lifting) the attached payload. The supply pressure (0.65 MPa abs.) for the system is provided by the proportional pressure regulator (Festo VPPM-6L-L1-G18-0L6H-V1N). A single 3/2 high speed on/off solenoid valve (Festo MHE2-1/8-MS1H-3/2G-M7) is controlled to actuate the muscle actuator and the payload. The solenoid is driven by pulsed valve control signal generated in DSpace and Matlab environment. An electronic amplifier is used to provide sufficient power to actuate the valve. The pressure and displacement of the actuator are measured. Flow restrictors are optional for reducing excessive pressure chattering. The tubing between the valve and the actuator is kept short and thus neglected in modeling.

2.2 McKibben muscle actuator

The McKibben muscle is an actuator that consists of a rubber tube with a non-extensible fiber surrounding [16]. This physical configuration causes the muscle to have variable-stiffness spring-like characteristics, nonlinear passive elasticity, physical flexibility, and very lightweight compared to other types of actuators [17]. The only commercially available muscle actuator (MAS) by Festo differs slightly from the general McKibben type muscle. The fiber of the fluidic muscle is knit into the tube, offering easy assembly and improved hysteretic behavior and linearity compared to conventional designs [18].

In recent years, a considerable amount of research has been performed to develop inexpensive servo-pneumatic systems using on/off solenoid valves with a pulse-width modulation (PWM) technique. In a PWM-controlled system, the power is delivered to the actuator in discrete packets of fluid mass, as the valve is either completely on or off. If the switching frequency of the valve is significantly higher than the system dynamics, the system will act as a low-pass filter responding similarly as to a continuous mass flow input. However, due to the discontinuous switching the development of an analytical dynamic model of the system is rather difficult, and often prevents the direct use of analytical control designs. Although previous work has shown the potential of PWM-controlled pneumatics, they have suffered due to the lack of an analytical approach for analyzing the system [1–4]. However, some effort has been made in the area of analytical modeling of such systems [5–15].

The objective of this research is to develop an analytical model of the pneumatic system which includes the nonlinearities of the system, and the transformation of the discontinuities into a continuous form. The use of analytical models enables the implementation of conventional analytical control approaches, such as sliding mode control, and provides a tool for the analysis of stability and robustness. In this paper, the modeling process is applied to a one degree of freedom pneumatic system where a McKibben muscle actuator mechanism is controlled by a single high-speed solenoid valve. A non-analytical and analytical mass flow rate model through the valve are developed and combined with the nonlinear model of the actuator and the mechanism. An extensive set of experimental tests are performed to characterize the dynamics of the overall system. The models are validated by a comparison of the simulated results with the experimental implementation of the system. Finally, a traditional PI-controller is tuned with the help of a mathematical model, and is implemented in the real system.

During pressurization of the muscle with air, the muscle widens in diameter and shortens in length. The maximum force is obtained at the beginning of the contraction and decreases with increasing contraction [19]. The actuator is unidirectional and its maximum contraction without load is typically 20% to 25%. The nominal force-to-contraction at different pressure levels is nonlinear, and adds to the difficulty of effectively modeling the muscle actuator. As with all actuation systems, effective application of pneumatic muscle actuators relies on being able to accurately model and predict the forces that will be generated under any operating conditions. A force equation, first proposed in [19] gives a basis for estimating the force generated by the muscle actuator as a function of pressure and displacement.

$$F = \frac{\pi D_0^2 p}{4}(3\cos^2\theta - 1) \tag{1}$$

Where F is the contractile muscle force, D_0 is the diameter of the actuator at the braid angle of 90° (theoretical maximum), and p is the muscle pressure. However, it fails to completely model the behaviour of braided muscle actuators due to the assumption of lossless operation. Subsequently, various hypotheses have been developed to account for the effects of tubing elasticity, internal frictions, braid thickness, stretching of the fibres, end cap diameter (i.e. non-cylindrical muscle shape) and material properties in order to provide more accurate models [16, 17, 20–25].

The muscle actuator introduces a variable spring and a damper in parallel. The variable spring component is described by the static muscle force equation. The damper component describes the dynamics of the actuator including the viscous friction effect. The maximum available force as a function of displacement is introduced by fitting a 4th-order polynomial function for the curve at the maximum pressure 0.6 MPa. As a result, the nonlinear curve shape of the force/displacement characteristics is captured. When the muscle displacement is held constant, the actuator force depends almost linearly on the pressure. However, the slope of the force per unit pressure changes as a function of the displacement and thus the muscle force can be described by:

$$F_{static} = F_{\max}(x) - (p_{\max} - p_m)(\frac{k_0 - k_1 x}{k_2}) \qquad (2)$$
$$F_{\max}(x) = a_0 + a_1 x + a_2 x^2 + a_3 x^3 + a_4 x^4$$

Where p_{max} is the maximum available muscle pressure and p_m is the current muscle pressure. Coefficients k_0 [N], k_1 [N/m], and k_2 [Pa] are found by using least-squares methods. Figure 2 (left) illustrates the predicted force plotted against the measured force data at different pressure levels (0.1 to 0.6 MPa). The model is able to predict the force reasonably well for almost every pressure. Some deterioration exists between the model and actual data at lower pressure levels (less than 0.2 MPa).

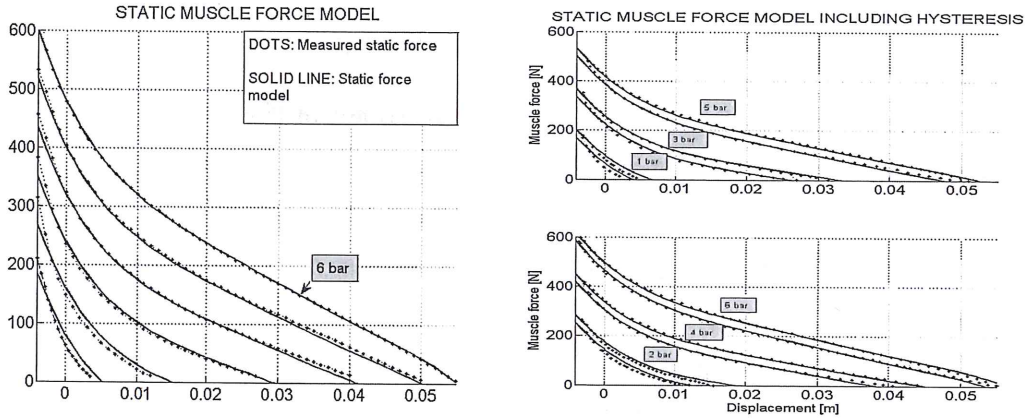

Figure 2: Averaged static muscle force model and model including the hysteresis

It has also been observed that there exists hysteresis in the muscles during operation caused mainly by friction present in the system [17,21]. For modeling the hysteresis, a similar approach as in [17] is used. The shape and the width of the hysteresis loops are almost the same for each pressure level as shown in Fig. 2. An average value for the width of the hysteresis loop resulted in 32 N. Thus a friction force offset F_C (Coulomb friction) of 16 N can be added into the static force model described by the equation (2), as follows:

$$F_{muscle} = F_{static} - F_C sign(\frac{dx}{dt}) - C_f \frac{dx}{dt} \qquad (3)$$

The equation includes also an experimentally obtained viscous friction component. In Fig. 2 (right) the muscle force model (equation (3)) is compared with the measured data in static case. As a conclusion, the model is able to provide a reasonably good prediction for the muscle force, including the effect of hysteresis.

2.3 Valve model

2.3.1 Non-analytic approach

The PWM pneumatic valve, that controls the airflow into and out of the actuator, is a fundamental component of the system. The valve considered in this study is a 3/2-high speed solenoid valve (Festo MHE2-1/8-MS1H-3/2G-M7) with a switching time of approximately 2 ms. We have found that the classical valve model, introduced in [26] and still in common usage, did not correspond well to the mass flow rate of the Festo valve. Instead, a theoretical model introduced in [7,27] is used:

$$\dot{m} = \begin{cases} C_v A \dfrac{p_{up}}{\sqrt{RT_{up}}} & \dfrac{p_{down}}{p_{up}} \le b_v \\ C_v A \dfrac{p_{up}}{\sqrt{RT_{up}}} \sqrt{1 - \left(\dfrac{\left(\dfrac{p_{down}}{p_{up}} \right) - b_v}{1 - b_v} \right)^2} & \dfrac{p_{down}}{p_{up}} \ge b_v \end{cases} \quad (4)$$

C_v is the valve discharge flow coefficient, and b_v is the critical pressure. The mass flow rate is studied in both direction (inflation 1->2 and deflation 2->3) separately using the experimental procedure introduced by ISO6358. In measurements three upstream pressure levels were used and the relevant experimental points were fitted by tuning two parameters (C_v, b_v) through equation (4). Figure 3 gives the parameters used and shows a good overlap between the simulated and experimental curves.

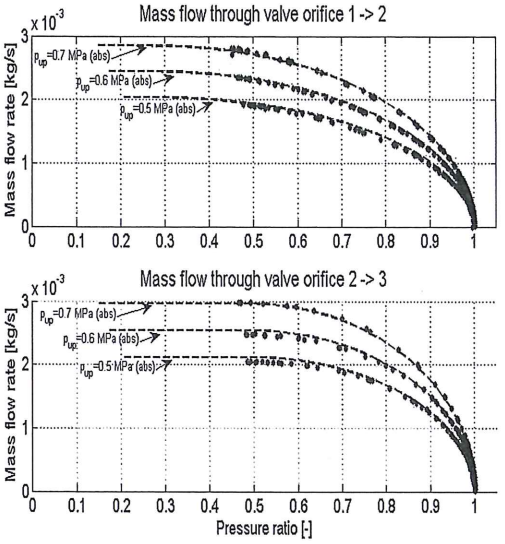

Parameter	Description	Value
R	Air constant	287 [J/(kg*K)]
T_{up}	Upstream temperature	293 [K]
p_{up}	Upstream pressure	0.5,0.6,0.7 [MPa] (abs)
A	Valve diameter	3.14e-6 [m^2]
C_v (1 -> 2)	Flow coefficient	0.36
C_v (2 -> 3)	Flow coefficient	0.39
b_v (1 -> 2)	Critical pressure	0.28
b_v (2 -> 3)	Critical pressure	0.49

Figure 3: Flow rate fits for passages 1->2 and 2->3

2.3.2 *Analytic approach*

In its place, a procedure similar to the one introduced in [28] is followed, where an equivalent mass flow rate model was determined for a proportional servo valve. The mass flow rate has nonlinear characteristics and is a function of pressure p inside the volume, and the control signal u (duty ratio [0-1]). Thus, one obtains a traditional representation for the pressure change as follows:

$$\dot{p} = \frac{kRT}{V}\dot{m}_{eq}(u,p) - kp\frac{\dot{V}}{V} \tag{5}$$

In equation (5), the second term can be computed once the volume V is known, and the pressure is given. In the first term, the nonlinear valve function is difficult to measure. Alternatively, the nonlinear valve characteristic can be approximated experimentally by charging and discharging a constant volume chamber. This causes the second term in equation (5) to disappear, allowing the mass flow rate to be calculated from the rate of change of pressure. A set of input signals with different duty cycles were applied to the valve and the pressure response in the constant volume chamber was measured. The averaged pressure signal is then differentiated in order to obtain the pressure change in the volume. By distributing the computed slopes of the pressure curve at the

corresponding parameter pairs (u and p), a parametric representation of the surface of the pressure change can be obtained. Using this surface, the mass flow rate can be estimated using equation (5). Figure 4 (left) illustrates the estimated/measured mass flow rate plotted as a function of input signal (duty ratio) and the relative actuator pressure. Note that a negative mass flow rate indicates a discharging flow.

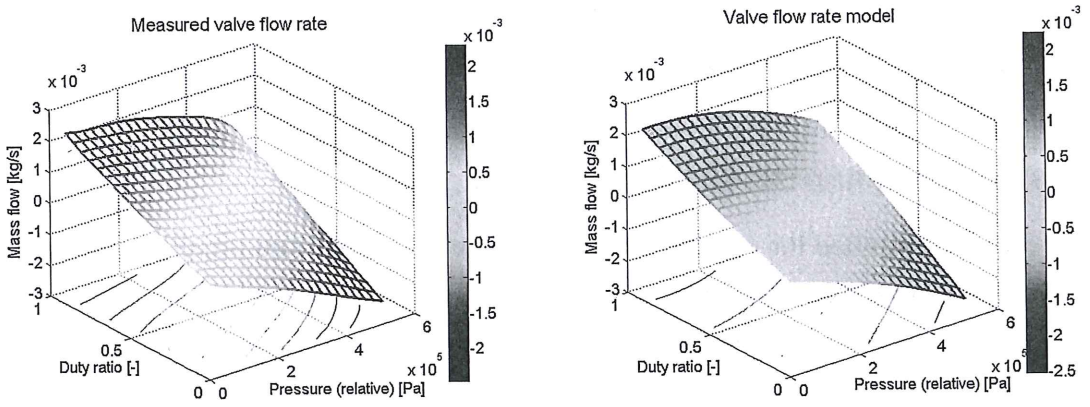

Figure 4: Estimated mass flow rate for on/off valve

In order to model the mass flow rate, a 2nd order bi-polynomial function was used, as follows:

$$\dot{m}_{eq}(u,P_m) = m_1 + m_2 P_m + m_3 P_m^2 + m_4 u + m_5 u P_m + m_6 u P_m^2 + m_7 u^2 + m_8 u^2 P_m + m_9 u^2 P_m^2 \quad (6)$$

Where $m_{1\text{-}9}$ are the coefficients found using the least-squares method. The output obtained from this function is plotted in Fig. 4 (right). It can be observed that the model approximates the averaged mass flow rate behavior of the valve quite well. The maximum fitting error is 1.96×10^{-4} kg/s, or 4.13 % of the range. The RMSE is 5.5×10^{-5} kg/s or 1.16 %.

2.4 Pressure dynamics

The pressure depends on the mass of the air and the volume of the muscle. The diameter and length of the muscle were measured, and the volume of the muscle was calculated assuming a cylindrical shape. The measurements indicate a nearly linear behavior, dependent on displacement:

$$V_m(x) = v_0 + v_1 x, \tag{7}$$

For calculating the pressure inside the muscle, it is assumed that the air is ideal gas and the process is adiabatic, such that the pressure change follows:

$$\dot{p}_m = \frac{kRT}{V_m(x)} \dot{m}_{eq}(u, p_m) - \frac{kp_m}{V_m(x)} \frac{dV_m(x)}{dx} \dot{x} \tag{8}$$

Where k (1.4 for adiabatic process), R, T, V_m and p_m denotes the specific heat ratio, gas constant, air temperature, volume of the muscle, and muscle pressure, respectively.

3 SIMULATION AND EXPERIMENTAL RESULTS

This section describes the results of validating the developed valve models and overall system model with measurements. In addition, the final system model is used for tuning the parameters of a traditional PI-controller, which is used to control the actuator to follow a desired displacement trajectory.

3.1 Valve model validation

The non-analytical valve model is based on equation (4) including the valve delay (~2 ms) in the switching phenomena when the valve changes its state and analytic model is based on equation (6). The measurements are carried out with a known constant volume and supply pressure 5.5 MPa (relative) and the initial pressure in the volume is zero. The volume is pressurized operating the solenoid valve with different duty ratios (25, 50 and 75 %) of 50 Hz PWM-signal. The chosen frequency is fast enough for the system dynamics and also provides a reasonable resolution for controlling the available duty ratio values. During the deflation process, the volume is first pressurized to a maximum value (5.5 MPa rel.), and then the valve is operated similarly with different duty ratios as in the inflation process.

Figure 5 illustrates the simulated and measured pressure responses for the inflation and deflation processes. The non-analytical valve model gives a good overall estimation for inflating pressure curves. However, the model is unable to completely estimate the pressure response during the deflation process. The deviation is caused by the silencer

that was attached to the third valve port. The use of the silencer is necessary because of the very loud noise caused by the high speed valve switching. The silencer clearly changes the characteristics of the flow through 2 -> 3 and the effects are strongest when the pressure inside the volume approaches the steady-state value. As the pressure drop across the valve decreases the silencer works like a flow restrictor. In consequence, the pressure in the simulations drops faster causing a steady-state offset compared to the measurements. The effects of the silencer at higher upstream pressure levels are almost negligible, and the model is able to follow the measured pressure curves quite accurately.

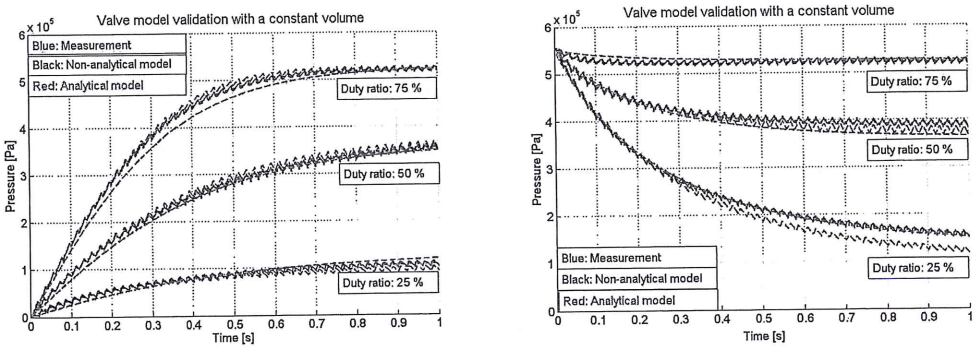

Figure 5: The validation of valve models when inflating and deflating a constant volume with different PWM-duty ratios

Despite some divergences between the model and the measurement the analytic model is able to estimate the pressure with reasonable accuracy. The advantage of the model is its suitability to be used for conventional control design, such as sliding mode control. The effectiveness of the model was proved in [29], where it was used successfully with the smooth variable structure filter (SVSF) to estimate the system states for the sliding mode controller (SMC). The 2nd -order bi-polynomial function (equation (6)) can be solved to find the desired duty ratio when the desired flow rate and the actuator pressure (measured) are known. The sliding mode controller and the filter are known to be very robust to parameter variations and other uncertainties, yielding an error tolerance for the estimated mass flow rate model.

3.2 System model validation

The motion equation of the muscle driving a constant payload attached in a vertical direction is defined (using Newton's Second Law) as follows:

$$M\ddot{x} = F_{static} - F_c sign(\frac{dx}{dt}) - C_f \frac{dx}{dt} - Mg \quad (9)$$

Where F_{static} is the static muscle force given in equation (7), M is the total mass of the system and payload, and g is the gravitational constant. F_c is the Coulomb friction and C_f is an experimentally approximated damping factor of the muscle actuator. The overall model was verified for both the non-analytic and analytic valve models. In the validation process, a set of input signals (duty ratio) of triangle waveform was applied to the system. The frequency of the waveform was varied and the duty ratio value changed between 0.05 and 0.95. The simulation and measurement results for input signal frequencies 0.08 and 0.25 Hz are shown in Fig. 6. The chosen PWM-frequency is high enough compared to the system dynamics as there exists no excessive chattering in the displacement signal.

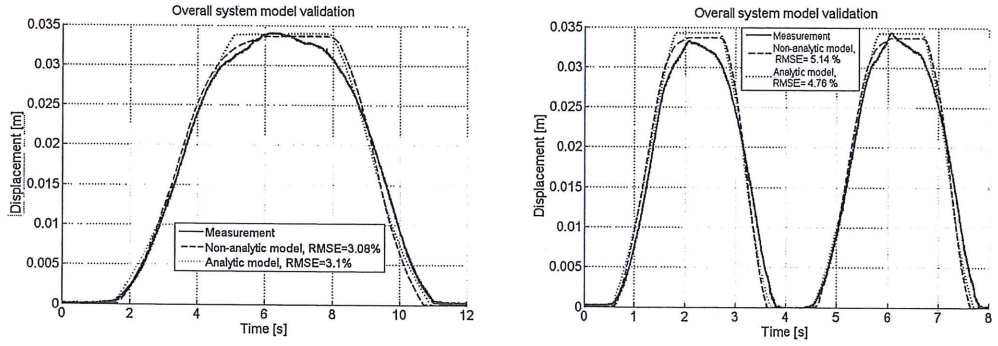

Figure 6: Simulated and measured displacement response for a triangle (f=0.08 Hz and f=0.25 Hz) input signal

The simulation results show that both models are able to estimate the displacement of the actuator and payload (9.6 kg) with reasonable good accuracy. An extremely good accuracy is obtained during the upward motion. The models fail to describe the creeping effect near the maximum displacement. It is a nominal effect for this type of actuator caused by material deformations. The largest modeling errors occur during the

downwards motion. This is caused by the simplified hysteresis model where a constant force offset is either reduced from or added into the static muscle force model depending on the sign of the actuator velocity. Thus, the model does not take into account the real transition between the inflating and deflating curves. In addition, the un-modeled silencer affects the accuracy of the non-analytical model. Altogether, both the models can estimate the real process reasonably well, as the maximum displacement error is approximately 10 % and the RMSE values for the displacement are around 3 - 5 %.

3.3 PI-controller

A PI-controller was tuned by trial-and-error using the non-analytical and analytical system models. During the operation it was noted that the system is very sensitive to oscillations and instability. The instability issue limited the maximum gains for the controller resulting in a lack of accuracy. A reasonable performance was gained with a derivative gain in the controller during the simulations, but due to the measurement noise it could not be used in the real system. Figure 7 illustrates the results when the input signal is sinusoidal with amplitude of0.01 m and frequencies of 0.5 and 1 rad/s. The tuned gains for the controller were P=25 and I=150. It can be seen that the system performance is quite poor with the PI-controller. The response for the initial step is slow, and the system is not able to follow the desired trajectory very well. A steady-state error of approximately 1.5-2.2 mm is present during the entire cycle. The RMSE is over 10 % and increases as the frequency of the desired trajectory is increased. It becomes apparent that pneumatic systems are very difficult to control accurately. The performance of traditional linear approaches like PI and PID controllers is poor with highly nonlinear pneumatic systems. Thus, nonlinear and robust approaches are needed for better performance. However, the models developed in this paper of the pneumatic muscle actuator system give a firm basis for the design of more advanced control strategies. The non-analytical model can be used to simulate the real process quite accurately. In addition, the analytical model can be used in the model-based controller and state estimator design.

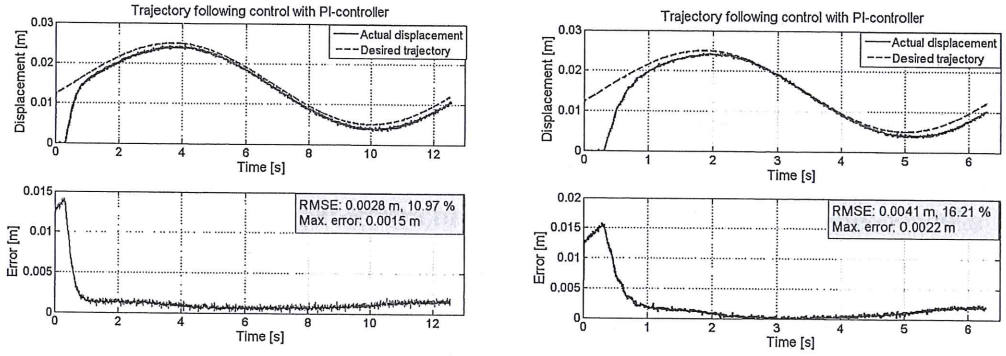

Figure 7: Trajectory (ω=0.5 and ω=1 rad/s) followed control with tuned PI-controller

CONCLUSIONS

In this paper, a nonlinear model for a pneumatic muscle actuator system controlled by an on/off solenoid valve was developed. The solenoid valve is operated by a pulse width modulated (PWM) scheme which gives an interesting alternative to develop low-cost pneumatic servo systems. On the other hand, accurate control of highly nonlinear pneumatic systems requires advanced control techniques that often use model-based approaches. Thus, the main focus of this research was to develop a model for control design approaches which capture the major nonlinearities present in the system with reasonable accuracy. In PWM-operated systems, the high speed switching of the valve results in discontinuities which are often difficult to handle from the viewpoint of control design. As a consequence, two valve models were developed in this study. The non-analytical model is able to describe the real operation of the system with relatively good accuracy, and including the nonlinear flow regimes and valve switching delays. The model is suitable for system analysis and for testing of controllers. The analytical model of the system which includes the nonlinearities of the system was developed to transform the discontinuities into a continuous form. This was accomplished by introducing a continuous flow model through the valve as a function of duty ratio of PWM-signal and actuator pressure. The use of this analytical model enables the implementation of conventional analytical control approaches, such as sliding mode control, and provides a tool for the analysis of stability and robustness.

ACKNOWLEDGEMENT

The work described in this article was partly supported by the Academy of Finland and Finnish Foundation for Technology Promotion.

REFERENCES

[1] **Morita, Y.S., Shimizu, M., and Kagawa, T.**, *An Analysis of Pneumatic PWM and its Application to a Manipulator,* Proc. of International Symposium of FluidControl and Measurement, Tokyo, pp. 3–8, 1985.

[2] **Noritsugu, T.**, *Development of PWM Mode Electro-Pneumatic Servomechanism, Part I: Speed Control of a Pneumatic Cylinder,* J. Fluid Control, 17–1, pp. 65–80, 1986

[3] **Noritsugu, T.**, *Development of PWM Mode Electro-Pneumatic Servomechanism, Part II: Position Control of a Pneumatic Cylinder*, J. Fluid Control, 17–2–, pp. 7–31, 1986

[4] **Lai, J.-Y., Singh, R., and Menq, C.-H.**, *Development of PWM Mode Position Control for a Pneumatic Servo System*, Journal of the Chinese Society of Mechanical Engineers, Vol. 13, No. 1, pp. 86–95, 1992.

[5] **Kunt, C., and Singh, R.**, *A Linear Time Varying Model for On-Off Valve Controlled Pneumatic Actuators*, ASME J. Dyn. Syst., Meas., Control, 112–4, pp. 740–747, 1990

[6] **Ye, N., Scavarda, S., Betemps, M., and Jutard, A.**, *Models of a PneumaticPWM Solenoid Valve for Engineering Applications*, ASME J. Dyn.Syst., Meas., Control, 114–4, pp. 680–688, 1992

[7] **Messina, A., Giannoccaro, N.I., and Gentile, A.**, *Experimenting and modeling the dynamics of pneumatic actuators controlled by pulse width modulated technique*, Mechatronics, No. 15, pp. 859–881, 2005.

[8] **Barth, E., Zhang, J., Goldfarb, M.**, *Sliding mode approach to PWM-controlled pneumatic systems*, Proceedings of the American Control Conference, pp. 2362-2367, Anchorage, AK, 2002

[9] **Ning, S., Bone, G.**, *Development of a nonlinear dynamic model for a servo pneumatic positioning system*, Proceedings of the IEEE International Conference on Mechatronics and Automation, pp. 43-48, Niagara Falls, Canada, 2005

[10] **Paul, A. K., Mishra, J. K., and Radke, M. G.**, *Reduced Order Sliding Mode Control for Pneumatic Actuator*, IEEE Trans. Control Syst. Technol., 2–30, pp. 271–276, 1994

[11] **Van Varseveld, R. B., and Bone, G. M.**, *Accurate Position Control of a Pneumatic Actuator Using On/Off Solenoid Valves*, IEEE/ASME Trans. Mechatron., 2–30, pp. 195–204, 1997

[12] **Barth, E. J., Zhang, J., and Goldfarb, M.**, *Control Design for Relative Stability in a PWM-Controlled Pneumatic System*, ASME J. Dyn. Syst., Meas., Control, 125–3, pp. 504–508, 2003

[13] **Shen, X., Zhang, J., Barth, E., and Goldfarb, M.**, *Nonlinear averaging applied to the control of pulse width modulated (PWM) pneumatic systems*, Proceedings of the American control Conference, pp. 4444–4448, Boston, 2004.

[14] **Shen, X., Zhang, J., Barth, E., and Goldfarb, M.**, *Nonlinear Model-Based Control of Pulse Width Modulated Pneumatic Servo Systems*, Journal of Dynamic Systems, Measurement and Control, Vol. 128, pp. 663–669, September 2006

[15] **Taghizadeh, M., Ghaffari, A., and Najafi, F.**, *A Linearization Approach in Control of PWM-Driven Servo-Pneumatic Systems*, 40th Southeastern Symposium on Systems Theory (SSST), pp. 395–399, March 2008

[16] **Schulte, R.A.**, *The characteristics of the McKibben artificial muscle, In the Applications of External Power in Prosthetics and Orthotics.* Publ. 874, Nas-RC, pp. 94–115, 1962.

[17] **Chou, P., and Hannaford, B.**, *Measurement and Modeling of a McKibben Pneumatic Artificial Muscles*, IEEE Transactions on Robotics and Automation, Vol. 12, No. 1, Feb 1996.

[18] **Festo**, *Fluidic Muscle MAS*, Festo Brochure, 2002

[19] **Gaylord, R. H.**, *Fluid Actuated Motor System and Stroking Device*, US Patent No. 2,844,126. July 22, 1958.

[20] **Inoue, K.**, *Rubbertuators and applications for robotics*, In 4th International Symposium on Robotics Research, pp. 57–63, 1987.

[21] **Tondu, B., and Lopez, P.**, *Modeling and Control of McKibben Artificial Muscle*, IEEE Control Systems Magazine, pp. 15–38, April 2000.

[22] **Klute, G. K., and Hannaford, B.**, Accounting for elastic energy storage in McKibben artificial muscle actuators, ASME Journal of Dynamic Systems, Measurement and Control, Vol. 122, 2000.

[23] **Delson, N., Hanak, T., Loewke, K., and Miller, D.N.**, *Modeling and implementation of McKibben Actuators for a Hopping Robot.*

[24] **Davis, S., and Caldwell, D. G.**, *Braid effects on contractile range and friction modeling in pneumatic muscle actuators*, The International Journal of Robotics Research, Vol. 25, No. 4, pp. 359–369, April 2006

[25] **Kerscher, T., Albiez, J., Zöllner, J. M., and Dillman, R.**, *FLUMUT – Dynamic Modelling of Fluidic Muscles Using Quick-Releases*, Proceedings of the 3rd International Symposium on Adaptive Motion in Animals and Machines, Illmenau, Germany, 2005

[26] **Shearer, J.L.**, *Study of pneumatic processes in the continuous control of motion with compressed air (I, II)*, ASME Trans., pp.233–249, 1956.

[27] **ISO6358**, *Pneumatic Fluid Power – Components using Compressible Fluids – Determination of Flow-rate Characteristics*, 1989

[28] **Rao, Z., and Bone, G. M.**, *Nonlinear modeling and control of servo pneumatic actuators*, IEEE Transactions on Control Systems Technology, Vol. 16, No. 3, pp. 562–569, May 2008.

[29] **Jouppila, V., Gadsden, A., Habibi, S., Bone, G. M., Ellman, A.**, *Sliding mode controller and filter applied to a pneumatic McKibben muscle actuator*, In ASME International Mechanical Engineering Congress and Exposition (IMECE2009), 10 pages, Lake Buena Vista, USA 2009

PUBLICATION 2

Position Control of PWM-actuated Pneumatic Muscle Actuator System

Ville Jouppila and Asko Ellman

Reprinted, with permission, from the *Proceeding of the ASME 2011 International Mechanical Engineering Congress and Exposition (ASME IMECE 2011)*, Denver, USA, 2011

Proceedings of the ASME 2011 International Mechanical Engineering Congress & Exposition
IMECE2011
November 11-17, 2011, Denver, Colorado, USA

IMECE2011-63370

POSITION CONTROL OF PWM-ACTUATED PNEUMATIC MUSCLE ACTUATOR SYSTEM

Ville Jouppila
Tampere University of Technology
Department of Mechanics and Design
Tampere, Finland

Asko Ellman
Tampere University of Technology
Department of Mechanics and Design
Tampere, Finland

ABSTRACT

Pneumatic servo positioning systems have been in use for long time and subject to wide spectrum of studies due to their numerous advantages: inexpensive, clean, safe and high ratio of power to weight. However, the compressibility of air and the inherent non-linearity of these systems continue to make achieving accurate position control a real challenge. Conventional pneumatic servo systems are based on cylinder actuators that are difficult to control precisely due to the aforementioned nonlinearities as well as the nonlinear behavior of the air flow through the valve, the friction between the cylinder and the piston, and the stick slip effect at the low velocity of the system. In this paper, a position servo control system using a pneumatic muscle actuator is studied. Pneumatic muscle actuator is a novel type of actuator which has even higher force to weight ratio than the cylinder. In addition, muscle actuator introduces a stick slip free operation giving an interesting option for positioning systems. However, significant hysteresis and position dependant force result in a highly nonlinear system, a real challenge for good control performance.

In this paper, pneumatic muscle actuator is controlled by a low-cost on/off valve with PWM-strategy instead of costly servo or proportional valve. The main processes of the system, including flow dynamics, pressure dynamics, force dynamics and load dynamics are derived to provide a full nonlinear model that captures all the major nonlinearities of the system. This model is used for analyzing and tuning the controller performances by simulations before implementing in the real system. In addition, a recently introduced method of using bi-polynomial functions to model the valve flow rate is utilized to provide a continuous and invertible description of flow for controller designs.

A proportional plus velocity plus acceleration controller with feed-forward component (PVA+FF) is designed based on the linearized system model. For a comparison, a sliding mode controller (SMC) based on linear as well as non-linear system model are designed. The performance of the designed controllers is studied by simulations. The stability and performance analysis includes the effects of friction modeling error and valve modeling error. The robustness of the controllers is tested by varying the payload mass of the system.

INTRODUCTION

Pneumatic systems have many properties that make them attractive for use in a variety of applications. Pneumatics does not have temperature limitations and exhausted air is not required to be collected making the fluid return lines unnecessary. In addition, high force-to-weight ratios, cleanliness, compactness, ease of maintenance, and the safety of pneumatic actuators offer desirable features for many industrial designs. A new type of pneumatic McKibben muscle actuator can provide an even higher force-to-weight ratio compared with conventional pneumatic systems, and is able to operate in a wide range of environments. However, the nonlinear characteristics of the actuator, compressibility of air, friction, and nonlinear air flow through the valve results in a complex and difficult system to model and control. These effects are the main reason that pneumatic systems are commonly avoided for advanced applications.

A review of the literature demonstrates that a large number of control strategies have been proposed to handle the effects of nonlinearities present in the muscle actuator. These include: PID control, adaptive control strategies [1,2,3], nonlinear PID [4], gain scheduling, neural networks, and fuzzy controllers [5,6,7], In [8] and [9] a sliding mode control strategy was applied to a muscle actuator system, where simulation results of

the effectiveness of the strategy were presented. Other sliding mode control approaches are presented in [10,11,12]. In [12], a SMC strategy was applied to control the muscle actuator system in an opposing pair configuration using a proportional flow control valve. Experimental results with sinusoidal tracking (with amplitude of 7.5 mm for a frequency range of 0.5 – 1.5 Hz) showed accuracies of +/- 0.5 mm to +/- 1.2 mm. Since the studied system is highly nonlinear and not completely known, the SMC strategy is chosen for the control of the muscle actuator. Previous studies on the SMC strategy have demonstrated it to be an efficient and robust control strategy for controlling pneumatic actuators. However, in these studies, a proportional or servo valve has been used to control the actuator. In this paper, the on/off valve is chosen for the control of the muscle actuator system in order to provide a low cost alternative to servo-pneumatic systems.

In recent years, a considerable amount of research has been performed to develop inexpensive servo-pneumatic systems using on/off solenoid valves with pulse-width modulation (PWM). Previous efforts have shown the potential of PWM-controlled pneumatics, although they have suffered from the lack of an analytical approach for studying the system [13,14,15]. In one article, the nonlinearities of the system were handled by proposing a switching controller based on a reduced order nonlinear model [16]. In [17], a novel valve pulsing algorithm was developed that allowed the use of multiple on/off solenoid valves in place of costly servo valves. The effectiveness of the proposed algorithm with a continuous state feedback controller (i.e., position, velocity and acceleration feedback) was successfully implemented and demonstrated through experiments on a pneumatic cylinder. Another notable paper was introduced in [18], where a discrete-time control method was developed for a PWM-controlled pneumatic servo system. A PID controller with added friction compensation and position feed-forward was successfully implemented with a worst case steady-state accuracy of 0.21 mm and S-curve trajectory following errors less than 2.0 mm. In [19], a linear state-space averaged model and a sliding mode controller with PWM based on a loop shaping approach was introduced for the control of a single degree of freedom pneumatic positioning system with a cylinder. This was later followed by a nonlinear averaged model and a sliding mode controller design [20]. Sinusoidal tracking with amplitude of 20 mm and frequencies from 0.25 to 1 Hz reportedly had accuracies from +/- 1 mm to +/- 3.5 mm. In [21], a sliding mode controller without PWM for a double-acting cylinder using four low-cost solenoid valves was introduced. The sinusoidal tracking error for a stroke +/- 20 mm at 0.5 Hz was less than +/- 2 mm. In [22], three linearization approaches for PWM-driven servo-pneumatic systems with a cylinder and a single on/off valve were introduced. Improved performances were achieved by using simple linear controllers with velocity feedback instead of complex and costly nonlinear ones. Tracking accuracies for a sinusoidal input with amplitude 20 mm at 1 Hz and 2 Hz were less than +/- 0.5 mm and +/- 1.5 mm, respectively.

The system architecture used in this study is illustrated in Figure 1. The Festo fluidic muscle (MAS10-300 mm) is mounted horizontally and attached to a cylinder piston. The supply pressure (0.65 MPa abs.) for the system is provided by the proportional pressure regulator (Festo VPPM). A 3/2 high speed on/off solenoid valve (Festo MHE2) is controlled to drive the muscle actuator. The valve is operated with a pulse width modulated signal by controlling the duty ratio. The cylinder pressure is set for a constant value that is maintained with another proportional pressure regulator providing a counterforce for the muscle actuator. The uncontrolled cylinder adds frictional effects that can be treated as system uncertainties. A muscle pressure and the displacement of the actuator (potentiometer) are measured. The other states (velocity and acceleration) are obtained by differentiation of the filtered position signal. The controller design and simulations are performed in the Matlab/Simulink environment.

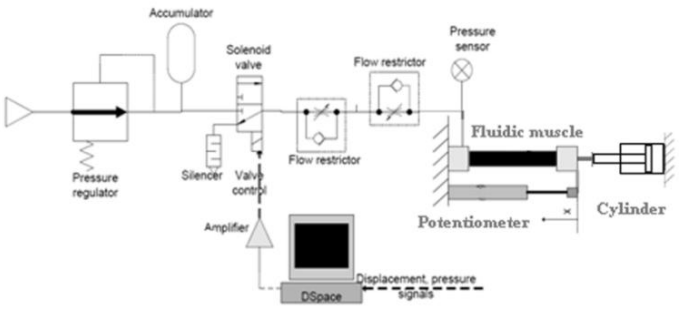

Fig. 1. System setup

The overall system is highly nonlinear and not completely known leading to un-modeled uncertainties. In order to capture the major nonlinearities of the system, the main subsystems including flow, pressure, force and load dynamics are derived to provide a full nonlinear model for simulations. A continuous valve model that captures the flow as a function of PWM duty ratio and actuator pressure is generated and utilized to describe the nonlinear flow through the valve. This enables the use of mass flow rate as a controller output, which is then converted to a real control variable (duty ratio) by using the inverse of the flow model. Thus, the nonlinear system from mass flow rate to actuator position can be linearized around an equilibrium point and conventional controller design can be applied for the system. Based on the linearized system model a proportional plus velocity plus acceleration controller combined with feed-forward compensation (PVA+FF) is derived. Also, a sliding mode control (SMC) strategy based on linear model as well as non-linear model is designed and applied with the goal of improved accuracy and robustness.

The performance of the controllers is demonstrated with a sinusoidal trajectory tracking task with different frequencies. The robustness of the controllers is tested by varying the payload from its nominal value.

MUSCLE ACTUATOR SYSTEM MODELLING

This section describes the modeling of the system, including the pneumatic muscle actuator with load mechanism, pressure and valve flow dynamics resulting in a nonlinear model of the system that can be used for verification of the controller performance.

Pneumatic Muscle Actuator

The pneumatic McKibben muscle actuator consists of a rubber tube with a non-extensible fiber surrounding [23]. This physical configuration causes the muscle to have variable-stiffness spring-like characteristics, nonlinear passive elasticity, physical flexibility, and is very lightweight compared to other types of actuators [24]. During pressurization, the muscle widens in diameter and shortens in length, and the maximum force is obtained at the beginning of the contraction and decreases with increasing contraction. The actuator is unidirectional and its maximum contraction is typically 20% to 25% of the nominal length. The advantage of the muscle actuator over the traditional cylinder is the higher force to weight ratio and the stick-slip free motion at low velocities. On the other hand, the force-to-contraction relation at different pressure levels is highly nonlinear, and adds to the difficulty of effectively modelling the muscle actuator.

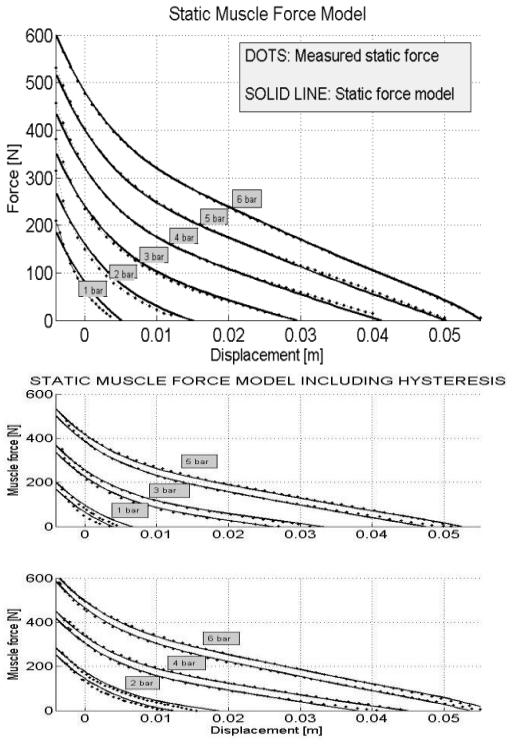

Fig. 2. Static muscle force characteristics and hysteresis

Figure 2 illustrates the nonlinear relationship between the force, pressure, and displacement. It should also be noted, that the actuator introduces a significant hysteresis phenomenon due to the material deformations. The hysteresis is extremely difficult to model accurately, especially during the transition phase when the direction of the movement changes. The simplest way to model hysteresis is to add a constant force offset to the mean static force curve. Thus, the hysteresis can be considered as static Coulomb friction. The mean static force (Fig. 2 (upper)) to be modeled is the averaged force from the upper and lower curves of the hysteresis force loop. The shape can be captured quite accurately by fitting a 3rd order polynomial function $F_{max}(x)$ for the curve at the maximum actuator pressure 6 bars. In order to model the force at different pressure levels, a force component that is subtracted from the maximum possible force is needed. It is also noted, that the force is proportional to the pressure when the actuator length is fixed. However, the proportionality factor changes as a function of displacement being at its maximum at $x = 0$ and decreasing with increased displacement resulting in the latter term in the overall muscle force equation [25]:

$$F_m(x, p_m) = F_{\max}(x) - (p_{\max} - p_m)\left(\frac{k_0 - k_1 x}{k_2}\right)$$
$$F_{\max}(x) = a_0 + a_1 x + a_2 x^2 + a_3 x^3 \qquad (1)$$

where p_{max} is the maximum muscle pressure, p_m is the actual muscle pressure, x is the displacement of the actuator, and $a_{0\text{-}3}$, k_0 [N], k_1 [N/m] and k_2 [Pa] are coefficients to match the model and measured data, respectively. Figure 2 illustrates that the model is able to describe the mean static force-pressure-displacement relation with good accuracy. By including a static Coulomb friction term also the hysteresis effect can be captured reasonably well as shown in Figure 2 (lower). The viscous friction of the actuator is extremely difficult to determine and model accurately, as it is dependent on the velocity as well as the pressure in the actuator. Thus, a constant damping factor B is usually introduced to describe the viscous friction. In a control design the frictional elements of the system are simplified where the discontinuous static and Coulomb friction are neglected and only viscous friction is taken into account.

Pressure dynamics

For calculating the pressure inside the muscle, it is assumed that the air is an ideal gas and the change of air is adiabatic, such that the pressure change is as follows:

$$\dot{p}_m = \frac{kRT}{V_m(x)}\dot{m}_{eq}(u_{duty}, p_m) - \frac{kp_m}{V_m(x)}\frac{dV_m(x)}{dx}\dot{x} \qquad (2)$$

where k (1.4 for adiabatic process), R, T, V_m and p_m denote the specific heat ratio, gas constant, air temperature, volume of the muscle, and muscle pressure, respectively. The equivalent mass flow rate $\dot{m}_{eq}(u_{duty}, p_m)$ is described as a function of a duty ratio u_{duty} and actuator pressure, and will be determined in the next section. Figure 3 shows that a linear approximation is

sufficient to describe the volume of the muscle actuator as a function of displacement:

$$V_m(x) = v_0 + v_1 x \tag{3}$$

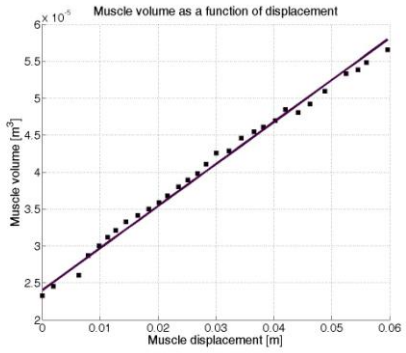

Fig. 3. Muscle volume in correlation with displacement

Valve flow dynamics

The mass flow rate model of the on/off valve controlling the muscle actuator is an essential part of the system model. The valve is controlled with the duty ratio u_{duty} of the PWM-modulated signal. The switching frequency f_{PWM} and the duty ratio determine how long the valve is open and closed during time period T_{PWM} (=1/ f_{PWM}). The PWM switching frequency has a significant effect on the system performance as the final control signal for the valve is updated at the PWM frequency used. Thus, a small PWM frequency results in poor control accuracy. On the other hand, the bandwidth of the used valve sets the limit to the maximum reasonable PWM frequency. The valve used in this work has a bandwidth of 300 Hz. Another factor affecting the performance is the sampling time used for creating the discrete (on/off) control of the valve. The sampling time is defined as T_S=0.1ms in order to provide sufficient control resolution. The resolution of the control signal can be simply calculated by $Resolution=1/(T_{PWM}/T_S)*100\%$. If a PWM frequency of 50 Hz is used the resolution will be 0.5 % and for 100 Hz it is 1 %, respectively. If the operating sampling time would be decreased e.g. to T_S=1ms, one would get the control resolutions of 5 and 10 % and the control accuracy would decrease considerably.

Due to the PWM switching, two modes exist in the system. During the 'on'-mode the valve charges the muscle actuator, and during the 'off'-mode the actuator is discharged. In addition, the flow can be either choked or un-choked depending on the ratio of downstream and upstream pressure. Assuming an ideal gas law and an adiabatic process, a widely accepted model for mass flow rate through the valve can be expressed

$$\dot{m} = \begin{cases} Cp_{up} & \frac{p_{down}}{p_{up}} \le b \\ Cp_{up}\sqrt{1-\left(\frac{\left(\frac{p_{down}}{p_{up}}\right)-b}{1-b}\right)^2}, & \frac{p_{down}}{p_{up}} \ge b \end{cases} \tag{4}$$

C is the valve conductance and b is the critical pressure ratio. In addition, the flow paths of the valve must be considered separately. In other words, the model should account for two possible flows. When the valve is open the flow path is through the orifice 1 -> 2 (inflation) and when the valve is closed the flow path is through the orifice 2-> 3 (deflation). When inflating, the upstream pressure is the constant supply pressure and downstream pressure is the pressure inside the actuator. When exhausting, the upstream pressure is the actuator pressure and the downstream pressure is the ambient pressure. In order to identify the pneumatic behavior of the valve a set of experiments according to the procedure introduced by ISO6358 were carried out. In measurements 3 upstream pressure levels were used and the relevant experimental points were fitted by tuning two parameters (C, b) through equation (4). The tuned flow rate parameters are reported in Table 1. Figure 4 shows a good overlap between the simulated and experimental curves. Note, that this flow model combined with switching delays (~2 ms) is used in simulation study when proposed controllers are tested against the "real" nonlinear system.

Parameter	Description	Value
p_{up}	Upstream pressure	0.5, 0.6, 0.7 [MPa] (abs.)
C (1->2)	Sonic conductance	3.48e-9 [kg/(s*MPa]
C (2->3)	Sonic conductance	3.77e-9 [kg/(s*MPa]
b (1->2)	Critical pressure ratio	0.39
b (2->3)	Critical pressure ratio	0.28

Table 1. Identified valve parameters

From the view-point of conventional/linear controller design, the discontinuous switching between the modes is difficult to handle. Thus, an alternative approach introduced in [26] and applied to on/off solenoid valve in [25] is needed to provide a continuous and invertible flow model for the proposed controller design. In order to obtain a precise valve mapping, a pressure response curve was measured while inflating and deflating a closed chamber while operating the valve with different duty ratios. In the measurements a constant supply pressure level of 0.55 MPa was used. By differentiating the filtered pressure curve and using Eqn. 2 for a constant

volume, the mass flow rate can be approximated. Furthermore, the nonlinear characteristics of the mass flow rate can be captured introducing the equivalent mass flow through the valve as a function of the control signal u_{duty} and the measured muscle pressure p_m. Then, a 2nd order bi-polynomial function can be matched with the measurements and describe the relationship between the variables with sufficient accuracy.

$$\dot{m}_{eq}(u_{duty}, p_m) = m_1 + m_2 p_m + m_3 p_m^2 + m_4 u_{duty} + m_5 u_{duty} p_m + m_6 u_{duty} p_m^2 + m_7 u_{duty}^2 + m_8 u_{duty}^2 p_m + m_9 u_{duty}^2 p_m^2 \quad (5)$$

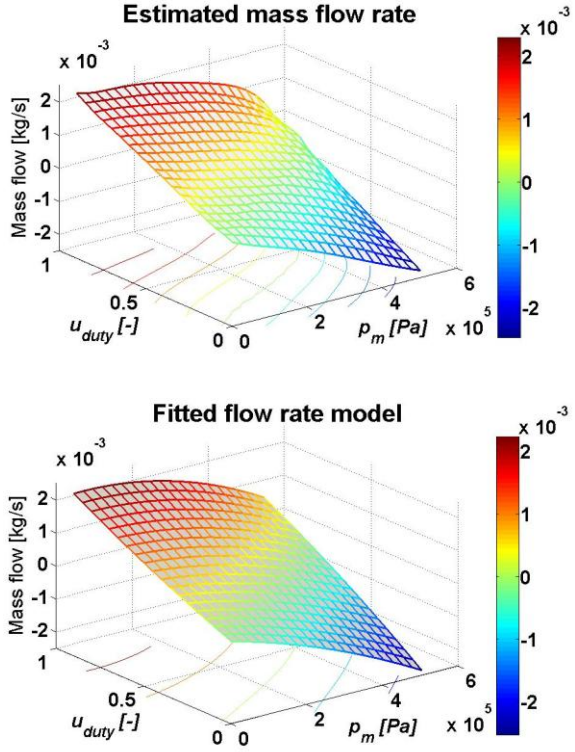

Fig. 4. Estimated and fitted mass flow rate

The output obtained from this function is plotted in Fig. 4. It can be observed that the model approximates the equivalent mass flow rate behaviour of the valve quite well. The maximum fitting error is 1.96×10^{-4} kg/s, or 4.13 % of the range. The RMSE is 5.5×10^{-5} kg/s or 1.16 %. Figure 5 illustrates the valve model validation when a test chamber (different from the chamber used for valve modeling) was pressurized and depressurized with different values of duty ratio.

Despite some divergences between the model and the measurement, the model is able to estimate the pressure response with reasonable accuracy. Furthermore, as the model is invertible, it can be used to convert the controller output (mass flow rate) into the duty ratio input for controlling the valve. In addition, the transformation takes into account the nonlinear behaviour of the flow through the valve.

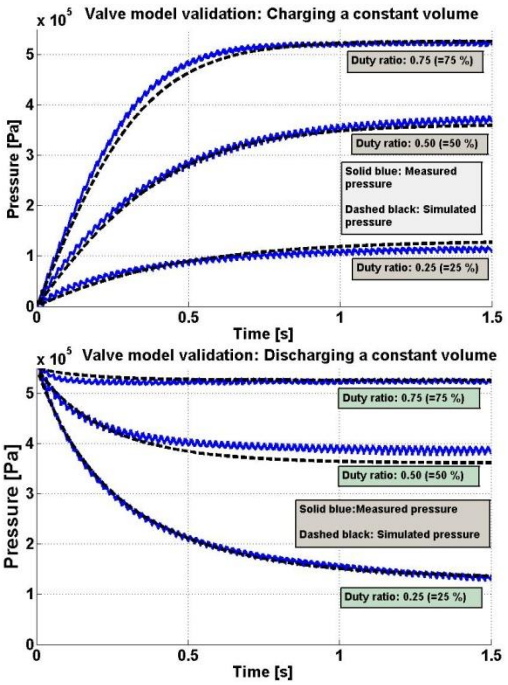

Fig. 5. Valve model validation for charging and discharging a constant volume chamber

Nonlinear system model

The overall nonlinear model of the muscle actuator system driving a constant mass load in horizontal configuration with a cylinder providing the counterforce can be derived as

$$\begin{aligned}
&M\ddot{x} = F_m(x, p_m) - F_f - p_{cyl} A_{cyl} \\
&F_m(x, p_m) = F_{\max}(x) - (p_{\max} - p_m)\left(\frac{k_0 - k_1 x}{k_2}\right) \\
&F_{\max}(x) = a_0 + a_1 x + a_2 x^2 + a_3 x^3 \\
&F_f = \left[F_C + (F_S - F_C) e^{-(\dot{x}/v_s)^2}\right] \mathrm{sgn}(\dot{x}) + B\dot{x} \\
&\dot{p}_m = \frac{kRT}{V_m(x)} \dot{m}_{eq}(u_{duty}, p_m) - \frac{k p_m}{V_m(x)} \frac{dV_m(x)}{dx} \dot{x} \\
&V_m(x) = v_0 + v_1 x \\
&\dot{m}_{eq} = \textit{see also equation (4)} \\
&\dot{m}_{eq}(u_{duty}, p_m) = m_1 + m_2 p_m + m_3 p_m^2 + m_4 u_{duty} + m_5 u_{duty} p_m + \\
&\qquad m_6 u_{duty} p_m^2 + m_7 u_{duty}^2 + m_8 u_{duty}^2 p_m + m_9 u_{duty}^2 p_m^2
\end{aligned} \quad (6)$$

The nonlinear system model is used in simulations for describing the behavior of the real system. The parameters for friction model were identified in [25], F_S=35 N, F_C=15 N, B=95 Ns/m and v_s=0.005 m/s. In simulations, the valve flow model described by equation (4) is used with valve delays in order to describe the real functionality of the valve.

Linearized system model

In order to apply conventional controller design, a linear model of the system is required. Linearization of the nonlinear

system model (eq. (6)) around an equilibrium point (p_e=0.35 MPa, x_e=0.015 m) results in a 3rd order transfer function between the actuator position and the mass flow rate

$$G_{ol}(s) = \frac{X(s)}{U(s)} = \frac{n_0}{s(s^2 + d_2 s + d_1 s)} \quad (7)$$

with parameters n_0=2.53e6, d_2=50, d_1=5248.

It should be noted, PWM operation is subject to sample-and-hold operation, which constrains the system such that the duty cycle can only be updated once per PWM period. The sample-and-hold operation can be approximated in a continuous expression as follows:

$$SAH(s) = \frac{1 - e^{-T_{PWM} s}}{T_{PWM} s} \quad (8)$$

Combining this with previously derived linear model we get:

$$G(s) = \frac{1 - e^{-T_{PWM} s}}{T_{PWM} s} G_{ol}(s) \quad (9)$$

For our system (with PWM frequency of 50 Hz), T_{PWM}=0.02 s. Figure 7 illustrates the effect of the sample-and-hold operation on the open loop characteristics of the linear model. It should be noted, that the sample-and-hold approximation attenuates the magnitude and decreases the phase near the PWM switching frequency. Therefore, the control design objective is to formulate a controller resulting in a robustly stable closed-loop system with a performance bandwidth well below the PWM switching frequency. Figure 8 illustrates the root locus of the linear system with sample-and-hold operation, indicating a critical negative feedback gain of 0.09.

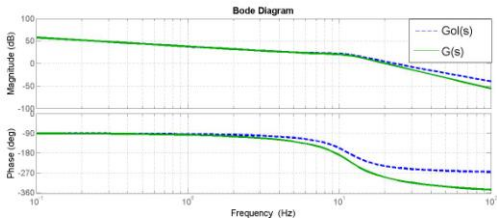

Fig. 7. Frequency characteristics of the linearized model with and without sample-and-hold approximation

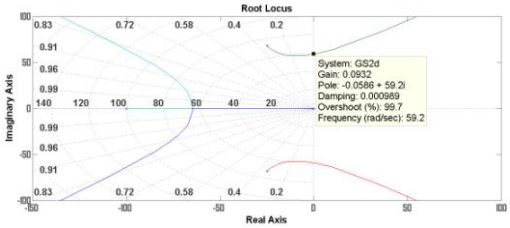

Fig. 8. Root locus of the linearized system with negative gain feedback

CONTROL DESIGN

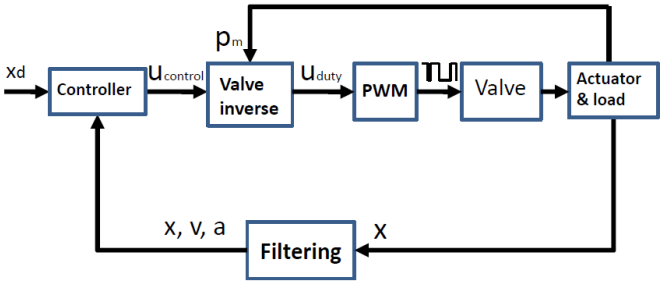

Fig. 9. Block diagram of the overall control system

Figure 9 depicts the block diagram of the overall control system. Actuator position and pressure are measured and velocity and acceleration are derived from the measured position signal in the filtering block. The output of the controller block is the mass flow rate $u_{control}$ which is then converted into a duty ratio u_{duty} of PWM signal in the "Valve inverse" –block. The bi-polynomial equation (5) reduces to the following quadratic equation in u_{duty}:

$$\begin{aligned} & C_{21} u_{duty}^{\ 2} + C_{11} u_{duty} + C_{01} = 0 \\ & where \\ & C_{01} = m_1 + m_2 p_m + m_3 p_m^2 - \dot{m}_{eq} \\ & C_{11} = m_4 + m_5 p_m + m_6 p_m^2 \\ & C_{21} = m_7 + m_8 p_m + m_9 p_m^2 \\ & \dot{m}_{eq} = u_{control} \end{aligned} \quad (10)$$

The correct value for desired input signal can be determined to be the most positive root, as follows:

$$u_{duty} = \frac{-C_{11} + \sqrt{C_{11}^2 - 4 C_{21} C_{01}}}{2 C_{21}} \quad (11)$$

Due to the numerical errors in the solution, the equivalent input control signal is bounded between 0 and 1 (as per the duty ratio signal which controls the valve). The remaining step is to convert the duty ratio u_{duty} to an applicable switching signal (0/1) for the on/off valve. In the PWM –block the duty ratio signal is sampled at the operating PWM frequency f_{PWM}. As we know, the duty ratio defines the time ($t_{on}=u_{duty}/f_{PWM}$) the valve is "on" during each PWM period $T_{PWM}=1/f_{PWM}$. Respectively, the valve is "off" for the remaining time of the PWM period. Based on this information the pulse width modulator outputs a discrete signal for the valve.

PVA+FF control design

The most common form of controller applied in practice to positioning systems is the proportional, velocity and acceleration (PVA) controller. Given x as the actuator position,

$u_{control}$ as the control signal and x_d as the reference position, a PVA controller is given as:

$$u_{control} = K_p e - K_v \dot{x} - K_a \ddot{x}$$
$$e = x_d - x \tag{12}$$

K_p, K_v and K_a as the proportional, velocity and acceleration gains, respectively. It is generally stated that both velocity and acceleration feedback are essential to ensure adequate performance in pneumatic servo applications. In practice, acceleration is often avoided as it is quite expensive to measure directly and alternatively the double differentiation of the position signal generally produces a noisy signal even with filtering. In addition, the PWM switching causes dither in the position signal which also can be regarded as noise. The magnitude of dither depends on the PWM frequency as well as the inertia of the system. It should be noted, that traditional filters (e.g. 2nd order Butterworth digital filter) introduce some phase lag between the real and filtered signal that also affects the control performance.

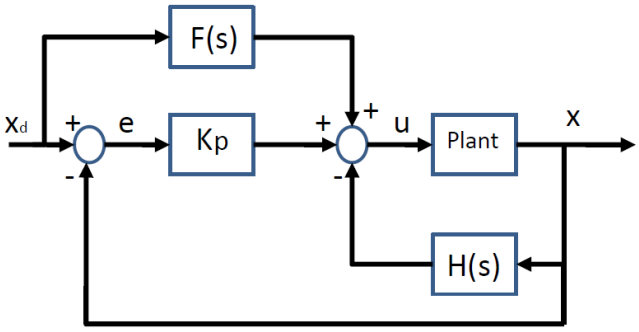

Fig. 10. Block diagram of the system with PVA+FF controller

The block diagram of the system with PVA controller plus feed-forward (FF) compensation is shown in Figure 10. Our PVA+FF controller design follows the work done [27]. In order to simplify the controller design, a plant transfer function (Eq.7) without sample-and-hold, is assumed. Then, assuming *F(s)=0*, the closed loop transfer function is

$$G_{cl}(s) = \frac{X(s)}{X_d(s)} = \frac{n_0 K_p}{s^3 + (d_2 + n_0 K_a)s^2 + (d_1 + n_0 K_v)s) + n_0 K_p} \tag{13}$$

Using the pole placement method, the desired closed-loop pole locations are defined as:

$$s_{1,2} = -\xi\omega_n \pm \omega_n\sqrt{1-\xi^2}, s_3 = -r\xi\omega_n \tag{14}$$

where ζ is the damping ratio, ω_n is the natural frequency and r is a constant. These pole locations produce the desired characteristics polynomial:

$$s^3 + (r\xi\omega_n + 2\xi\omega_n)s^2 + (2\xi^2\omega_n^2 r + \omega_n^2)s + r\xi\omega_n^3 \tag{15}$$

Equating (15) with the denominator of equation (13) and solving for the gains gives the design solution:

$$K_p = r\xi\omega_n^3 / n_0$$
$$K_v = (2\xi^2\omega_n^2 r + \omega_n^2 - d_1)/n_0 \tag{16}$$
$$K_a = (r\xi\omega_n + 2\xi\omega_n - d_2)/n_0$$

The desired natural frequency ω_n and damping ζ can also be related to the performance specifications of:

$$T_{settle} = \frac{4}{\xi\omega_n}$$
$$M_p = 100e^{-\xi\pi/\sqrt{1-\xi^2}} \tag{17}$$

with T_s as the ±2 percent settling time and M_p as the percent overshoot. The initial values for the PVA gains are determined by setting ζ=0.3, ω_n =50 rad/s and r=10 (with T_{settle}=0.27s and M_p=37 %) resulting in K_p=0.148, K_v=0.0007 and K_a=5e-5. The gains will be re-tuned with the nonlinear system model.

Feed-forward (FF) control is commonly used to improve tracking control performance. The goal of the FF design is to make the output track the reference input perfectly, i.e. $X_d(s)/X(s)$=1. This objective is accomplished by setting:

$$F(s) = (1 + G_{ol}(s)H(s))/G_{ol}(s)$$
$$H(s) = K_a s^2 + K_v s \tag{18}$$

In practice, modeling error, sensor noise and disturbances prevent perfect tracking from being realized.

Sliding mode control (SMC) design with linear model

Unlike the PVA+FF algorithm, sliding mode control considers model uncertainty and is a form of robust control. SMC is a form of variable structure control, which utilizes a discontinuous switching plane along some desired trajectory [28,29]. This plane is often referred to as a sliding surface, in which the objective is to keep the state values along this surface by minimizing the state errors (between the desired trajectory and the estimated or actual values). Ideally, if the state value is off or away from the surface, a switching gain would be used to push the state towards the sliding surface. Once on the surface, the states slide along the surface in what is called the sliding mode [29]. The switching brings inherent stability and robustness to the control strategy, while also introducing chattering (high-frequency switching) that is undesirable in

practice and can excite un-modelled dynamics. A boundary layer may be introduced along the sliding surface in order to saturate and smooth out the chattering within a region referred as the smoothing boundary region.

As our system is of 3rd order we can define a second order sliding surface as:

$$S = \ddot{x} - \ddot{x}_d + 2\zeta\lambda\left(\dot{x} - \dot{x}_d\right) + \lambda^2\left(x - x_d\right) \tag{19}$$

where λ corresponds to control bandwidth/natural frequency similarly as ω_n with the PVA+FF design and ζ is the damping factor. With a critically damped system ($\zeta = 1$), the system gets a commonly used sliding surface form. However, with noisy velocity and acceleration signals, it would be reasonable to adjust the damping factor for determining the relative significance of the velocity and acceleration in the control action.

We will apply the equivalent control design method from [29] the purpose of which is to keep the system state on the sliding surface after it has reached it. The state will stay on the surface when $dS/dt=0$. As the nominal plant (eq.7) can be rewritten in the form

$$\dddot{x} = -d_2\ddot{x} - d_1\dot{x} + n_0 u \tag{20}$$

The equivalent control signal, u_{eq}, is therefore obtained by taking the derivative of equation (19), substituting equation (20) for $\dddot{x}$, setting $dS/dt=0$ and solving for u_{eq} to give

$$u_{eq} = \frac{1}{n_0}\left[\dddot{x}_d + d_2\ddot{x} + d_1\dot{x} - 2\zeta\lambda\left(\ddot{x} - \ddot{x}_d\right) - \lambda^2\left(\dot{x} - \dot{x}_d\right)\right] \tag{21}$$

The necessary condition for the reachability of the sliding surface is given by

$$\frac{1}{2}\frac{d}{dt}S^2 \le -\eta\,|S| \tag{22}$$

where η is a design parameter that impacts the converging rate of the sliding surface. In order to satisfy the condition, the switching control component that accommodates the model uncertainties and disturbances is defined by

$$\begin{aligned} u_{sw} &= -K_{SMC}\,sat\left(\frac{S}{\phi}\right) \\ sat\left(\frac{S}{\phi}\right) &= \begin{cases} S/\phi & |S/\phi| \le 1 \\ \mathrm{sgn}(S/\phi) & |S/\phi| > 1 \end{cases} \end{aligned} \tag{23}$$

where K_{SMC} is a switching gain (maximum valve flow in our case). The boundary layer thickness ϕ can be tuned to reduce the amount of chattering of u_{sw}. The total control signal is then

$$u_{SMC} = u_{eq} + u_{sw} \tag{24}$$

It should be noted, that the SMC is actually a modification of a traditional PVA+FF controller. The equivalent control term corresponds to feed-forward term FF and the switching control term corresponds to PVA term. Once the system enters the boundary layer, SMC becomes a state feedback controller of the form $u=-K\mathbf{x}$ with gains $K=(K_{SMC}/\phi)*[\lambda^2\ 2\zeta\lambda\ 1]$ and the state vector given as $\mathbf{x}=[x-x_d\ \ \dot{x}-\dot{x}_d\ \ \ddot{x}-\ddot{x}_d]$. In order to compare the controllers, we can determine equivalent proportional, velocity and acceleration gains for SMC as

$$\begin{aligned} K_{p\_eq} &= \frac{K_{SMC}\lambda^2}{\phi} \\ K_{v\_eq} &= \frac{2K_{SMC}\xi\lambda}{\phi} \\ K_{a\_eq} &= \frac{K_{SMC}}{\phi} \end{aligned} \tag{25}$$

For example, the following set of controller parameters $\lambda=55$, $\zeta=0.13$, $\phi=40$ and $K_{SMC}=2e\text{-}3$ would result in equivalent gains K_{p_eq}=0.15, K_{v_eq}=0.00069 and K_{a_eq}=5e-5. The final tuning of the SMC parameters will be made by the help of the simulations with nonlinear system model.

Ideally, SMC should enable higher gains than PVA controller resulting in better tracking performance and robustness for system uncertainties and disturbances. However, SMC is very sensitive to delays that might lead to inefficient control performance. In PWM systems, the sample-and-hold operation can limit the efficient use of SMC.

Sliding mode control (SMC) design with nonlinear model

SMC design enables also the use of nonlinear system model. With nonlinear system model we can better exploit the knowledge of the system in the feed-forward path and improve the control performance. Using the system model equation (Eq. 6) and determining the state vector for the system as follows:

$$\mathbf{x} = [x \quad \dot{x} \quad \ddot{x} \quad p_m]^T \tag{26}$$

For a controller design, the system (eq. (6)) needs to be formulated as a standard single input, single output (SISO) canonical form:

$$\dot{\mathbf{x}} = f(\mathbf{x}) + b(\mathbf{x})u \tag{27}$$

where u is the control input and $\mathbf{x}$ is the state vector. It can be seen, that the real control input (duty ratio) appears in the definition of the equivalent mass flow rate (eqn. 5), and it is rather difficult to obtain equations such that it appears in the system motion equation. By defining the equivalent mass flow rate as a new control input u_{flow} we get:

$$\ddot{x} = f(\mathbf{x}) + b(\mathbf{x})u_{flow} = \frac{1}{M}\left[C\dot{m}_{eq} + H\dot{x} - B\ddot{x}\right]$$
$$f(\mathbf{x}) = \frac{H\dot{x} - B\ddot{x}}{M},\ b(\mathbf{x}) = \frac{C}{M},\ u_{flow} = \dot{m}_{eq}$$
$$H = a_1 + 2a_2x + 3a_3x^2 + 4a_4x^3 + (p_{\max} - p_m)\frac{k_1}{k_2} - \frac{kp_mv_1}{V_m(x)}\frac{k_0 - k_1x}{k_2} \quad (28)$$
$$C = \frac{k_0 - k_1x}{k_2}\frac{kRT}{V_m(x)}$$

Where equations (6) are used and rearranged to terms *H* and *C* in order to simplify the expression.

Applying the equivalent control method with previously defined sliding surface *S* (Eq. (19)) we get

$$u_{eq} = \frac{\dddot{x}_d - \hat{f}(\mathbf{x}) - 2\xi\lambda\ddot{e} - \lambda^2\dot{e}}{\hat{b}(\mathbf{x})} \quad (29)$$

$$\hat{b}(\mathbf{x}) = \sqrt{b_{\min}(x)b_{\max}(x)}$$
$$\hat{f}(\mathbf{x}) = \frac{f_{\min}(x) + f_{\max}(x)}{2} \quad (30)$$

Where $\hat{f}(\mathbf{x})$ and $\hat{b}(\mathbf{x})$ are estimates of *f(x)* and *b(x)*, respectively. The main uncertainty in the system is the payload mass M which is assumed to vary between 1 and 4 kg (nominal M=2 kg). Using equations 28-30 we can determine $b_{min}(x)$, $f_{min}(x)$ and $b_{max}(x)$, $f_{max}(x)$ and get the estimates $\hat{f}(\mathbf{x})$ and $\hat{b}(\mathbf{x})$. Note also that estimates $\hat{f}(\mathbf{x})$ and $\hat{b}(\mathbf{x})$ are time varying functions. The overall control and the switching control component are defined similarly as in the previous SMC design with linear system model (see equations 23-24).

SIMULATION RESULTS

Procedure

The three controllers were designed for the system with a nominal payload mass of M=2kg. The controller parameters were re-tuned by trial error using simulations with nonlinear system model. Sinusoidal 1 Hz tracking was used to tune the controllers, in order to provide stable and accurate tracking up to 1 Hz. SMC parameters were first tuned by simulating the controller performance using only the switching control component without the equivalent control component. The resulting parameter values for both SMC designs (linear and non-linear) were: λ=70 rad/s, ζ=0.1, K_{SMC}=0.002 and φ=40. These parameters will result in PVA equivalent gains (Eq. (25)) K_{p_eq}=0.245, K_{v_eq}=0.0007 and K_{a_eq}=5e-5, that are used also with PVA+FF controller. During the tuning process it was noted, that the SMC does not enable higher gains than PVA+FF controller.

Performance analysis of the controllers was performed with a sinusoidal input trajectory with 15 mm amplitude and various frequencies (0.25, 0.5, 0.75 and 1 Hz). The required velocity signal for the controllers was obtained by using a backward finite difference of the position signal followed by a 2nd order 30-Hz Butterworth digital filter. The acceleration was computed in the same way from the filtered velocity. Band-limited white noise was added to the position signal in order to include the sensor noise for simulations. The controller performance was analyzed by calculating the root mean square error (RMSE) using the equation:

$$RMSE = \sqrt{\frac{1}{N}\sum_{i=1}^{N} e_i^2} \quad (31)$$

where i is the current sample number, e_i is the error for the current sample, and N is total number of samples.

The robustness of the controllers was tested by changing the nominal payload mass from 2kg to 1kg and 4kg.

Performance with nominal payload

The RMSE values for the three controllers with no mismatch between the nominal and actual payload masses and with PWM frequency 50 and 100 Hz are listed in Table 2. As expected, the tracking performance worsened as the sine wave frequency increased, mainly due to saturation of the valve input signal and physical limits of the system. The similarity of PVA+FF and SMC based on the linear model is evident as tracking performances in every case are almost identical. Thus, SMC works only as a conventional PVA+FF controller without improvement in tracking accuracy and robustness.

Sine freq. [Hz]	**PVA+FF** *(PWM 50Hz)*	**SMC** linear *(PWM 50Hz)*	**SMC** nonlinear *(PWM 50Hz)*	**PVA+FF** *(PWM 100Hz)*	**SMC** linear *(PWM 100Hz)*	**SMC** nonlinear *(PWM 100Hz)*
0.25	0.414	0.396	0.307 *(-26 %)*	0.366	0.364	0.317 *(-13 %)*
0.5	0.587	0.573	0.397 *(-32 %)*	0.532	0.533	0.376 *(-29 %)*
0.75	0.842	0.823	0.503 *(-40 %)*	0.756	0.753	0.464 *(-39 %)*
1.0	1.055	1.032	0.636 *(-40 %)*	1.009	0.984	0.577 *(-43 %)*

Table 2. Comparison of RMSE (mm) values for nominal payload (2 kg) with PWM frequencies 50 and 100 Hz

The use of PWM frequency 100 Hz instead of 50 Hz, improves the tracking performance in overall by 10 %. This is mainly caused by the smaller dither magnitude as the control signal is updated more often. On the other hand, at lower input frequencies the poorer control resolution decreases the control performance.

It can be clearly seen, that SMC based on the nonlinear system model improves the tracking performance significantly (between 13-43 %) compared to PVA+FF and linear SMC. Thus, a significant improvement can be obtained by a proper nonlinear modeling of the system affecting through the

equivalent control component. However, a retuning of the SMC gains by trying to make the performance better did not work. This indicates that the control delay caused by the PWM operation degrades the advantages commonly stated with SMC strategy.

Figures 11 and 12 show the controller performance for a nominal payload mass for sinusoidal tracking 1 Hz and with PWM frequency 50 and 100 Hz. Note also, that higher PWM frequency decreases the dither in the position signal. Maximum tracking errors for 1 Hz sinusoidal tracking are *+/-2 mm* for PVA+FF and linear SMC, and *+/- 1.2 mm* for SMC nonlinear with PWM frequency 50 Hz. A slight improvement in terms of maximum tracking errror is obtained with PWM frequency 100 Hz *(+/-1.8 mm* for PVA+FF, *+/- 1 mm* SMC nonlinear). Maximum tracking errors for 0.25 Hz sinusoidal tracking are *-0.8..+1.2 mm* for PVA+FF and SMC linear, *-0.7..+0.9 mm* for SMC nonlinear with PWM frequency 50 Hz. For PWM 100 Hz, maximum errors are *-0.8..+0.6 mm* and are *-0.7..+0.6 mm*.

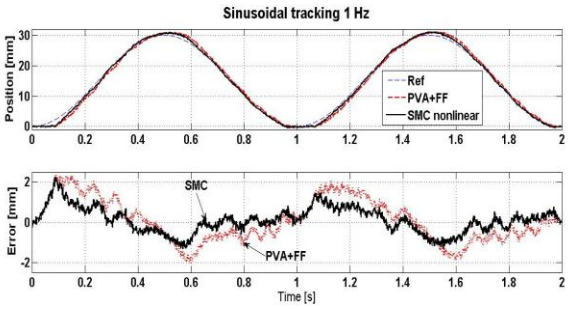

Fig. 11. Comparison of tracking accuracy for a 1.0 Hz sine wave trajectory with nominal payload mass and f_{PWM}=50 Hz

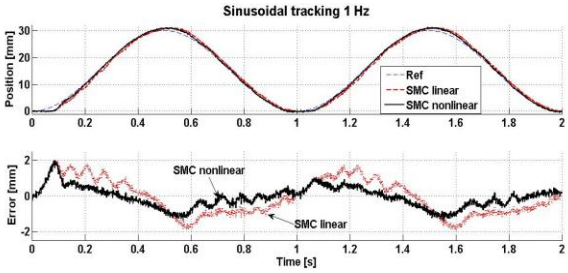

Fig. 12. Comparison of tracking accuracy for a 1.0 Hz sine wave trajectory with nominal payload mass and f_{PWM}=100 Hz

Robustness of the controllers

The robustness of the controllers was analyzed by varying the payload mass from its nominal value (2kg) to 1 kg and to 4 kg. The RMSE values for the controllers with decreased payload mass and PWM frequency 50 and 100 Hz are listed in Table 3. In the brackets below the RMSE value is shown the relative change in tracking accuracy compared to the nominal case. Each controller can handle the decreased payload mass well as they are able to maintain the stability in the system. Slightly increased tracking errors with PWM 50 Hz are explained by the increased dither magnitude due to smaller inertia. With PWM 100 Hz, the RMSE values are almost the same as in the nominal case.

Sine freq. [Hz]	**PVA+FF** *(PWM 50Hz)*	**SMC** linear *(PWM 50Hz)*	**SMC** nonlinear *(PWM 50Hz)*	**PVA+FF** *(PWM 100Hz)*	**SMC** linear *(PWM 100Hz)*	**SMC** nonlinear *(PWM 100Hz)*
0.25	0.527 *(+27 %)*	0.454 *(+15 %)*	0.346 *(+13 %)*	0.363 *(-0 %)*	0.361 *(-0 %)*	0.314 *(-0 %)*
0.5	0.661 *(+13 %)*	0.625 *(+9 %)*	0.430 *(+8 %)*	0.533 *(-0 %)*	0.532 *(-0 %)*	0.375 *(-0 %)*
0.75	0.920 *(+9 %)*	0.889 *(+10 %)*	0.552 *(+10 %)*	0.761 *(+1 %)*	0.752 *(-0 %)*	0.462 *(-0 %)*
1.0	1.091 *(+3 %)*	1.066 *(+3 %)*	0.654 *(+3 %)*	1.033 *(+2 %)*	0.991 *(+1 %)*	0.574 *(-0 %)*

Table 3. Comparison of RMSE (mm) values for decreased payload (1 kg = 50 % less than nominal) with PWM frequencies 50 and 100 Hz

Sine freq. [Hz]	**PVA+FF** *(PWM 50Hz)*	**SMC** linear *(PWM 50Hz)*	**SMC** nonlinear *(PWM 50Hz)*	**PVA+FF** *(PWM 100Hz)*	**SMC** linear *(PWM 100Hz)*	**SMC** nonlinear *(PWM 100Hz)*
0.25	0.379 *(-8 %)*	0.372 *(-6 %)*	0.302 *(-1 %)*	0.366 *(+0 %)*	0.365 *(+0 %)*	0.318 *(+0 %)*
0.5	0.568 *(-3 %)*	0.562 *(-2 %)*	0.398 *(+0 %)*	0.533 *(+0 %)*	0.532 *(+0 %)*	0.379 *(+0 %)*
0.75	0.820 *(-3 %)*	0.806 *(-2 %)*	0.560 *(+11 %)*	0.756 *(+0 %)*	0.748 *(-0 %)*	0.471 *(+2 %)*
1.0	1.083 *(+3 %)*	1.076 *(4 %)*	0.821 *(+29 %)*	1.000 *(-0 %)*	0.989 *(+0 %)*	0.653 *(+13 %)*

Table 4. Comparison of RMSE (mm) values for decreased payload (4 kg = 100 % more than nominal) with PWM frequencies 50 and 100 Hz

Table 4 gathers the RMSE values with increased payload mass (100 % more than nominal) and PWM frequency 50 and 100 Hz. PVA+FF and SMC linear are robust to increased payload mass as the RMSE tracking error does not change much. Slightly improved performance with PWM frequency 50 Hz can be explained by increased inertia that decreases the dither magnitude. In the case of nonlinear SMC, it is interesting to see that increased payload degrades the performance especially at higher input frequencies. This can be clearly seen in Figure 13 where the system with nonlinear SMC oscillates more than the system with PVA+FF controller. The reason for this is the equivalent control term of nonlinear SMC that uses estimated velocity and acceleration to calculate the equivalent control term. As it uses nonlinear system model, its' effect on the overall control action is stronger than the one of the linear SMC which uses linear model. Thus, the noise in velocity and acceleration affects the performance of SMC designs also through the equivelent control part and might lead to some degraded performance as can be seen with nonlinear SMC. It should also be noted, that feed-forward component of PVA+FF controller uses only desired velocity, acceleration and jerk signals, not measured or estimated ones. The results with PWM 100 Hz shown in Figure 14 indicate an improved performance

as the magnitude of SMC oscillation has clearly decreased. Thus it can be stated, that the higher PWM frequency (less delay) can provide a slight improvement in the sense of robustness to parameter uncertainties.

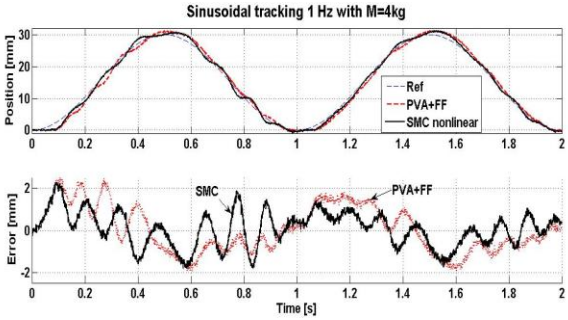

Fig. 13. Comparison of tracking accuracy for a 1 Hz sine wave trajectory with increased payload mass M=4kg and f_{PWM}=50 Hz

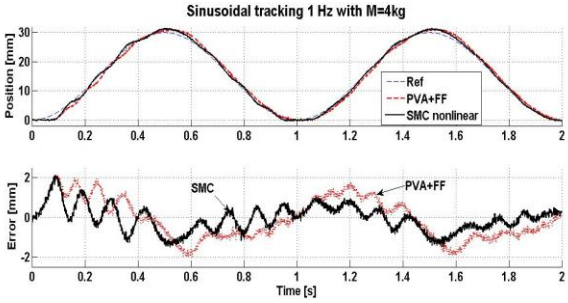

Fig. 11. Comparison of tracking accuracy for a 1 Hz sine wave trajectory with increased payload mass M=4kg and f_{PWM}=100 Hz

CONCLUSIONS

This paper provides a low-cost approach to control pneumatic systems by using high-speed on/off valves with PWM technique instead of costly proportional and servo valves. A full nonlinear modelling of the system was derived and used to analyze the performance of the proposed controllers. The valve model (pressure, flow, and load dynamics) is continuous and invertible, such that it can be exploited in the control design of the pneumatic system. The valve model is used to convert the controller output (mass flow rate) into duty ratio signal that simplifies the control design.

Performance of two common control strategies (SMC and PVA+FF) was compared by simulations to sinusoidal input trajectories. In the SMC design, a linear and nonlinear approach was presented. In addition, the effects of the PWM frequency on the system performance were studied with PWM frequencies 50 and 100 Hz. Under nominal conditions, it was demonstrated that the linear SMC strategy and PVA+FF performed quite equally. Ideally, SMC is a high-gain PVA+FF controller that utilizes switching robust component to ensure better robustness to uncertainties and disturbances. However, it was noted that the SMC design dis not enable higher gains than PVA+FF design. The reason for this, is the control delay caused by the PWM sampling, where the control signal is updated only once per PWM period. The delay deteriorates the performance of the SMC and it works actually as a conventional PVA+FF controller.

For a comparison to linear control approaches, also a SMC based on the nonlinear model was designed. As the more accurate modeling of the system affects through the equivalent control term, the nonlinear SMC approach resulted in a significant improvement (up to 40 %) in terms of tracking accuracy.

The robustness of the controllers was tested by varying the payload mass from its nominal value. Each of the controllers were able to handle the decreased mass well but with increased payload mass (100 % increase) nonlinear SMC started to chatter more than linear control approaches. This was expected to be caused by noisy velocity and acceleration estimates affecting through the equivalent/feed-forward path.

As the performance and effectiveness of the SMC strategy is dependent on the delay in the system it was noted that SMC performed slightly better against payload variations with increased PWM frequency 100 Hz. This is due to a fact that the control action is twice faster than with PWM frequency 50 Hz.

The simulation results show that the use of SMC based on a nonlinear system model with PWM technique can provide sufficient accuracy for controlling a pneumatic muscle actuator system. However, the delay caused by the PWM sampling degrades the performance of the SMC. Thus, the advantages of SMC, such as robustness to uncertainties and disturbances, can not be fully exploited. One possible option for improving the performance of SMC could be the use of predictor that compensates the delay. The next step is to verify the simulation results experimentally by implementing the proposed controllers in a real system.

ACKNOWLEDGMENTS

This study was funded by Academia of Finland.

REFERENCES

[1] D. G. Caldwell, G. A. Medrano-Cerda, and M. J. Goodwin, "Control of Pneumatic Muscle Actuators," in *IEEE Control Systems Magazine*, vol. 15, No.1, 1995, pp. 40-48.

[2] J. Lilly, "Adaptive Tracking for Pneumatic Muscle Actuators in Bicep and Tricep Configurations," in *IEEE Transaction of Neural Systems and Rehabilitation Engineering*, vol. 11, No. 3, 2003, pp. 333-339.

[3] G. A. Medrano-Cerda, C. J. Bowler, and D. G. Caldwell, "Adaptive Position Control of Antagonistic Pneumatic Muscle Actuators," in *IEEE/RSJ International Conference on Intelligent Robots and Systems*, vol. 1, Pittsburgh, USA, 1995, pp. 378-383.

[4] G. A. Medrano-Cerda, C. J. Bowler, and D. G. Caldwell, "Adaptive Position Control of Antagonistic Pneumatic Muscle Actuators," in *IEEE/RSJ International Conference on*

Intelligent Robots and Systems, vol. 1, Pittsburgh, USA, 1995, pp. 378-383.
[5] T. Hesselroth, K. Sarkar, P. Van der Smagt, and K. Schulten, "Neural Network Control of a Pneumatic Robot Arm," in *IEEE Transaction of Systems, Man and Cybernetics*, vol. 24, No.1, 194, pp. 28-38.
[6] S. W. Chan, J. H. Lilly, D. W. Repperger, and J. E. Berlin, "Fuzzy PD+I Learning Control for a Pneumatic Muscle ," in *Proceedings of 2003 IEEE International Conference on Fuzzy Systems*, St Louis, USA, 2003, pp. 278-283.
[7] K. Balasubramanian and K. S. Rattan, "Feedforward Control of a Nonlinear Pneumatic Muscle System Using Fuzzy Logic," in *IEEE International COnference of Fuzzy Systems*, vol. 1, 2003, pp. 272-277.
[8] J. H. Lilly and L. Yang, "Sliding Mode Tracking for Pneumatic Muscle Actuators in Opposing Pair Configuration," in *IEEE Transactions on Control Systems Technology*, vol. 13, 2005, pp. 550-558.
[9] P. Carbonell, Z. P. Jiang, and D. W. Repperger, "Nonlinear Control of a Pneumatic Muscle Actuator: Backstepping vs. Sliding Mode," in *Proceedings of the IEEE International Conference on Control Applications*, 2001, pp. 167-172.
[10] B. Tondu and P. Lopez, "Modeling and Control of McKibben Artificial Muscle," in *IEEE Control Systems Magazine*, 2000, pp. 15-38.
[11] H. Aschemann and D. Schindele, "Sliding-mode Control of a High-Speed Linear Axis Driven by Pneumatic Muscle Actuators," *IEEE Transactions on Industrial Electronics*, vol. 11, no. 55, pp. 3855-3864, 2008.
[12] X. Shen, "Nonlinear Model-Based Control of Pneumatic Artificial Muscle Actuator Systems," *Control Engineering Practice*, vol. 18, pp. 311-317, 2010.
[13] J. Y. Lai, R. Singh, and C. H. Menq, "Development of PWM mode Position Control for a Pneumatic Servo System," *Journal of the Chinese Society of Mechanical Engineers*, vol. 13, no. 1, pp. 86-95, 1992.
[14] T. Noritsugu, "Development of PWM Mode Electro-Pneumatic Servomechanism, Part I: Speed Control of a Pneumatic Cylinder," *Journal of Fluid Control*, vol. 17-1, pp. 65-80, 1986.
[15] Y. S. Morita, M. Shimizu, and T. Kagawa, "An Analysis of Pneumatic PWM and Its Application to a Manipulator," in *Proceedings of International Symposium of Fluid Control and Measurement*, Tokyo, Japan, 1985, pp. 3-8.
[16] A. K. Paul, J. K. Mishra, and M. G. Radke, "Reduced Order Sliding Mode Control for Pneumatic Actuator," *IEEE Transaction on Control Systems Technology*, vol. 2, no. 30, pp. 271-276, 1994.
[17] K. Ahn and S. Yokota, "Intelligent Switching Control of Pneumatic Actuator using On/Off Solenoid Valves," *Mechatronics*, vol. 15, pp. 683-702, 2005.
[18] R. B. Van Varseveld and G. M. Bone, "Accurate Position Control of a Pneumatic Actuator Using On/Off Solenoid Valves," *IEEE/ASME Transaction on Mechatronics*, vol. 2, no. 30, pp. 195-2004, 1997.
[19] E. J. Barth, J. Zhang, and M. Goldfarb, "Control Design for Relative Stability in a PWM-Controlled Pneumatic Systems," *ASME Journal of Dynamic Systems, Measurement and Control*, vol. 125, no. 3, pp. 504-508, 2003.
[20] X. Shen, J. Zhang, E. Barth, and M. Goldfarb, "Nonlinear Model-Based Control of Pulse Width Modulated Pneumatic Servo Systems," *ASME Journal of Dynamic Systems, Measurement and Control*, vol. 128, pp. 663-669, 2006.
[21] T. Nguyen, J. Leavitt, F. Jabbari, and J. E. Bobrow, "Accurate Sliding-Mode Control of Pneumatic Systems Using Low-Cost Solenoid Valves," *IEEE/ASME Transactions on Mechatronics*, vol. 12, no. 2, pp. 216-219, April 2007.
[22] M. Taghizadeh, A. Ghaffari, and F. Najafi, "A Linearization Approach in Control of PWM-driven Servo-Pneumatic Systems," in *Proceedings of the 40th Southeastern Symposium on System Theory*, New Orleans, LA, USA, 2008, pp. 395-399.
[23] R. A. Schulte, "The Characteristics of the McKibben Artificial Muscle," *The Applications of External Power in Prosthetics and Orthotics*, pp. 94-115, 1962.
[24] P. Chou and B. Hannaford, "Measurement and Modeling of a McKibben Pneumatic Artificial Muscles," *IEEE Transaction on Robotics and Automation*, vol. 12, no. 1, 1996.
[25] V. T. Jouppila, S. A. Gadsden, and A. U. Ellman, "Modeling and Identification of a Pneumatic Muscle Actuator System Controlled by an On/Off Solenoid Valve," in *Proceedings of 7th International Fluid Power Conference*, Aachen, Germany, 2010, p. 16.
[26] Z. Rao and G. M. Bone, "Nonlinear Modeling and Control of Servo Pneumatic Actuators," *IEEE Transactions on Control Systems Technology*, vol. 16, pp. 562-569, 2008.
[27] S. Ning and G. M. Bone, "Experimental Comparison of Two Pneumatic Servo Position Control Algorithms," Proceedings of the *IEEE International Conference on Mechatronics & Automation*, pp. 37-42, Niagara Falls, Canada, 200
[28] V. I. Utkin, *Sliding Modes and Their Application in Variable Strucure Systems*. Moscow, Russia: MIR Publishers, 1978.
[29] J. J. Slotine and W. Li, *Applied Nonlinear Control*. Englewood Cliffs, New Jersey, USA: Prentice-Hall,1991

PUBLICATION 3

Sliding Mode Control of a Pneumatic Muscle Actuator System with a PWM Strategy

Ville Jouppila, Andrew Gadsden, Gary Bone, Asko Ellman, Saeid Habibi

This is the authors accepted manuscript of an article published in *International Journal of Fluid Power, Vol.15, No.1, March 2014*, permission to use admitted.

SLIDING MODE CONTROL OF A PNEUMATIC MUSCLE ACTUATOR SYSTEM WITH A PWM STRATEGY

Ville T. Jouppila[1], S. Andrew Gadsden[2], Gary M. Bone[2], Asko U. Ellman[1], and Saeid R. Habibi[2]

1. Department of Engineering Design, Tampere University of Technology, Tampere, Finland
2. Department of Mechanical Engineering, McMaster University, Hamilton, Ontario, Canada
ville.jouppila@tut.fi

Abstract

In this paper, a sliding mode control (SMC) strategy is applied to a pulse width modulation (PWM)-driven pneumatic muscle actuator system using high speed on/off solenoid valves. Servo-pneumatic systems with PWM-driven on/off valves can be used instead of expensive servo valves to decrease complexity, weight, and cost of servo-pneumatic systems. Due to the highly nonlinear nature of pneumatics, the system is difficult to model accurately which leads to un-modelled dynamics and uncertainties. In this paper, a robust and nonlinear SMC approach is implemented in order to control the system with sufficient accuracy. A nonlinear model is developed in a single-input single-output form by studying the flow, pressure, and force dynamics of the system. The SMC strategy is applied to three different system configurations: single on/off valve, two on/off valves, and a servo valve. The performance and effectiveness of these configurations are investigated under sinusoidal tracking at different frequencies. The robustness of the controllers is studied by varying the inertia of the system and by applying external disturbances to the system.

Keywords: pneumatic actuator, sliding mode control, solenoid valves, pulse width modulation

1 Introduction

Pneumatic systems have many properties that make them attractive for use in a variety of environments. They are less sensitive to temperature than hydraulic systems and it is not necessary to collect exhaust air which removes the need for fluid return lines. In addition, high force-to-weight ratios, cleanliness, compactness, ease of maintenance, and the safety of pneumatic actuators offer desirable features for many industrial designs. Pneumatic McKibben muscle actuators, invented by Gaylord (Gaylord, 1958), provide a higher force-to-weight ratio compared with pneumatic cylinders. However, there are a number of nonlinearities present that makes it rather difficult and complex to model effectively.

This manuscript was submitted August, 2012.

Nonlinear characteristics of the actuator, air compressibility, friction, and nonlinear airflow through the valves are the main reasons that pneumatic systems are commonly avoided for advanced applications. Literature demonstrates that a large number of control strategies have been proposed to handle the effects of the nonlinearities present. These include the following: PID control (Chou & Hannaford, 1996), adaptive control strategies (Caldwell;Medrano-Cerda;& Goodwin, 1995; Lilly J. , 2003; Medrano-Cerda;Bowler;& Caldwell, 1995), nonlinear PID (Than & Ahn, 2006), neural networks (Hesselroth, Sarkar, Van der Smagt, & Schulten, 1994), and fuzzy controllers (Lilly J. , 2003; Medrano-Cerda, Bowler, & Caldwell, 1995; Chan, Lilly, Repperger, & Berlin, 2003; Balasubramanian & Rattan, 2003). In (Lilly & Yang, 2005) and (Carbonell, Jiang, & Repperger, 2001), a sliding mode control (SMC) strategy was applied to a muscle actuator system, but only simulation results of the effectiveness of the strategy were presented. Other SMC approaches are presented in

(Tondu & Lopez, 2000; Aschemann & Schindele, 2008; Shen, Nonlinear Model-Based Control of Pneumatic Artificial Muscle Actuator Systems, 2010). In (Tondu & Lopez, 2000), modelling and control of pneumatic muscle actuators in an antagonistic configuration for a 2-DOF SCARA-type robot prototype was studied. The system was controlled by a sliding mode control strategy based on an identified 2nd order model, from pressure input to joint angle. An additional integrative term in the close neighbourhood of desired angle position was used to improve the tracking accuracy. A static joint accuracy of $\pm 0.2°$, and mean dynamic accuracy of $\pm 0.5°$ for a trapezoidal velocity profile ($0.5\ \mathrm{rad/s}$ cruising speed and a $0.5\ \mathrm{rad/s^2}$ slope) was reported. In (Aschemann & Schindele, 2008), a cascaded SMC scheme was presented for a pneumatic linear actuator. A guided carriage was driven by a nonlinear mechanism consisting of a rocker with an antagonistic pair of pneumatic muscle actuators arranged at both sides. The differential flatness of the system was exploited in combination with sliding mode techniques to stabilize the error dynamics in view of un-modelled dynamics. The internal pressure of each pneumatic muscle was controlled by a fast underlying control loop. The control of the outer control loop involved a decoupling of rocker angle as well as mean internal pressure of both pneumatic muscles as flat outputs. Additionally, model uncertainties such as friction were directly counteracted by an observer-based disturbance compensation which reduces the chattering problem. Experimental results emphasize the excellent closed-loop performance with maximum position errors of approximately $3.5\ \mathrm{mm}$ during the movements, negligible steady-state position error, and a steady-state pressure error of less than $0.03\ \mathrm{bar}$.

In the most recent work (Shen, Nonlinear Model-Based Control of Pneumatic Artificial Muscle Actuator Systems, 2010), an SMC strategy was applied to control a muscle actuator system in an opposing pair configuration using a proportional flow control valve. Experimental results with sinusoidal tracking (with amplitude $7.5\ \mathrm{mm}$ and frequency $0.5 - 1.5\ Hz$) showed accuracies of $\pm 0.5\ \mathrm{mm}$ to $\pm 1.2\ \mathrm{mm}$. This work and previous SMC studies have demonstrated that it is an efficient and robust control strategy for pneumatic actuator applications. However, in these studies, a proportional or servo valve has been used to control the actuator. In this paper, on/off valve(s) are chosen for the control of the muscle actuator system in order to provide a low cost alternative to servo valve-based pneumatic systems.

In recent years, effort has been made to develop inexpensive servo-pneumatic systems using on/off solenoid valves with pulse-width modulation (PWM). Previous efforts have shown the potential of PWM-controlled pneumatics; although they typically lack an analytical approach when studying the system (Lai, Singh, & Menq, 1992; Noritsugu, 1986; Morita, Shimizu, & Kagawa, 1985). In one article, the nonlinearities of the system were handled by proposing a switching controller based on a reduced order nonlinear model of the system (Paul, Mishra, & Radke, 1994). In (Ahn & Yokota, 2005), a modified PWM valve pulsing algorithm was developed. The proposed algorithm (with a continuous state feedback controller) was successfully implemented, and demonstrated its effectiveness on pneumatic cylinder experiments. In (Van Varseveld & Bone, 1997), a controller based on discrete-time control methods was developed for a PWM-controlled pneumatic servo system. A PID controller with friction compensation and a position feed-forward term was successfully implemented with a worst case steady-state error of $0.21\ \mathrm{mm}$ and S-curve trajectory following errors of less than $2.0\ \mathrm{mm}$. In (Barth, Zhang, & Goldfarb, 2003), a linear state-space averaged model and an SMC with a PWM strategy based on a loop shaping approach was introduced for the control of a single degree of freedom pneumatic positioning system with a cylinder. This was followed by a nonlinear averaging approach (Shen, Zhang, Barth, & Goldfarb, 2006) where originally discontinuous and possibly non-affine system in the input was transformed into equivalent continuous-time nonlinear system (that was also affine in control input) for which SMC strategy could be applied. Their approach was demonstrated with a pneumatic cylinder controlled by a pair of 3-way solenoid valves. Sinusoidal tracking with amplitude of $20\ \mathrm{mm}$ and frequencies $0.25 - 1\ \mathrm{Hz}$ reportedly had accuracies from $\pm 1\ \mathrm{mm}$ to $\pm 3.5\ \mathrm{mm}$. In (Nguyen, Leavitt, Jabbari, & Bobrow, 2007), a SMC strategy using four low cost solenoid valves without PWM to control a double-acting cylinder was introduced. The sinusoidal tracking error for a stroke of $\pm 20\ \mathrm{mm}$ at $0.5\ \mathrm{Hz}$ was less than $2\ \mathrm{mm}$.

The aforementioned studies of pneumatic PWM on/off valve systems applied their approaches to systems with pneumatic cylinders. However, in this paper, a pneumatic muscle actuator which differs significantly from the traditional cylinder is used. Due to highly nonlinear characteristics of the muscle actuator, a significant effort is applied for modeling the actuator. In addition, previous studies like (Shen;Zhang;Barth;& Goldfarb, 2006) have assumed a linear relation between duty ratio and effective valve opening area, combined with traditional mass flow rate models with choked and un-choked flow. In order to better approximate the mass flow rate through the valve, this paper utilizes a nonlinear continuous model where the mass flow rate is described as a 2nd order bi-polynomial function of actuator pressure and PWM duty ratio. Being a continuous and invertible function, the actual PWM duty ratio control signal for the valve(s) can be solved based on the knowledge of actuator pressure and desired mass flow rate given by the SMC controller output. As a result, the mass flow rate model can be separated from the control law and the system model can be given in a SISO control canonical form for which the SMC strategy can be easily applied.

Most studies lack a thorough review of PWM on/off valve systems and comparisons with proportional/servo valve systems. This paper provides an experimental study of PWM on/off valve systems, including a study of system robustness. A comparative study between on/off valve approaches and traditional servo valve approach is performed.

In this paper, the muscle actuator system shown in Fig. 1 is studied. Three different valve configurations will be implemented separately. An SMC strategy will be designed for each configuration and the resulting closed-loop performances compared. The actuator is a Festo fluidic muscle (MAS10-300). It is mounted horizontally and attached to a pneumatic cylinder (Festo DNC-40) whose pressure is controlled by an electronic regulator to provide an adjustable unidirectional returning force for the muscle. Note that the cylinder adds frictional uncertainties for the system that the control strategy needs to compensate. In the first system configuration, a single 3/2 high-speed on/off solenoid valve (Festo MHE2-MS1H-3/2G-M7, cost: $50 USD) drives the muscle actuator. The valve is controlled by varying the duty ratio of a PWM signal. In the second system configuration, two 2/2 solenoid valves (Festo MHE2-MS1H-3/2G-M7 with third port plugged) are used to control the inflow and outflow independently. For comparison purposes, a servo valve (Festo MPYE-5-M5-010-B, cost: $450 USD) is also used to control the actuator in the third system architecture, denoted Case 3 in Fig. 1. The controller is programmed in the Matlab Simulink environment and is implemented using the Real-Time Windows Target. The controller output signal is transmitted to an electronic amplifier that supplies sufficient power to actuate the valve. The muscle pressure and the displacement of the actuator are measured using Festo SDE1 pressure sensors, and a linear potentiometer, respectively. The velocity and acceleration are obtained by differentiation of the position signal with a digital Butterworth low-pass filter.

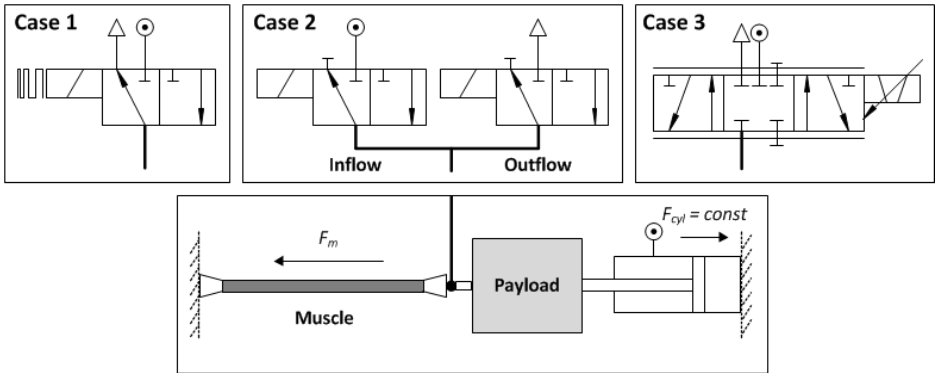

Fig. 1: *Muscle actuator system with three different valve configurations.*

As the system under study is highly nonlinear, a simulation model is needed for the initial tuning process and studying the performance of the controller. In Section 2 a nonlinear system model is presented which takes into account the flow, pressure, force, and load dynamics covering the main nonlinearities present in the system. In Section 3, a model-based SMC strategy is designed. Section 4 discusses the tuning of the controller, and compares the performance of the SMC strategy with three different valve configurations. Section 5 presents the conclusions of the research.

2 Muscle Actuator System Modelling

This section describes the modelling of the system; including the experimental setup, pneumatic muscle actuator, pressure and valve flow dynamics, and the overall system model in single-input single-output (SISO) form.

2.1 Pneumatic Muscle Actuator

The pneumatic McKibben muscle actuator consists of a rubber tube covered with a double helical braid (Schulte, 1962). During pressurization, the muscle increases in diameter and shortens in length. The maximum force is obtained at the beginning of the contraction and decreases with increasing contraction. The actuator is unidirectional and its maximum contraction is typically 20% to 25% of the nominal length. The advantage of the muscle actuator over the traditional cylinder is the higher force-to-weight ratio and the stick-slip free motion at low velocities. However, the force-to-contraction relationship at different pressure levels is highly nonlinear, and adds to the difficulty of modelling the muscle actuator effectively. As with all actuation systems, the effective application of the pneumatic muscle actuator relies on being able to accurately model and predict the forces that will be generated under any operating condition.

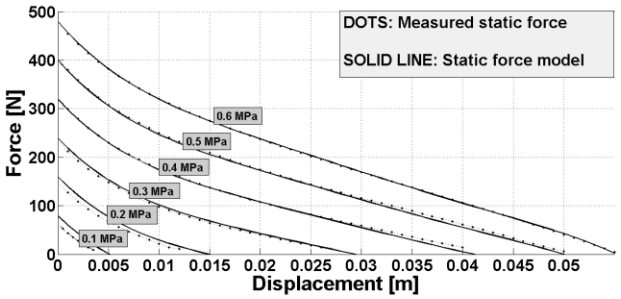

(a) Mean static muscle force characteristics

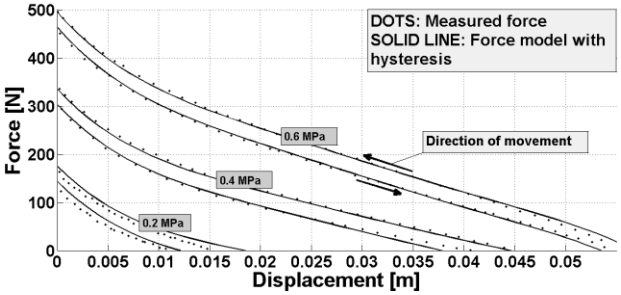

(b) Force model including hysteresis

Fig. 2: *Modelling of the muscle static force.*

Figure 2 illustrates the measured nonlinear relationship between the force, pressure, and displacement. Note that the actuator introduces a significant hysteresis phenomenon due to material deformations and the presence of friction. The hysteresis is difficult to model accurately, especially during the transition phase when the direction of the movement changes. In this study, a simple model of hysteresis is used where a force offset is added to the mean static force curve. In this case, the hysteresis can be considered as static Coulomb friction.

The mean static force shown in Fig. 2 (a) is the averaged force from the upper and lower curves of the hysteresis force loop. The shape of the curves is quite similar for different pressures, and can be captured accurately by fitting a third-order polynomial function $F_{max}(x)$ for the curve at the maximum actuator pressure 0.6 MPa, where x is the contraction/displacement of the muscle.

In order to model the force at different pressure levels, a force term that is subtracted from the maximum possible force is needed. Note that the force is proportional to the pressure when the actuator length is fixed. However, the proportionality factor decreases as contraction increases. This results in the last term in the overall muscle force equation, defined as follows:

$$F_m(x, p_m) = F_{max}(x) - (p_{max} - p_m)(k_0 - k_1 x)$$
$$F_{max}(x) = a_0 + a_1 x + a_2 x^2 + a_3 x^3 \qquad (1)$$

where p_{max} is the maximum muscle pressure, p_m is the actual muscle pressure, and a_{0-3}, k_0, and k_1 are the fitted model parameters.

Figure 2 illustrates that the model is able to describe the mean static force-pressure-displacement behaviour with good accuracy. By also including a static Coulomb friction term, the hysteresis effect can be captured reasonably well as shown in Fig. 2 (b). The viscous friction of the actuator is extremely difficult to determine and model accurately, as it is dependent on the velocity as well as the pressure in the actuator. In this paper a constant damping factor B is used to approximate the viscous friction. In the SMC design described in Section 3, the discontinuous static and Coulomb friction are treated as a disturbance.

2.2 Pressure Dynamics

For calculating the pressure inside the muscle, it is assumed that air is an ideal gas with an adiabatic process such that the change of pressure is as follows:

$$\dot{p}_m = \frac{kRT}{V_m(x)}\dot{m}_{eq}(u_{duty}, p_m) - \frac{kp_m}{V_m(x)}\frac{dV_m(x)}{dx}\dot{x} \qquad (2)$$

where k (1.4 for adiabatic process), R, T, and V_m denote the specific heat ratio, gas constant, air temperature, volume of the muscle, and muscle pressure, respectively. The equivalent mass flow rate $\dot{m}_{eq}$ is a function of the PWM duty ratio u_{duty} and actuator pressure p_m, and will be determined in the next section. An empirical linear approximation is used to describe the volume of the muscle actuator as a function of displacement, as follows (Jouppila, Gadsden, & Ellman, 2010):

$$V_m(x) = v_0 + v_1 x \qquad (3)$$

where v_0 and v_1 are fitted parameters.

2.3 Valve Mass Flow Rate Dynamics

The mass flow rate model of the 3/2 valve controlling the muscle actuator is an essential part of the system model. The switching frequency f_{PWM} and u_{duty} determine how long the valve is open and closed during the time PWM period ($1/f_{PWM}$). The PWM switching frequency has a significant effect on the system performance as the final control signal for the valve is updated at the implemented PWM frequency. In other words the sampling frequency is equal to the PWM frequency. A small PWM frequency results in poor tracking precision since the sampling frequency should be significantly higher than the natural frequency of the system. However, the switching delay (about 2 ms) sets the limit to the maximum reasonable PWM frequency.

Due to the PWM switching, two modes exist in the system. During the on-mode the valve charges the muscle actuator, and during the off-mode the actuator is discharged. In addition, the flow can be either choked or un-choked depending on the ratio of downstream and

upstream pressure. Assuming an ideal gas law and an adiabatic process, a widely accepted model for mass flow rate through the valve is expressed as follows (Pneumatic Fluid Power, 2005):

$$\dot{m} = \begin{cases} Cp_{up}, & \frac{p_{down}}{p} \leq b \\ Cp_{up}\sqrt{1-\left(\frac{\frac{p_{down}}{p_{up}}-b}{1-b}\right)^2}, & \frac{p_{down}}{p_{up}} > b \end{cases} \quad (4)$$

where C is defined as the valve conductance and b is the critical pressure ratio. While the valve is open the air flows into the actuator, and the upstream pressure is defined by $p_{up} = p_s$ (supply pressure) and the downstream pressure is $p_{down} = p_m$. While the valve is closed, the air flows out of the actuator, $p_{up} = p_m$ and $p_{down} = p_0$ (atmosphere pressure), respectively. In order to identify the pneumatic behavior of the valve, a set of experiments were carried out according to the procedure introduced by ISO6358 (Pneumatic Fluid Power, 2005). The two parameters (C and b) were found by using Eq. (4) with a least squares fitting method for measured data with upstream pressure 0.7 MPa. These results are found in Table 1.

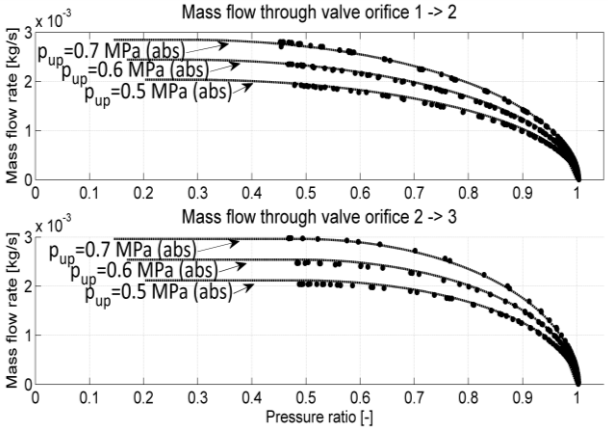

Fig. 3: *Mass flow rate model (based on ISO6358).*

Table 1: Identified parameters for mass flow rate model.

Parameter	Description	Value
p_{up}	Upstream pressure	0.5, 0.6, 0.7 MPa
C_{in}	Sonic conductance for charging	3.48×10^{-3} $\frac{\text{kg}}{\text{sMPa}}$
C_{out}	Sonic conductance for discharging	3.77×10^{-3} $\frac{\text{kg}}{\text{sMPa}}$
b_{in}	Critical pressure ratio for charging	0.39
b_{out}	Critical pressure ratio for discharging	0.28

The RMS fitting error for upstream pressure 0.7 MPa was 0.252×10^{-4} kg/s or 0.9% (flow path 1-2) of the range and 0.212×10^{-4} kg/s or 0.7% (flow path 2-3). Figure 3 shows a relatively good overlap also for upstream pressures 0.6 and 0.5 MPa. Note that this flow model combined with valve switching delays is used in the simulation study for the initial tuning of the controller parameters.

(i) System with One 3/2 Valve

The discontinuous switching between the on-mode and off-mode is difficult to handle in terms of controller design. An alternative approach introduced in (Jouppila, Gadsden, & Ellman, 2010; Rao & Bone, 2008) is employed to provide a continuous and invertible flow model for the proposed controller design. In order to obtain a precise valve mapping, a pressure response curve was measured while inflating and deflating a closed chamber while operating the valve with different duty ratios. By differentiating the filtered pressure curve and using Eq. (2) for a constant volume, the mass flow rate can be approximated. The nonlinear characteristics of the mass flow rate can be captured by the following second-order bi-polynomial function (see details in (Jouppila;Gadsden;& Ellman, 2010)):

$$\begin{aligned} \dot{m}_{eq}(u_{duty}, p_m) = m_1 + m_2 p_m + m_3 p_m^2 \\ + m_4 u_{duty} \\ + m_5 u_{duty} p_m + m_6 u_{duty} p_m^2 + m_7 u_{duty}^2 \\ + m_8 u_{duty}^2 p_m + m_9 u_{duty}^2 p_m^2 \end{aligned} \quad (5)$$

The parameters of (5) were determined using nonlinear least squares. The maximum fitting error was 1.96×10^{-4} kg/s or 4.13% of the range. The RMSE was 5.5×10^{-5} kg/s or 1.16%.

(ii) System with Two 2/2 Valves

Similar valve modelling approaches can be used for determining the flow characteristics in the case where two 2/2 valves are used to control the actuator. The first valve is used for controlling the inflow, and the second for the outflow. With this configuration, unnecessary valve switching can be avoided when the state of the system is close to the desired state (by closing both valves). This helps to save energy and increases the lifetime of the valves.

(iii) System with Servo Valve

The chosen servo valve has a nominal flow rate of 100 L/min, which is equivalent to the nominal flow rate specifications for the solenoid valves allowing an opportunity for comparison. The inflow and outflow of the servo valve are also captured using the 2nd order bi-polynomial fitting function (Eq.(5)) by replacing u_{duty} with u_{servo}.

2.4 System Model for Control Design

In this paper and system, the muscle actuator drives a pneumatic cylinder in a horizontal configuration resulting in additional and unknown friction. For the sliding mode control design, a continuous system model is needed and discontinuous frictional elements (static or Coulomb) are neglected in the system model. The overall model can be derived as:

$$M\ddot{x} = F_m(x, p_m) - B_{eff}\dot{x} - p_{cyl}A_{cyl} \quad (6)$$

where F_m is the static muscle force described in Eq.(1), M is the mass of moving parts (dominated by the payload mass), and p_{cyl} and A_{cyl} are the cylinder pressure and effective piston rod side area, respectively. The frictional force includes viscous friction, where $B_{eff} = 95$ Ns/m is an experimentally identified effective viscous friction factor. Coulomb and static friction that are present in the real system can be considered as modelling uncertainties and disturbances that the SMC control strategy shall compensate for. The state vector for the system studied in this paper is defined as follows:

$$\boldsymbol{x} = [x \quad \dot{x} \quad \ddot{x} \quad p_m]^T \quad (7)$$

For a controller design, the following single-output (SISO) canonical form is considered:

$$\dot{\boldsymbol{x}} = F(\boldsymbol{x}) + G(\boldsymbol{x})u_{control}, h(\boldsymbol{x}) = x \quad (8)$$

where $u_{control}$ is the control input, and $\boldsymbol{x}$ is the state vector, F and G vectors and h is the output of interest (position). The actual control input (duty ratio) appears in the definition of the equivalent mass flow rate defined in Eq. (4). Note that it is rather difficult to obtain equations such that it also appears in the system motion equation.

However, if the inverse of the valve flow model is used as a part of the control structure as shown in Fig. 4, the equivalent mass flow rate can be defined as a control input $u_{control}$. Differentiating Eq. (6) yields the following:

$$\begin{gathered}\dddot{x} = f(\boldsymbol{x}) + g(\boldsymbol{x})u_{control}, \quad where \\ f(\boldsymbol{x}) = L_f^3 h(\boldsymbol{x}) = \frac{H\dot{x} - B_{eff}\ddot{x}}{M}, \\ g(\boldsymbol{x}) = L_G L_F^2 h(\boldsymbol{x}) = \frac{C}{M}, \\ u_{control} = \dot{m}_{eq} \\ H = a_1 + 2a_2 x + 3a_3 x^2 + (p_{max} - p_m)k_1 \\ -\frac{kp_m v_1}{V_m(x)}(k_0 - k_1 x) \\ C = (k_0 - k_1 x)\frac{kRT}{V_m(x)}\end{gathered} \quad (9)$$

where Eqs. (1-3) are substituted into Eq. (6), and rearranged as terms H and C to simplify the expression. Figure 4 illustrates the block diagram of the overall control system in single on/off valve configuration. Note, that dead-zone configuration is not used with single valve configuration, but is necessary with two valve configuration.

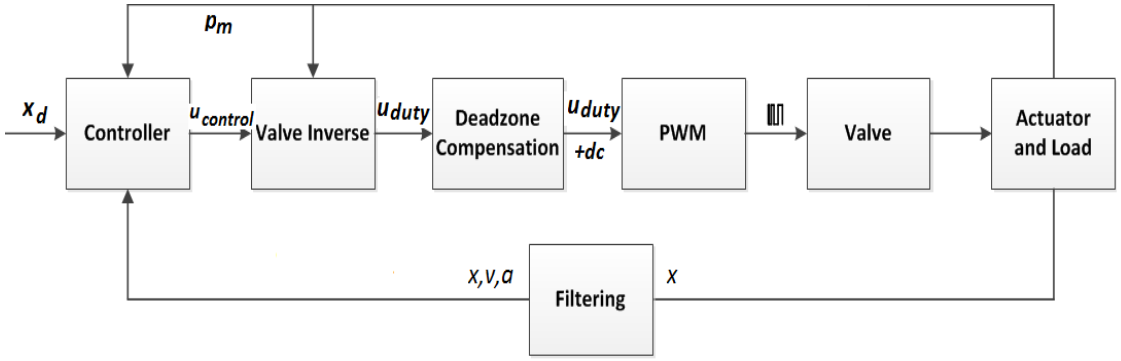

Fig. 4: *Block diagram of the overall control system with single on/off valve configuration.*

3 Sliding Mode Control Design

SMC is a form of variable structure control that utilizes a plane in the state space termed the sliding surface (Utkin, 1978; Slotine & Li, 1991). The objective is to keep the state values close to this surface by minimizing the state errors (between the desired trajectory and the estimated or actual values). Ideally, if the state value is away from the surface, a switching gain would be used to push the state towards the sliding surface. Once on the surface, the states slide along the surface in what is called the sliding mode (Slotine & Li, 1991). The switching brings inherent stability and robustness to the control strategy, while also introducing chattering (high-frequency switching) that is undesirable in practice and can excite un-modelled dynamics. A

boundary layer may be introduced within a region of the sliding surface to minimize chattering.

The order of the overall system is three. A common approach is to define a sliding surface of one degree less than the controlled system, as follows:

$$S = \left(\frac{d}{dt} + \lambda\right)^2 e = \ddot{e} + 2\lambda\dot{e} + \lambda^2 e \tag{10}$$

where S is the sliding surface, λ is the control bandwidth and e is the position error defined by:

$$e = x - x_d \tag{11}$$

The above definition for a sliding surface assumes a critically damped ($\xi = 1$) closed loop control dynamics. However, quite often the estimated or measured velocity can be very noisy which will affect the performance. In cases where a clean estimation of velocity and acceleration is difficult to obtain, the following alternative sliding surface definition can be used:

$$S = \ddot{e} + 2\xi\lambda\dot{e} + \lambda^2 e \tag{12}$$

where the damping factor is defined by ξ.

Since PWM is being used with the on/off valves the equivalent control approach to SMC may be used (Slotine & Li, 1991). The equivalent control approach utilizes the system model, and the purpose of it is to keep the system state on the sliding surface once it has been reached. The state will stay on the surface when $dS/dt = 0$, which yields the equivalent control as follows:

$$\begin{aligned} u_{eq} &= \frac{\dddot{x}_d - \hat{f}(\boldsymbol{x}) - 2\lambda\xi\ddot{e} - \lambda^2\dot{e}}{\hat{g}(\boldsymbol{x})} \\ \hat{f}(\boldsymbol{x}) &= \frac{f_{min}(\boldsymbol{x}) + f_{max}(\boldsymbol{x})}{2} \\ \hat{g}(\boldsymbol{x}) &= \sqrt{g_{min}(\boldsymbol{x}) g_{max}(\boldsymbol{x})} \\ \beta^{-1} \le \frac{\hat{g}(\boldsymbol{x})}{g(\boldsymbol{x})} &= \beta, \beta = \sqrt{\frac{g_{max}(\boldsymbol{x})}{g_{min}(\boldsymbol{x})}} \end{aligned} \tag{13}$$

where $\hat{g}(\boldsymbol{x})$ and $\hat{f}(\boldsymbol{x})$ are estimates of $g(\boldsymbol{x})$ and $f(\boldsymbol{x})$, respectively. The estimate $\hat{f}(\boldsymbol{x})$ can be approximated by calculating the mean of minimum and maximum bounds of $f(\boldsymbol{x})$ based on uncertainties in the model parameters. A natural choice for estimate $\hat{g}(\boldsymbol{x})$ is the geometric mean of the upper and lower bounds while β is the gain margin of the design. The necessary condition for the reachability of the sliding surface is given by the following:

$$\frac{1}{2}\frac{d}{dt}S^2 \le -\eta|S| \tag{14}$$

where η is a design parameter that impacts the convergence rate of the sliding surface. In order to satisfy the condition, a switching control that accommodates the model uncertainties and disturbances (such as static friction) is defined as follows:

$$u_{sw} = -K_{SMC}\, sign(S) \tag{15}$$

The switching gain K_{SMC} can be defined as a constant or as a function of upper bounds on modelling and system uncertainties as in (Slotine & Li, 1991)

$$K_{SMC} \ge \beta(F + \eta) + (\beta - 1)\left|u_{eq}\right|, F = \alpha\left|\hat{f}(\boldsymbol{x})\right| \tag{16}$$

where F describes the estimation error on $f(\boldsymbol{x})$ with and uncertainty factor α.

A robust control law can be obtained by combining the equivalent control with the switching control:

$$u_{control} = u_{eq} + u_{sw} \tag{17}$$

In this application both the equivalent and switching control terms are given in terms of mass flow rate. Due to finite sampling frequency and delays the state trajectory may start to chatter around the sliding surface. In order to reduce the chattering, a smoothing boundary layer φ is often introduced around the sliding surface, as follows:

$$u_{sw} = -K_{SMC}\, sat\left(\frac{S}{\varphi}\right) \tag{18}$$

Inside the boundary layer, the discontinuous switching function is interpolated by a continuous saturation function to avoid control signal discontinuities. Although the boundary layer design reduces the chattering effect, it no longer drives the tracking error to the origin, but to a small region around the origin. As a consequence, there exists a design conflict or trade-off between the requirements on smoothness of control signal and tracking precision.

As the SMC controller outputs the desired mass flow rate, the remaining step is to convert the controller output to a respective valve control signal. With servo valves, the valve control signal is an electrical voltage. With on/off valves, it is the duty ratio of the PWM signal. This conversion may be accomplished by using the second-order bi-polynomial fitting Eq. (5) with the given values for the mass flow rates and the pressure measurement p_m. The bi-polynomial Eq. (5) reduces to the following quadratic equation with u_{duty}:

$$\begin{aligned} C_{21}u_{duty}^2 + C_{11}u_{duty} + C_{01} &= 0 \\ C_{01} = m_1 + m_2 p_m + m_3 p_m^2 - \dot{m}_{eqd} \\ C_{11} = m_4 + m_5 p_m + m_6 p_m^2 \\ C_{21} = m_7 + m_8 p_m + m_9 p_m^2 \\ \dot{m}_{eqd} = u_{control} = u_{eq} + u_{sw} \end{aligned} \tag{19}$$

The correct value for desired input signal was determined to be the most positive root, as follows:

$$u_{duty} = \frac{-C_{11} + \sqrt{C_{11}^2 - 4C_{21}C_{01}}}{2C_{21}} \tag{20}$$

In the case of two on/off valves and the servo valve, Eq.(17) is solved separately for both the inflow u_{inflow} and outflow $u_{outflow}$ cases:

$$u_{inflow} = \begin{cases} 0 & u_{control} \le 0 \\ d_{min} & 0 < u_{control}, u_{duty} \le d_{min} \\ u_{duty} & 0 < u_{control}, d_{min} \le u_{duty} \end{cases}$$
$$u_{outflow} = \begin{cases} 0 & u_{control} \ge 0 \\ d_{min} & 0 > u_{control}, u_{duty} \le d_{min} \\ u_{duty} & 0 > u_{control}, d_{min} \le u_{duty} \end{cases} \tag{21}$$

where experimentally determined $d_{min} = 0.08$ is used to compensate for the dead zone of the valves as there is no flow with $u_{duty} < d_{min}$. Similarly, the control signal of the servo valve U_{servo} with dead zone compensation $u_{dz} = 0.25$ V is defined as:

$$U_{servo} = \begin{cases} u_0 + u_{dz} & 0 < u_{control}, u_{servo} < u_{dz} \\ u_0 + u_{servo} & 0 < u_{control}, u_{servo} \ge u_{dz} \\ u_0 - u_{dz} & 0 > u_{control}, u_{servo} < u_{dz} \\ u_0 - u_{control} & 0 > u_{control}, u_{servo} \ge u_{dz} \end{cases} \tag{22}$$

where $u_0 = 5\ V$ (spool in mid-position).

4 Experimental Results

Experiments were conducted to demonstrate the performance of the SMC strategy with the aforementioned valve configurations. For the implementation of the SMC strategy, the system states defined by Eq. (7) are required. The velocity was obtained by differentiating the measured position signal which was then filtered by a second-order Butterworth low pass filter with a cut-off frequency of 65 Hz. The acceleration estimate was obtained by differentiating the velocity estimate, and filtering it again by a similar low-pass filter (cut-off frequency 50 Hz). The cut-off frequencies were tuned experimentally to provide the best result.

The experiments were performed for sinusoidal desired trajectories (amplitude 14 mm) for frequencies of 0.25 Hz, 0.5 Hz, and 1 Hz. The cylinder force was set at 50 N. With the on/off valve configurations, a PWM frequency of 100 Hz was used. Each experiment was repeated five times, and the averaged root mean square error (RMSE) values were calculated as follows:

$$RMSE = \sqrt{\frac{1}{N}\sum_{i=1}^{N} e_i^2} \tag{23}$$

where i is the current sample number, e_i is the error for the current sample, and N is the total number of samples. The experiment length of time was 8 sec with a 1000 Hz sampling rate.

4.1 Controller Tuning

Based on simulation and experimental results with a nominal payload of 2 kg, the control bandwidth was set to $\lambda = 85$ rad/s and the damping ratio was set to $\xi = 0.1$. The switching gain should be large enough to provide robustness to parameter uncertainties. Note that it also determines how quickly the system states converge towards the sliding surface. Figure 5 (a) illustrates the step responses of the system with different values of K_{SMC} and control law defined by Eq. (13), Eq. (15) and Eq. (17). In order to provide enough flow to follow a sinusoidal curve (amplitude of 14 mm at 1 Hz), K_{SMC} was set to 0.6×10^{-3}kg/s. As described earlier, excessive control chattering can be reduced by a boundary layer based control law with saturation. Figure 5 (b) illustrates the tracking performance as a function of boundary layer thickness for each configuration: single on/off valve, dual on/off valves, and a servo valve.

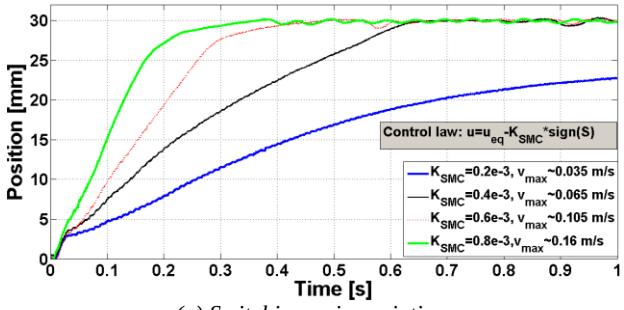

(a) Switching gain variation

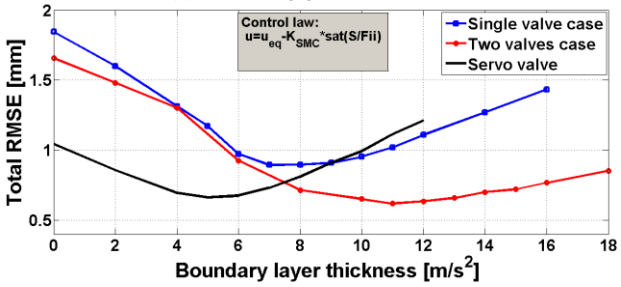

(b) Boundary layer thickness variation

Fig. 5: *Determination of important control parameters.*

In Figure 5 (b), the *total RMSE* is defined as the sum of RMSE values for sinusoidal input frequencies 0.25 Hz, 0.5 Hz, and 1 Hz. For every valve configuration, the boundary layer width improves the

tracking performance up to a certain point, after which the control accuracy begins to degrade.

It is also interesting to note that the system with two on/off valves can provide a better tracking performance than the system with the servo valve. This is assumed to be caused by the friction in the system as the PWM switching decreases the static friction of the system. The boundary layer thickness values are chosen based on the these curves and the amount of control signal chattering resulting in $\varphi = 9$ for single valve; $\varphi = 12$ for two on/off valves; and $\varphi = 5$ for the servo valve.

4.2 Sinusoidal Tracking (Normal Conditions)

Table 2 lists the mean RMSE values for the valve configurations with sinusoidal tracking and the nominal payload. As demonstrated by these results, the dual valve configuration provides the best tracking with sinusoidal frequencies 0.25 Hz and 0.5 Hz. The dual valve and servo valve configurations improve the tracking performance up to 30% when compared with the single on/off valve case. It is also notable that the tracking performance with the dual valve configuration is slightly better than compared to the servo valve system (overall).

Figure 6 illustrates the performance for sinusoidal tracking at 0.5 Hz for the single valve and dual valve configurations. The performances for sinusoidal tracking at 1 Hz for the dual valve and servo valve configurations are shown in Fig. 7.

Note that slight oscillations occur in the control performance during the negative direction movement. This may be due to the cylinder acting like a driving force, and the muscle actuator acting like a brake; which is more difficult to control as the air is released from the actuator. Finally, note also that the magnitude of the oscillation is smaller in the servo valve system due to its faster sampling rate.

Table 2: Comparison of RMSE values [mm] averaged over five tests for the three valve configurations (as per Figs. 6 and 7).

Frequency	Single On/Off	Dual On/Off	Servo Valve
0.25 Hz	0.196	**0.087**	0.091
0.5 Hz	0.268	**0.170**	0.205
1 Hz	0.448	0.378	**0.367**
Total RMSE	0.912	**0.635**	0.663

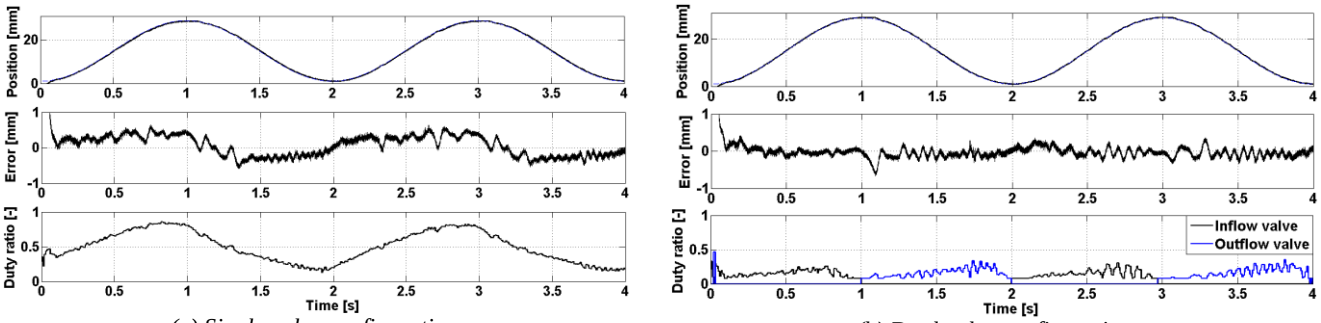

(a) Single valve configuration *(b) Dual valve configuration*

Fig. 6: *Sinusoidal tracking (at* 0.5 Hz *with* $M = 2$kg*).*

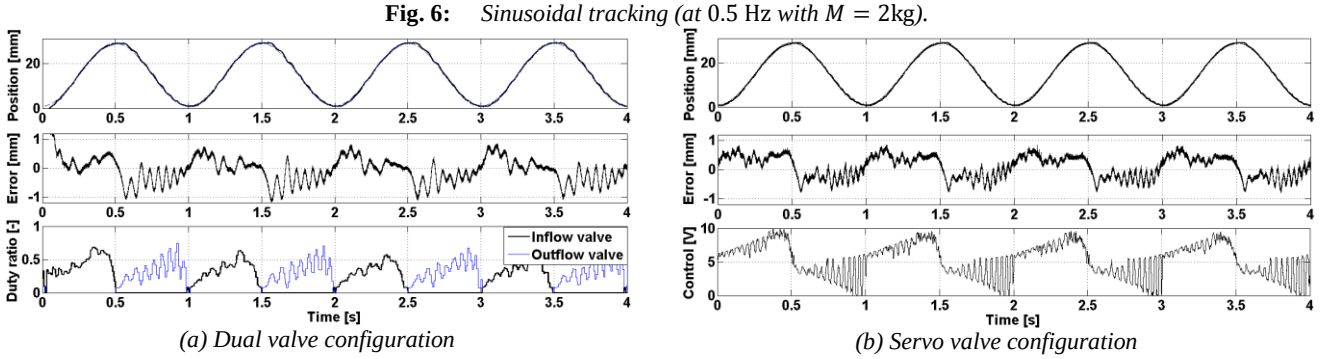

(a) Dual valve configuration *(b) Servo valve configuration*

Fig. 7: *Sinusoidal tracking (at* 1 Hz *with* $M = 2$kg*).*

4.3 Robustness to Payload Variation

The RMSE results of this section are summarized in Tables 3 and 4. The payload was decreased to $M = 0.5$ kg and also increased to $M = 4$ kg. It is interesting to observe that the on/off valve configurations are extremely robust to decreased payload mass as the total RMSE is actually improved when compared with the nominal case. Conversely, the total RMSE of the servo valve configuration increases with payload mass $M = 0.5$ kg by approximately 37% when compared with the nominal case. This is most likely due to the control effort being excessive for the decreased inertia which leads to increased chattering around the sliding surface.

For the second payload variation ($M = 4$ kg), the performance of the case with two on/off valves degrades

79% on average, and 46% with the single valve compared with the nominal case. In terms of robustness, the best performance with the increased payload mass is obtained with the servo valve configuration, as the total RMSE increases by only 16%. With all of the valve configurations, oscillations occurred in the motion signal with increased inertia. This is due to a relatively low damping ratio $\xi = 0.1$ of the closed loop control dynamics, which begins to affect the performance as the inertia of the system increases.

Figure 8 illustrates the damping ratio effect on the control performance with the nominal payload mass $M = 2$ kg and increased payload mass $M = 4$ kg with each system configuration. The calculated tracking accuracy is the sum of the RMSE values with sinusoidal inputs 0.25 Hz and 0.5 Hz. With the nominal payload $M = 2$ kg, the tracking performance degrades significantly while increasing the damping ratio. A higher damping ratio magnifies the noise in the system, which results in poor performance, especially when studying the on/off valve configurations. The servo valve configuration has a faster control loop, which provides better robustness to increased noise. Under the $M = 4$ kg condition, the systems start to oscillate when low damping ratios are implemented, thus a higher damping ratio is needed. The best performance is obtained by using a damping ratio of 0.4 with the servo valve and two valves systems, and 0.7 with the single valve system. Note also that a high damping ratio decreases the tracking accuracy which can be seen amongst all of the configurations.

Table 3: Comparison of average RMSE [mm] with payload $M = 0.5$ kg (as per Fig. 9).

Frequency	Single On/Off	Two On/Off	Servo Valve
0.25 Hz	0.163	**0.079**	0.135
0.5 Hz	0.230	**0.142**	0.232
1 Hz	0.470	**0.354**	0.543
Total RMSE	0.863	**0.575**	0.910

Table 4: Comparison of average RMSE [mm] with payload $M = 4$ kg (as per Fig. 9).

Frequency	Single On/Off	Two On/Off	Servo Valve
0.25 Hz	0.231	0.193	**0.131**
0.5 Hz	0.356	0.313	**0.209**
1 Hz	0.748	0.633	**0.434**
Total RMSE	1.335	1.139	**0.774**

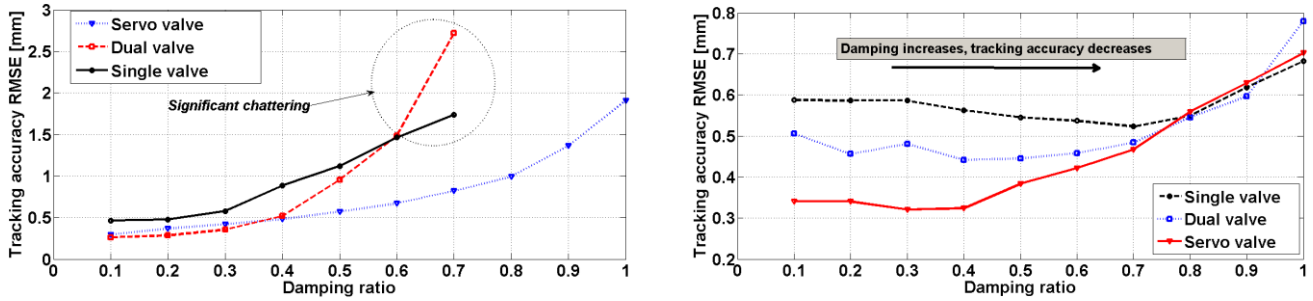

(a) Effect with $M = 2$kg *(b) Effect with $M = 4$kg*

Fig. 8: *Effect of damping ratio (dr) with various payloads ($M = 2$kg and $M = 4$kg).*

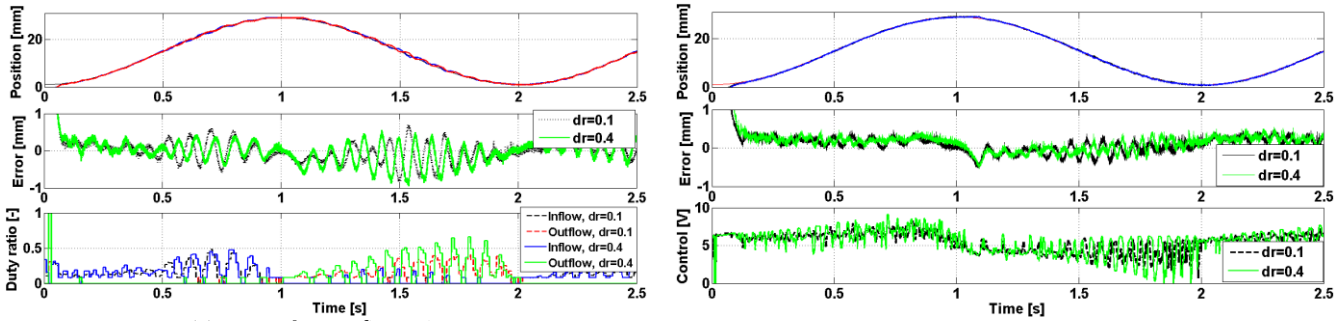

(a) Two valve configuration *(b) Servo valve configuration*

Fig. 9: *Sinusoidal tracking (at 0.5 Hz with $M = 4$kg).*

Figure 9 illustrates the effect of the damping ratio on the performances of the two valves and servo valve configurations. As stated earlier, it is observed that the servo valve configuration provides a much better damping of oscillations due to the faster control loop. With the PWM-actuated on/off valve systems, the PWM sampling introduced unwanted delay decreases the overall robustness of the SMC strategy.

4.4 Robustness to External Disturbances

Robustness to external disturbances was tested by applying sinusoidal and square wave force profiles with

the pneumatic cylinder. The amplitude of the force disturbance was 25 N and the mean value was 50 N. Frequencies of 1 Hz and 2 Hz were used for the sinusoidal disturbance, and 0.75 Hz for the square wave disturbance.

Table 5 summarizes the RMSE values when the desired trajectory is sinusoidal with an amplitude of 10 mm at 0.25 Hz. Although each of the valve configurations is capable of providing a reasonable response for the applied disturbance signals, the best performance is obtained with the servo valve configuration. Figure 10 illustrates the tracking performance of the two valves and servo valve systems, with sinusoidal (2 Hz) and square wave (0.75 Hz) disturbances.

As illustrated by the results for the sinusoidal disturbance, the two valve system has a maximum tracking error of ± 0.75 mm, whereas the servo valve system error is in the range of roughly ± 0.5 mm. For the stepwise disturbance, the respective errors are about ± 1.4 mm and ± 1 mm. Based on these results, due to a faster control loop, the servo valve configuration provides the best response to the studied external disturbances.

Table 5: Comparison of average RMSE [mm] with external disturbance (as per Fig. 10).

Disturbance	Single On/Off	Two On/Off	Servo Valve
1 Hz (Sine)	0.173	0.149	**0.120**
2 Hz (Sine)	0.288	0.238	**0.178**
0.75 Hz (Step)	0.280	0.237	**0.177**
None	0.123	**0.083**	0.097

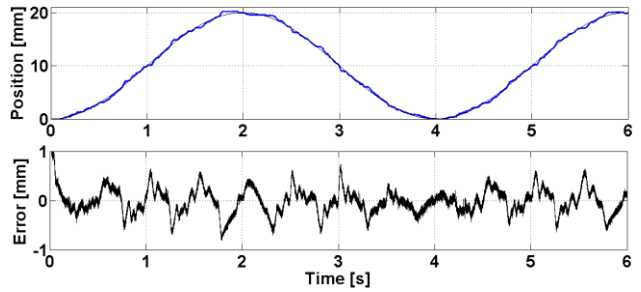

(a) Two valve configuration (2 Hz sinusoidal disturbance)

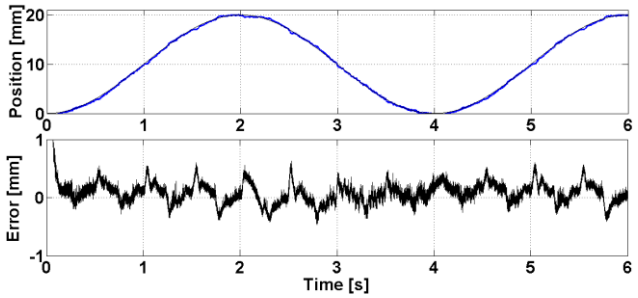

(b) Servo valve configuration (2 Hz sinusoidal disturbance)

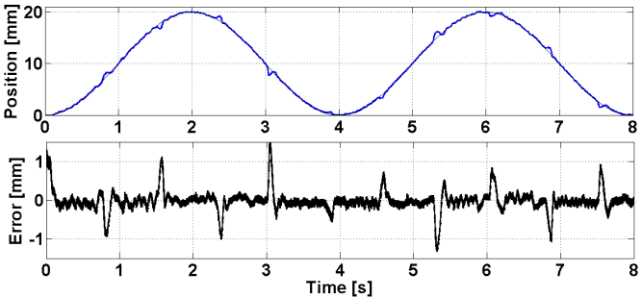

(c) Two valve configuration (0.75 Hz stepwise force disturbance)

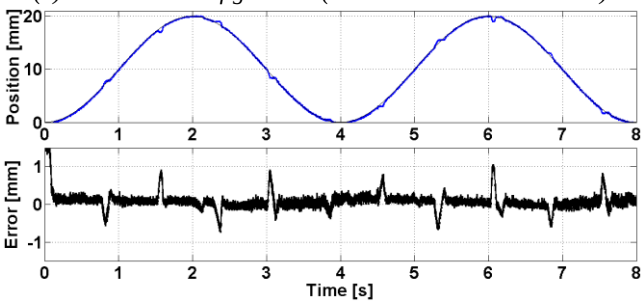

(d) Servo valve configuration (0.75 Hz stepwise force disturbance)

Fig. 10: *Sinusoidal tracking (0.25 Hz) performance with various disturbances (with $M = 2$kg).*

5 Conclusions

This paper provides a low cost approach to control pneumatic systems by using high-speed on/off valves, instead of costly proportional and servo valves. A full nonlinear system model was derived and provided for use with PWM-driven pneumatic applications. The valve model (pressure and flow dynamics) is continuous and invertible, such that an equivalent control method such as a SMC strategy may be implemented. A comparison of three valve configurations was made: single on/off valve, two on/off valves, and a servo valve. In nominal conditions, the two valves and servo valve configurations are capable of providing a 30% reduction in RMSE compared with the single on/off valve case. In general, the two valve system provided slightly better tracking accuracy compared with the servo valve system.

The robustness of the control configurations was tested by changing the payload mass and by applying an external force disturbance. When decreasing the payload mass, the two on/off valves configuration was the most robust. However, when increasing the payload mass, the servo valve configuration provided the best results. Against external force disturbances, the servo valve also provided the best robustness. Overall, the PWM-actuated on/off valve controlled muscle actuator system provided a low cost option with a performance almost similar to servo valve controlled systems.

Nomenclature

Symbol	Description	Unit
A_{cyl}	cylinder effective piston rod side area	$[m^2]$

b	Critical pressure ratio	$[-]$
B_{eff}	Effective viscous friction	[Ns/m]
C	Valve conductance	$[\frac{\text{kg}}{\text{sMPa}}]$
d_{min}	Min. duty ratio to provide flow	$[-]$
f_{PWM}	PWM frequency	[Hz]
F_m	Muscle actuator force	[N]
F_{max}	Max. muscle actuator force	[N]
k	Specific heat ratio	$[-]$
K_{SMC}	Switching gain	[kg/s]
$\dot{m}$	Mass flow rate	[kg/s]
$\dot{m}_{eq}$	Equivalent mass flow rate	[kg/s]
M	Payload mass	[kg]
p_{cyl}	Cylinder pressure	[Pa]
p_{down}	Downstream pressure	[Pa]
p_m	Muscle actuator pressure	[Pa]
p_{max}	Max. muscle actuator pressure	[Pa]
p_s	Supply pressure	[Pa]
p_{up}	Upstream pressure	[Pa]
p_0	Atmosphere pressure	[Pa]
R	Gas constant	[J/(kgK)]
S	Sliding surface	$[\text{m/s}^2]$
T	Air temperature	[K]
$u_{control}$	Control input	[kg/s]
u_{duty}	PWM duty ratio	$[-]$
u_{dz}	Valve dead zone compensation	$[-]$
u_{eq}	Equivalent control term	[kg/s]
u_{inflow}	Duty ratio for inflow valve	$[-]$
$u_{outflow}$	Duty ratio for outflow valve	$[-]$
u_{sw}	Switching control term	[kg/s]
U_{servo}	Servo valve control signal	[V]
V_m	Muscle actuator volume	$[\text{m}^3]$
x	Position of the actuator	[m]
x_d	Desired position	[m]
α	Uncertainty factor	$[-]$
β	Gain margin	$[-]$
η	Control design parameter [	$\text{m/s}^3]$
λ	Control bandwidth	[rad/s]
ξ	Damping factor	$[-]$
φ	Boundary layer width	$[\text{m/s}^2]$

The following is a list of important parameters used with corresponding definitions and values, where applicable.

Parameter	Value
a_0	$484\ [N]$
a_1	$-1.97e4\ [N/m]$
a_2	$4.34e5\ [N/m^2]$
a_3	$-4.33e6\ [N/m^3]$
k	1.4
k_0	$0.00079\ [N/Pa]$
k_1	$0.00751\ [\frac{N}{Pa}m^{-1}]$
m_1	$-2.26 \times 10^{-4}\ [kg/s]$
m_2	$-3.05 \times 10^{-9}\ [kg/sPa]$
m_3	$-3.3 \times 10^{-15}\ [kg/sPa^2]$
m_4	$0.002\ [kg/s]$
m_5	$5.35 \times 10^{-9}\ [kg/sPa]$
m_6	$-2.35 \times 10^{-15}\ [kg/sPa^2]$
m_7	$6.01 \times 10^{-4}\ [kg/s]$
m_8	$-1.5 \times 10^{-9}\ [kg/sPa]$
m_9	$-1.62 \times 10^{-15}\ [kg/sPa^2]$
B_{eff}	$95\ [Ns/m]$
M	$2\ [kg]$
p_{max}	$0.6\ [MPa]$
R	$287\ [J/(kgK)]$
T	$293\ [K]$
v_0	$2.4 \times 10^{-5}\ [m^3]$
v_1	$5.6 \times 10^{-4}\ [m^2]$

References

anon. (2005). ISO-6358 Pneumatic Fluid Power - Components Using Compressible Fluids - Determination of Flow-Rate Characteristics. International Organization for Standardization. Geneve.

Ahn, K., & Yokota, S. (2005). Intelligent Switching Control of Pneumatic Actuator using On/Off Solenoid Valves. *Mechatronics, 15*, 683-702.

Aschemann, H., & Schindele, D. (2008). Sliding-mode Control of a High-Speed Linear Axis Driven by Pneumatic Muscle Actuators. *IEEE Transactions on Industrial Electronics, 11*(55), 3855-3864.

Balasubramanian, K., & Rattan, K. S. (2003). Feedforward Control of a Nonlinear Pneumatic Muscle System Using Fuzzy Logic. *IEEE International Conference of Fuzzy Systems, 1*, pp. 272-277.

Barth, E. J., Zhang, J., & Goldfarb, M. (2003). Control Design for Relative Stability in a PWM-Controlled Pneumatic Systems. *ASME Journal of Dynamic Systems, Measurement and Control, 125*(3), 504-508.

Caldwell, D. G., Medrano-Cerda, G. A., & Goodwin, M. J. (1995). Control of Pneumatic Muscle Actuators. *IEEE Control Systems Magazine, 15, No.1*, pp. 40-48.

Carbonell, P., Jiang, Z. P., & Repperger, D. W. (2001). Nonlinear Control of a Pneumatic Muscle Actuator: Backstepping vs. Sliding Mode. *Proceedings of the IEEE International Conference on Control Applications*, (pp. 167-172).

Chan, S. W., Lilly, J. H., Repperger, D. W., & Berlin, J. E. (2003). Fuzzy PD+I Learning Control for a Pneumatic Muscle . *Proceedings of 2003 IEEE International Conference on Fuzzy Systems*, (pp. 278-283). St Louis, USA.

Chou, P., & Hannaford, B. (1996). Measurement and Modeling of a McKibben Pneumatic Artificial Muscles. *IEEE Transaction on Robotics and Automation, 12*(1).

Gaylord, R. H. (1958). *Patent No. 2,844,126.* U.S.A.

Hesselroth, T., Sarkar, K., Van der Smagt, P., & Schulten, K. (1994). Neural Network Control of a Pneumatic Robot Arm. *IEEE Transaction of Systems, Man and Cybernetics, 24, No.1*, pp. 28-38.

Jouppila, V. T., Gadsden, S. A., & Ellman, A. U. (2010). Modeling and Identification of a Pneumatic Muscle Actuator System Controlled by an On/Off Solenoid Valve. *Proceedings of 7th International Fluid Power Conference*, (p. 16). Aachen, Germany.

Lai, J. Y., Singh, R., & Menq, C. H. (1992). Development of PWM mode Position Control for a Pneumatic Servo System. *Journal of the Chinese Society of Mechanical Engineers, 13*(1), 86-95.

Lilly, J. (2003). Adaptive Tracking for Pneumatic Muscle Actuators in Bicep and Tricep Configurations. *IEEE Transaction of Neural Systems and Rehabilitation Engineering, 11, No. 3*, pp. 333-339.

Lilly, J. H., & Yang, L. (2005). Sliding Mode Tracking for Pneumatic Muscle Actuators in Opposing Pair Configuration. *IEEE Transactions on Control Systems Technology, 13*, pp. 550-558.

Medrano-Cerda, G. A., Bowler, C. J., & Caldwell, D. G. (1995). Adaptive Position Control of Antagonistic Pneumatic Muscle Actuators. *IEEE/RSJ International Conference on Intelligent Robots and Systems, 1*, pp. 378-383. Pittsburgh, USA.

Morita, Y. S., Shimizu, M., & Kagawa, T. (1985). An Analysis of Pneumatic PWM and Its Application to a Manipulator. *Proceedings of International Symposium of Fluid Control and Measurement*, (pp. 3-8). Tokyo, Japan.

Nguyen, T., Leavitt, J., Jabbari, F., & Bobrow, J. E. (2007, April). Accurate Sliding-Mode Control of Pneumatic Systems Using Low-Cost Solenoid Valves. *IEEE/ASME Transactions on Mechatronics, 12*(2), 216-219.

Noritsugu, T. (1986). Development of PWM Mode Electro-Pneumatic Servomechanism, Part I: Speed Control of a Pneumatic Cylinder. *Journal of Fluid Control, 17-1*, 65-80.

Paul, A. K., Mishra, J. K., & Radke, M. G. (1994). Reduced Order Sliding Mode Control for Pneumatic Actuator. *IEEE Transaction on Control Systems Technology, 2*(30), 271-276.

Rao, Z., & Bone, G. M. (2008). Nonlinear Modeling and Control of Servo Pneumatic Actuators. *IEEE Transactions on Control Systems Technology, 16*, 562-569.

Schulte, R. A. (1962). The Characteristics of the McKibben Artificial Muscle. *The Applications of External Power in Prosthetics and Orthotics*, 94-115.

Shen, X. (2010). Nonlinear Model-Based Control of Pneumatic Artificial Muscle Actuator Systems. *Control Engineering Practice, 18*, 311-317.

Shen, X., Zhang, J., Barth, E., & Goldfarb, M. (2006). Nonlinear Model-Based Control of Pulse Width Modulated Pneumatic Servo Systems. *ASME Journal of Dynamic Systems, Measurement and Control, 128*, 663-669.

Slotine, J. J., & Li, W. (1991). *Applied Nonlinear Control.* Englewood Cliffs, New Jersey, USA: Prentice-Hall.

Than, T., & Ahn, K. (2006). Nonlinear PID Control to Improve the Control Performance of 2 Axes Pneumatic Artificial Muscle Manipulator Using Neural Networks. *Mechatronics, 16*, 577-587.

Tondu, B., & Lopez, P. (2000). Modeling and Control of McKibben Artificial Muscle. *IEEE Control Systems Magazine*, (pp. 15-38).

Utkin, V. I. (1978). *Sliding Modes and Their Application in Variable Strucure Systems.* Moscow, Russia: MIR Publishers.

Van Varseveld, R. B., & Bone, G. M. (1997). Accurate Position Control of a Pneumatic Actuator Using On/Off Solenoid Valves. *IEEE/ASME Transaction on Mechatronics, 2*(30), 195-2004.

PUBLICATION 4

A Pneumatic Position Servo Based on On/Off Valve Actuated Muscle Actuators in Opposing Pair Configuration

Ville Jouppila and Asko Ellman

Reprinted, with permission, from the *Proceedings of Bath/ASME Symposium on Fluid Power & Motion Control (FPMC 2012), Bath, UK, 2012*

A Pneumatic Position Servo Based on On/Off Valve Actuated Muscle Actuators in Opposing Pair Configuration

Ville Jouppila, Asko Ellman
Tampere University of Technology, Department of Mechanics and Design
Korkeakoulunkatu 6, 33101 Tampere, Finland
ville.jouppila@tut.fi, asko.ellman@tut.fi

ABSTRACT

Pneumatic muscle actuator is a novel type of actuator which has even higher force to weight ratio than a cylinder. In addition, muscle actuator introduces a stick slip free operation giving an interesting option for positioning systems. However, due to highly nonlinear characteristics of the actuator and pneumatic system, obtaining a good control performance is a real challenge. Instead of using relatively expensive servo valve, a proposal for controlling pneumatic muscle actuators in an opposing pair configuration by four low-cost on/off valves with a PWM strategy is introduced. PWM-technique allows control laws derived for servo valves to be used with on/off valves. As the overall pneumatic system is highly nonlinear and not completely known, a sliding mode control (SMC) strategy is chosen for control law.

The system with on/off valves is formulated in a nonlinear SISO canonical control form for which the SMC control law can be designed. The same approach is used also for servo valve approach enabling a direct comparison of these approaches. The SMC control algorithms designed for this pneumatic position servo system and their performance is compared experimentally with sinusoidal tracking tasks. The robustness of the approaches is verified by varying loading conditions of the system.

Keywords: Pneumatic muscle actuator, pulse width modulation (PWM), on/off valve, servo-pneumatics, sliding mode control (SMC)

1 INTRODUCTION

Pneumatic systems have many properties that make them attractive for use in a variety of environments. High force-to-weight ratios, cleanliness, compactness, ease of maintenance, and the safety of pneumatic actuators offer desirable features for many industrial designs. In addition, a pneumatic McKibben muscle actuator provides an even higher force-to-weight ratio compared with other conventional designs, and is able to operate in a wide range of environments. However, there are a number of nonlinearities present in the system, which makes it rather difficult and complex to control accurately. Nonlinear characteristics of the muscle actuator, air compressibility, friction, and nonlinear airflow through the

Fluid Power and Motion Control 2012 Edited by Dr D N Johnston and Professor A R Plummer

valves are the main reason that pneumatic systems are commonly avoided for advanced applications. Literature demonstrates that a large number of control strategies have been proposed to handle the effects of nonlinearities present. These include the following: adaptive control strategies (1,2,3), nonlinear PID (4), neural networks (5), and fuzzy controllers (6,7). In (8,9) a sliding mode control (SMC) strategy was applied to a muscle actuator system, but only simulation results of the effectiveness of the strategy were presented. Other SMC approaches are presented in (10-12). In the most recent work (12) a SMC strategy was applied to control the muscle actuator system in an opposing pair configuration (similar system as used in this work as a reference to on/off valve approach) using a servo valve. Experimental results with sinusoidal tracking (with amplitude 7.5 mm and frequency $0.5 - 1.5\ Hz$) and payload mass 10.8 kg showed accuracies of $\pm 0.5\ mm$ to $\pm 1.2\ mm$. In this work, SMC strategy was chosen for the control of the muscle actuator since the system studied was highly nonlinear and not well-defined. Previous SMC studies have demonstrated that it is an efficient and robust control strategy for pneumatic actuator applications. However, in these studies, a proportional or servo valve has been used to control the actuator. In this paper, the on/off valves are chosen for the control of the muscle actuator system in order to provide a low cost alternative to servo-pneumatic systems.

In recent years, effort has been made to develop inexpensive servo-pneumatic systems using on/off solenoid valves with pulse-width modulation (PWM). In a PWM-controlled system, the power to an actuator is delivered with discrete packets of energy via a valve that is either completely on or completely off. If the PWM frequency is significantly faster than the system dynamics (i.e. dynamics of the actuator and load), the system will respond in a manner similar to the continuous case. Unlike the continuous case, little to no power is dissipated in the process. Specifically, in the ideal on-state, no flow resistance is offered, and thus no power is dissipated as the flow orifice is fully opened. In the ideal off-state, no flow occurs (if flow to atmosphere is blocked), and thus no power is dissipated. A PWM-controlled system is therefore capable of delivering a significant amount of controlled power to an actuator while dissipating essentially none. Previous works have shown the potential of PWM-controlled pneumatics (13-18). In (19), a modified PWM valve pulsing algorithm was developed that enabled the use of multiple on/off solenoid valves instead of costly servo valves. The proposed algorithm (with a continuous state feedback controller) was successfully implemented, and demonstrated its effectiveness on pneumatic cylinder experiments. In (20), a nonlinear state-space averaged model and a sliding mode controller with PWM was introduced for the control of a single degree of freedom pneumatic positioning system with a cylinder. Sinusoidal tracking with amplitude of 20 *mm* and frequencies from 0.25 to 1 Hz reportedly had accuracies from +/- 1 *mm* to +/- 3.5 *mm*. In (21), a sliding mode controller without PWM for a double-acting cylinder using four low-cost solenoid valves was introduced. The sinusoidal tracking error for a stroke +/- 20mm at 0.5 Hz was less than +/- 2 *mm*. In (22) three linearization approaches for PWM-driven servo-pneumatic systems with a cylinder and a single on/off valve were introduced. Improved performances were achieved by using simple linear controllers with velocity feedback instead of complex and costly nonlinear ones although no real comparison was introduced. Tracking accuracies for a sinusoidal input with amplitude 20 *mm* at 1 Hz and 2 Hz were less than +/- 0.5 *mm* and +/- 1.5 *mm*, respectively.

In this paper, a muscle actuator system with two Festo Fluidic Muscle (MAS10-300 *mm*) actuators mounted horizontally and coupled to a linear slide carrying a payload is studied

(Fig. 1). The system is controlled by 4 on/off valves where an individual valve is used for controlling the inflow and outflow of each muscle actuator. The valves are operated with a PWM-based signal by controlling the PWM duty ratio. For a comparison to on/off valve approach, a servo valve approach is also presented. The SMC controller is designed in the Matlab Simulink environment and is coded by a real-time windows target toolbox, where reference values are generated, data from the sensors (potentiometer, pressures) are read, and the controller output signal is calculated. The output signal is then distributed to an electronic amplifier that supplies the sufficient power to actuate the valves. Actuator pressures and the displacement of the actuator (potentiometer) are measured. The other kinematic states (velocity and acceleration) are obtained by differentiation of the position signal; which adds noise that the controller needs to overcome.

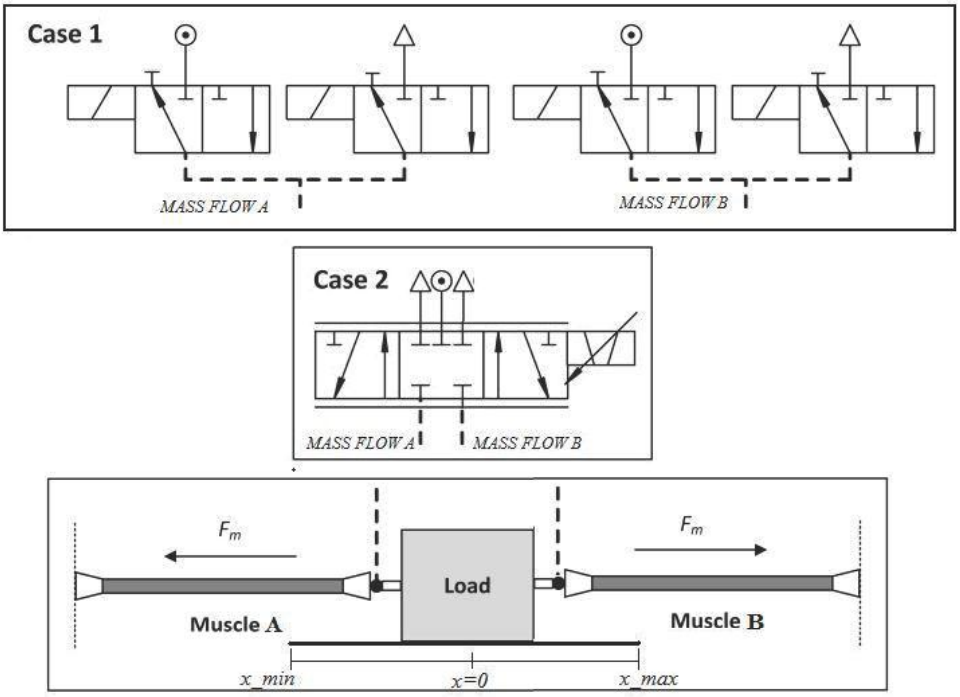

Figure 1: A Muscle Actuator System Controlled by 4 On/Off Valves and Servo Valve

2 MODELING OF THE PNEUMATIC SYSTEM

2.1 Load Dynamics

The load dynamics of the system can be written as

$$M\ddot{x} = F_B - F_A - B\dot{x} - F_{ext} \tag{1}$$

where M is the total payload, B is the viscous friction coefficient, F_A and F_B are the actuation forces of the muscle actuators and F_{ext} is the external force. Coulomb and static friction that are present in the real system are neglected in the control design and can be considered as modeling uncertainties and disturbances.

2.2 Muscle Actuator Force Dynamics

The pneumatic McKibben muscle actuator consists of a rubber tube with a non-extensible fiber surrounding. The physical configuration causes the muscle to have variable-stiffness spring-like characteristics and being very light-weight compared to other types of actuators (23, 24). During pressurization, the muscle widens in diameter and shortens in length, and the maximum force is obtained at the beginning of the contraction and decreases with increasing contraction. The generated force is unidirectional and its maximum contraction is typically 20% to 25% of the nominal length. The advantage of the muscle actuator over the traditional cylinder is the higher force to weight ratio and the stick-slip free motion at low velocities. On the other hand, the force-to-contraction relation at different pressure levels is highly nonlinear, and adds to the difficulty of effectively modelling the muscle actuator. As with all actuation systems, effective application of pneumatic muscle actuators relies on being able to accurately model and predict the forces that will be generated under any operating conditions. Figure 2 illustrates the nonlinear relationship between the force, pressure and displacement for the muscle actuators working in opposing pair configuration. Since the pneumatic muscle actuator is assumed to be non-stretchable, it is necessary, to initially contract both muscles of respectively $x_{0A}=x_{0B}=x_0$. Typically the initial contraction/displacement is determined as half the maximum stroke with an initial reference pressure $p_{A0}=p_{B0}=p_0$. In a typical configuration, the movement is produced by a pressure differential variation between the muscle actuator.

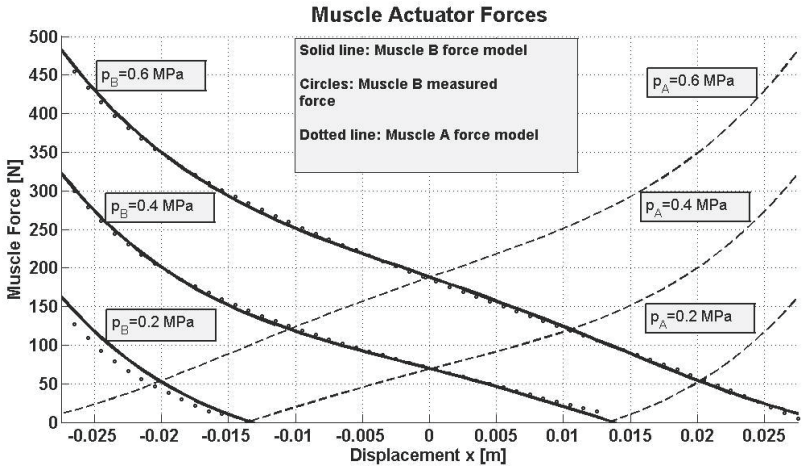

Figure 2: Nonlinear muscle actuator force characteristics

The nonlinear muscle forces can be described by equations

$$F_A(x,p_A) = a_0 + a_1(x_0 - x) + a_2(x_0 - x)^2 + a_3(x_0 - x)^3 + a_4(x_0 - x)^4 - (p_{\max} - p_A)\left(\frac{k_0 - k_1(x_0 - x)}{k_2}\right) \quad (2)$$

$$F_B(x,p_B) = a_0 + a_1(x_0 + x) + a_2(x_0 + x)^2 + a_3(x_0 + x)^3 + a_4(x_0 + x)^4 - (p_{\max} - p_B)\left(\frac{k_0 - k_1(x_0 + x)}{k_2}\right)$$

where p_{max} (=0.6 MPa) is the maximum muscle pressure, and $a_{0\text{-}3}$, k_0 [N], k_1 [N/m] and k_2 [Pa] are coefficients to match the model and measured data, respectively. The details of the actuator force modeling can be found in our previous work (25).

2.3 Pressure Dynamics

For calculating the pressure inside the actuators, it is assumed that the air is an ideal gas and the change of air is adiabatic, such that the pressure change is as follows:

$$\dot{p}_{A,B} = \frac{kRT}{V_{A,B}(x)}\dot{m}_{A,B} - \frac{kp_{A,B}\dot{V}_{A,B}}{V_{A,B}(x)} \quad (3)$$

where k (=1.4 for adiabatic process), R, T, $V_{A,B}$ and $\dot{m}_{A,B}$ denote the specific heat ratio, universal gas constant, air temperature, volume of the actuators and mass flow rate into the actuator. The volume of the muscle actuators can be described by a linear approximation (25)

$$V_A = V_0 - v_1 x, \quad V_B = V_0 + v_1 \quad (4)$$

2.4 Valve Mass Flow Dynamics

The on/off solenoid valve (Festo MHE2,Q_N=100 l/min) is controlled with the duty ratio u_{duty} of the PWM-modulated signal. The switching frequency f_{PWM} and the duty ratio determine how long the valve is open and closed during time period T_{PWM} (=1/f_{PWM}). PWM-technique allows control laws derived for servo valves to be used with on/off valves. It should be noted, that the PWM switching frequency has a significant effect on the system performance as the final control signal for the valve is updated at the PWM frequency used. In order to provide sufficient performance the PWM frequency should be significantly higher than the natural frequency of the system. On the other hand, the bandwidth (300 Hz) of the used valve sets the limit to the maximum reasonable PWM frequency. The PWM frequency used in this work is 100 Hz.

For a comparison to on/off valve approach, a servo valve (FESTO MPYE-5-M5-010-B, Q_N=100 l/min) with the same nominal flow capacity is also used to control the system. The spool position of the servo valve is controlled by a control voltage signal (0-10 V) where the spool is in the center position with control signal 5 V. Due to high bandwidth (125 Hz) the spool dynamics can be ignored and the valve control signal can be calculated based on the desired spool position.

The mass flow rate through the control valve is one of the major nonlinearities in pneumatic systems. Thus, the modeling of valve flow characteristics plays an important role, when a sufficient performance of pneumatic servo systems is required. A traditional equation for modeling the mass flow is based on a flow of an ideal gas through a converging nozzle, and related to the valve control signal by the following relation:

$$\dot{m}(p_u, p_d) = U\Psi(p_u, p_d),$$

$$\Psi(p_u, p_d) = \begin{cases} Cp_{up} & \frac{p_{down}}{p_{up}} \le b \\ Cp_{up}\sqrt{1-\left(\frac{\left(\frac{p_{down}}{p_{up}}\right)-b}{1-b}\right)^2}, & \frac{p_{down}}{p_{up}} \ge b \end{cases} \tag{5}$$

where p_u and p_d are the upstream and downstream pressures, respectively, C is the valve conductance, and b is the critical pressure ratio that divides the flow regimes into un-choked and choked flow through the orifice, and U is the control signal. The definition of valve control signal is defined here as a normalized control signal [-1…1]. In case of on/off valve approach, the control signal is directly the desired duty ratio $U=u_{duty}$ and in case of servo valve $U= G^{-1}*U_{servo}$. Note that, a positive valve command will pressurize the muscle B and exhaust the muscle A, while a negative command corresponds to opposite. The resulting equations for mass flow rates are

$$\dot{m}_A = -U\Psi_A, \quad \Psi_A = \begin{cases} \Psi(p_A, p_{atm}), & if\ U \ge 0 \\ \Psi(p_s, p_A), & if\ U < 0 \end{cases}$$

$$\dot{m}_B = U\Psi_B, \quad \Psi_B = \begin{cases} \Psi(p_s, p_B), & if\ U \ge 0 \\ \Psi(p_B, p_{atm}), & if\ U < 0 \end{cases} \tag{6}$$

where p_s is the supply pressure (=0.65 MPa (abs.)). Figure 3 shows a comparison of the estimated mass flow rate (Eq. (5)) and experimental data for servo valve while charging actuator B. The parameters of the equation (5) are obtained by searching the best fit for the experimental data. It can be seen that the model is capable of providing sufficient accuracy at higher control signals, while the modeling accuracy degrades at small control signals. Similar modeling approach is used also for negative control signals while discharging actuator B. Note, that the servo valve is assumed to be symmetric for mass flow rates A and B. Figure 3 illustrates also the measured mass flow rate as a function of control signal with constant pressure drop across the valve. Note the dead zone and linearity of the curves. Due to a valve dead zone, compensation is added to the final control signal of a servo valve as follows

$$U_{servo} = \begin{cases} U_0 - GU + u_{dz} sign(U), & if \quad U \le 0 \\ U_0 + GU + u_{dz} sign(U), & if \quad U > 0 \end{cases} \tag{7}$$

where U_0=5V and u_{dz}=0.25V is experimentally determined dead zone range.

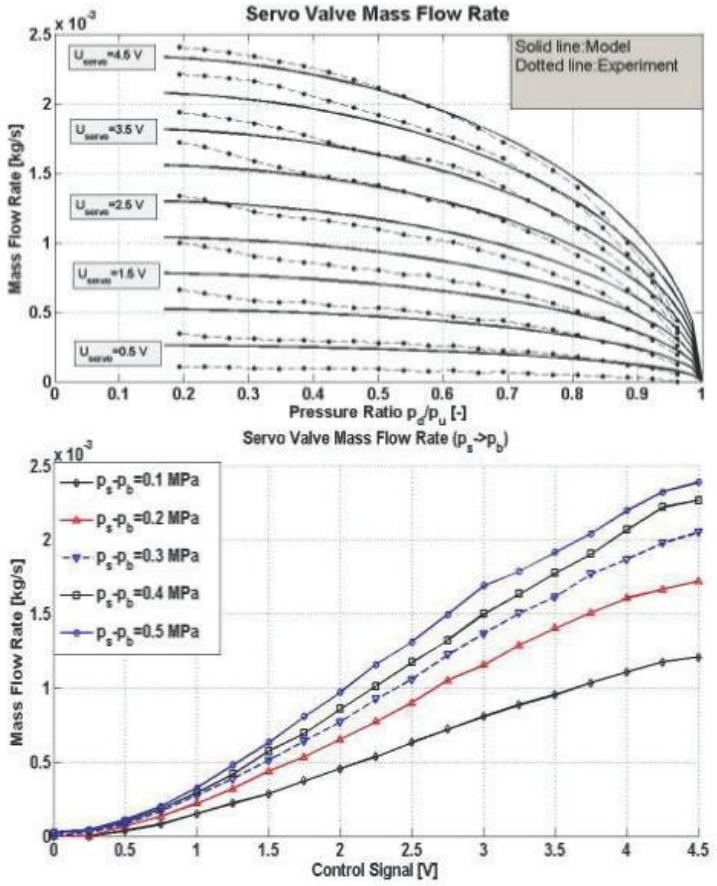

Figure 3: Servo valve mass flow rate while charging actuator B

Similar modeling approach can be utilized with a PWM controlled on/off valve where the control signal is PWM duty ratio (-1...1). Figure 4 illustrates that the traditional flow equation can reasonably well describe the nonlinear flow characteristics. Note also the linear region between control signals 0.1 and 0.9 and the valve dead zone with control values less than 0.05 and flow saturation with control values higher than 0.9. With a dead zone compensation (u_{dz}=0.05) the respective valve control signals are

$$u_{dutyA\_in}, u_{dutyB\_out} = \begin{cases} U + u_{dz}, & if\ U < 0 \\ 0 & if\ U \geq 0 \end{cases}$$
$$u_{dutyA\_out}, u_{dutyB\_in} = \begin{cases} U + u_{dz}, & if\ U > 0 \\ 0 & if\ U \leq 0 \end{cases} \quad (8)$$

Note that this kind of modeling approach results in identical controller structure providing a possibility for a direct comparison of on/off and servo approaches.

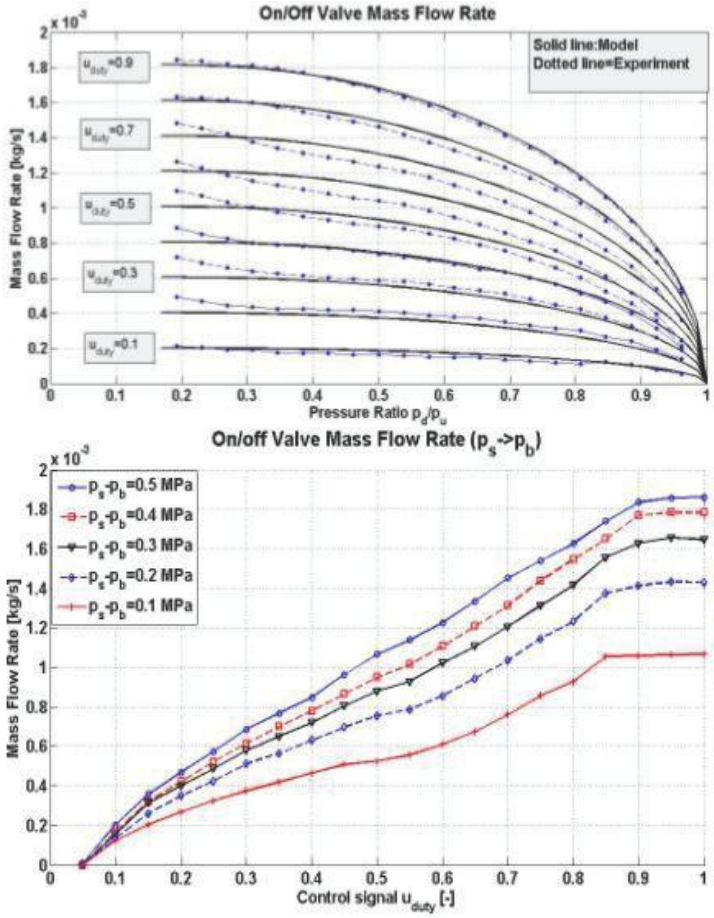

Figure 4: On/off valve mass flow rate while charging actuator B

2.5 Overall system model

The full nonlinear SISO model from the control input U to the displacement of the load x can be defined as

$$\dddot{x} = f(\mathbf{x}) + b(\mathbf{x})U \Rightarrow \dddot{x} = \frac{K}{M}\dot{x} - \frac{B}{M}\ddot{x} + \left(\frac{C_a\psi_a + C_b\psi_b}{M}\right)U \quad \textit{where}$$

$$f(\mathbf{x}) = \frac{K}{M}\dot{x} - \frac{B}{M}\ddot{x},\ b(\mathbf{x}) = \frac{C_a\psi_a + C_b\psi_b}{M}$$

$$\begin{aligned} K = {} & 2a_1 + 4a_2x_0 + 6a_3x_0^2 + 8a_4x_0^3 + 3x^2(2a_3 + 8a_4x_0) \\ & - \frac{k_1}{k_2}(p_A + p_B - 2p_{\max}) - \left(\frac{k_0 - k_1(x_0 + x)}{k_2}\right)\frac{kv_1p_B}{V_B(x)} \\ & - \left(\frac{k_0 - k_1(x_0 - x)}{k_2}\right)\frac{kv_1p_A}{V_A(x)} \end{aligned} \tag{9}$$

$$C_a = -\left(\frac{k_0 - k_1(x_0 - x)}{k_2}\right)\frac{kRT}{V_A(x)}, \qquad C_b = \left(\frac{k_0 - k_1(x_0 + x)}{k_2}\right)\frac{kRT}{V_B(x)}$$

The state vector **x** consists of the pressure in each muscle actuator, along with the position, velocity and acceleration of the load

$$\mathbf{x} = \begin{bmatrix} x & \dot{x} & \ddot{x} & p_A & p_B \end{bmatrix}^T \tag{10}$$

3 SLIDING MODE CONTROL (SMC) DESIGN

SMC is a form of variable structure control and regarded as one of the most effective nonlinear robust control approaches (26, 27). SMC utilizes a discontinuous switching plane along some desired trajectory. The plane is often referred to as a sliding surface *S* that models the desired closed loop performance in the state variable space. The objective is to keep the state values along this surface by minimizing the state errors (between the desired trajectory and the estimated or actual values). Then, the control law is designed so that the system state trajectories are forced towards the sliding surface and stay on it. The choice of the control law that satisfies the following sliding condition is:

$$S\dot{S} < 0 \tag{11}$$

which ensures the attractivity of the sliding surface in the state space. The switching brings inherent stability and robustness to the control strategy, while also introducing chattering (high-frequency switching) that is undesirable in practice and can excite un-modelled dynamics. A boundary layer may be introduced along the sliding surface in order to saturate and smooth out the chattering within a region referred as the smoothing boundary region.

The sliding surface for this configuration is selected as

$$S = (\ddot{x} - \ddot{x}_d) + 2\lambda\xi(\dot{x} - \dot{x}_d) + \lambda^2(x - x_d) = \ddot{e} + 2\lambda\xi\dot{e} + \lambda^2 e \tag{12}$$

with $\lambda > 0$ (control bandwidth) and ζ damping ratio. A robust control law can be obtained by combining an equivalent control component u_{eq} with a robust switching component u_{sw} (27)

$$U = u_{eq} + u_{sw} \tag{13}$$

where the equivalent control component is used to achieve the desired motion on the sliding surface

$$\dot{S} = 0 \Rightarrow u_{eq} = \frac{\ddot{x}_d - \hat{f}(\mathbf{x}) - 2\lambda\xi\dot{e} + \lambda^2 e}{\hat{b}(\mathbf{x})}, \qquad \hat{b}(\mathbf{x}) = \sqrt{b_{\min}(x) b_{\max}(x)}, \quad \hat{f}(\mathbf{x}) = \frac{f_{\min}(\mathbf{x}) + f_{\max}(\mathbf{x})}{2} \tag{14}$$

where $\hat{f}(\mathbf{x})$ and $\hat{b}(\mathbf{x})$ are the nominal or estimate values of $f(\mathbf{x})$ and $b(\mathbf{x})$, respectively. In order to satisfy the reaching condition Eq.(14), the switching control component that accommodates the model uncertainties and disturbances is defined as follows

$$u_{sw} = -\frac{K_{SMC}}{\hat{b}(\mathbf{x})} sat\left(\frac{S}{\Phi}\right)$$
$$K_{SMC} \geq \beta(F(\mathbf{x}) + \eta) + (\beta - 1) \mid \hat{b}(\mathbf{x}) \cdot u_{eq} \mid, \tag{15}$$
$$\beta = \sqrt{\frac{b_{\max}(x)}{b_{\min}(x)}}, \quad \mid f(\mathbf{x}) - \hat{f}(\mathbf{x}) \mid \leq F(\mathbf{x}) = \alpha \hat{f}(\mathbf{x})$$

where β is the gain margin, $F(\mathbf{x})$ is the estimation error on $f(\mathbf{x})$, α is the uncertainty factor, and Φ is the boundary layer thickness.

4 RESULTS

Experiments were conducted to demonstrate the performance of the SMC strategy with aforementioned control strategies. For the implementation of the sliding mode control law, the system states including the pressure in the muscle actuators, the position, velocity, and acceleration of the load are required. The velocity was obtained by differentiating the measured position signal which was then filtered by 2nd order Butterworth low pass filter with cut-off frequency 65 Hz. The acceleration estimate was obtained by differentiating the velocity estimate and filtering it by similar low-pass filter with cut-off frequency 50 Hz. The cut-off frequencies for the filters were found with the help of simulations and finally tuned experimentally to provide optimal result. It should be noted, that in order to obtain acceleration estimate for the SMC controller, also a direct measurement of acceleration, estimation of acceleration using pressure measurement or using state estimation strategies such as extended Kalman filter for nonlinear systems, could also been used here.

The experiments were performed with sinusoidal tracking (amplitude 15 mm) for frequencies 0.25, 0.50, 0.75, 1.0, 1.5 and 2.0 Hz. Each experiment was repeated 5 times to gauge the repeatability of the closed-loop performance and root mean square error (RMSE) values were used as performance indicator.

Initial controller tuning was done with the help of simulations and final tuning was done with the experimental setup in order to guarantee a sufficient accuracy for sinusoidal tracking in normal conditions (M=2 kg). Also, in the controller tuning a focus was to avoid significant chattering in the control signal. For the servo valve configuration, the control parameters were λ=85 rad/s, ζ =0.3, K_{SMC} = 3000 and Φ=50. Note that the damping ratio was set to a small value in order to minimize the amplification of noise in the estimated velocity and acceleration signals. In order to compare the valve approaches similar set of parameters were sed with the on/off valve approach. However, the performance was also studied with higher gains by decreasing the boundary layer thickness resulting in a better tracking accuracy at the cost of increased control signal chattering with both valve configurations.

4.1 Normal conditions

The mean RMSE values and maximum tracking errors for the control performance of the servo valve and 4 on/off valves configuration with SMC approach for sinusoidal tracking with nominal payload (M=2 kg) are gathered in Table 1. It can be seen that on/off valve approach results in only 22 % poorer performance in total than the servo valve approach for the whole input frequency range. However, the majority of this difference becomes at higher input frequencies (1.5 and 2.0 Hz) as the servo valve is capable of providing more flow than on/off valves (see Figures 3 and 4). At lower input frequencies (< 1 Hz) on/off valve approach is capable of providing surprisingly good performance as the performance is almost identical to servo valve approach. It is notable that servo valve approach provides better accuracy in terms of maximum tracking error in overall. The maximum error occurs mostly at times when the direction of movement is changed when the effect of muscle actuator hysteresis is the most significant. With servo valve approach the control loop is much faster (1 ms) than with on/off valve approach (10 ms) resulting in better response at motion reversals. Figures 5-7 illustrates the performance of the approaches for 0.25, 1.0 and 1.5 Hz sinusoidal tracking.

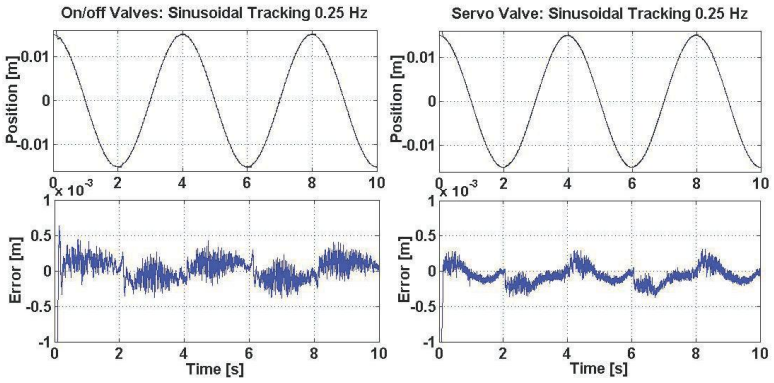

Figure 5: Sinusoidal tracking 0.25 Hz

Frequency of the sine wave trajectory	*On/Off Valves*	*Tracking error*	*Servo valve*	*Tracking error*
0.25 Hz	0.143 (-0 %)	-0.4…+0.4 mm	0.144	-0.35…+0.35 mm
0.5 Hz	0.195 (+0 %)	-0.5…+0.6 mm	0.195	-0.5…+0.3 mm
0.75 Hz	0.220 (-8%)	-0.5…+0.6 mm	0.240	-0.6…+0.3 mm
1.0 Hz	0.348 (+7 %)	-0.6…+0.7 mm	0.324	-0.6…+0.45 mm
1.5 Hz	0.725 (+45 %)	-1.1…+1.5 mm	0.500	-0.8…+0.7 mm
2.0 Hz	1.126 (+50 %)	-1.5…+2 mm	0.750	-1.15…+1.0 mm
Sum RMSE	2.757 *(+22%)*	----------	2.153	----------

Table 1: Comparison of RMSE (mm) values and maximum tracking error of the valve configurations with nominal payload mass M=2 kg and SMC approach.

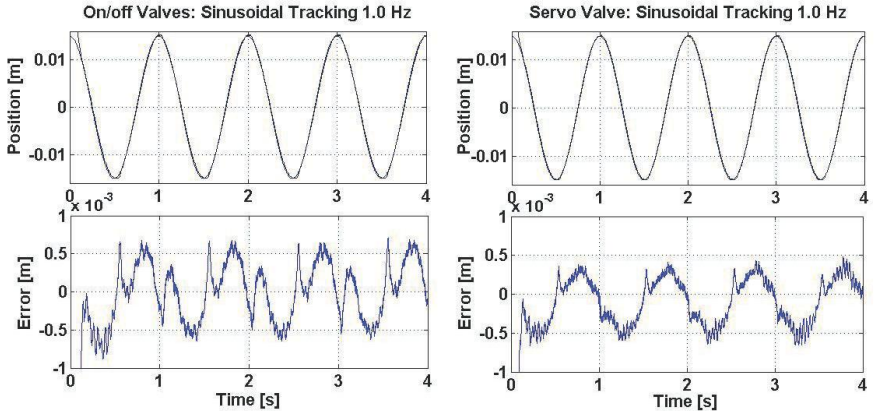

Figure 6: Sinusoidal Tracking 1 Hz

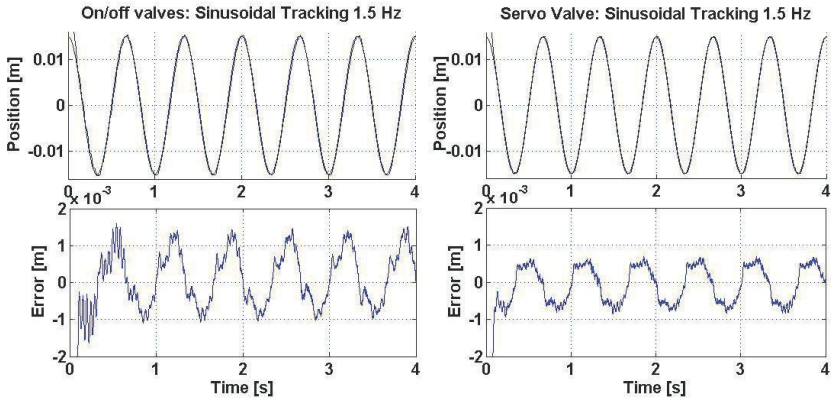

Figure 7: Sinusoidal Tracking 1.5 Hz

4.2 Robustness to payload variation

Although there has been many studies on PWM servo-pneumatics most of them lack analysis of robustness to parameter variations in the process. In this paper, the robustness analysis in terms of increased payload mass is performed. Figure 8 illustrates the resulting control performance of the approaches as a function of increased payload. The sum of the mean RMSE values of control performances for sinusoidal tracking at 0.25, 0.5, 0.75 and 1.0 Hz is used as a robustness indicator. It is interesting to see, that servo valve approach is extremely robust to increased payload mass as the tracking performance is maintained up to M=6 kg. In contrast, the on/off valve approach is capable of maintaining reasonable robustness up to M=4 kg after which the performance starts to degrade more clearly. A significantly better robustness of servo valve approach is due its faster control loop combined with smaller noise in the system. As the SMC strategy is quite sensitive to delay and noise, it starts to affect the performance with PWM strategy that results in a 10 ms control delay and more noise due to PWM switching. In order to demonstrate the effect of control delay, the servo valve approach was used with a sampling time T_s=10 ms that corresponds with the PWM 100 Hz. It can be seen, that the control delay degrades the control performance especially at higher payload masses decreasing the robustness of the controller. With on/off valve approach the effect of control delay and system noise has a more significant effect on the performance.

Another critical factor affecting the controller performances is the value of damping ratio used in the sliding surface design. A smaller damping ratio significantly decreases the magnitude of sensor noise (velocity, acceleration) and in the nominal case a higher value of damping ratio than 0.3 resulted in a poor performance due to magnified noise. It should be noted, that the damping ratio determines the damping properties of the control dynamics. Thus, a small value will provide fast response with low damping resulting in a poor performance with increased system inertia. A higher damping ratio will provide better damping properties with slower response resulting in better performance especially with increased inertia. For that reason, the controllers were not able to provide good results with payload masses much higher than M=6 kg with a damping ratio 0.3.

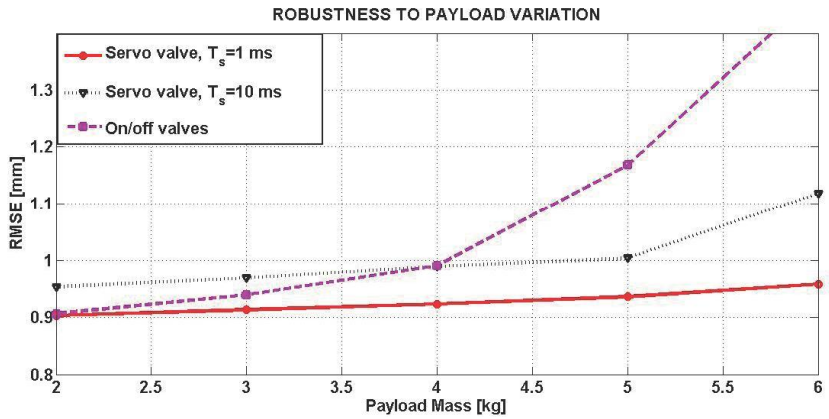

Figure 8: Robustness to Increased Payload

5 CONCLUSIONS

This paper provides a low-cost approach to control pneumatic systems by using high-speed on/off valves instead of costly proportional and servo valves. The mechatronic system under study consisted of pneumatic muscle actuators in the opposing pair configuration driven by four PWM operated on/off valves. In order to provide a comparison between on/off valve and servo valve approaches, a full nonlinear modelling of the system in SISO canonical control form was derived for which SMC strategy was applied. As the resulting controller structure was same for both valve configurations, a direct comparison between the approaches was possible. In nominal conditions, the on/off valve approach resulted in good results as the tracking accuracy was almost identical with the servo valve approach. In terms of maximum tracking error, the servo valve approach provided slightly better performance due to its faster control response at motion reversals when the muscle actuator hysteresis is the most significant. At higher tracking frequencies servo valve approach performed better mostly due to its higher flow capacity compared to on/off valve approach. The robustness of the approaches was tested by increasing the payload mass up to 6 kg. It was noted, that servo valve approach was extremely robust against it, but the performance of on/off valve approach started to degrade clearly at higher payloads. This difference between the approaches is caused by the combination of PWM switching introduced control delay and higher system noise that significantly affects the performance of SMC controlled PWM approaches. However, the results indicate that on/off valve approach can provide a reasonable performance and an interesting option for servo-pneumatic systems with limited uncertainties and parameter variations.

References

[1] Caldwell, D. G.;Medrano-Cerda, G. A.;& Goodwin, M. J. (1995). Control of Pneumatic Muscle Actuators. *IEEE Control Systems Magazine*, *15, No.1*, pp. 40-48.

[2] Lilly, J. (2003). Adaptive Tracking for Pneumatic Muscle Actuators in Bicep and Tricep Configurations. *IEEE Transaction of Neural Systems and Rehabilitation Engineering*, *11, No. 3*, ss. 333-339.
[3] Medrano-Cerda, G. A.;Bowler, C. J.;& Caldwell, D. G. (1995). Adaptive Position Control of Antagonistic Pneumatic Muscle Actuators. *IEEE/RSJ International Conference on Intelligent Robots and Systems*, *1*, ss. 378-383. Pittsburgh, USA.
[4] Than, T.;& Ahn, K. (2006). Nonlinear PID Control to Improve the Control Performance of 2 Axes Pneumatic Artificial Muscle Manipulator Using Neural Networks. *Mechatronics , 16*, 577-587.
[5] Hesselroth, T.;Sarkar, K.;Van der Smagt, P.;& Schulten, K. (1994). Neural Network Control of a Pneumatic Robot Arm. *IEEE Transaction of Systems, Man and Cybernetics*, *24, No.1*, ss. 28-38.
[6] Chan, S. W.;Lilly, J. H.;Repperger, D. W.;& Berlin, J. E. (2003). Fuzzy PD+I Learning Control for a Pneumatic Muscle . *Proceedings of 2003 IEEE International Conference on Fuzzy Systems*, (ss. 278-283). St Louis, USA.
[7] Balasubramanian, K.;& Rattan, K. S. (2003). Feedforward Control of a Nonlinear Pneumatic Muscle System Using Fuzzy Logic. *IEEE International COnference of Fuzzy Systems*, *1*, ss. 272-277.
[8] Lilly, J. H.;& Yang, L. (2005). Sliding Mode Tracking for Pneumatic Muscle Actuators in Opposing Pair Configuration. *IEEE Transactions on Control Systems Technology*, *13*, ss. 550-558.
[9] Carbonell, P.;Jiang, Z. P.;& Repperger, D. W. (2001). Nonlinear Control of a Pneumatic Muscle Actuator: Backstepping vs. Sliding Mode. *Proceedings of the IEEE International Conference on Control Applications*, (ss. 167-172).
[10] Tondu, B.;& Lopez, P. (2000). Modeling and Control of McKibben Artificial Muscle. *IEEE Control Systems Magazine*, (ss. 15-38).
[11] Aschemann, H.;& Schindele, D. (2008). Sliding-mode Control of a High-Speed Linear Axis Driven by Pneumatic Muscle Actuators. *IEEE Transactions on Industrial Electronics , 11* (55), 3855-3864.
[12] Shen, X.;Zhang, J.;Barth, E.;& Goldfarb, M. (2006). Nonlinear Model-Based Control of Pulse Width Modulated Pneumatic Servo Systems. *ASME Journal of Dynamic Systems, Measurement and Control , 128*, 663-669.
[13] Morita, Y. S.;Shimizu, M.;& Kagawa, T. (1985). An Analysis of Pneumatic PWM and Its Application to a Manipulator. *Proceedings of International Symposium of Fluid Control and Measurement*, (ss. 3-8). Tokyo, Japan.
[14] Noritsugu, T. (1986). Development of PWM Mode Electro-Pneumatic Servomechanism, Part I-II: *Journal of Fluid Control , 17-1*, 65-80.
[15] Lai, J. Y.;Singh, R.;& Menq, C. H. (1992). Development of PWM mode Position Control for a Pneumatic Servo System. *Journal of the Chinese Society of Mechanical Engineers , 13* (1), 86-95.
[16] Paul, A. K.;Mishra, J. K.;& Radke, M. G. (1994). Reduced Order Sliding Mode Control for Pneumatic Actuator. *IEEE Transaction on Control Systems Technology , 2* (30), 271-276.
[17] Van Varseveld, R. B.;& Bone, G. M. (1997). Accurate Position Control of a Pneumatic Actuator Using On/Off Solenoid Valves. *IEEE/ASME Transaction on Mechatronics , 2* (30), 195-2004.

[18] Barth, E. J.;Zhang, J.;& Goldfarb, M. (2003). Control Design for Relative Stability in a PWM-Controlled Pneumatic Systems. *ASME Journal of Dynamic Systems, Measurement and Control , 125* (3), 504-508.
[19] Ahn, K.;& Yokota, S. (2005). Intelligent Switching Control of Pneumatic Actuator using On/Off Solenoid Valves. *Mechatronics , 15*, 683-702.
[20] Shen, X.;Zhang, J.;Barth, E.;& Goldfarb, M. (2006). Nonlinear Model-Based Control of Pulse Width Modulated Pneumatic Servo Systems. *ASME Journal of Dynamic Systems, Measurement and Control , 128*, 663-669.
[21] Nguyen, T.;Leavitt, J.;Jabbari, F.;& Bobrow, J. E. (2007). Accurate Sliding-Mode Control of Pneumatic Systems Using Low-Cost Solenoid Valves. *IEEE/ASME Transactions on Mechatronics , 12* (2), 216-219.
[22]Taghizadeh, M.;Ghaffari, A.;& Najafi, F. (2008). A Linearization Approach in Control of PWM-driven Servo-Pneumatic Systems. *Proceedings of the 40th Southeastern Symposium on System Theory*, (ss. 395-399). New Orleans, LA, USA.
[23] Schulte, R. A. (1962). The Characteristics of the McKibben Artificial Muscle. *The Applications of External Power in Prosthetics and Orthotics* , 94-115.
[24] Chou, P.;& Hannaford, B. (1996). Measurement and Modeling of a McKibben Pneumatic Artificial Muscles. *IEEE Transaction on Robotics and Automation , 12* (1).
[25] Jouppila, V. T.;Gadsden, S. A.;& Ellman, A. U. (2010). Modeling and Identifiacation of a Pneumatic Muscle Actuator System Controlled by an On/Off Solenoid Valve. *Proceedings of 7th International Fluid Power Conference*, (s. 16). Aachen, Germany.
[26] Utkin,V. I., Sliding Modes and Their Application in Variable Strucure Systems. Moscow, Russia: MIR Publishers, 1978.
[27] Slotine, J. J. and Li, W., Applied Nonlinear Control. Englewood Cliffs, New Jersey, USA: Prentice-Hall, 1991.

PUBLICATION 5

Experimental Comparisons of Sliding Mode Controlled Pneumatic Muscle and Cylinder Actuator

Ville Jouppila, Andrew Gadsden and Asko Ellman

This is the authors accepted manuscript of an article published in *ASME Journal of Dynamic Systems, Measurement and Control, Vol.36, No.4, April 2014*, permission to use admitted.

Experimental Comparisons of Sliding Mode Controlled Pneumatic Muscle and Cylinder Actuators

Ville Jouppila[1*], S. Andrew Gadsden[2*], and Asko Ellman[1]

1. Department of Mechanics and Design, Tampere University of Technology, Tampere, Finland
2. Department of Mechanical Engineering, McMaster University, Hamilton, Ontario, Canada
* Correspondence: ville.jouppila@tut.fi or gadsden@mcmaster.ca

Abstract

Pneumatic muscle actuators offer a higher force-to-weight ratio compared to traditional cylinder actuators, and introduces stick-slip free operation which offers an interesting option for positioning systems. Despite several advantages, pneumatic muscle actuators are commonly avoided in industrial applications, mainly due to rather different working principles. Due to the highly nonlinear characteristics of the muscle actuator and pneumatic system, a reliable control strategy is required. Although muscle actuators are widely studied, the literature lacks detailed studies where the performance for servo systems is compared with traditional pneumatic cylinders. In this paper, a pneumatic servo actuation system is compared with a traditional cylinder actuator. As the overall system dynamics are highly nonlinear and not well defined, a sliding mode control (SMC) strategy is chosen for the control action. In order to improve the tracking performance, a SMC strategy with an integral action (SMCI) is also implemented. The control algorithms are experimentally applied on the pneumatic muscle and the cylinder actuator, for the purposes of position tracking. The robustness of the systems are verified and compared by varying the applied loads.

Keywords

Pneumatic muscle actuator; servo pneumatics; sliding mode control

1.0 Introduction

Pneumatic systems have a number of properties that make them attractive for use in a variety of environments. High force-to-weight ratios, cleanliness, compactness, ease of maintenance, and the safety of pneumatic actuators offer desirable features for many industrial designs. Usually, cylinder actuators are used in pneumatic systems for generating force and motion. However, during the last couple of decades, pneumatic muscle actuators have gained attention and found some applications, especially in robotics. Pneumatic muscle actuators are contractile devices that are characterized by a decrease in actuator length and an increase in actuator diameter when pressurized [1-3]. The physical configuration of the muscle results in a variable-stiffness spring like characteristics, nonlinear passive elasticity, physical flexibility, and very light weight; compared to other kinds of artificial actuators [4,5]. A significantly higher force-to-weight ratio [6-9] compared with conventional cylinder actuators, as well as the stick-slip free operation [10], offer an interesting option for pneumatic applications. However, there are a number of nonlinearities present in this type of system, which makes it rather difficult and complex to control accurately. In addition to air compressibility and nonlinear airflow through the control valve, the muscle actuators' nonlinear force-length-pressure characteristics and hysteresis result in a highly nonlinear system. Also, the different structure and working principles compared with the cylinder actuator are reasons why muscle actuators are still rarely used in industrial applications.

The literature demonstrates that a large number of control strategies have been proposed to handle the effects of nonlinearities present. These include the following: adaptive control strategies [11-13], artificial neural networks [14], fuzzy controllers [15,16], flatness based control [17,18]. In [19,20], a sliding mode control (SMC) strategy was applied to a muscle actuator system; however, only simulation results of the effectiveness of the strategy were presented. Other SMC approaches were presented in [8,21,22]. In the most recent work [22], a SMC strategy was applied to control the muscle actuator system in an opposing pair configuration using a servo valve. Experimental results with sinusoidal tracking (amplitude $7.5\ \mathrm{mm}$ and frequency $0.5-1.5\ \mathrm{Hz}$) and a payload mass of $10.8\ \mathrm{kg}$ showed accuracies of $\pm 0.5\ \mathrm{mm}$ to $\pm 1.2\ \mathrm{mm}$. In this research, an SMC strategy was chosen for the control of the muscle actuator due to the nonlinearities and uncertainties present in the system. Previous SMC studies have demonstrated that this strategy is an efficient and robust control strategy for pneumatic actuator applications.

When comparing actuators and actuation technologies, in order to find the best compromise for

a particular application, there are number factors to consider: power/force-weight ratio, energy to volume ratio, energy losses (friction, hysteresis), air consumption, reliability, tracking accuracy, and so forth. Although pneumatic muscle actuators have widely been studied and its advantages clearly addressed, the literature still lacks studies where the muscle actuators are sufficiently compared with cylinder actuators for pneumatic servo actuation. Therefore, the objective of this paper is to provide an experimental comparison of pneumatic muscle and conventional cylinder actuators for servo actuation in terms of steady-state positioning accuracy, tracking accuracy, and robustness to payload variations.

In this paper, as shown in Fig. 1, a muscle actuator system with two Festo fluidic muscle (MAS10-300 mm) actuators are mounted horizontally and coupled to a linear slide carrying a payload. The payload system is also driven by a conventional pneumatic cylinder (Festo DSNU-25-100-PPV). A servo valve (FESTO MPYE-5-M5-010-B) is used to control the inflow and outflow of the actuator chambers. The SMC controller is designed in the Matlab Simulink environment and is coded by a real-time windows target toolbox; where reference values are generated, data from the sensors (potentiometer, pressures) are read, and the controller output signal is calculated. The other kinematic states (velocity and acceleration) are obtained by differentiation of the position signal with a second-order Butterworth low-pass filter.

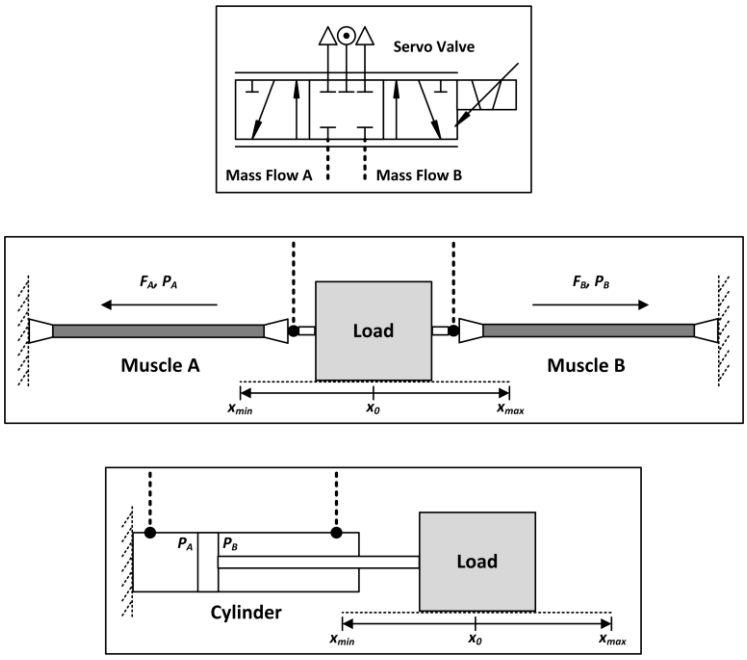

Figure 1. Pneumatic servo system with muscle actuators (middle) and cylinder actuator (bottom)

The system dynamics are modeled in the following section. The SMC design is discussed in Section 3, and the experimental results are shown and discussed in Section 4. The paper then concludes with a summary of the main findings.

2.0 Modeling of System Dynamics

This section describes the modeling of the system, including load dynamics, force dynamics, pressure dynamics, and flow dynamics.

2.1 Load Dynamics

The load dynamics of the system with muscle actuators and cylinder actuator can be written as follows:

$$M\ddot{x} = F_B - F_A - B\dot{x} - F_{ext}$$
$$M\ddot{x} = P_A A_A - P_B A_B - P_0 A_{rod} - B\dot{x} - F_{ext} \quad (1)$$

where M is the total moving mass (payload, slide mechanism, actuators), B is the viscous friction coefficient, F_A and F_B are the actuation forces of the muscle actuators, F_{ext} is the external force, P_A and P_B are the absolute pressures of actuator chamber A and chamber B respectively, and P_0 is the atmospheric pressure. Note that the Coulomb and static friction that are present in the actual system are neglected in the control design, and can be considered as modeling uncertainties and disturbances.

2.2 Muscle Actuator Force Dynamics

The pneumatic McKibben muscle actuator consists of a rubber tube with a non-extensible fiber surrounding. The physical configuration causes the muscle to have variable-stiffness spring-like characteristics, and is very light-weight compared with other types of actuators [4,5]. During pressurization, the muscle widens in diameter and shortens in length, and the maximum force is obtained at the beginning of the contraction and decreases with increasing contraction [4]. The generated force is unidirectional and its maximum contraction is typically 20% to 25% of the nominal (resting) length. The advantage of the muscle actuator over the traditional cylinder is the higher force to weight ratio and the stick-slip free motion at low velocities. However, the force-to-contraction relation is highly nonlinear, and adds to the difficulty of effectively modeling the muscle actuator [4-8,23-25]. As with all actuation systems, effective application of pneumatic muscle actuators relies on being able to accurately model and predict the forces that will be generated under any operating conditions. Figure 2 illustrates the nonlinear relationship between the force, pressure, and displacement for the muscle

actuators working in opposing pair configuration. Note that an initial contraction x_0 of both muscles must be allowed in order to operate in an opposing pair configuration. The nonlinear muscle forces can be described by the following:

$$\begin{aligned} F_A(x,P_A) &= a_0 + a_1(x_0 - x) + a_2(x_0 - x)^2 + a_3(x_0 - x)^3 + a_4(x_0 - x)^4 \\ &\quad - (P_{max} - P_A)\left(\frac{k_0 - k_1(x_0 - x)}{k_2}\right) \\ F_B(x,P_B) &= a_0 + a_1(x_0 + x) + a_2(x_0 + x)^2 + a_3(x_0 + x)^3 + a_4(x_0 + x)^4 \\ &\quad - (P_{max} - P_B)\left(\frac{k_0 - k_1(x_0 + x)}{k_2}\right) \end{aligned} \tag{2}$$

where P_{max} (0.7 MPa, absolute) is the maximum muscle pressure, and a_{0-4}, k_0 [N], k_1 [N/m], and k_2 [Pa] are coefficients to fit the model and measured data, respectively. The details of the actuator force modeling can be found in our previous publication [26]. Figure 2 illustrates the selected operating region (-15…+15 mm) and the maximum cylinder force at 0.6 MPa. It can be seen that both systems provide similar range of forces within the specified operating region justifying the comparison the systems.

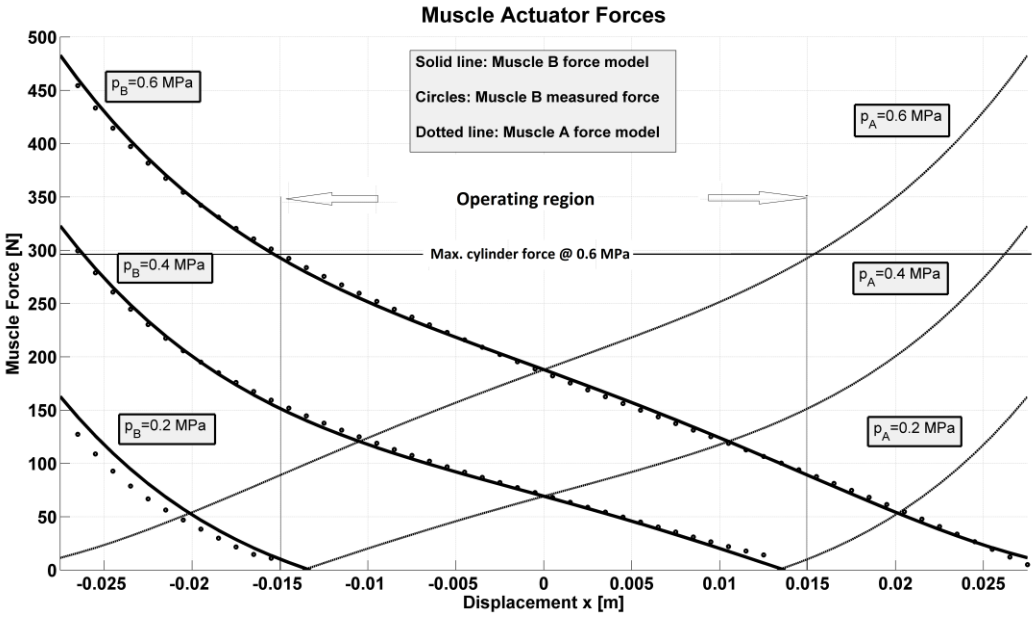

Figure 2. Nonlinear muscle actuator force characteristics, maximum cylinder force and specified operating region

2.3 Pressure Dynamics

For calculating the pressure inside the actuator, it is assumed that the air is an ideal gas and the change of air is adiabatic, such that the pressure change is defined as follows:

$$\dot{P}_{A,B} = \frac{kRT}{V_{A,B}(x)}\dot{m}_{A,B} - \frac{kP_{A,B}\dot{V}_{A,B}}{V_{A,B}(x)} \tag{3}$$

where k (1.4 for adiabatic process), R, T, $V_{A,B}$ and $\dot{m}_{A,B}$ respectively denote the specific heat ratio, universal gas constant, air temperature, volume of the actuators, and mass flow rate into the actuator. The volume of the muscle actuators and cylinder chambers is given by the following:

$$\begin{gathered} V_A = V_0 - v_1 x, \quad V_B = V_0 + v_1 x \\ V_A = A_A\left(\tfrac{1}{2}L - x\right) + V_{A0}, \quad V_B = A_B\left(\tfrac{1}{2}L + x\right) + V_{B0} \end{gathered} \tag{4}$$

where V_0 is the initial muscle volume at midpoint, v_1 is the volume rate, V_{A0} and V_{B0} are the dead volumes in cylinder chambers, and L is the cylinder stroke.

2.4 Mass Flow Dynamics

The servo valve (FESTO MPYE-5-M5-010-B) features a position-controlled spool with a bandwidth of 125 Hz. The spool position is controlled by a control voltage signal ($0 - 10$ V) where the spool is in the center position with a control signal (5 V). A traditional equation for modeling the mass flow rate is based on the flow of an ideal gas through a converging nozzle, and is related to the valve control signal by the following relation [27]:

$$\begin{gathered} \dot{m}(P_u, P_d) = U\psi(P_u, P_d) \\ \psi(P_u, P_d) = \begin{cases} CP_{up}, & if\ P_{down}/P_{up} \le b \\ CP_{up}\sqrt{1 - \left(\dfrac{P_{down}/P_{up} - b}{1 - b}\right)^2}, & if\ \dfrac{P_{down}}{P_{up}} > b \end{cases} \end{gathered} \tag{5}$$

where P_u and P_d are the upstream and downstream pressures, respectively. C is the valve conductance, and b is the critical pressure ratio that divides the flow regimes into un-choked and choked flows through the orifice. A positive valve command will pressurize the muscle/cylinder chamber (B) and exhaust the muscle/cylinder chamber (A), while a negative command corresponds to the opposite. The resulting equations for the mass flow rates are as follows:

$$\dot{m}_A = U\psi_A, \quad \psi_A = \begin{cases} \psi(P_A, P_{atm}), & if\ U \geq 0 \\ \psi(P_s, P_A), & if\ U < 0 \end{cases}$$
$$\dot{m}_B = U\psi_B, \quad \psi_B = \begin{cases} \psi(P_s, P_B), & if\ U \geq 0 \\ \psi(P_B, P_{atm}), & if\ U < 0 \end{cases} \tag{6}$$

where P_s is the supply pressure (0.65 MPa, absolute). Due to the valve dead zone in the mid spool position, dead zone compensation is required, defined as follows:

$$U_{servo} = \begin{cases} U_0 - U + u_{dz} sign(U), & if\ U \leq 0 \\ U_0 + U + u_{dz} sign(U), & if\ U > 0 \end{cases} \tag{7}$$

where $U_0 = 5$ V and $u_{dz} = 0.4$ V is the experimentally determined dead zone range. The parameters of the estimated mass flow rate (5)) are obtained by searching the best fit for the experimental data. The model is capable of providing sufficient accuracy at higher control signals; however, the modeling accuracy decreases with small control signals.

2.5 Overall System Model

The overall nonlinear single-input, single-output (SISO) system model, with muscle actuators from the valve command U to the displacement of the load, can be defined as follows:

$$\dddot{x} = f(\boldsymbol{x}) + b(\boldsymbol{x})U \rightarrow \dddot{x} = \frac{K}{M}\dot{x} - \frac{B}{M}\ddot{x} + \left(\frac{C_a\psi_A + C_b\psi_B}{M}\right)U, \quad where$$

$$f(\boldsymbol{x}) = \frac{K}{M}\dot{x} - \frac{B}{M}\ddot{x}$$

$$b(\boldsymbol{x}) = \frac{C_a\psi_A + C_b\psi_B}{M}$$

$$\boldsymbol{x} = [x \quad \dot{x} \quad \ddot{x} \quad P_A \quad P_B]^T$$

$$K = 2a_1 + 4a_2x_0 + 6a_3x_0^2 + 8a_4x_0^3 + 3x^3(2a^3 + 8a_4x_0) - \frac{k_1}{k_2}(P_A + P_B - 2P_{max}) \tag{8}$$
$$- \left(\frac{k_0 - k_1(x_0 + x)}{k_2}\right)\frac{kv_1P_B}{V_B(x)} - \left(\frac{k_0 - k_1(x_0 - x)}{k_2}\right)\frac{kv_1P_A}{V_A(x)}$$

$$C_a = \left(\frac{k_0 - k_1(x_0 + x)}{k_2}\right)\frac{kRT}{V_A(x)}$$

$$C_b = \left(\frac{k_0 - k_1(x_0 + x)}{k_2}\right)\frac{kRT}{V_B(x)}$$

Similarly, in the case of the pneumatic cylinder:

$$\ddot{x} = f(\boldsymbol{x}) + b(\boldsymbol{x})U \rightarrow \ddot{x} = \frac{K}{M}\dot{x} - \frac{B}{M}\ddot{x} + \left(\frac{C_a\psi_A + C_b\psi_B}{M}\right)U, \quad where$$

$$f(\boldsymbol{x}) = \frac{K}{M}\dot{x} - \frac{B}{M}\ddot{x}$$

$$b(\boldsymbol{x}) = \frac{C_a\psi_A + C_b\psi_B}{M}$$

$$\boldsymbol{x} = [x \quad \dot{x} \quad \ddot{x} \quad P_A \quad P_B]^T \tag{9}$$

$$K = -\frac{kP_AA_A^2}{V_A(x)} - \frac{kP_BA_B^2}{V_B(x)}$$

$$C_a = \frac{kRT}{V_A(x)}$$

$$C_b = \frac{kRT}{V_B(x)}$$

A list of the nomenclature and corresponding parameters used throughout this paper may be found in Table 1. The parameters are identified either based on manufacturer data (e.g. actuator dimensions), or measurements (e.g. viscous friction, muscle force, muscle volume, mass flow, etc.). Details of muscle actuator modeling can be found in [26].

Table 1. List of important nomenclature and corresponding parameters

Parameter	Value	Description
A_A	490×10^{-6} m^2	Piston area
A_B	411×10^{-6} m^2	Piston (rod side) area
A_{rod}	79×10^{-6} m^2	Rod area
B_c	48 kg/s	Viscous friction (cylinder)
B_m	95 kg/s	Viscous friction (muscle)
C	kg/sPa	Valve conductance
M	5 kg	Payload mass
L	0.1 m	Cylinder stroke
R	287 J/kgK	Air constant
T	293 K	Air temperature
V_{0A}	0.1×10^{-5} m^3	Dead volume
V_{0B}	0.1×10^{-5} m^3	Dead volume
a_0	483 N	Identified coefficient
a_1	-2.3×10^{-4} N/m	Identified coefficient
a_2	8.2×10^{5} N/m^2	Identified coefficient
a_3	-1.68×10^{7} N/m^3	Identified coefficient
a_4	1.23×10^{8} N/m^4	Identified coefficient
b	0.21	Critical pressure ratio
k	1.4	Specific heat ratio

k_0	80 N	Identified coefficient
k_1	750 N/m	Identified coefficient
k_2	1.0×10^5 Pa	Identified coefficient
P_{max}	7.0×10^5 Pa	Maximum muscle pressure
P_s	6.5×10^5 Pa	Supply pressure
v_0	2.4×10^{-5} m^3	Initial muscle volume
v_1	5.6×10^{-4} m^2	Muscle volume rate
x_0	2.1×10^{-2} m	Initial muscle displacement

3.0 Sliding Mode Control Design

SMC is a form of variable structure control and is regarded as one of the most effective nonlinear robust control approaches [28,29]. SMC utilizes a discontinuous switching plane along some desired trajectory. The plane is often referred to as a sliding surface S that models the desired closed loop performance in the state variable space. The objective is to keep the state values along this surface by minimizing the state errors (between the desired trajectory and the estimated or actual values). The control law is designed so that the system state trajectories are forced towards the sliding surface and stays within a region of it. The choice of the control law that satisfies the sliding condition is as follows:

$$S\dot{S} < 0 \tag{10}$$

which ensures the sliding surface is attracted towards the state space. The switching brings inherent stability and robustness to the control strategy, while also introducing chattering (high-frequency switching) that is undesirable in practice and can excite un-modeled dynamics. A boundary layer may be introduced along the sliding surface in order to saturate and smooth out the chattering within a region referred as the smoothing boundary region.

A sliding surface for a third-order system is selected as follows:

$$S = \ddot{e} + 2\xi\lambda\dot{e} + \lambda^2 e \tag{11}$$

where λ (> 0) is the control bandwidth and ζ is the damping ratio. Selecting a damping ratio $\zeta = 1$ results in critically damped closed-loop dynamics. The SMC design requires full state feedback (position, velocity, and acceleration), such that the noise in the estimated velocity and acceleration can decrease the overall performance of the controller. By selecting a small damping ratio, the amount of noise can be reduced.

In order to improve the tracking accuracy, a sliding surface with integral action can be selected as follows:

$$\begin{aligned} S_{int} &= \left(\frac{d}{dt}+\lambda\right)\left(\frac{d^2}{dt}+2\lambda\xi\frac{d}{dt}+\lambda^2\right)\int e d\tau \\ &= \ddot{e}+(2\lambda\xi+\lambda)\dot{e}+(2\lambda^2\xi+\lambda^2)e+\lambda^3\int e d\tau \end{aligned} \tag{12}$$

A robust control law can be obtained by combining an equivalent control component u_{eq} with a robust switching component u_{sw} as follows [29]:

$$U = u_{eq} + u_{sw} \tag{13}$$

where the equivalent control component is used to achieve the desired motion on the sliding surface, as follows:

$$\begin{aligned} \dot{S}, \dot{S}_{int} \rightarrow u_{eq} &= \frac{\dddot{x}_d - \hat{f}(\boldsymbol{x}) - 2\lambda\xi\ddot{e} - \lambda^2\dot{e}}{\hat{b}(\boldsymbol{x})} \\ u_{eq,int} &= \frac{\dddot{x}_d - \hat{f}(\boldsymbol{x}) - (2\lambda\xi+\lambda)\ddot{e} - (2\lambda^2\xi+\lambda^2)\dot{e} - \lambda^3 e}{\hat{b}(\boldsymbol{x})} \\ \hat{b}(\boldsymbol{x}) &= \sqrt{b_{min}(\boldsymbol{x})b_{max}(\boldsymbol{x})} \\ \hat{f}(\boldsymbol{x}) &= \frac{f_{min}(\boldsymbol{x})+f_{max}(\boldsymbol{x})}{2} \end{aligned} \tag{14}$$

where $\hat{f}(\boldsymbol{x})$ and $\hat{b}(\boldsymbol{x})$ are the nominal or estimate values of $f(\boldsymbol{x})$ and $b(\boldsymbol{x})$, respectively. In order to satisfy the reaching condition (10), the switching control component that accommodates the model uncertainties and disturbances may be defined as follows [29]:

$$\begin{aligned} u_{sw} &= -\frac{K_{SMC}}{\hat{b}(\boldsymbol{x})} sat\left(\frac{S}{\phi}\right), \quad where \\ K_{SMC} &\geq \beta(F(\boldsymbol{x})+\eta)+(\beta-1)\left|\hat{b}(\boldsymbol{x})u_{eq}\right| \\ \beta &= \sqrt{\frac{b_{max}(\boldsymbol{x})}{b_{min}(\boldsymbol{x})}} \\ \left|f(\boldsymbol{x})-\hat{f}(\boldsymbol{x})\right| &\leq F(\boldsymbol{x}) = \alpha\hat{f}(\boldsymbol{x}) \end{aligned} \tag{15}$$

where β is the gain margin, $F(\boldsymbol{x})$ is the estimation error on $f(\boldsymbol{x})$, α is the uncertainty factor, and ϕ is the boundary layer thickness. The final control signal is obtained by substituting U into (7).

4.0 Experimental Results

Experiments were conducted in an effort to demonstrate and compare the performance of the muscle actuator and cylinder system, for a simple step-wise positioning task, as well as for a sinusoidal position tracking task (from 0.25 Hz to 2 Hz and amplitude 15 mm). Each experiment was repeated 5 times to gauge the repeatability of the closed-loop performance. The root mean square error (RMSE) values and maximum tracking error were used as indicators of performance.

For the implementation of the sliding mode control law, the system states including the pressure in the muscle actuators, the position, velocity, and acceleration of the load are required. The velocity was obtained by differentiating the measured position signal, which was then filtered by a second-order Butterworth low-pass filter with a cut-off frequency of 65 Hz. The acceleration estimate was obtained by differentiating the velocity estimate, and filtering it by a similar low-pass filter with a cut-off frequency of 50 Hz. The optimal cut-off frequencies for the filters were found by using simulations, and were finally tuned experimentally to provide the best result.

Initial controller tuning was performed with the help of simulations, and tuning was refined experimentally in order to guarantee a sufficient accuracy for sinusoidal tracking under normal conditions ($M = 5$ kg). The first task was to select the sliding surface control bandwidth λ. In the literature, several rules have been provided to select an appropriate value. A larger value yields a faster closed-loop dynamics. Another critical sliding surface parameter is the damping factor ζ, which determines the damping properties of the closed-loop control dynamics. A constant switching gain was used instead of (15) in an effort to avoid noise affecting in the velocity and acceleration estimates. The boundary layer thickness was selected for each case by minimizing the following cost function:

$$J = RMSE_e + RMSE_U = \sqrt{\frac{1}{N}\sum_{i=1}^{N} e_i^2} + R\sqrt{\frac{1}{N}\sum_{i=1}^{N} U_i^2} \tag{16}$$

where N is the number samples, R is a weighting factor, and U_N is the normalized control signal. The goal of the cost function is to find the best control performance for sinusoidal tracking $0.25-1.0$ Hz, while minimizing the chattering in the control signal.

Table 2. Control parameters used in the experiment

Parameter	Muscle SMC	Muscle SMCI	Cylinder SMC	Cylinder SMCI
λ (rad/s)	75	45	75	45
ζ	0.3	0.3	0.3	0.3
K_{SMC}	3,000	3,000	3,000	3,000
ϕ	115	70	100	55

4.1 Point-to-Point Positioning Task

Figures 3 and 4 illustrate the control performance of the cylinder and muscle actuator configurations with the SMC and SMCI control strategies. It is interesting to note that the muscle actuator configuration is capable of providing significantly better steady-state accuracy compared to the cylinder configuration. The cylinder friction introduces a maximum steady-state error of approximately 0.2 mm with SMC. With SMCI, the integral action attempts to decrease the steady-state error; however, due to the presence of friction, it introduces overshooting around the target position. The muscle actuator configuration with SMC provides better overall steady-state accuracy compared to the cylinder approach with a maximum steady-state error of 0.2 mm. With SMCI, the steady-state error was reduced to approximately ± 0.1 mm, with a small dither around the target position. With SMCI approaches, note the overshooting for step-wise commands. This is due to integral action that decreases the overall system damping, combined with a relative small closed-loop damping factor $\zeta = 0.3$. Note also, that the cylinder configuration is capable for faster dynamic response (smaller rise time) than the muscle configuration indicating of broader closed loop control bandwidth.

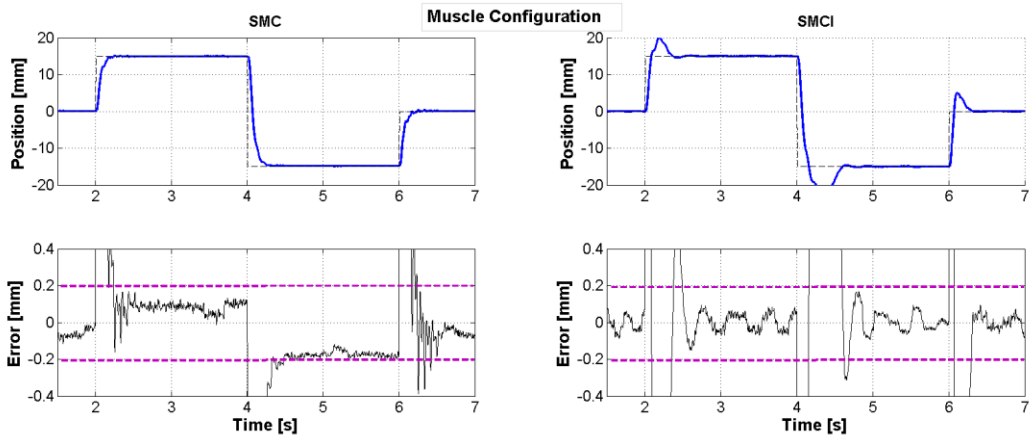

Figure 3. Point-to-point positioning with muscle configuration

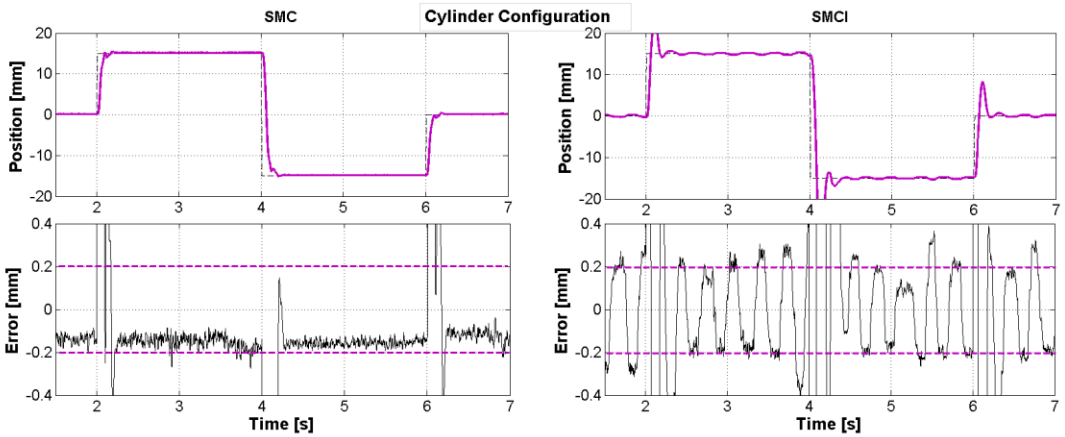

Figure 4. Point-to-point positioning with cylinder configuration

4.2 Sinusoidal Tracking Task

The mean RMSE values for the sinusoidal tracking with a nominal payload $M = 5$ kg are presented in Table 3. The maximum errors are shown in Table 4. Based on the experimental results, the integral action provides a better tracking performance compared to traditional SMC, especially at lower input frequencies. At higher input frequencies, the integral action causes overshooting at reversals of motion, which results in decreased performance (see the maximum error values). Also, note that the best performance at low input frequencies (< 0.5 Hz) was obtained with a muscle actuator configuration and the SMCI strategy. As the muscle actuator can provide a stick-slip free motion, the maximum error at motion reversals is smaller than the cylinder; which is reflected in the RMSE value. At higher tracking frequencies, the cylinder actuator performs better than the muscle actuator. This is caused mainly by the higher bandwidth of the cylinder actuator, and partly due to larger modeling uncertainties in the muscle actuators. Figures 5-7 illustrate the performance of the muscle actuator and the cylinder system with an SMCI control law, for sinusoidal tracking of 0.25 Hz, 1.0 Hz, and 1.5 Hz.

Table 3. Comparison with a nominal payload of 5 kg (RMSE [mm])

Frequency	Muscle SMC	Muscle SMCI	Cylinder SMC	Cylinder SMCI
0.25 Hz	0.164	**0.062**	0.189	0.106
0.50 Hz	0.325	**0.131**	0.209	0.138
0.75 Hz	0.437	0.268	0.231	**0.159**
1.00 Hz	0.560	0.439	0.242	**0.191**
1.50 Hz	0.784	0.865	0.291	**0.268**
2.00 Hz	1.020	1.510	**0.299**	0.332
Total RMSE	3.290	3.276	1.461	1.194

Table 4. Comparison with a nominal payload of 5 kg (maximum error [mm])

Frequency	Muscle SMC	Muscle SMCI	Cylinder SMC	Cylinder SMCI
0.25 Hz	$-0.35 \dots 0.33$	$\mathbf{-0.16 \dots 0.20}$	$-0.45 \dots 0.22$	$-0.41 \dots 0.33$
0.50 Hz	$-0.57 \dots 0.40$	$\mathbf{-0.33 \dots 0.38}$	$-0.56 \dots 0.34$	$-0.53 \dots 0.63$
0.75 Hz	$-0.73 \dots 0.62$	$-0.56 \dots 0.58$	$-0.70 \dots 0.38$	$\mathbf{-0.51 \dots 0.47}$
1.00 Hz	$-0.95 \dots 0.82$	$-0.86 \dots 0.86$	$-0.70 \dots 0.36$	$\mathbf{-0.53 \dots 0.60}$
1.50 Hz	$-1.30 \dots 1.10$	$-1.60 \dots 1.60$	$-0.74 \dots 0.50$	$\mathbf{-0.67 \dots 0.70}$
2.00 Hz	$-1.60 \dots 1.60$	$-2.50 \dots 2.60$	$\mathbf{-0.73 \dots 0.46}$	$-0.71 \dots 0.75$

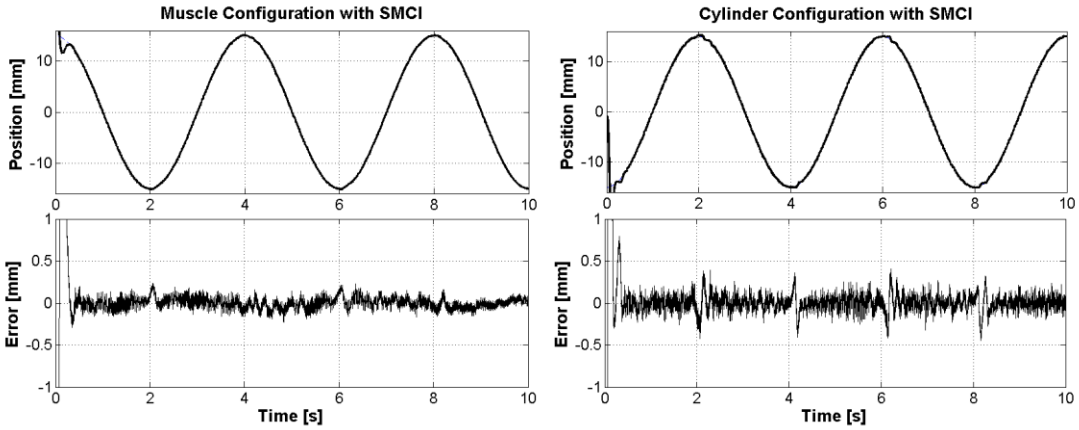

Figure 5. Sinusoidal tracking with 0.25 Hz

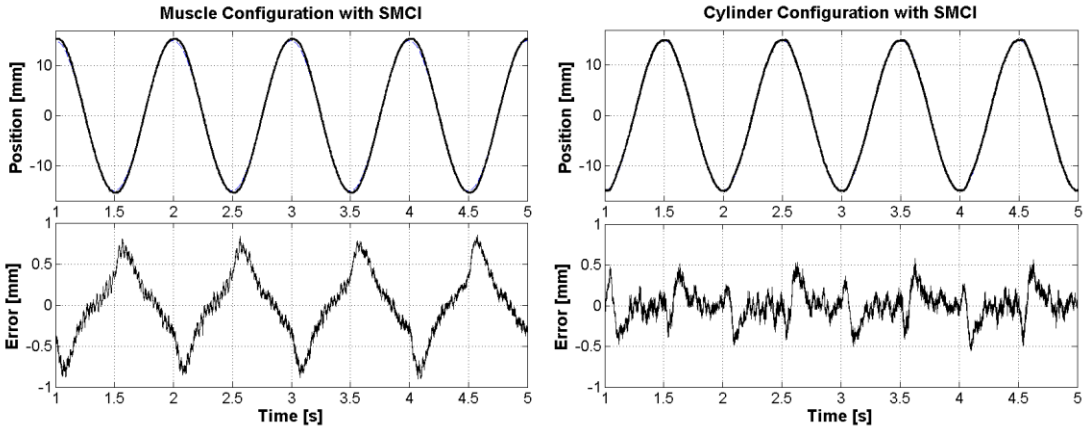

Figure 6. Sinusoidal tracking with 1.0 Hz

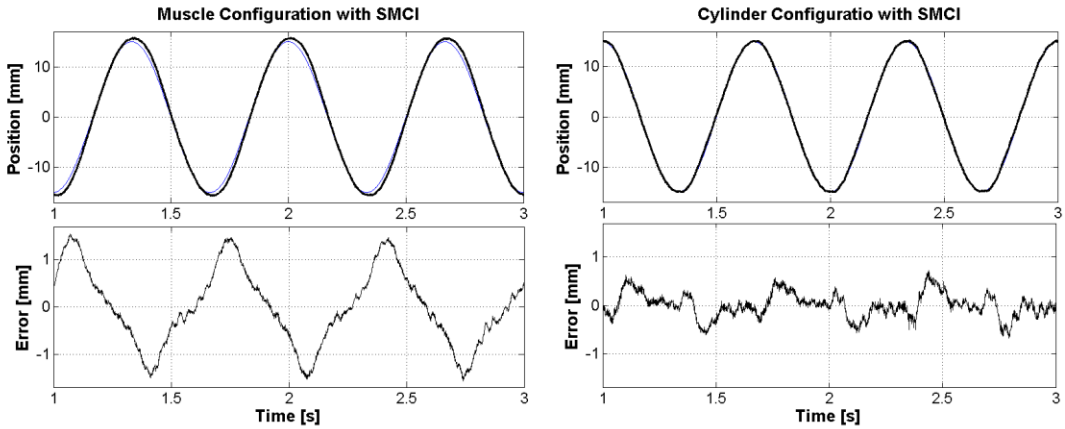

Figure 7. Sinusoidal tracking with 1.5 Hz

4.3 Robustness to Payload Variation

The robustness of the control approaches were tested by changing the payload mass from the nominal $M = 5$ kg. The robustness was validated by calculating the sum of the averaged RMSE values (five measurements for each) for input frequencies 0.25 Hz, 0.5 Hz, 0.75 Hz, and 1.0 Hz. The values were normalized with respect to the nominal case. Figure 8 illustrates that the SMC strategy is not very robust against decreased payload mass. With decreased inertia, the control effort is effectively too strong which results in increased chattering. This may be avoided by selecting a smaller control gain, at the cost of reduced tracking accuracy in the nominal case. Against increased payload mass, the control laws are quite insensitive, providing a reasonably good overall performance. This corresponds well and agrees with the fact that the SMC strategy is commonly stated as a robust control law [29]. However, note that the system with muscle actuators provides very good robustness as the performance hardly changes from the nominal case. In the case of the cylinder actuator, the performance starts to degrade slightly, especially at higher inertias mostly due to friction being present at low velocities.

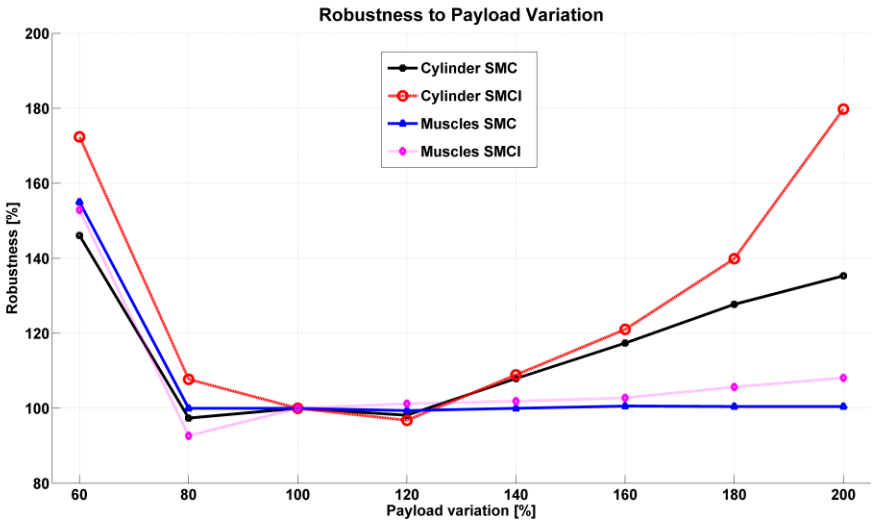

Figure 8. Robustness to payload variation

5.0 Conclusions

In this paper, the focus was to experimentally verify and compare the performance of the position servo system composed of muscle actuators with the traditional cylinder actuator. Based on the derived system models given in a SISO affine form, a sliding mode control (SMC) method, and SMC with an integral action (SMCI) were applied. As the actuator force ranges within the specified operating region were similar and the resulting controller structures were the same for both configurations, a direct comparison between the approaches was made possible.

The system performances were verified with a simple positioning task and also with sinusoidal position tracking tasks. A maximum tracking error and RMSE values were used as performance criteria. It was interesting to note that the muscle actuator configuration resulted in a smaller steady-state error and RMSE, compared to the cylinder configuration; for the positioning task and low frequency (< 0.5 Hz) sinusoidal tracking task. This was caused by the stick-slip free smooth operation of muscle actuators at low velocities, whereas the static friction degrades the performance with the cylinder. At higher tracking frequencies, the cylinder actuator outperformed the muscle actuators. This is due to the higher bandwidth of the cylinder actuator, and fewer modeling errors. With the SMCI approach, the system performance was significantly improved at low tracking frequencies. At higher frequencies, the overshooting at motion reversals started to negatively affect the tracking performance. Furthermore, the steady-state error increased with the cylinder actuator and SMCI method compared to the SMC

method, as the friction caused small oscillations around the target position. For the muscle actuators case, this phenomenon was significantly smaller.

The robustness of the approaches was tested by changing the payload mass from 60% to 200% of nominal. The system with muscle actuators was very robust to increased payload, resulting in minimal change in performance compared with the nominal case. The cylinder performance began to degrade at higher payload masses (more with SMCI), mostly due to friction at smaller tracking frequencies. Furthermore, the performance of both approaches started to decrease at smaller inertias, which is common for SMC strategies due to increased chattering.

Although the advantages and application potential of pneumatic muscle actuators have previously been recognized, the literature has lacked sufficient comparative studies of cylinder actuators mostly used in pneumatic applications. The results of this study indicate that, with a good modeling effort and choice of control law, pneumatic muscle actuators can be practical for use as well in pneumatic servo positioning systems. In addition to many desirable features, such as high force/energy-to-weight ratio and inherent compliance, the operation without stick-slip friction is a significant advantage compared to cylinder actuators when smooth and delicate positioning or tracking is required.

6.0 References

[1] Pierce, R. C., 1940, "Expansible Cover," USA Patent 2,211,478.

[2] De Haven, H., 1949, "Tensioning Device for Producing a Linear Pull," USA Patent 2,483,088.

[3] Gaylord, R. H., 1958, "Fluid Actuated Motor System and Stroking Device," USA Patent 2,844,126.

[4] Schulte, R. A., 1961, "The Characteristics of the McKibben Artificial Muscle," *The Applications of External Power in Prosthetics and Orthotics: A Report*, National Academy of Sciences, National Research Council, pp. 94-115.

[5] Chou, P., and Hannaford, B., 1996, "Measurement and Modeling of McKibben Pneumatic Artificial Muscles," IEEE Transactions on Robotics and Automation, **12**(1), pp. 90-102.

[6] Caldwell, D. G., Medrano-Cerda, G. A., and Bowler, C. J., 1997, "Investigation of Bipedal Robot Locomotion Using Pneumatic Muscle Actuators," *IEEE Proceedings of the International Conference on Robotics and Automation,* Albuquerque, New Mexico, USA, Vol. 1, pp. 799-804.

[7] Klute, G. K., and Hannaford, B., 2000, "Accounting for Elastic Energy Storage in McKibben Artificial Muscle Actuators," J Dyn Syst-T ASME, **122**(2), pp. 386-388.

[8] Tondu, B., and Lopez, P., 2000, "Modeling and Control of McKibben Artificial Muscles," IEEE Control Systems, **20**(2), pp. 15-38.

[9] Plettenburg, D. H., 2005, "Pneumatic Actuators: a Comparison of Energy-to-Mass Ratio's," *Proceedings of the 2005 IEEE 9th International Conference on Rehabilitation Robotics,* Chicago, IL, USA, pp. 545-549.

[10] Festo, 2002, "Fluidic Muscle MAS, Festo Brochure."

[11] Caldwell, D. G., Medrano-Cerda, G. A., and Goodwin, M. J., 1995, "Control of Pneumatic Muscle Actuators," IEEE Control Systems, **15**(1), pp. 40-48.

[12] Lilly, J. H., 2003, "Adaptive Tracking for Pneumatic Muscle Actuators in Bicep and Tricep Configurations," IEEE Transactions of Neural Systems and Rehabilitation Engineering, **11**(3), pp. 333-339.

[13] Medrano-Cerda, G. A., Bowler, C. J., and Caldwell, D. G., 1995, "Adaptive Position Control of Antagonistic Pneumatic Muscle Actuators." *IEEE/RSJ International Conference on Intelligent Robots and Systems,* Pittsburgh, USA, pp. 378-383.

[14] Hesselroth, T., Sarkar, K., Van der Smagt, P., and Schulten, K., 1994, "Neural Network Control of a Pneumatic Robot Arm," IEEE Transactions of Systems, Man and Cybernetics, **24**(1), pp. 28-38.

[15] Chan, S. W., Lilly, J. H., Repperger, D. W., and Berlin, J. E., 2003, "Fuzzy PD+I Learning Control for a Pneumatic Muscle," *The 12th IEEE International Conference on Fuzzy Systems,* St. Louis, USA, Vol. 1, pp. 278-283.

[16] Balasubramanian, K., and Rattan, K. S., 2003, "Feedforward Control of a Nonlinear Pneumatic Muscle System Using Fuzzy Logic," *The 12th IEEE International Conference on Fuzzy Systems,* St. Louis, USA, Vol. 1, pp. 272-277.

[17] Hildebrandt, A., Sawodny, O., Neumann, R., and Hartmann, A., 2002, "A Flatness Based Design For Tracking Control of Pneumatic Muscle Actuators," *Proceedings of 7th International Conference on Automation, Robotics and Vision,* Singapore, pp. 1151-1161.

[18] Aschemann, H., and Hofer, E. P., 2004, "Flatness-based Trajectory Control of Pneumatically Driven Carriage with Uncertainties," *Proceedings of 6th IFAC Symposium on Nonlinear Control Systems (NOLCOS 2004),* F. Allgöwer, and M. Zeitz, eds., Elsevier, Kidlington, Oxford, Vol. 1, pp. 225-230.

[19] Carbonell, P., Jiang, Z. P., and Repperger, D. W., 2001, "Nonlinear Control of a Pneumatic Muscle Actuator: Backstepping vs. Sliding Mode," *IEEE Proceedings of International Conference on Control Applications,* Mexico City, Mexico, pp. 167-172.

[20] Lilly, J. H., and Yang, L., 2005, "Sliding Mode Tracking for Pneumatic Muscle Actuators in Opposing Pair Configuration," IEEE Transactions on Control Systems Technology, **13**(4), pp. 550-558.

[21] Aschemann, H., Schindele, D., 2008, "Sliding-Mode Control of a High-Speed Linear Axis Driven by Pneumatic Muscle Actuators," IEEE Transactions on Industrial Electronics, **11**(55), pp. 3855-3864.

[22] Shen, X., 2010 "Nonlinear Model-Based Control of Pneumatic Artificial Muscle Actuator Systems," Control Engineering Practice, **18**(3), pp. 311-317.

[23] Tsagarakis, N., and Caldwell, D. G., 2000, "Improved Modeling and Assessment of Pneumatic Muscle Actuators," *Proceedings of the IEEE International Conference on Robotics and Automation,* San Francisco, USA, pp. 3641-3646.

[24] Davis, S., Tsagarakis, N. G., Canderle, J., and Caldwell, D. G., 2003, "Enhanced modelling and performance in braided pneumatic muscle actuators," The International Journal of Robotics Research, **22**(3-4), pp. 213-227.

[25] Davis, S., and Caldwell, D. G., 2006, "Braid Effects on Contractile Range and Friction Modeling in Pneumatic Muscle Actuators," The International Journal of Robotics Research, **25**(4), pp. 359-369.

[26] Jouppila, V., Gadsden, S. A., and Ellman, A., 2010, "Modeling and Identification of a Pneumatic Muscle Actuator System Controlled by an On/Off Solenoid Valve," *Workshop Proceedings of the 7th International Fluid Power Conference,* Aachen, Germany, pp. 167-182.

[27] ISO6358, 1989, "Pneumatic Fluid Power - Components using Compressible Fluids - Determination of Flow-rate Characteristics."

[28] Utkin, V. I., 1978, *Sliding Modes and Their Application in Variable Structure Systems,* Mir Publishers, Moscow.

[29] Slotine, J. J. E., and Li, W., 1991, *Applied Nonlinear Control,* Prentice-Hall, NJ, USA, Chap. 7.

Tampereen teknillinen yliopisto
PL 527
33101 Tampere

Tampere University of Technology
P.O.B. 527
FI-33101 Tampere, Finland

ISBN 978-952-15-3258-0
ISSN 1459-2045